

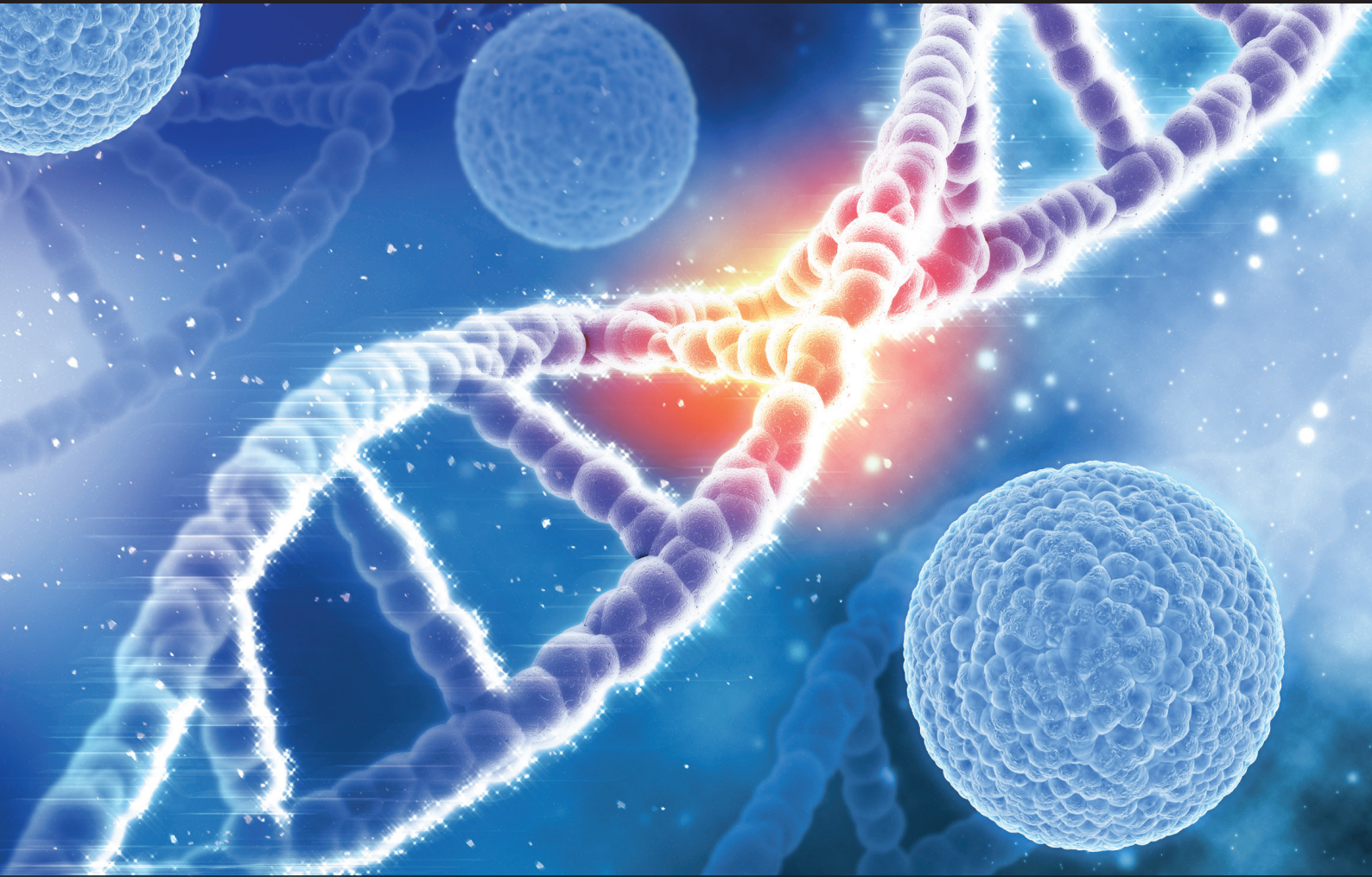
ISSN 2602-2575 - EISSN 2618-6144

# EUROPEAN JOURNAL OF BIOLOGY

OFFICIAL JOURNAL OF ISTANBUL UNIVERSITY'S SCIENCE FACULTY

VOLUME 82 • NUMBER 1 • JUNE 2023

<https://iupress.istanbul.edu.tr/en/journal/ejb/home>



**Indexing and Abstracting**

SCOPUS

TUBITAK ULAKBIM TR Index

Zoological Record - Clarivate Analytics

CAB Abstracts

DOAJ

CABI

- AgBiotechNet Database

- Animal Science Database

- VetMed Resource

- Environmental Impact Database

- Horticultural Science Database

- Nutrition and Food Sciences Database

Chemical Abstracts Service (CAS)

EBSCO Central & Eastern European Academic Source

SOBIAD

Cabells Journalytics

**Owner**

Prof. Dr. Tansel AK  
Istanbul University, Istanbul, Turkiye

**Responsible Manager**

Prof. Dr. Sehnaz BOLKENT  
Istanbul University, Istanbul, Turkiye  
[sbolkent@istanbul.edu.tr](mailto:sbolkent@istanbul.edu.tr)

**Correspondence Address**

Istanbul University Faculty of Science  
Department of Biology, 34134 Vezneciler, Fatih, Istanbul, Turkiye  
Phone: +90 (212) 455 57 00 (Ext. 20318)  
Fax: +90 (212) 528 05 27  
E-mail: [ejb@istanbul.edu.tr](mailto:ejb@istanbul.edu.tr)  
<https://iupress.istanbul.edu.tr/en/journal/ejb/home>

**Publisher**

Istanbul University Press  
Istanbul University Central Campus,  
34452 Beyazit, Fatih, Istanbul, Turkiye  
Phone: +90 (212) 440 00 00

**Printed by**

İlbey Matbaa Kağıt Reklam Org. Müc. San. Tic. Ltd. Şti.  
2. Matbaacılar Sitesi 3NB 3 Topkapı / Zeytinburnu,  
Istanbul, Turkiye  
[www.ilbeymatbaa.com.tr](http://www.ilbeymatbaa.com.tr)  
Certificate No: 51632

---

Authors bear responsibility for the content of their published articles.

The publication language of the journal is English.

This is a scholarly, international, peer-reviewed and open-access journal published biannually in June and December.

---

**Publication Type:** Periodical

---

## EDITORIAL MANAGEMENT BOARD

---

### Editor-in-Chief

**Prof. Sehnaz BOLKENT**–Istanbul University, Faculty of Science, Department of Biology, Istanbul, Turkiye – [sbolkent@istanbul.edu.tr](mailto:sbolkent@istanbul.edu.tr)

### Co-Editor-in-Chief

**Prof. Fusun OZTAY**–Istanbul University, Faculty of Science, Department of Biology, Istanbul, Turkiye – [fusoztay@istanbul.edu.tr](mailto:fusoztay@istanbul.edu.tr)

**Dr. Pinar UYSAL ONGANER**–University of Westminster, London, United-Kingdom – [p.onganer@westminster.ac.uk](mailto:p.onganer@westminster.ac.uk)

### Editorial Management Board Members

**Prof. Fusun OZTAY**–Istanbul University, Faculty of Science, Department of Biology, Istanbul, Turkiye – [fusoztay@istanbul.edu.tr](mailto:fusoztay@istanbul.edu.tr)

**Prof. Gulriz BAYCU KAHYAOGU**–Istanbul University, Faculty of Science, Department of Biology, Istanbul, Turkiye – [gulrizb@istanbul.edu.tr](mailto:gulrizb@istanbul.edu.tr)

**Assoc. Prof. Aysegul MULAYIM**–Istanbul University, Faculty of Science, Department of Biology, Istanbul, Turkiye – [aysegulm@istanbul.edu.tr](mailto:aysegulm@istanbul.edu.tr)

### Section Editors

**Prof. Filiz GUREL**–University of Maryland, Department of Plant Science & Landscape Architecture, Maryland, USA – [filiz@umd.edu](mailto:filiz@umd.edu)

**Prof. Gulriz BAYCU KAHYAOGU**–Istanbul University, Faculty of Science, Department of Biology, Istanbul, Turkiye – [gulrizb@istanbul.edu.tr](mailto:gulrizb@istanbul.edu.tr)

**Prof. Bekir KESKIN**–Ege University, Faculty of Science, Department of Biology, Izmir, Turkiye – [bekir.keskin@ege.edu.tr](mailto:bekir.keskin@ege.edu.tr)

**Assoc. Prof. Aysegul MULAYIM**–Istanbul University, Faculty of Science, Department of Biology, Istanbul, Turkiye – [aysegulm@istanbul.edu.tr](mailto:aysegulm@istanbul.edu.tr)

**Assoc. Prof. Pinar CAGLAYAN**–Marmara University, Department of Biology, Istanbul, Turkiye – [pinar.caglayan@marmara.edu.tr](mailto:pinar.caglayan@marmara.edu.tr)

### Language Editors

**Elizabeth Mary EARL**–Istanbul University, School of Foreign Languages (English), Istanbul, Turkiye – [elizabeth.earl@istanbul.edu.tr](mailto:elizabeth.earl@istanbul.edu.tr)

**Rachel Elana KRISS**–Istanbul University, School of Foreign Languages (English), Istanbul, Turkiye – [rachel.kriss@istanbul.edu.tr](mailto:rachel.kriss@istanbul.edu.tr)

### Statistics Editor

**Prof. Ahmet DIRICAN**–Istanbul University-Cerrahpasa, Faculty of Cerrahpasa Medicine, Department of Biostatistics, Istanbul, Turkiye – [adirican@iuc.edu.tr](mailto:adirican@iuc.edu.tr)

### Publicity Manager

**Dr. Ozgecan KAYALAR**–Koc University, Research Center for Translational Medicine, Istanbul, Turkiye – [okayalar@ku.edu.tr](mailto:okayalar@ku.edu.tr)

### Editorial Assistant

**Oykum GENÇ**–Istanbul University, Faculty of Science, Department of Biology, Istanbul, Turkiye – [oykumgenc@istanbul.edu.tr](mailto:oykumgenc@istanbul.edu.tr)

## EDITORIAL BOARD

---

**Hafiz AHMED** – University of Maryland, Maryland, USA – [hahmed@som.umaryland.edu](mailto:hahmed@som.umaryland.edu)

**Ugur AKSU** – Istanbul University, Istanbul, Turkiye – [uguraksu@istanbul.edu.tr](mailto:uguraksu@istanbul.edu.tr)

**Elif Damla ARISAN** – Gebze Technical University, Istanbul, Turkiye – [d.arisan@gtu.edu.tr](mailto:d.arisan@gtu.edu.tr)

**Ahmet ASAN** – Trakya University, Edirne, Turkiye – [ahasan@trakya.edu.tr](mailto:ahasan@trakya.edu.tr)

**Meral BIRBIR** – Marmara University, Istanbul, Turkiye – [mbirbir@marmara.edu.tr](mailto:mbirbir@marmara.edu.tr)

**Ricardo Antunes DE AZEVEDO** – Universidade de Sao Paulo, Sao Paulo, Brazil – [raa@usp.br](mailto:raa@usp.br)

**Kasim BAJROVIC** – University of Sarajevo, Sarajevo, Bosnia – [kasim.bajrovic@ingeb.unsa.ba](mailto:kasim.bajrovic@ingeb.unsa.ba)

**Levent BAT** – Sinop University, Sinop, Turkiye – [leventb@sinop.edu.tr](mailto:leventb@sinop.edu.tr)

**Mahmut CALISKAN** – Istanbul University, Istanbul, Turkiye – [mahmut.caliskan@istanbul.edu.tr](mailto:mahmut.caliskan@istanbul.edu.tr)

**Carmela CAROPPO** – Institute for Coastal Marine Environment, Rome, Italy – [carmela.caroppo@iamc.cnr.it](mailto:carmela.caroppo@iamc.cnr.it)

**Mustafa DJAMGOZ** – Imperial College, London, United Kingdom – [m.djamgoz@imperial.ac.uk](mailto:m.djamgoz@imperial.ac.uk)

**Mehmet Haluk ERTAN** – The University of New South Wales (UNSW), Sydney, Australia – [hertan@unsw.edu.au](mailto:hertan@unsw.edu.au)

**Rafael Ruiz De La HABA** – University of Sevilla, Sevilla, Spain – [rrh@us.es](mailto:rrh@us.es)

**Onder KILIC** – Istanbul University, Istanbul, Turkiye – [okilic@istanbul.edu.tr](mailto:okilic@istanbul.edu.tr)

**Ayten KIMIRAN** – Istanbul University, Istanbul, Turkiye – [kimiran@istanbul.edu.tr](mailto:kimiran@istanbul.edu.tr)

**Armagan KOCER** – University of Twente, Enschede, The Netherlands – [a.kocer@utwente.nl](mailto:a.kocer@utwente.nl)

**Domenico MORABITO** – Universite d’Orleans, Orleans, France – [domenico.morabito@univ-orleans.fr](mailto:domenico.morabito@univ-orleans.fr)

**Michael MOUSTAKAS** – Aristotle University, Thessaloniki, Greece – [moustak@bio.auth.gr](mailto:moustak@bio.auth.gr)

**Gokhan M. MUTLU** – University of Chicago, Chicago, USA – [gmutlu@medicine.bsd.uchicago.edu](mailto:gmutlu@medicine.bsd.uchicago.edu)

**Maxim NABOZHENKO** – Dagestan State University, Dagestan, Russia – [nalassus@mail.ru](mailto:nalassus@mail.ru)

**Selda OKTAYOGLU** – Istanbul University, Istanbul, Turkiye – [selgez@istanbul.edu.tr](mailto:selgez@istanbul.edu.tr)

**Nesrin OZOREN** – Bogazici University, Istanbul, Turkiye – [nesrin.ozoren@boun.edu.tr](mailto:nesrin.ozoren@boun.edu.tr)

**Majeti Narasimha VARA PRASAD** – University of Hyderabad, Hyderabad, India – [mnvsl@uohyd.ernet.in](mailto:mnvsl@uohyd.ernet.in)

**Thomas SAWIDIS** – Aristotle University, Thessaloniki, Greece – [sawidis@bio.auth.gr](mailto:sawidis@bio.auth.gr)

**Jaswinder SINGH** – McGill University, Quebec, Canada – [jaswinder.singh@mcgill.ca](mailto:jaswinder.singh@mcgill.ca)

**Lejla PAŠIĆ** – University Sarajevo School of Science and Technology, Sarajevo, Bosnia and Herzegovina – [lejla.pasic@ssst.edu.ba](mailto:lejla.pasic@ssst.edu.ba)

**Nico M. Van STRAALLEN** – Vrije Universiteit, Amsterdam, The Netherlands – [n.m.van.straalen@vu.nl](mailto:n.m.van.straalen@vu.nl)

**Ismail TURKAN** – Ege University, Izmir, Turkiye – [ismail.turkan@ege.edu.tr](mailto:ismail.turkan@ege.edu.tr)

**Refiye YANARDAG** – Istanbul University-Cerrahpasa, Istanbul, Turkiye – [yanardag@iuc.edu.tr](mailto:yanardag@iuc.edu.tr)

## AIMS AND SCOPE

European Journal of Biology (Eur J Biol) is an international, scientific, open access periodical published in accordance with independent, unbiased, and double-blinded peer-review principles. The journal is the official publication of Istanbul University Faculty of Science and it is published biannually on June and December. The publication language of the journal is English. European Journal of Biology has been previously published as IUFS Journal of Biology. It has been published in continuous publication since 1940.

European Journal of Biology aims to contribute to the literature by publishing manuscripts at the highest scientific level on all fields of biology. The journal publishes original research and review articles, and short communications that are prepared in accordance with the ethical guidelines in all fields of biology and life sciences.

The scope of the journal includes but not limited to; animal biology and systematics, plant biology and systematics, hydrobiology, ecology and environmental biology, microbiology, cell and molecular biology, biochemistry, biotechnology and genetics, physiology, toxicology, cancer biology, developmental and stem cell biology.

The target audience of the journal includes specialists and professionals working and interested in all disciplines of biology.

The editorial and publication processes of the journal are shaped in accordance with the guidelines of the International Committee of Medical Journal Editors (ICMJE), World Association of Medical Editors (WAME), Council of Science Editors (CSE), Committee on Publication Ethics (COPE), European Association of Science Editors (EASE), and National Information Standards Organization (NISO). The journal is in conformity with the Principles of Transparency and Best Practice in Scholarly Publishing ([doaj.org/bestpractice](http://doaj.org/bestpractice)).

European Journal of Biology is currently indexed SCOPUS, TUBITAK ULAKBIM TR Index, Zoological Record - Clarivate Analytics, CAB Abstracts, DOAJ, CABI, Chemical Abstracts Service (CAS), EBSCO Central & Eastern European Academic Source, SOBIAD, Cabells Journalytics.

Processing and publication are free of charge with the journal. No fees are requested from the authors at any point throughout the evaluation and publication process. All manuscripts must be submitted via the online submission system, which is available at [dergipark.gov.tr/iufsjb](http://dergipark.gov.tr/iufsjb). The journal guidelines, technical information, and the required forms are available on the journal's web page.

All expenses of the journal are covered by the Istanbul University.

Statements or opinions expressed in the manuscripts published in the journal reflect the views of the author(s) and not the opinions of the Istanbul University Faculty of Science, editors, editorial board, and/or publisher; the editors, editorial board, and publisher disclaim any responsibility or liability for such materials.

All published content is available online, free of charge at <https://dergipark.org.tr/tr/pub/iufsjb>. Printed copies of the journal are distributed free of charge.



**Editor in Chief:** Prof. Dr. Sehnaz BOLKENT

**Address:** Istanbul University, Faculty of Science, Department of Biology, 34134 Vezneciler, Fatih, Istanbul, Turkiye

**Phone:** +90 212 4555700 (Ext. 20318)

**Fax:** +90 212 5280527

**E-mail:** [sbolkent@istanbul.edu.tr](mailto:sbolkent@istanbul.edu.tr); [ejb@istanbul.edu.tr](mailto:ejb@istanbul.edu.tr)

## INSTRUCTIONS TO AUTHORS

European Journal of Biology (Eur J Biol) is an international, scientific, open access periodical published in accordance with independent, unbiased, and double-blinded peer-review principles. The journal is the official publication of Istanbul University Faculty of Science and it is published biannually on June and December. The publication language of the journal is English. European Journal of Biology has been previously published as IUFS Journal of Biology. It has been published in continuous publication since 1940.

European Journal of Biology aims to contribute to the literature by publishing manuscripts at the highest scientific level on all fields of biology. The journal publishes original research and review articles, and short communications that are prepared in accordance with the ethical guidelines in all fields of biology and life sciences.

The scope of the journal includes but not limited to; animal biology and systematics, plant biology and systematics, hydrobiology, ecology and environmental biology, microbiology, cell and molecular biology, biochemistry, biotechnology and genetics, physiology, toxicology, cancer biology, developmental and stem cell biology.

The editorial and publication processes of the journal are shaped in accordance with the guidelines of the International Council of Medical Journal Editors (ICMJE), the World Association of Medical Editors (WAME), the Council of Science Editors (CSE), the Committee on Publication Ethics (COPE), the European Association of Science Editors (EASE), and National Information Standards Organization (NISO). The journal conforms to the Principles of Transparency and Best Practice in Scholarly Publishing ([doaj.org/bestpractice](http://doaj.org/bestpractice)).

Originality, high scientific quality, and citation potential are the most important criteria for a manuscript to be accepted for publication. Manuscripts submitted for evaluation should not have been previously presented or already published in an electronic or printed medium. Manuscripts that have been presented in a meeting should be submitted with detailed information on the organization, including the name, date, and location of the organization.

Manuscripts submitted to European Journal of Biology will go through a double-blind peer-review process. Each submission will be reviewed by at least three external, independent peer reviewers who are experts in their fields in order to ensure an unbiased evaluation process. The editorial board will invite an external and independent editor to manage the evaluation processes of manuscripts

submitted by editors or by the editorial board members of the journal. The Editor in Chief is the final authority in the decision-making process for all submissions.

An approval of research protocols by the Ethics Committee in accordance with international agreements (World Medical Association Declaration of Helsinki “Ethical Principles for Medical Research Involving Human Subjects,” amended in October 2013, [www.wma.net](http://www.wma.net)) is required for experimental, clinical, and drug studies. If required, ethics committee reports or an equivalent official document will be requested from the authors.

For manuscripts concerning experimental research on humans, a statement should be included that shows the written informed consent of patients and volunteers was obtained following a detailed explanation of the procedures that they may undergo. Information on patient consent, the name of the ethics committee, and the ethics committee approval number should also be stated in the Materials and Methods section of the manuscript. It is the authors’ responsibility to carefully protect the patients’ anonymity. For photographs that may reveal the identity of the patients, signed releases of the patient or of their legal representative should be enclosed.

European Journal of Biology requires experimental research studies on vertebrates or any regulated invertebrates to comply with relevant institutional, national and/or international guidelines. The journal supports the principles of Basel Declaration ([basel-declaration.org](http://basel-declaration.org)) and the guidelines published by International Council for Laboratory Animal Science (ICLAS) ([iclas.org](http://iclas.org)). Authors are advised to clearly state their compliance with relevant guidelines.

European Journal of Biology advises authors to comply with IUCN Policy Statement on Research Involving Species at Risk of Extinction and the Convention on the Trade in Endangered Species of Wild IUCN Policy Statement on Research Involving Species at Risk of Extinction and the Convention on the Trade in Endangered Species of Wild Fauna and Flora.

All submissions are screened by a similarity detection software (iThenticate by CrossCheck).

In the event of alleged or suspected research misconduct, e.g., plagiarism, citation manipulation, and data falsification/fabrication, the Editorial Board will follow and act in accordance with COPE guidelines.

Each individual listed as an author should fulfil the authorship criteria recommended by the International Committee of Medical Journal Editors (ICMJE - [www.icmje.org](http://www.icmje.org)).

The ICMJE recommends that authorship be based on the following 4 criteria:

1. Substantial contributions to the conception or design of the work; or the acquisition, analysis, or interpretation of data for the work; AND
2. Drafting the work or revising it critically for important intellectual content; AN
3. Final approval of the version to be published; AND
4. Agreement to be accountable for all aspects of the work in ensuring that questions related to the accuracy or integrity of any part of the work are appropriately investigated and resolved.

In addition to being accountable for the parts of the work he/she has done, an author should be able to identify which co-authors are responsible for specific other parts of the work. In addition, authors should have confidence in the integrity of the contributions of their co-authors.

All those designated as authors should meet all four criteria for authorship, and all who meet the four criteria should be identified as authors. Those who do not meet all four criteria should be acknowledged in the title page of the manuscript.

European Journal of Biology requires corresponding authors to submit a signed and scanned version of the authorship contribution form (available for download through the journal's web page) during the initial submission process in order to act appropriately on authorship rights and to prevent ghost or honorary authorship. If the editorial board suspects a case of "gift authorship," the submission will be rejected without further review. As part of the submission of the manuscript, the corresponding author should also send a short statement declaring that he/she accepts to undertake all the responsibility for authorship during the submission and review stages of the manuscript.

European Journal of Biology requires and encourages the authors and the individuals involved in the evaluation process of submitted manuscripts to disclose any existing or potential conflicts of interests, including financial, consultant, and institutional, that might lead to potential bias or a conflict of interest. Any financial grants or other supports received for a submitted study from individuals or institutions should be disclosed to the Editorial Board. To disclose a potential conflict of interest, the ICMJE Potential Conflict of Interest Disclosure Form should be filled and submitted by all contributing authors. Cases of a potential conflict of interest of the editors, authors, or

reviewers are resolved by the journal's Editorial Board within the scope of COPE and ICMJE guidelines.

The Editorial Board of the journal handles all appeal and complaint cases within the scope of COPE guidelines. In such cases, authors should get in direct contact with the editorial office regarding their appeals and complaints. When needed, an ombudsperson may be assigned to resolve cases that cannot be resolved internally. The Editor in Chief is the final authority in the decision-making process for all appeals and complaints.

When submitting a manuscript to European Journal of Biology, authors accept to assign the copyright of their manuscript to Istanbul University Faculty of Science. If rejected for publication, the copyright of the manuscript will be assigned back to the authors. European Journal of Biology requires each submission to be accompanied by a Copyright Transfer Form (available for download at the journal's web page). When using previously published content, including figures, tables, or any other material in both print and electronic formats, authors must obtain permission from the copyright holder. Legal, financial and criminal liabilities in this regard belong to the author(s).

Statements or opinions expressed in the manuscripts published in European Journal of Biology reflect the views of the author(s) and not the opinions of the editors, the editorial board, or the publisher; the editors, the editorial board, and the publisher disclaim any responsibility or liability for such materials. The final responsibility in regard to the published content rests with the authors.

## MANUSCRIPT SUBMISSION

European Journal of Biology endorses ICMJE-Recommendations for the Conduct, Reporting, Editing, and Publication of Scholarly Work in Medical Journals (updated in December 2015 - <http://www.icmje.org/icmje-recommendations.pdf>). Authors are required to prepare manuscripts in accordance with the CONSORT guidelines for randomized research studies, STROBE guidelines for observational original research studies, STARD guidelines for studies on diagnostic accuracy, PRISMA guidelines for systematic reviews and meta-analysis, ARRIVE guidelines for experimental animal studies, TREND guidelines for non-randomized public behaviour, and COREQ guidelines for qualitative research.

Manuscripts can only be submitted through the journal's online manuscript submission and evaluation system, available at the journal's web page. Manuscripts submitted via any other medium will not be evaluated.

Manuscripts submitted to the journal will first go through



a technical evaluation process where the editorial office staff will ensure that the manuscript has been prepared and submitted in accordance with the journal's guidelines. Submissions that do not conform to the journal's guidelines will be returned to the submitting author with technical correction requests.

During the initial submission, authors are required to submit the following:

- Copyright Agreement Form,
- Author Contributions Form, and

ICMJE Potential Conflict of Interest Disclosure Form (should be filled in by all contributing authors). These forms are available for download at the journal's web page.

## Preparation of the Manuscript

Title page: A separate title page should be submitted with all submissions and this page should include:

- The full title of the manuscript as well as a short title (running head) of no more than 50 characters,
- Name(s), affiliations, and highest academic degree(s) of the author(s),
- Grant information and detailed information on the other sources of support,
- Name, address, telephone (including the mobile phone number) and fax numbers, and email address of the corresponding author,
- Acknowledgment of the individuals who contributed to the preparation of the manuscript but who do not fulfil the authorship criteria.

**Abstract:** Abstract with subheadings should be written as structured abstract in submitted papers except for Review Articles and Letters to the Editor. Please check Table 1 below for word count specifications (250 words).

**Keywords:** Each submission must be accompanied by a minimum of three to a maximum of six keywords for subject indexing at the end of the abstract. The keywords should be listed in full without abbreviations.

## Manuscript Types

**Original Articles:** This is the most important type of article since it provides new information based on original research. A structured abstract is required with original articles and it should include the following subheadings: Objective, Materials and Methods, Results and Conclu-

sion. The main text of original articles should be structured with Introduction, Materials and Methods, Results, Discussion, and Conclusion subheadings. Please check Table 1 for the limitations of Original Articles. Statistical analysis to support conclusions is usually necessary. Statistical analyses must be conducted in accordance with international statistical reporting standards. Information on statistical analyses should be provided with a separate subheading under the Materials and Methods section and the statistical software that was used during the process must be specified. Units should be prepared in accordance with the International System of Units (SI).

**Short Communications:** Short communication is for a concise, but independent report representing a significant contribution to Biology. Short communication is not intended to publish preliminary results. But if these results are of exceptional interest and are particularly topical and relevant will be considered for publication. Short Communications should include an abstract and should be structured with the following subheadings: "Introduction", "Materials and Methods", "Results and Discussion".

**Editorial Comments:** Editorial comments aim to provide a brief critical commentary by reviewers with expertise or with high reputation in the topic of the research article published in the journal. Authors are selected and invited by the journal to provide such comments. Abstract, Keywords, and Tables, Figures, Images, and other media are not included.

**Review Articles:** Reviews prepared by authors who have extensive knowledge on a particular field and whose scientific background has been translated into a high volume of publications with a high citation potential are welcomed. These authors may even be invited by the journal. Reviews should describe, discuss, and evaluate the current level of knowledge of a topic in clinical practice and should guide future studies. The main text should contain Introduction, Experimental and Clinical Research Consequences, and Conclusion sections. Please check Table 1 for the limitations for Review Articles.

**Letters to the Editor:** This type of manuscript discusses important parts, overlooked aspects, or lacking parts of a previously published article. Articles on subjects within the scope of the journal that might attract the readers' attention, particularly educative cases, may also be submitted in the form of a "Letter to the Editor." Readers can also present their comments on the published manuscripts in the form of a "Letter to the Editor." Abstract, Keywords, and Tables, Figures, Images, and other media should not be included. The text should be unstructured. The

manuscript that is being commented on must be properly cited within this manuscript.

### Tables

Tables should be included in the main document, presented after the reference list, and they should be numbered consecutively in the order they are referred to within the main text. A descriptive title must be placed above the tables. Abbreviations used in the tables should be defined below the tables by footnotes (even if they are defined within the main text). Tables should be created using the “insert table” command of the word processing software and they should be arranged clearly to provide easy reading. Data presented in the tables should not be a repetition of the data presented within the main text but should be supporting the main text.

### Figures and Figure Legends

Figures, graphics, and photographs should be submitted as separate files (in TIFF or JPEG format with 1200 dpi for graphic and 600 dpi for colour images) through the submission system. The files should not be embedded in a Word document or the main document. When there are figure subunits, the subunits should be labeled merged to form a single image. Each subunit should be submitted separately through the submission system. Images should be labeled (a, b, c, etc.) to indicate figure subunits.

Thick and thin arrows, arrowheads, stars, asterisks, and similar marks can be used on the images to support figure legends. Like the rest of the submission, the figures too should be blind. Any information within the images that may indicate an individual or institution should be blinded. The minimum resolution of each submitted figure should be 300 DPI. To prevent delays in the evaluation process, all submitted figures should be clear in resolution and large in size (minimum dimensions: 100 × 100 mm). Figure legends should be listed at the end of the main document.

All acronyms and abbreviations used in the manuscript should be defined at first use, both in the abstract and in the main text. The abbreviation should be provided in parentheses following the definition.

When a drug, chemical, product, hardware, or software program is mentioned within the main text, product information, including the name of the product, the producer of the product, and city and the country of the company (including the state if in USA), should be provided in parentheses in the following format: “Discovery St PET/CT scanner (General Electric, Milwaukee, WI, USA)”

All references, tables, and figures should be referred to within the main text, and they should be numbered consecutively in the order they are referred to within the main text.

Limitations, drawbacks, and the shortcomings of original articles should be mentioned in the Discussion section before the conclusion paragraph.

### References

European Journal of Biology uses the **AMA citation style**. In the paper, you are writing, materials are cited using superscript numerals. The first reference used in a written document is listed as 1 in the reference list, and a 1 is inserted into the document immediately next to the fact, concept, or quotation being cited. If the same reference is used multiple times in one document, use the same number to refer to it throughout the document.

### Example:

Finding treatments for breast cancer is a major goal for scientists.<sup>1,2</sup> Some classes of drugs show more promise than others. Gradishar evaluated taxanes as a class.<sup>3</sup> Other scientists have investigated individual drugs within this class, including Andre and Zielinski<sup>2</sup> and Joensuu and Gligorov.<sup>4</sup> Mita et al’s investigation of cabazitaxel<sup>5</sup> seems to indicate a new role for this class of drugs.

While citing publications, preference should be given to the latest, most up to date publications. If an ahead of print publication is cited, the DOI number should be provided. Authors are responsible for the accuracy of references. Journal titles should be abbreviated in accordance with the journal abbreviations in Index Medicus/ MEDLINE/PubMed. When there are six or fewer authors, all authors should be listed. If there are seven or more authors, the first six authors should be listed followed by “et al.”

At the end of the document, include a reference list with full citations to each item. The reference styles for different types of publications are presented in the following examples.

### Print journal article with six or fewer authors:

Kayalar O, Oztay F, Ongen HG. Gastrin-releasing peptide induces fibrotic response in MRC5s and proliferation in A549s. *Cell Commun Signal*. 2020;18(1):96-107.

Kazerouni NN, Currier RJ, Hodgkinson C, Goldman S, Lorey F, Roberson M. Ancillary benefits of prenatal maternal serum screening achieved in the California program. *Prenat Diagn*. 2010;30 (10):981-987.

**Table 1.** Limitations for each manuscript type

Type of manuscript	Word limit	Abstract word limit	Reference limit	Table limit	Figure limit
Original Article	4500	250 (Structured)	No limit	6	Maximum 10
Short Communication	2500	200	30	3	4
Review Article	5500	250	No limit	5	6
Letter to the Editor	500	No abstract	5	No tables	No media

**Print journal article with more than six authors:**

Baba Y, Yoshida N, Kinoshita K, et al. Clinical and prognostic features of patients with esophageal cancer and multiple primary cancers: A retrospective single-institution study. *Ann Surg.* 2018;267(3):478-483.

**Online journal article:**

Florez H, Martinez R, Chakra W, Strickman-Stein M, Levis S. Outdoor exercise reduces the risk of hypovitaminosis D in the obese. *J Steroid Biochem Mol Bio.* 2007;103(3-5):679-681. doi:10.1016/j.jsbmb.2006.12.032.

**Journal article with no named author or group name:**

Centers for Disease Control and Prevention (CDC). Li-censure of a meningococcal conjugate vaccine (Menveo) and guidance for use-Advisory Committee on Immunization Practices (ACIP), 2010. *MMWR Morb Mortal Wkly Rep.* 2010;59(9):273

**Book:**

Brownson RC. *Evidence-based Public Health.* 2nd ed. New York, N.Y.: Oxford University Press; 2011.

**Book Chapter:**

Guyton JL, Crockarell JR. Fractures of acetabulum and pelvis. In: Canale ST, ed. *Campbell's Operative Orthopaedics.* 10th ed. Philadelphia, PA: Mosby, Inc; 2003:2939-2984.

**Webpage:**

Fast facts. National Osteoporosis Foundation website. <http://www.nof.org/osteoporosis/diseasefacts.htm>. Accessed August 27, 2007.

**Official organization report published on a webpage:**

Office of Women's Health, California Department of Public Health. California Adolescent Health 2009. <http://www.cdph.ca.gov/pubsforms/Pubs/OWH-AdolHealthReport09.pdf>. Accessed January 5, 2011.

**Conference Proceedings:**

Fritz TC, Soni MG. Use of dietary supplements in sports drinks: Consumption and safety determinations for regulatory compliance. Poster presented at: *Annual International Society of Sports Nutrition Conference and Expo;* June 16-18, 2005; New Orleans, LA.

**Thesis**

Yildirim M. The determination of effective long non-coding RNA on human pulmonary fibrosis in an in vitro model. Istanbul University, Science Institute, Master Thesis, 2018.

**REVISIONS**

When submitting a revised version of a paper, the author must submit a detailed "Response to the reviewers" that states point by point how each issue raised by the reviewers has been covered and where it can be found (each reviewer's comment, followed by the author's reply and line numbers where the changes have been made) as well as an annotated copy of the main document. Revised manuscripts must be submitted within 30 days from the date of the decision letter. If the revised version of the manuscript is not submitted within the allocated time, the revision option may be cancelled. If the submitting author(s) believe that additional time is required, they should request this extension before the initial 30-day period is over. Accepted manuscripts are copy-edited for grammar, punctuation, and format. Once the publication process of a manuscript is completed, it is published online on the journal's webpage as an ahead-of-print publication before it is included in its scheduled issue. A PDF proof of the accepted manuscript is sent to the corresponding author and their publication approval is requested within 2 days of their receipt of the proof.

**Editor in Chief:** Prof. Dr. Sehnaz BOLKENT

**Address:** Istanbul University, Faculty of Science, Department of Biology,

34134 Vezneciler, Fatih, Istanbul, Turkiye

**Phone:** +90 212 4555700 (Ext. 20318)

**Fax:** +90 212 5280527

**E-mail:** [sbolkent@istanbul.edu.tr](mailto:sbolkent@istanbul.edu.tr)

## CONTENTS

---

### RESEARCH ARTICLES

- 1 *In Silico* Approach for Identification of PI3K/mTOR Dual Inhibitors for Multiple Myeloma Treatment  
**Ilke Masalaci, Yaren Akdogan, Ozge Mutlu, Hande Eyvaz, Yagmur Kiraz**
- 12 Effects of Salicylic Acid and Microorganisms on Morphological and Physiological Characteristics (*Satureja hortensis* L.) under Drought Stress  
**Mahmood Ghojavand, Porang Kasraei, Hamid Reza Tohidi Moghadam, Mohammad Nasri, Hamid Reza Larijani**
- 23 Evaluation of Oxidative Protein Damage in Patients with Type 1 and 2 Diabetes Mellitus in Bangladesh  
**Sanjeda Tamanna, Rocky Sheikh, Taslimul Jannat, Laila Noor Islam**
- 31 Morphological and Biochemical Investigation of the Protective Effects of *Panax ginseng* on Methotrexate-Induced Testicular Damage  
**Fatma Bedia Karakaya-Cimen, Caglar Macit, Guzin Goksun Sivas, Tugba Tunali Akbay, Goksel Sener, Feriha Ercan**
- 38 Anti-Bacterial, Anti-Mycobacterial and Anti-Fungal Properties of *Punica granatum* as Natural Dye  
**Pinar Guner, Tulin Askun**
- 49 The Senescence Program is Reduced in Proteasome Inhibitor Bortezomib-Resistant PC3 Prostate Cancer Cell Line  
**Ertan Kanbur, Semih Seker, Ferah Budak, Azmi Yerlikaya**
- 59 Morphological and Molecular Identification of *Trichoderma* Isolates Used as Biocontrol Agents by DNA Barcoding  
**Yuksel Gezgin, Gulce Guralp, Ayse Bercin Barlas, Rengin Eltem**
- 70 Screening of Antibiotics Biodegradability from Wastewater  
**Saim Souhila, Mokrani Slimane, Isabel Martínez-Alcalá, Ramazan Erenler**

### REVIEW ARTICLES

- 86 The Use of Plant Steroids in Viral Disease Treatments: Current Status and Future Perspectives  
**Pinar Obakan Yerlikaya, Elif Damla Arisan, Leila Mehdizadehtapeh, Pinar Uysal-Onganer, Ajda Coker-Gurkan**
- 95 The Role of Akt Signalling Pathway in Neurological and Cardiovascular Pathologies  
**Akshat D. Modi, Aahmad Ali Mahoon, Dharmeshkumar M. Modi**
- 109 Impact of Toxic Heavy Metals and Their Concentration in *Zygophyllum* Species, *Mentha longifolia*, and *Thymus vulgaris* Traditional Medicinal Plants Consumed in Setif-Algeria  
**Meriem Djarmouni, Ilham Sekia, Djamila Ameni, Tassadit Ikessoulen, Abderrahmane Baghiani**

# *In Silico* Approach for Identification of PI3K/mTOR Dual Inhibitors for Multiple Myeloma Treatment

Ilke Masalaci<sup>1</sup>,  Yaren Akdogan<sup>1</sup>,  Ozge Mutlu<sup>1</sup>,  Hande Eyvaz<sup>1</sup>,  Yagmur Kiraz<sup>1</sup> 

<sup>1</sup>Izmir University of Economics, Faculty of Engineering, Department of Genetics and Bioengineering, Izmir, Turkiye

## ABSTRACT

**Objective:** Multiple myeloma is a hematologic malignancy in which targeting phosphoinositide 3 kinase (PI3K) and/or the mammalian target of rapamycin (mTOR) individually has been shown to have anti-proliferative effects, however, inhibiting both proteins simultaneously has been reported to have more effective results for its treatment. The aim of this study is to determine the molecular interactions and predicted inhibitory effects of 40 different dual inhibitors on mTOR, PI3K $\delta$ , and PI3K $\gamma$  to propose potentially the most effective dual inhibitor that targets the PI3K $\delta$  and PI3K $\gamma$  isoforms as well as the mTOR proteins since those isoforms are known to be predominant in multiple myeloma patients. Therefore, the focus in this study is built around the specific targeting of the PI3K $\delta$  and PI3K $\gamma$  isoforms from the multiple myeloma perspective.

**Materials and Methods:** *In silico* docking experiments were conducted to determine the binding energies for different ligands that target mTOR, PI3K $\delta$ , and PI3K $\gamma$ . Protein-dual inhibitor complexes and the amino acids and bond types were visualized to identify molecular interactions. The absorption, distribution, metabolism, and excretion properties of dual inhibitors were analyzed and evaluated.

**Results:** The binding affinity values were found to be between -7 and -9.9 kcal/mol. The toxicity prediction values of the selected dual inhibitors were obtained from the Pro-Tox-II web tool and classified according to the globally harmonized system of classification of labeling of chemicals.

**Conclusion:** Correspondingly, among all dual inhibitors, Vistusertib is determined to be a promising compound against multiple myeloma cells by inhibiting both PI3K $\delta$  and PI3K $\gamma$  as well as mTORC1/2.

**Keywords:** *In silico* search, docking, dual inhibition, PI3K/mTOR pathway

## INTRODUCTION

Phosphatidylinositol 3-kinases (PI3Ks) are a type of lipid kinases which are responsible for the regulation of various cellular activities. The PI3K pathway is important in cancer proliferation and one of the most promising therapeutic targets due to its activities over other downstream effectors such as Akt serine-threonine kinase (Akt) and mTOR (mammalian target of rapamycin).<sup>1</sup> Multiple PI3K isoforms are found, which can be classified into three groups based on structural similarity, substrate selectivity, and regulatory mechanism. Class I PI3Ks are the isoforms which significantly contributes to driving oncogenesis and are split into two classes as receptor tyrosine kinases activated Class IAs and GPCR activated Class IBs.<sup>2</sup>

mTORC1 and mTORC2 are two multiprotein mTOR complexes made up of separate proteins and partners. Abnormal activation of the mTOR signaling pathway has been commonly

observed in many cancers. As a result, it's gotten a lot of attention as a potential target for oncology drug discovery.

Targeting both PI3K and mTOR has been the most common approach to dual inhibition, by taking advantage of structural similarities between the catalytic site of mTOR and ATP-binding domain of p110.<sup>2</sup> The PI3K/Akt/mTOR is one of the hub pathways in multiple myeloma (MM) because it is abnormally activated in a significant portion of MM patients. mTOR is an Akt downstream target that is important in MM progression, proliferation and gene and protein synthesis. Because the PI3K/Akt/mTOR pathway is a large signaling network and engaged with other pathways, inhibiting an upstream element such as Akt or mTOR may not be sufficient to inhibit downstream effectors.<sup>3,4</sup> Targeting two critical sites of the same pathway can result in more efficacy, overcome feedback inhibition caused by blocking mTOR activity, and reduce the possibility of the generation of chemoresistance that would emerge if

**Corresponding Author:** Yağmur Kiraz E-mail: yagmur.kiraz@ieu.edu.tr

Submitted: 21.09.2022 • Revision Requested: 28.11.2022 • Last Revision Received: 16.03.2023 • Accepted: 17.03.2023



This article is licensed under a Creative Commons Attribution-NonCommercial 4.0 International License (CC BY-NC 4.0)

only one p110 isoform was targeted. Indeed, dual PI3K/mTOR inhibitors have performed better than targeting PI3K isoform inhibitors, all PI3K isoform inhibitors, and mTOR inhibitors in the preclinical context.<sup>5</sup>

MM is a heterogeneous disease that complicates the diagnosis and detection of the molecular origin of the disease. In MM progression, naive B cells, before they get fully developed into plasma cells, proliferate in an uncontrolled manner and over-produce antibodies.<sup>6,7</sup> Although the mortality of the disease has decreased with newer strategies, more effective treatments are still needed in order to reach higher survival rates.<sup>8</sup>

Proteasome inhibitors have been used to treat cancer for over 20 years. Bortezomib (Velcade, PS-341) is a proteasome inhibitor that was approved first for multiple myeloma treatment which advanced quickly from bench to initial approval in 2003. It is approved for the use as a first-line treatment as well as in patients who have relapsed or are resistant to prior therapies. Bortezomib causes immunogenic stress and cell death in multiple myeloma cells; which is the mechanism of its therapeutic efficacy.<sup>9</sup> Although Bortezomib was a significant advancement in the treatment of multiple myeloma, about 20% of individuals have primary resistance, and a lot of patients relapsed after using it alone or in combination, which results in a lack of response to treatment.<sup>10-12</sup> Using data from prior research, the combination therapy of Bortezomib has been demonstrated to be promising. In the combined treatments of Bortezomib, Gedatolisib, Omipalisib and Dactolisib, Panulisib and Vistusertib have been investigated with very promising results in preclinical leukemia models, including acute lymphoblastic leukemia (ALL) and acute myeloid leukemia (AML).<sup>12-15</sup>

There is a continuously growing need to discover novel dual PI3K/mTOR inhibitors to be developed into therapeutic possibilities for cancer treatment. The demand for new dual inhibitors of PI3K/mTOR to be converted into therapeutic options for cancer therapy is constantly growing.

The objective in this study is to search for the most potent suitable dual inhibitor that would target mTOR and PI3K isoforms PI3K $\delta$ , and PI3K $\gamma$  since those two isoforms have been detected in multiple myeloma patients. Although there are generic dual inhibitors against PI3K and mTOR, the main goal here is to potentially identify the most effective inhibitor that could be proposed to use for multiple myeloma treatment.

This study is organized into two main parts: theoretical and *in silico* experimental to achieve potentially the most promising candidate to be proposed for therapeutic purposes. The theoretical section gives a quick rundown of the most recent scientific results. The second part, the experimental component, is devoted to a holistic view and comparative analysis of the aforesaid dual inhibitors in PI3K/mTOR inhibitors for multiple myeloma treatment utilizing *in silico* methodologies starting with docking. In addition, *in silico* the absorption, distribution, metabolism, and excretion (ADME) parameters, physicochemical descriptors,

lipophilicity, solubility, pharmacokinetic properties, drug-like nature, and suitability for medicinal chemistry were examined using the SwissADME online tool to predict dual inhibitor compatibility and behavior, while toxicity was investigated using the ProTox II web server. These preliminary results, which provide pharmacological information, are indicative of designing and developing new treatment agents. Acute toxicity, cytotoxicity, hepatotoxicity, mutagenicity, immunotoxicity, carcinogenicity, adverse outcomes pathways, and toxicity targets of the candidate chemicals were predicted with Pro-Tox-II according to molecular similarity, fragment propensities, pharmacophores, and machine-learning models. The PyRx software was used for insertion experiments for the target proteins PI3K $\delta$  and PI3K $\gamma$ , and mTOR, whereas Discovery Studio (Accelrys, San Diego, CA), a powerful simulation tool, was employed for imaging. The hypothesis in the project had the possibility to be successfully analyzed in numerous ways with the help of these tools.<sup>16</sup>

## MATERIALS AND METHODS

### Compound Selection and Preparation

The identified compounds were downloaded in SDF format for 40 dual inhibitors with 3-dimensional structure as well as their CAS numbers in the PubChem database. All of the compounds were used as dual inhibitors and had a 3D structure. 40 dual inhibitors that target PI3K delta and gamma isoforms and mTOR were selected according to literature (Table 1).<sup>12</sup> ArgusLab was used to remove bound ligands and water molecules, insert hydrogen atoms, merge non-polar hydrogens, and Gasteiger charges were included to prepare the structure of the protein for docking.<sup>17</sup>

### Docking Studies

Molecular docking was conducted to calculate the ligand library's binding energy in PI3K isoform proteins and mTOR. 3D macromolecular structures of the mammalian target of rapamycin (mTOR) (PDB ID: 4JT6), phosphoinositide 3 kinase delta (PI3K $\delta$ ) (PDB ID: 4GB9) and phosphoinositide 3 kinase gamma (PI3K $\gamma$ ) (PDB ID: 6C1S) were obtained from Protein Data Bank (www.pdb.org) which is an online database used to search for molecule structures as pdb format. In the protein preparation step, all crystallographic water molecules are removed unless they are known to be tightly bound to the protein.<sup>18</sup> *In silico* docking calculations were performed with the PyRx (PyRx-Python Prescription 0.8) software's AutoDock Vina option which is open-source software for computer-aided drug design. Energy minimization was performed for the loaded proteins, which is essential for determining the appropriate molecular arrangement in space. Initially, the active sites to which the proteins will bind to the ligand were determined. A 25-angstrom grid box was defined for the X, Y, and Z dimen-

**Table 1.** PIK3/mTOR dual pathway.

Ligand	Target	Ligand	Target
Dactolisib	PI3K ( $\alpha$ , $\beta$ , $\gamma$ + $\delta$ ) + mTOR	TORKinib	mTOR
Omipalisib	PI3K ( $\alpha$ , $\beta$ , $\gamma$ + $\delta$ ) + mTOR	Copanlisib	PI3K ( $\alpha$ , $\delta$ )
Duvelisib	PI3K ( $\delta$ , $\gamma$ )	PQR-530	PI3K ( $\alpha$ , $\beta$ , $\gamma$ + $\delta$ ) + mTOR
MK-2206	AKT 1,2+3	Bimiralisib	PI3K ( $\alpha$ , $\beta$ , $\gamma$ + $\delta$ ) + mTOR
Miransertib	AKT 1,2+3	Onatasertib	PI3K $\alpha$ + mTOR
Pictilisib	PI3K ( $\alpha$ , $\beta$ , $\gamma$ + $\delta$ )	Gdc 0084	PI3K ( $\alpha$ , $\beta$ , $\gamma$ + $\delta$ ) + mTOR
Pilaralisib	PI3K ( $\alpha$ , $\beta$ + $\delta$ )	GSK-2636771	PI3K $\beta$
PKI-402	PI3K $\alpha$ + mTOR	PF-04691502	PI3K ( $\alpha$ , $\beta$ , $\gamma$ + $\delta$ )
Gedatolisib	PI3K ( $\alpha$ + $\gamma$ ) + mTOR	AZD 8186	PI3K $\beta$
Vistusertib	PI3K ( $\alpha$ , $\beta$ , $\gamma$ + $\delta$ ) + mTOR	Uprosertib	AKT 1,2+3
Taselisib	PI3K ( $\alpha$ , $\gamma$ + $\delta$ )	PKI 179	PI3K ( $\alpha$ , $\beta$ , $\gamma$ + $\delta$ ) + mTOR
Alpelisib	PI3K $\alpha$	SN-32976	PI3K ( $\alpha$ , $\beta$ , $\gamma$ + $\delta$ ) + mTOR
Panulisib	PI3K + mTOR	PWT-33597	PI3K $\alpha$ + mTOR
BGT-226	PI3K ( $\alpha$ , $\beta$ , $\gamma$ + $\delta$ ) + mTOR	Buparlisib	PI3K ( $\alpha$ , $\beta$ , $\gamma$ + $\delta$ )
Fimepinostat	PI3K ( $\alpha$ , $\beta$ , $\delta$ )	VS-5584	PI3K ( $\alpha$ , $\beta$ , $\gamma$ + $\delta$ ) + mTOR
Apitolisib	PI3K ( $\alpha$ , $\beta$ , $\gamma$ + $\delta$ ) + mTOR	Sapanisertib	PI3K ( $\alpha$ , $\gamma$ + $\delta$ ) + mTOR
Ipatasertib	AKT 1,2+3	Voxtalisib	PI3K (mostly $\gamma$ ) + mTOR
PI-103	PI3K ( $\alpha$ , $\beta$ , $\gamma$ + $\delta$ ) + mTOR	GNE-477	PI3K $\alpha$ + mTOR
LY 294002	PI3K ( $\alpha$ , $\beta$ + $\delta$ )	Capivasertib	AKT 1,2+3
Samatolisib	class I PI3K isoforms + mTOR	PF-04979064	PI3K ( $\alpha$ , $\gamma$ + $\delta$ ) + mTOR

sions. The refined low-energy structures of the proteins were coupled with each ligand. The binding affinities of the proteins were then calculated. Significant identifiers and relevant pharmaceutical properties were predicted for the compounds.

### *In silico* ADME and Toxicity Screening Predictions

A drug candidate must be measurably effective in order to be approved. The candidate molecule has to have an adequate concentration when it reaches its target in the body and stays there actively so that it can actually do the work it is assigned to. The approach to the development of the drug involves ADME. The molecules were analyzed and evaluated with the SwissADME web tool according to their physicochemical properties, pharmacokinetics, lipophilicity, water-solubility, drug-likeness, and medicinal chemistry.<sup>19</sup> The prediction of the toxicity of the compounds is performed in the Pro-Tox-II web tool. Pro-Tox-II offers data on molecular similarity, fragment propensities, frequently observed features, and machine learning, based on a total of 33 models, for the prediction of various toxicity endpoints, including acute toxicity, hepatotoxicity, cytotoxicity, carcinogenicity, mutagenicity, immunotoxicity, adverse outcomes (Tox21) pathways, and toxicity targets. Toxicity classes are classified in 6 levels, all defined by a globally accepted system of classification of labeling of chemicals (GHS).<sup>20</sup>

### Visualizing Protein-Ligand Complexes

mTOR (PDB ID: 4JT6), PI3K $\delta$  (PDB ID: 4GB9), PI3K $\gamma$  (PDB ID: 6C1S) proteins and ligand (Dactolisib, Gedatolisib, Panulisib, Pki-179, Omipalisib, Vistusertib) complexes were visualized with Discovery Studio. As an outcome of the docking combination of three proteins and six ligands, a total of 18 samples were accessible in Discovery Studio. The 2D Show of each of the 18 samples revealed amino acid interactions between the protein structures and ligands.

## RESULTS

### Docking Calculations

A library of 40 dual inhibitors was docked with selected PI3K $\delta$ , PI3K $\gamma$  and mTOR proteins and their binding affinities with one another were obtained in order to select the best possible drug candidate in a way where previous literature is conducted upon.<sup>21</sup> The first 16 ligands with binding values of -7 kcal/mol and lower (down to -9.9) were selected, while significant interactions were found to ensure the highest binding affinity and efficiency. This selection adjusted the number of ligands used for further analysis. The results of the molecular docking experiments were represented as binding affinities of the evaluated

**Table 2.** Ligand-protein binding energies of selected 16 ligand molecules and 3 identified target proteins.

Ligand	Binding Affinity with PI3K $\gamma$ (kcal/mol)	Binding Affinity with PI3K $\delta$ (kcal/mol)	Binding Affinity with mTOR (kcal/mol)
Dactolisib	-9.9	-9.8	-9.5
Omipalisib	-9.4	-7.7	-9.7
Duvelisib	-8.5	-7.7	-9.1
MK-2206	-8.6	-7.5	-8.6
Miransertib	-8.3	-8.9	-9.2
Pictilisib	-8.3	-7	-8.9
Pilaralisib	-8.4	-8.1	-9.2
PKI-402	-8.8	-7.5	-9.5
Gedatolisib	-8.3	-8	-9.9
Vistusertib	-8.4	-7.7	-9.3
Taselisib	-8.2	-7.2	-8.8
PKI-179	-8.8	-7.6	-9.7
Panulisib	-9.8	-9.4	-9.1
BGT-226	-8.8	-7.8	-8.9
Fimepinostat	-8.7	-7.4	-8.3
Apitolisib	-8.5	-7.3	-9.3

ligands on mTOR, PI3K $\delta$ , and PI3K $\gamma$ , and are listed in Table 2. Results reported as mean square deviation (RMSD) lower bound and upper bound values were used to compare displacement and conformational changes, based on results with the highest conformation (0 Angstrom). Also, aspirin, which is not known to be a compound that targets PI3K $\delta$ , PI3K $\gamma$  or mTOR, was selected as a negative control and molecular docking results have been presented in Table 1.

### ***In silico* ADME and Toxicity Screening Predictions**

The canonical SMILES formats of the formerly selected 16 dual inhibitors, according to the results of the dockings, were listed on the online tool of SwissADME. *In silico* physicochemical properties and predictions have to be checked in order for a drug to be investigated efficiently. Properties such as molecular weight, number of heavy atoms, Fraction Csp3, number of aromatic heavy atoms, number of rotatable bonds, number of H-bond acceptors, number of H-bond donors, molar refractivity, and TPSA (Topological Polar Surface Area), and lipophilicity provide information of log Po/w values and help to determine the access of a potential drug. Water solubility, the pharmacokinetics of the compounds according to GI absorption, BBB permanent, P-gp substrate, CYP inhibitors (CYP1A2, CYP2C19,

CYP2C9, CYP2D6, and CYP3A4), log Kp (skin permeation) were analyzed while drug-likeness was scored with respect to Lipinski, Ghose, Veber, Egan, Muegge filters\* and the bioavailability score of the compound (Tables 3 and 4). Medicinal chemistry properties such as lead-likeness and synthetic accessibility are also checked to investigate how difficult it is for drug candidates' molecular fragments to be obtained with also the relationship of the molecules' synthesis taken into consideration. The Egan BOILED-Egg (Brain or IntestinaL EstimateD) permeation predictive model diagram is used for the visualization of the 16 dual inhibitors as in vivo prediction as well as passive human gastrointestinal absorption, blood-brain barrier permeation, and the presence or absence of P-glycoprotein parameters are checked (Figure 1). The molecules represented in the BOILED-Egg model predicted that 10 of the selected compounds can be passively absorbed by the gastrointestinal tract while 6 of the further selected molecules are not expected to be absorbed by the gastrointestinal tract or permeated through the blood brain barrier (Figure 1).<sup>22</sup>

The elimination of the dual inhibitors was conducted with respect to the drug-likeness filters. There are several expert criteria that are used in drug design for how "drug-like" a substance is with respect to factors like bioavailability, such as Lipinski, Ghose, Veber, and Egan rules, etc. While 5 filters



**Table 3.** Selected physicochemical and pharmacokinetic properties of the analyzed compounds.

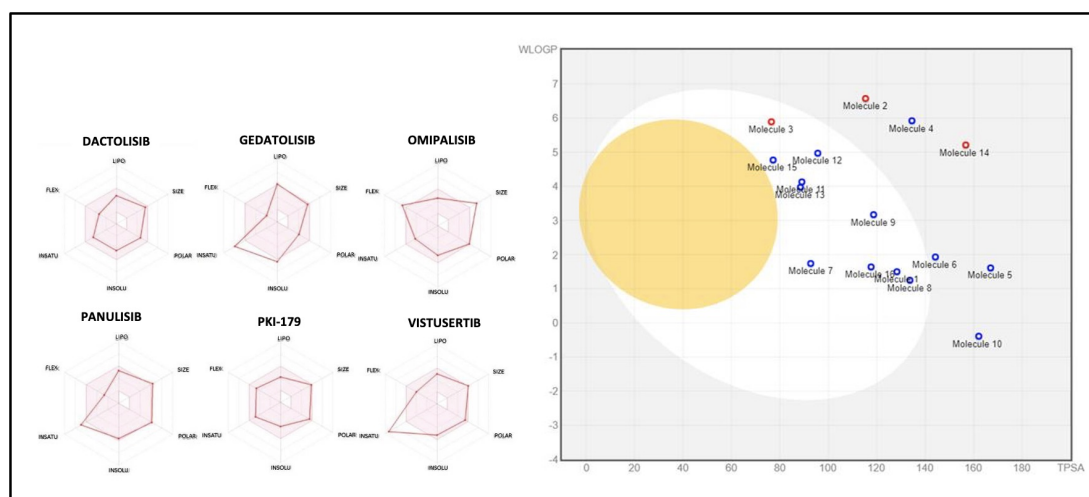
Chemical-Physical Properties									
Compound	Heavy atoms	Aromatic heavy atoms	Fraction Csp3	Rotatable bonds	H-bond acceptors	H-bond donors	MW (g/mol)	MR	TPSA
Gedatolisib	45	18	0.47	10	8	2	615.73	182.07	128.29
Omipalisib	36	28	0.04	6	9	1	505.5	129.52	115.34
Dactolisib	36	29	0.13	3	4	0	469.54	143.88	76.5
Panulisib	39	25	0.19	4	9	1	527.5	138.46	134.49
Vistusertib	34	16	0.44	5	6	1	462.54	136.83	92.71
PKI-179	36	18	0.4	7	7	2	488.54	140.73	117.63
Pharmacokinetic									
Compound	GI	BBB	P-gp substrate	CYP1A2	CYP2C19	CYP2C9	CYP2D6	CYP3A4	Log Kp (cm/s)
Gedatolisib	High	No	Yes	No	No	Yes	Yes	Yes	-8.34
Omipalisib	Low	No	No	No	No	Yes	Yes	Yes	-7.03
Dactolisib	High	No	No	No	Yes	Yes	No	No	-5.43
Panulisib	Low	No	Yes	No	No	Yes	No	No	-6.87
Vistusertib	High	No	Yes	No	No	Yes	Yes	Yes	-7.15
PKI-179	High	No	Yes	No	No	Yes	Yes	Yes	-7.92

**Table 4.** Drug-likeness predictions of the analyzed compounds.

Drug-likeness						
Compound	Lipinski # violations	Ghose # violations	Veber # violations	Egan # violations	Muegge # violations	Bioavailability score
Gedatolisib	2	3	0	0	1	0.17
Omipalisib	1	2	0	1	0	0.55
Dactolisib	0	2	0	1	1	0.55
Panulisib	1	3	0	2	0	0.55
Vistusertib	0	1	0	0	0	0.55
PKI-179	1	2	0	0	0	0.55
Medicinal Chemistry						
Compound	PAINS	Brenk	Leadlikeness	Synthetic Accessibility		
Gedatolisib	0	0	2	4.65		
Omipalisib	0	0	1	3.57		
Dactolisib	0	0	2	3.39		
Panulisib	0	1	2	3.93		
Vistusertib	0	0	1	4.4		
PKI-179	0	0	1	4.95		

were identified according to the values of molecular weight, Log P, number of H-bond donors, and number of H-bond acceptors, the ones that violated the rules could not serve as a great candidate. Therefore, while deciding on the most proper dual inhibitor for this study, the number of violations of the Lipinski, Ghose, Veber, Egan, and Muegge rules are evaluated as well as bioavailability scores and synthetic accessibility are decided to be chosen as parameters. After the dual inhibitors' ADME results were obtained and analyzed, 6 dual inhibitors were found to be the most effective among the 16, which are Omipalisib, Vistusertib, Panulisib, Gedatolisib, PKI-179 and Dactolisib (Figure 2). After ADME *in vivo* predictions, the toxicity of the possible drugs was analyzed. Toxicity estimates, shown as inactive (green) and/or active (red), also help decide

which dual inhibitor would be most beneficial to use and classify drug candidates according to lethal doses. The predicted LD50 values, the predicted toxicity classes, average similarity, and prediction accuracy of the dual inhibitors were evaluated as well as the radar chart that analyzes the probabilities for activity. From the data, it was obtained that Omipalisib and Panulisib were predicted to be active for hepatotoxicity, immunotoxicity, hepatotoxicity, carcinogenicity, and cytotoxicity respectively. For this reason, the candidate dual inhibitor number decreased to 4. While deciding on one dual inhibitor only, the data obtained both from ADME and toxicity were evaluated in combination, and Vistusertib was decided to be the most promising for the inhibition of PI3K $\delta$ , PI3K $\gamma$ , and mTOR complexes in multiple myeloma treatment.



**Figure 1.** (A) Bioavailability radar (pink area exhibits optimal range of particular property) for studied compounds [LIPO lipophilicity as in XLOGP3; SIZE indicates size as molecular weight; POLAR means polarity as TPSA (topological polar surface area); INSOLU is insolubility in water by log S scale; INSATU means insaturation as per fraction of carbons in the sp<sup>3</sup> hybridization and FLEX indicates the flexibility as per rotatable bonds]. (B) Egan-BOILED-Egg model of the candidate dual inhibitors. The molecules represented as circles located in the yellow region (yolk) is the ones to be expected to passively permeated through blood-brain barrier (BBB), on the other hand, other molecules within the white region are the molecules predicted to be passively absorbed by the gastrointestinal tract (HIA). [To estimate the toxicity of the candidate compounds, the Pro-Tox-II web server is used, which classifies the chemicals according to the LD50 (the median lethal dose) values [mg/kg], Class I being the fatal dose ( $LD50 \leq 5$ ) and Class VI being the non-toxic ( $LD50 > 5000$ ). By selecting additional models to predict, Organ toxicity (Hepatotoxicity), Toxicity endpoints (Carcinogenicity, Immunotoxicity, Mutagenicity, Cytotoxicity), Tox21 Nuclear receptor signaling pathways (Aryl hydrocarbon Receptor (AhR), Androgen Receptor (AR), Androgen Receptor Ligand Binding Domain (AR-LBD), Aromatase, Estrogen Receptor Alpha (ER), Estrogen Receptor Ligand Binding Domain (ER-LBD), Peroxisome Proliferator-Activated Receptor Gamma (PPAR-Gamma)) and Tox21 Stress response pathways (Nuclear factor (erythroid-derived 2)-like 2/antioxidant responsive element (nrf2/ARE), Heat shock factor response element (HSE), Mitochondrial Membrane Potential (MMP), Phosphoprotein (Tumor Suppressor) p53, ATPase family AAA domain-containing protein 5 (ATAD5)) can be further computed.

### Amino Acid Interactions Between Indicated Protein-Ligand Complexes

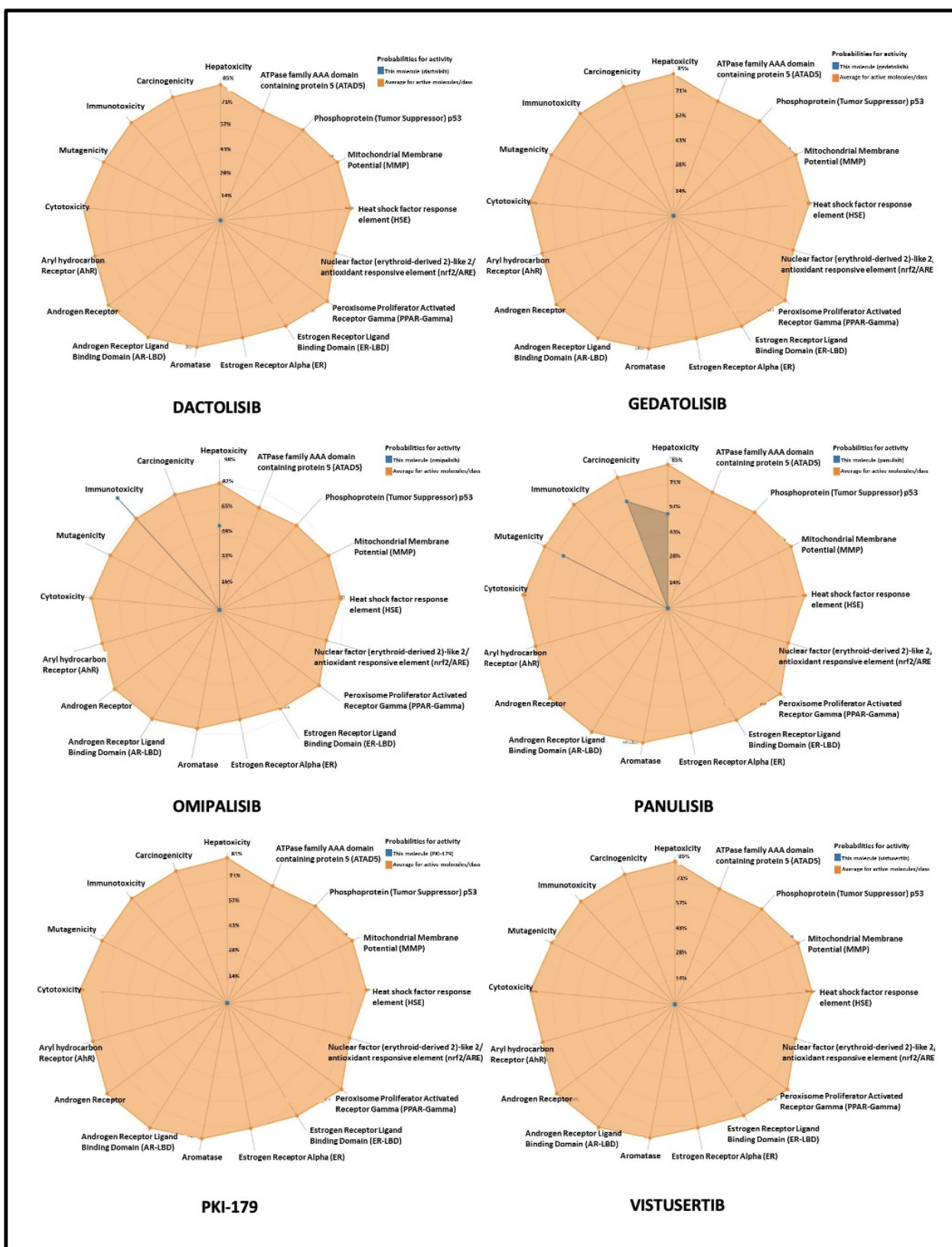
Ligand-protein complexes were categorized according to their amino acid interactions. Hydrogen bonds count, interactions in the amino acids with the ligands, hydrophobic amino acids that include the interactions in the complexes were determined. Discovery Studio 2D shows that Vistusertib is positioned at 2423 of the TYR, with a single hydrogen bond only to the 4JT6 protein in Supplementary Table 2. Omipalisib ligand appears to be located at LYS 890, LYS 756, SER 806, and VAL 882 with 4 hydrogen bonds to the 4GB9 protein and 2 hydrogen bonds to the 6C1S protein at LYS 833 and TYR 867, as shown in Table 2. As seen, the Dactolisib ligand appears to be positioned at TYR 1776, with a single hydrogen bond to the 4JT6 protein. The Panulisib ligand has been observed to be located in GLN 2499 and ILE 2498 with 2 hydrogen bonds to 4JT6 protein, 2 hydrogen bonds to 4GB9 protein in TYR 867, and LYS 833, 2 hydrogen bonds to 6C1S protein in TYR 867 and ASP 964. It has been observed that the Gedatolisib ligand is located in GLN 1901, GLU 1799, and ARG 1905 with 3 hydrogen bonds to the 4JT6 protein, in LYS 890 with a single hydrogen bond to the 4GB9 protein, and in ALA 805 with a single hydrogen bond to the 6C1S protein. PKI-179 possesses four hydrogen bonds in its ligand to the 4GB9 protein in LYS 890, MET 804, LYS 833 and ASP 964, and three hydrogen bonds to the 6C1S protein in ASP 950, ASP 964, and LYS 890. The Discovery Studio's

visualization tool showed any amino acid residues implicated in hydrophobic interactions in addition to the formation of hydrogen bonds between ligands and proteins (Figure 3). Table 3 lists the amino acid residues that reacted with the ligand.

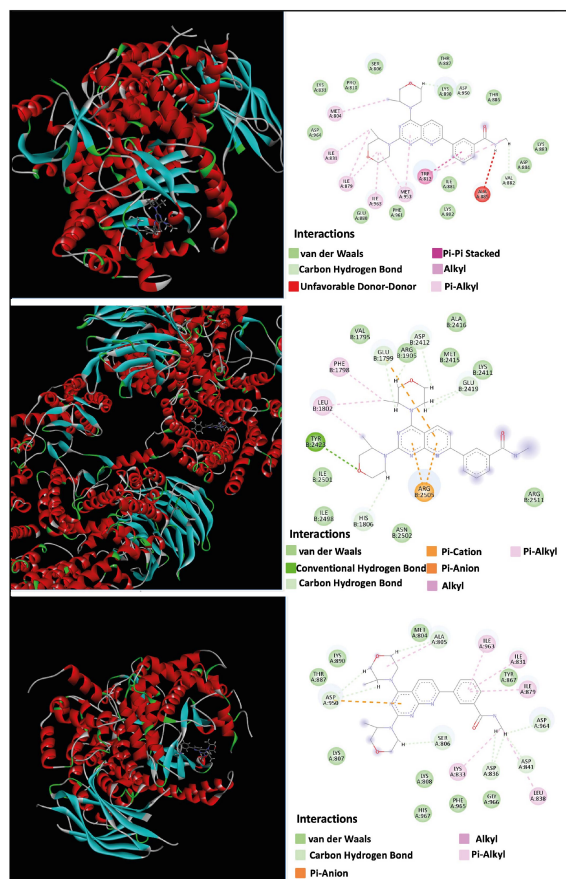
### DISCUSSION

Many cancers, including different types of leukemia, lymphoma, and multiple myeloma, are known to have dysregulation of the PI3K/Akt signaling pathway. Overactivation of PI3K/Akt results in chemoresistance and poor outcomes, whereas knocking down PI3K or Akt results in cancer cell death. As a result, the PI3K/Akt pathway has been regarded as a promising candidate to be used in cancer treatment since its inhibition was shown to trigger apoptosis in MM cells. Therefore, many PI3K/Akt signaling pathway inhibitors, such as CAL-101, NVP-BKM120, and Perifosine, have been developed and tried as treatment agents for MM and are in the ongoing clinical trials. However, there still is a high demand for new PI3K inhibitors to be developed with more potent and efficient effects.<sup>23</sup>

The PI3K/Akt/mTOR pathway is a key regulator of various cancer cell activities including their survival, proliferation and drug resistance. The route is especially critical for lymphoma cells, and blocking it with drugs has demonstrated to be beneficial to patients with various lymphoproliferative neoplasms.<sup>12</sup> Many intracellular and extracellular myeloma



**Figure 2.** ProTox radar plots for selected 6 compounds. ProTox-II classification is represented in the scheme; as orange dots/lines show the average probability of the compound's active class, acquired by computing from the trained model.



**Figure 3.** 2D representation of intermolecular interactions depicted using Discovery Studio Visualizer (A) 4GB9 protein with Vistusertib, (B) 4JT6 protein with Vistusertib, (C) 6C1S protein with Vistusertib. Dashed lines represent the different interactions and line color represents the interaction type. Amino acid residue numbers are shown in colored circles with their three letter code.

growth cytokines activate the PI3K/Akt pathway, concluding the probability that inhibiting PI3K will improve anti myeloma effects even further.<sup>24</sup>

Among the different classes of PI3K, Class I PI3Ks are the only ones shown to be correlated with cancer, and no confirmed study was found that shows the involvement of Class II PI3Ks or Class III PI3K (Vsp34p) in cancer progression. Class I PI3K is a dimeric formed enzyme, together with one catalytic and one regulatory subunit. The catalytic subunit is formed and can be found in four different isoforms designated as p110 $\alpha$ , p110 $\beta$ , p110 $\gamma$ , and p110 $\delta$ . It is thought to be related to the fact that PIP2 is used to generate PIP3, and PIP3 is a molecule that is shown to have a role in cell growth and cell replication, which only Class I PI3K can achieve. This molecule has the ability to confer tumorigenic capacity to lipid kinase. p110 $\gamma$  and p110 $\delta$  are leukocyte-specific, and their genetic inactivation leads to defective immune responses. Constant overexpression of p110 $\delta$  has been detected in acute myeloblastic leukemia, and p110 $\delta$  inhibitors prevent the proliferation of leukemic cells, suggesting

the role of p110 $\delta$  as an oncoprotein. Also in different studies, increased expression levels of p110 $\gamma$  were shown in chronic myeloid leukemia.<sup>25</sup>

The involvement of p110 $\delta$  and p110 $\gamma$  in hematological malignancies and cellular signaling has been shown to be important especially for studying the inhibitors targeting these two isoforms simultaneously, which turned to be a success and led to clinical trials for B- and T-cell lymphomas. In a study, p110 $\gamma$  inhibition was shown to inhibit myeloid cell migration into the tumor area which results in decreased malignancy through being able to target tumor microenvironment. Another study pointed that inhibition of p110 $\delta$  suppressed tumor progression by interfering regulatory T-cell mediated immune response. These findings indicate novel approaches for targeting p110 $\delta$  or p110 $\gamma$  selectively could be discussed as new treatment options in cancer.<sup>26</sup> In the light of these studies, it is thought that inhibiting both isoforms PI3K $\delta$  and PI3K $\gamma$ , as well as mTOR complexes, might lead to a significant inactivation of the tumor cells' irrepressible proliferation. This is why, in this study, a dual inhibitor that targets these proteins is decided to be used against multiple myeloma cell lines.

PI3K activation is induced by IL-6 and many other cytokines and growth factors, which activates Akt and consequently mTOR. Akt signaling activation is assumed to be responsible for MM cell survival and proliferation. mTOR activation in MM has a reducing effect on apoptosis in myeloma cells.<sup>24</sup> Thus, it can be deduced that both PI3K and mTOR are suitable targets in MM. Here, we describe the prominent inhibitors when describing PI3K/mTOR dual inhibitors for multiple myeloma treatment.<sup>27</sup>

Molecular docking data of the 40 best-known mTOR inhibitors was defined by extensive binding interactions within the same active site in research targeting mTOR inhibitors for the treatment of breast cancer, and SF1126 was identified as the best protein-ligand complexes in this study. The docking score of this chosen inhibitor was -8,705 kcal/mol, and the free binding energy was found to be -36.926.<sup>28</sup>

In another study, the PI3K/Akt/mTOR axis was targeted with selected *Olea europaea* phenolic compounds in PIK3CA mutant colorectal cancer. Luteolin, which gave the best results, was found to have a binding energy of -9.4 kcal/mol to the PI3K protein, -8.1 kcal/mol to the Akt protein, and -8.8 kcal/mol to the mTOR protein.<sup>29</sup>

In a study conducted on the COVID-19 disease, Atranorin was the ligand with the best binding affinity (-7.0 kcal/mol) among other ligands, while the binding energies in our research range from -7 to -9.9 kcal/mol.<sup>30</sup>

In a study conducted with *in silico* drug screening analysis in the literature evaluated the selected final compounds using the ProTox-2 server depending on the toxicity of candidates' compounds in order to assess their drug-like characteristics.

The selected molecules were subjected to various toxicity elements. Researchers checked parameters of hepatotoxicity, cytotoxicity, mutagenicity, and Oral LD50 value. Predicted toxicity classes were obtained as Class IV, which is also the same for the compounds we analyzed.<sup>21</sup>

Dactolisib (BEZ235) is a dual pan-PI3K/mTOR inhibitor that is known to have oral activity against MM in animal models.<sup>14</sup> It was found to induce cell cycle arrest and death in HER2-overexpressed, PIK3CA-mutated, or other PI3K pathway mutations in breast cancer cells as well. Dactolisib has recently completed approximately 10 clinical trials in which it was combined with trastuzumab, everolimus, paclitaxel, and newer agents such as MEK162 and Buparlisib.<sup>9,31</sup>

Both *in vitro* and *in vivo*, Gedatolisib (PKI-587/PF-05212384) has shown promising outcomes in breast cancer tissues. Lower activity on phosphorylation of p70S6K and 4EBP1 residues in Akt and mTOR showed a link between tumor growth inhibition and PI3K pathway signaling inhibition.<sup>9</sup> When PI3K/mTOR signal inhibitors were observed, Gedatolisib was investigated in acute lymphoblastic leukemia and resulted in long-term animal survival and almost extinction, and thus, its use in other advanced cancer patients is being discussed.<sup>32</sup> In the light of these data, the ADME results indicate that Gedatolisib violated more rules than the other compounds, and the bioavailability score is lower than the other 5 inhibitors as well, which is why it was not a suitable candidate for MM. PKI-179 was structurally studied previously using computational approaches, and the inhibitory mechanism of an active PI3K/mTOR dual inhibitor was explored by checking its binding modes to PI3K $\gamma$  and mTOR.<sup>33</sup> The *in vitro* effects of dual inhibitor Omipalisib (GSK458) and its inhibition on PI3K/Akt/mTOR pathway were investigated in chemotherapy resistant and sensitive Burkitt lymphoma (BL) cell line models. Inhibition of PI3K and mTOR by the dual inhibitor Omipalisib suppressed the activation of the PI3K/Akt/mTOR pathway, leading to disruption of BL cell proliferation by induction of G1 cell cycle arrest and altering apoptosis in chemotherapy-resistant cell line models of Burkitt lymphoma.<sup>34</sup> Panulisib was unsuitable for use in leukemia models due to insufficient data.

Vistusertib was found to be effective in diffuse large B-cell lymphoma patients after the phase I/2 trials when used with Acalabrutinib (Bcr tyrosine kinase inhibitor). Studies on the TMD8 tumor model also show that the combination of Acalabrutinib and Vistusertib succeeds in promoting tumor regression.<sup>35</sup> Considering studies using Vistusertib in combination, a study with the non-allosteric mTORC1/2 inhibitor Vistusertib showed that a combination therapy of Vistusertib and paclitaxel resulted in a significant regression in tumor growth and an elevated level of apoptosis.<sup>36</sup> Also, Vistusertib previously showed synergistic effects with some inhibitors in acute myeloid leukemia cells.<sup>13</sup>

Summing up, based on previous combination studies, Vistusertib provides tumor regression, has a short half-life, and is in phase II trials for lymphoma models. Although Vistusertib has not been used for the treatment of blood cancer on its own up to date, *in silico* modeling and testing the physicochemical nature of the dual inhibitor with tools like ADME and Pro-Tox-II indicate that it is an important candidate for inhibiting myeloma cell growth, believed to be able to fight multiple myeloma cells in the long run.

*In silico* prediction and toxicity analysis studies have shown that certain parameters need to be achieved for an agent to be proposed for *in vitro* tests. The four parameters that should be correlated with solubility and permeability are molecular weight, Log P, number of H-bond donors, and number of H-bond acceptors. The cutoff values for these parameters were close to 5, leading to a simple mnemonic called the "rule of 5".<sup>37</sup> The "rule of 5" regarding solubility and permeability poor absorption or permeability is more likely if: more than 5 H bond donors, MWT above 500, Log P above 5 (or MLogP above 4.15), There are more than 10 H-bond acceptors. Substrates are the exception to this rule.<sup>37</sup> Based on these pharmacokinetic scores and analyses, this study revealed the suitability of Vistusertib to be tested on multiple myeloma cells based on its selective efficiency on PI3K isoforms and mTOR.

All in all, PI3K/mTOR is an important pathway for hematological malignancies that are being studied to develop new therapeutic approaches. The negative consequences of this pathway are high toxicity rates observed in solid tumors, low clinical activity levels, and the numerous unknown targets for inhibition. Based on these results, dual PI3K/mTOR inhibitors are valued, which are part of ongoing research and make it possible to avoid toxicity. This study revealed the binding properties and molecular interactions of ranked 6 dual inhibitors with PI3K $\delta$ , PI3K $\gamma$ , and mTOR using molecular docking analyses. Potent inhibitors that are specific and have lower toxicity can be optimized further based on the docking results. Recent information on Vistusertib *in silico* action is promising, and clinical trial needs are accumulating. More translational research into its action and toxicity is expected to lead to the development and clinical success.

## CONCLUSION

In conclusion, the PI3K/Akt/mTOR pathway plays a significant role in cancer cell activities, including survival, proliferation, and drug resistance. The Class I PI3K isoforms, p110 $\delta$  and p110 $\gamma$ , have been found to be involved in hematological malignancies, cellular signaling, and tumor progression, making them a target of interest for selective inhibition. The inhibition of PI3K and mTOR has shown promising results in the treatment of MM. Several inhibitors have been developed, and their binding interactions with the target proteins have been studied

using molecular docking. The use of dual inhibitors that target both PI3K and mTOR could lead to a significant inactivation of tumor cells' irrepressible proliferation. Future studies could evaluate selected final compounds using the ProTox-2 server, depending on the toxicity of candidate compounds, to assess their drug-like characteristics.

**Peer Review:** Externally peer-reviewed.

**Author Contributions:** Conception/Design of Study- Y.K.; Data Acquisition- I.M., Y.A., O.M., H.E.; Data Analysis/Interpretation- I.M., Y.A., O.M., H.E., Y.K.; Drafting Manuscript-I.M., Y.A., O.M., H.E.; Critical Revision of Manuscript- Y.K.; Final Approval and Accountability- I.M., Y.A., O.M., H.E., Y.K.

**Conflict of Interest:** Authors declared no conflict of interest.

**Financial Disclosure:** Authors declared no financial support.

### ORCID IDs of the authors

Ilke Masalaci	0000-0002-7989-7767
Yaren Akdogan	0000-0002-5930-2113
Ozge Mutlu	0000-0001-5237-7887
Hande Eyvaz	0000-0002-4642-3442
Yagmur Kiraz	0000-0003-3508-5617

### REFERENCES

- Wang L, Lin N, Li Y. The PI3K/AKT signaling pathway regulates ABCG2 expression and confers resistance to chemotherapy in human multiple myeloma. *Oncol Rep.* 2019;41:1678-1690.
- McKenna M, McGarrigle S, Pidgeon GP. The next generation of PI3K-Akt-mTOR pathway inhibitors in breast cancer cohorts. *Biochim Biophys Acta Rev Cancer.* 2018;1870:185-197.
- John L, Krauth MT, Podar K, Raab MS. Pathway-directed therapy in multiple myeloma. *Cancers.* 2021;13(7):1668.
- Ramakrishnan V, Kumar S. PI3K/AKT/mTOR pathway in multiple myeloma: from basic biology to clinical promise. *Leuk Lymphoma.* 2018;59(11):2524-2534.
- Tarantelli C, Lupia A, Stathis A, Bertoni F. Is there a role for dual PI3K/mTOR inhibitors for patients affected with lymphoma? *Int J Mol Sci.* 2020;21(3):1060. doi: 10.3390/ijms21031060.
- Jourdan M, Caraux A, De Vos J, et al. An in vitro model of differentiation of memory B cells into plasmablasts and plasma cells including detailed phenotypic and molecular characterization. *Blood.* 2009;114(25):5173-5181.
- Corre J, Munshi NC, Avet-Loiseau H. Risk factors in multiple myeloma: is it time for a revision? *Blood.* 2021;137(1):16-19.
- Clinical pathways to address the challenges of treatment resistance and relapse in multiple myeloma. *J Clin Pathw.* Accessed March 16, 2023. <https://www.journalofclinicalpathways.com/white-paper/clinical-pathways-address-challenges-treatment-resistance-and-relapse-multiple>
- Zitvogel L, Kroemer G. Bortezomib induces immunogenic cell death in multiple myeloma. *Blood Cancer Discov.* 2021;2(4):405-407.
- Robak P, Szymraj J, Mikulski D, Drozd I, Robak T. Prognostic value of resistance proteins in plasma cells from multiple myeloma patients treated with bortezomib. *J Clin Med.* 2021;10(21):5028. doi:10.3390/jcm10215028
- Teicher BA, Tomaszewski JE. Proteasome inhibitors. *Biochem Pharmacol.* 2015;96:1-9.
- Painuly U, Kumar S. Efficacy of bortezomib as first-line treatment for patients with multiple myeloma. *Clin Med Insights Oncol.* 2013;7:53-73.
- Mologni L, Marzaro G, Redaelli S, Zamboni A. Dual kinase targeting in leukemia. *Cancers.* 2021;13. doi:10.3390/cancers13010119.
- Abramson HN. Kinase inhibitors as potential agents in the treatment of multiple myeloma. *Oncotarget.* 2016;7:81926-81968.
- Musiol R. An overview of quinoline as a privileged scaffold in cancer drug discovery. *Expert Opin Drug Discov.* 2017;12:583-597.
- BIOVIA Discovery Studio - BIOVIA - Dassault Systèmes®. Dassault Systèmes. Accessed July 18, 2022.
- Thompson MA. molecular docking using ArgusLab, an efficient shape-based search algorithm and the a score scoring function. ACS meeting, Philadelphia. Scientific Research Publishing. Accessed July 18, 2022.
- Wong SE, Lightstone FC. Accounting for water molecules in drug design. *Expert Opin Drug Discov.* 2011;6:65-74.
- Daina A, Michielin O, Zoete V. SwissADME: a free web tool to evaluate pharmacokinetics, drug-likeness and medicinal chemistry friendliness of small molecules. *Sci Rep.* 2017;7:42717. doi:10.1038/srep42717
- Banerjee P, Eckert AO, Schrey AK, Preissner R. ProTox-II: a webserver for the prediction of toxicity of chemicals. *Nucleic Acids Res.* 2018;46:W257-W263.
- Fareed MM, El-Esawi MA, El-Ballat EM, et al. *In silico* drug screening analysis against the overexpression of PGAM1 gene in different cancer treatments. *Biomed Res Int.* 2021;2021:5515692. doi: 10.1155/2021/5515692
- Bojarska J, Remko M, Breza M, et al. A supramolecular approach to structure-based design with a focus on synthons hierarchy in ornithine-derived ligands: review, synthesis, experimental and *in silico* studies. *Molecules.* 2020;25(5):1135. doi: 10.3390/molecules25051135
- Han K, Xu X, Chen G, et al. Identification of a promising PI3K inhibitor for the treatment of multiple myeloma through the structural optimization. *J Hematol Oncol.* 2014;7:9. doi: 10.1186/1756-8722-7-9
- Harvey RD, Lonial S. PI3 kinase/AKT pathway as a therapeutic target in multiple myeloma. *Future Oncol.* 2007;3(6):639-647.
- Zhao L, Vogt PK. Class I PI3K in oncogenic cellular transformation. *Oncogene.* 2008;27(41):5486-5496.
- Thorpe LM, Yuzugullu H, Zhao JJ. PI3K in cancer: divergent roles of isoforms, modes of activation and therapeutic targeting. *Nat Rev Cancer.* 2015;15(1):7-24.
- Baumann P, Schneider L, Mandl-Weber S, Oduncu F, Schmidmaier R. Simultaneous targeting of PI3K and mTOR with NVP-BGT226 is highly effective in multiple myeloma. *Anticancer Drugs.* 2012;23(2):131-138.
- Patidar K, Panwar U, Vuree S, et al. An *in silico* approach to identify high affinity small molecule targeting m-TOR inhibitors for the clinical treatment of breast cancer. *Asian Pac J Cancer Prev.* 2019;20(4):1229-1241.

29. Sain A, Kandasamy T, Naskar D. *In silico* approach to target PI3K/Akt/mTOR axis by selected *Olea europaea* phenols in PIK3CA mutant colorectal cancer. *J Biomol Struct Dyn*. 2021;1–16.
30. Putra PP, Abdullah SS, Rahmatunisa R, Junaidin J, Ismed F. Structure, activity, and drug-likeness of pure compounds of Sumatran lichen (*Stereocaulon halei*) for the targeted ACE2 protein in COVID-19 disease. *Pharmaciana*. 2020;10(2):135–146.
31. Schult C, Dahlhaus M, Glass A, et al. The dual kinase inhibitor NVP-BEZ235 in combination with cytotoxic drugs exerts anti-proliferative activity towards acute lymphoblastic leukemia cells. *Anticancer Res*. 2012;32:463–474.
32. Tasian SK, Teachey DT, Li Y, et al. Potent efficacy of combined PI3K/mTOR and JAK or ABL inhibition in murine xenograft models of Ph-like acute lymphoblastic leukemia. *Blood*. 2017;129:177–187.
33. Mohd Rehan. A structural insight into the inhibitory mechanism of an orally active PI3K/mTOR dual inhibitor, PKI-179 using computational approaches. *J Mol Graph Model*. 2015;62:226–234.
34. Ippolito T, Tang G, Mavis C, Gu JJ, Hernandez-Ilizaliturri FJ, Barth MJ. Omipalisib (GSK458), a novel Pan-PI3K/mTOR inhibitor, exhibits in vitro anti-lymphoma activity in chemotherapy-sensitive and -resistant models of burkitt lymphoma. *Blood*. 2016;128:5376. doi: 10.1182/blood.V128.22.5376.5376
35. Collins GP, Clevenger TN, Burke KA, et al. A phase 1/2 study of the combination of acalabrutinib and vistusertib in patients with relapsed/refractory B-cell malignancies. *Leuk Lymphoma*. 2021;62:2625–2636.
36. Rinne N, Christie EL, Ardasheva A, et al. Targeting the PI3K/AKT/mTOR pathway in epithelial ovarian cancer, therapeutic treatment options for platinum-resistant ovarian cancer. *Cancer Drug Resist*. 2021;4:573–595.
37. Lipinski CA, Lombardo ational approaches to estimate solubility and permeability in drug discovery and development settings IPII of original article: S0169-409X(96)00423-1. The article was originally published in *Advanced Drug Delivery Reviews 23 (1997) 3–25.I. Adv Drug Deliv Rev*. 2001;46:3–26.

### How cite this article

Masalaci I, Akdogan Y, Mutlu O, Eyvaz H, Kiraz Y. *In Silico* Approach for Identification of PI3K/mTOR Dual Inhibitors for Multiple Myeloma Treatment. *Eur J Biol* 2023;82(1): 1-11. DOI: 10.26650/EurJBiol.2023.1178214

# Effects of Salicylic Acid and Microorganisms on Morphological and Physiological Characteristics (*Satureja hortensis* L.) under Drought Stress

Mahmood Ghojavand<sup>1</sup>,  Porang Kasraei<sup>1</sup>,  Hamid Reza Tohidi Moghadam<sup>1</sup>,  Mohammad Nasri<sup>1</sup>,   
Hamid Reza Larijani<sup>1</sup> 

<sup>1</sup>Department of Agronomy, Faculty of Agricultural, Islamic Azad University, Varamin-Pishva Branch, Tehran, Iran

## ABSTRACT

**Objective:** As a critical limitation of plant growing, drought stress has always received a lot of attention from botanical researchers. This study intends to investigate the role of salicylic acid and the Mycorrhiza and Azotobacter bio-fertilizer on *Satureja hortensis* L. under drought stress.

**Materials and Methods:** Salicylic acid and bio-fertilizers have been shown to improve drought tolerance in growing plants. To evaluate the synergistic effect of salicylic acid, *Azotobacter chroococcum* bacteria, and arbuscular mycorrhizal fungi under drought stress (-3.5 atm: W1), (- 6.5 atm: W2), and (-10 atm: W3), a 2-year (2016 to 2018) field experiment was organized based on split-plot factorial statistical in a randomized complete block design, with three replicates.

**Results:** The main findings of this study showed that the combinable use of bio-fertilizers and salicylic acid diminished the disadvantageous effects of drought stress. Co-application of bio- fertilizers and salicylic acid significantly increased chlorophyll a and b (22% and 31.5%), carotenoid (30.7%) contents, aerial fresh (38.3%) and dry (64.1%) weights, root fresh (55.8%), and dry (45%) weights, auxin (15%), percentage of essential oil (30.7%) in *S. hortensis* while it decreased the proline content (48.8%) under severe stress as compared to the control groups, which confirmed the efficacy of this approach and its role in drought tolerance.

**Conclusion:** The results demonstrated that this new suggested treatment could effectively alleviate drought stress symptoms and improve *S. hortensis* growth under spreading drought conditions and limited water resources.

**Keywords:** Arbuscular Mycorrhizal Fungi, Bio-Fertilizers, Drought Stress, Phytohormone, *Satureja hortensis*

## INTRODUCTION

Medicinal plants are plants whose quality of materials is far more important and necessary than their quantity. Therefore, in order to achieve maximum quality, knowledge and awareness of the factors affecting the growth and development of medicinal plants is very important. Knowledge of environmental, plant and agronomic factors has an important role in the success of medicinal plants.<sup>1</sup> Among the factors affecting the growth, development and production of active ingredients of medicinal plants and aromatic plants, the lack of which more than other inputs affects the reduction of production. Although extensive and comprehensive research has been done on the effect of water stress on crops, the behavior of medicinal plants in such conditions has not been well studied.<sup>1</sup> To understand the existence and survival of medicinal plants in arid and semi-arid regions, which also cover a large part of our country, exten-

sive research is needed on plants with medicinal value and the application of various treatments.<sup>2</sup>

The use of *Azotobacter* has been considered as a biological fertilizer in agriculture due to its ability to stabilize molecular nitrogen in cooperation with plants as well as the production of growth-promoting hormones. In addition to the significant potential it has shown to improve the growth of host plants, this bacterium has been considered for other reasons such as the wide range of host plants, species diversity, and modulating the effects of environmental stresses. It is effective<sup>3</sup>. There are successful reports of the use of this bio-fertilizer to combat dehydration in plants<sup>4</sup>. Also, since the global approach in the production of medicinal plants is effective in improving the quantity and quality of material, it seems that the healthy nutrition of plants through the use of bio-fertilizers is most in

**Corresponding Author:** Porang Kasraei **E-mail:** dr.kasraei@yahoo.com

**Submitted:** 14.11.2022 • **Revision Requested:** 26.01.2023 • **Last Revision Received:** 27.03.2023 • **Accepted:** 05.04.2023



This article is licensed under a Creative Commons Attribution-NonCommercial 4.0 International License (CC BY-NC 4.0)



line with the objectives of the production of medicinal plants.<sup>5</sup> Salicylic acid (SA) is a phenolic compound in plants that is considered a hormone-like regulator and plays an important protective role in defense mechanisms against biological and environmental stresses. Induction of flowering, growth and development, ethylene synthesis, orifice closure and respiration are important roles of SA<sup>6</sup>. This substance has increased resistance to water shortage in wheat.<sup>7</sup> In view of the above, this study intends to investigate the role of SA and the Mycorrhiza and Azotobacter bio-fertilizer on *Satureja hortensis* under drought stress.

## MATERIALS AND METHODS

### Plant Material

In order to study the effect of the application of Azotobacter (Az), Arbuscular Mycorrhizal Fungi (AMF) and SA on quantitative and qualitative properties of savoury (*S. hortensis* L) in drought stress conditions of this study in Zamanabad the village of Shahr-e Ray (Tehran province) for two cropping years (2016 and 2017); the crushed randomized complete block design (RCBD) was performed in three replications. Main plot of three irrigation levels (soil moisture potential -3.5 atm or crop capacity (FC), potential of -6.5 atm as medium stress and potential of -10 atm as severe stress), sub-factors including biological fertilizers of Az and Mycorrhiza with inoculation levels with Az strain, combination of seeds with AMF and combined use of Azotobacter-mycorrhiza (AM) and SA with non-foliar application and foliar application (with a concentration of 0.6 mM) were assigned. The physical and chemical characteristics of farm soil are shown in Tables 1 and 2.

**Table 1.** Physical properties the soil of field.

Texture	Clay(%)	Silt (%)	Sand (%)	S.P. (%)
Clay	35.71	37.78	25.51	35.29

S.P.: Poorly graded sand

### Measurement of Photochemical Activity

#### *Chlorophyll and Carotenoids*

To measure the photosynthetic pigments (e.g., chlorophyll a, b and total chlorophyll), fully expanded mature leaves were sampled and dissolved in acetone (80%) and after being centrifuged, the absorbance of each sample was measured using a spectrophotometer (Perkin Elmer, Lambda 25, UV/VIS Spectrophotometer) in wavelengths of 663.2, 646.8 and 470 nm for chlorophyll a, chlorophyll b and total chlorophyll content, and according to the following relations the amount of pigments were calculated based on the µg/g fresh weigh.<sup>8</sup>

### Extraction of Essential Oil

Precisely weighed *S. hortensis* powder (200 g) was mixed with distilled water (3000 ml). The mixture was heated, and kept at a low boil for 4.5 h till the amount of oil in the vessel no longer increased, and then the heating was stopped. After 1 h, the volume of essential oil was recorded. The percentage of essential oil yield was calculated using the formula volume of essential oil divided by the weight of the sample powder. The volatile extract obtained was kept at 4 °C after drying with anhydrous sodium sulphate. The upper yellow oil was used as the sample for further analysis.

### Analysis of Essential Oil

A GCMS-QP2010 Plus Mass Spectrometer (Shimadzu, Kyoto, Japan), equipped with a DB-5 MS capillary column (30.0 m × 0.25 mm; film thickness, 0.25 µm) and a mass spectrometry (MS) detector was used for GC-MS analysis. The injector temperature was 250 °C. The oven temperature was programmed from 50 °C (1 min isothermal) to 180 °C at a rate of 5 °C/min and then to 250 °C at a rate of 10 °C/min, and then kept for 6 min. The interface was kept at 280 °C. The mass spectra were obtained at 70 eV. The sector mass analyser was set to scan from 30 to 550 amu. Helium was used as a carrier gas with a flow rate of 1 mL/min. Essential oil (0.1 mL) of the sample was injected (in split mode 20:1). Volatile oil components were calculated as a relative percentage of the total oil using peak area. Retention index of all the components were determined by Kovats method using n-alkanes (C6–C32) as standards. Identification of individual constituents was accomplished by comparing their MS spectra by matching the mass spectral data with those from the NIST (NIST 08, NIST 08s; National Institute of Standards and Technology, Gaithersburg, MD, USA), and by comparison of their MS spectra and GC retention indices with those of standard compounds available in the laboratory and also by comparison with some other relevant references.<sup>9</sup>

### Auxin

In order to measure the amount of auxin (IAA), 1 gr of leaf tissue from the leaves near the top of the stem (leaf+stem) and the root was boiled separately in 10 ml of 80% ethanol, and after grinding, it was passed through filter paper and then an amount of 1 ml A litre of the obtained extracts was poured into separate test tubes and 2 ml of Salkowski's reagent was added to each test tube. (In order to prepare Salkowski's reagent, 0.5 M ferric chloride (FeCl<sub>3</sub>) solution was first prepared. Then, one ml of this solution was mixed with 50 ml of 35% perchloric acid and after stirring the mixture, Salkowski's reagent was prepared). Then, the tubes were placed in a Bain-Marie at 40-50°C for 15 minutes until the complete reaction and the presence of IAA in the extract was revealed with a pink colour. At the end, the

**Table 2.** Chemical properties the soil of field.

<b>K (Available)</b>	<b>P (Available)</b>	<b>Zn (ppm)</b>	<b>Fe (ppm)</b>	<b>Organic C (%)</b>	<b>Total N (%)</b>	<b>H</b>	<b>EC (dS m<sup>-1</sup>)</b>
580	8.16	0.37	3.18	1.33	0.09	0.48	1.02

EC: Electrical conductivity

optical absorbance of the samples was measured at 530 nm by a Pharmacia LKB-Novaspac spectrophotometer. The amount of IAA in the samples was calculated using a standard curve in the range of 0 to 40 mg/L. Pure IAA was used to draw the standard curve.<sup>10</sup>

### Proline

Proline content was estimated using ninhydrin reaction.<sup>11</sup> A portion (0.5 g) of shoot was homogenized with 10 mL of 3% (w/v) sulphosalicylic acid and passed through Whatman filter paper (no. 2; Whatman, Maidstone, UK). Ninhydrin reagent (2 mL) (Sigma, St. Louis, Missouri, USA) and glacial acetic acid (2 mL) were added to 2 mL of the filtered extract. The mixture was then incubated at 100°C for 1 h and the reaction was terminated by placing it on ice. The reaction mixture was extracted with 4 mL toluene and the absorption of chromophore was measured at 520 nm, against toluene as blank, using the spectrophotometer. Proline content was calculated using L-proline (Sigma) as a standard curve. Plants were harvested at the time of flowering and the samples were dried in the drying at 105 °C up to constancy for the required time and then weighed to measure dry weight. After determining the dry weight, 10 g of the leaves and flowering twigs of each sample was sent to the laboratory. The percentage of essential oil by water distillation was measured by Clevenger Model 500HM6. Essential oil yield was calculated by multiplying the percentage of essential oil by the dry weight of the vegetative body.

### Statistical Analysis

Data analysis with software SAS 9.4 and comparison of the mean of treatments with least significant difference (LSD) test was performed at a probability level of 0.05%. Graphs were drawn using Excel software.

## RESULTS

### Aerial Fresh Weight (AFW) and Aerial Dry Weight (ADW)

This study showed that AMF, Az, SA, and Az+AMF with SA had improved AFW and ADW in all irrigation levels. On the other hand, drought stress reduced AFW and ADW by 40.8% and 55.4% under the W3 drought than the control (Table 3). The inoculation with Az+AMF+0.6 mM SA spraying in every

irrigation regime had the most positive effect on *S. hortensis* AFW and ADW compared with control. AFW and ADW plants sprayed with 0.6 mM of SA in some of the treatments did not show any significant difference comparing to non-sprayed plants in the same treatments. Nevertheless, inoculated with Az+AMF enhanced the AFW and ADW 17.1% and 34.4% at W1 conditions, while inoculation with Az+AMF+SA causes increased AFW and ADW 23.6% and 57.3%. Also, under drought stress conditions (W2 and W3) application of bio-fertilizers, SA either or together showed no significant difference compared with the control (13.6 and 8.1 g) for ADW. The highest AFW (103 g) and ADW (28.8 g) were observed from the inoculation with Az+AMF and 0.6 mM SA spraying under W1 irrigation conditions (Table 3).

### Root Fresh Weight (RFW) and Root Dry Weight (RDW)

Drought stress diminished the RFW and RDW. The RFW and RDW decreased under the mild drought stress W2 (24.7% and 22.8%) and severe drought stress W3 (52.6% and 49.2%) as compared with the control (3.63 and 1.4 g). Under W2 and W3 conditions, the RFW and RDW indicated a non-significant difference between means with application Az, AMF, SA, and compound with SA as compared with the control treatments, while using of AMF+SA, Az+AMF alone and with SA caused a significant improvement in the root fresh and dry weight in W1 irrigation conditions. Also, the greatest the root fresh (6.2 g) and dry (2.2 g) weight was seen in plants treated with Az+AMF and sprayed with SA in W1 condition (Table 4).

### Chlorophyll and Carotenoid Contents

The results of this work showed various levels of drought (W2 and W3) caused a reduction in the concentration of photosynthetic pigments. The lowest chlorophyll a, b, and carotenoid were obtained in W3 stress, which indicated a decrease of 40%, 39.4%, and 48%, respectively, than W1 irrigation conditions (Table 5). Moreover, it has been reported that the chlorophyll decline may be due to the chloroplast disintegration and the instability of the chlorophyll protein complex. The chlorophyll a, b significantly enhanced with the application of AMF and Az+AMF alone or with SA at W1 and W3 watered conditions in comparison with control groups, but under the W2 situation, just the Az+AMF+SA treatment had increased the chlorophylls a and b contents. Carotenoid was significantly enhanced by the

**Table 3.** Comparison of two-year means of aerial fresh weight (AFW) and aerial dry weight (ADW) of *Satureja hortensis* by different bio-fertilizers and SA treatments under different irrigation levels.

Treatment		AFW (g)			ADW (g)		
Bio-fertilizers	SA (mM)	W1	W2	W3	W1	W2	W3
Non-inoculation	0	83.3 <sup>c-f</sup>	71.2 <sup>e-h</sup>	49.3 <sup>j</sup>	18.3 <sup>d-f</sup>	13.6 <sup>f-i</sup>	8.1 <sup>i</sup>
	0.6	85.7 <sup>b-e</sup>	72.7 <sup>d-h</sup>	53.8 <sup>ij</sup>	18.6 <sup>c-f</sup>	14.6 <sup>f-h</sup>	10.6 <sup>hi</sup>
Azotobacter (Az)	0	87.5 <sup>b-d</sup>	73.2 <sup>d-h</sup>	60 <sup>h-j</sup>	18.6 <sup>c-f</sup>	15.3 <sup>e-h</sup>	10.6 <sup>hi</sup>
	0.6	87.5 <sup>b-d</sup>	73.7 <sup>d-h</sup>	61 <sup>h-j</sup>	21.1 <sup>b-e</sup>	15.3 <sup>e-h</sup>	11.1 <sup>hi</sup>
Mycorrhiza (AMF)	0	88.7 <sup>a-d</sup>	75.3 <sup>d-h</sup>	61.3 <sup>h-j</sup>	21.6 <sup>b-d</sup>	16 <sup>d-h</sup>	11.1 <sup>hi</sup>
	0.6	95.5 <sup>a-c</sup>	78.7 <sup>d-g</sup>	65.2 <sup>g-i</sup>	24 <sup>a-c</sup>	17.1 <sup>d-g</sup>	12.1 <sup>g-i</sup>
Co-inoculation with Az+AMF	0	97.7 <sup>ab</sup>	79.5 <sup>d-g</sup>	65.5 <sup>g-i</sup>	24.6 <sup>ab</sup>	17.3 <sup>d-g</sup>	13.1 <sup>f-i</sup>
	0.6	103 <sup>a</sup>	80.3 <sup>c-g</sup>	62.8 <sup>g-i</sup>	28.8 <sup>a</sup>	17.8 <sup>d-g</sup>	13.3 <sup>f-i</sup>

Means followed by the same letter in each column are not significantly different according to the LSD test ( $p=0.05$ ). Control: W1 (Field capacity); *Medium stress*: W2 (6.5 atm); *Severe stress*: W3 (10 atm); SA: Salicylic acid.

**Table 4.** Comparison of two-year means of root fresh weight (RFW) and root dry weight (RDW) of *Satureja hortensis* by different bio-fertilizers and SA treatments under different irrigation levels.

Treatment		RFW (g)			RDW (g)		
Bio-fertilizers	SA (mM)	W1	W2	W3	W1	W2	W3
Non-inoculation	Control	3.63 <sup>d.g</sup>	2.73 <sup>f.j</sup>	1.72 <sup>j</sup>	1.40 <sup>d.g</sup>	1.08 <sup>g.j</sup>	0.71 <sup>k</sup>
	0.6	3.77 <sup>d.f</sup>	2.79 <sup>f.i</sup>	1.9 <sup>l.j</sup>	1.42 <sup>c.f</sup>	1.08 <sup>g.j</sup>	0.83 <sup>jk</sup>
Azotobacter (Az)	0	3.85 <sup>de</sup>	2.79 <sup>f.i</sup>	2.32 <sup>h.j</sup>	1.48 <sup>c.e</sup>	1.15 <sup>f.j</sup>	0.92 <sup>i.k</sup>
	0.6	3.88 <sup>de</sup>	2.82 <sup>f.i</sup>	2.35 <sup>h.j</sup>	1.55 <sup>c.e</sup>	1.23 <sup>e.i</sup>	0.95 <sup>h.k</sup>
Mycorrhiza (AMF)	0	4.27 <sup>cd</sup>	3.18 <sup>e.h</sup>	2.38 <sup>h.j</sup>	1.63 <sup>cd</sup>	1.26 <sup>d.i</sup>	0.95 <sup>h.k</sup>
	0.6	5.02 <sup>bc</sup>	3.43 <sup>d.g</sup>	2.41 <sup>h.j</sup>	1.78 <sup>c</sup>	1.28 <sup>d.i</sup>	0.96 <sup>h.k</sup>
Co-inoculation with Az+AMF	0	5.37 <sup>ab</sup>	3.48 <sup>d.g</sup>	2.62 <sup>g.j</sup>	2.10 <sup>ab</sup>	1.33 <sup>d.h</sup>	1 <sup>h.k</sup>
	0.6	6.20 <sup>a</sup>	3.51 <sup>d.g</sup>	2.68 <sup>g.j</sup>	2.27 <sup>a</sup>	1.33 <sup>d.h</sup>	1.03 <sup>g.k</sup>

Means followed by the same letter in each column are not significantly different according to the LSD test ( $p=0.05$ ). Control: W1 (Field capacity); *Medium stress*: W2 (6.5 atm); *Severe stress*: W3 (10 atm); SA: Salicylic acid.

application of AMF+SA and Az+AMF alone or with SA at W1 conditions (Table 5). The highest mean of the carotenoid ( $0.35 \text{ mg g}^{-1}$ ) was achieved in the W1 irrigation level and integrated application of Az+AMF and SA. Under the W2 irrigation condition, integrated application of Az+AMF with SA had a significant effect on carotenoid content compared to the control, but under W3 drought stress application of bio-fertilizers and SA showed no significant effect between treatments (Table 5).

### Proline

The results of the analysis of 2-year data showed the impact of drought stress, bio-fertilizers, SA, and their interaction was significant on the proline content. As shown in Table 6, with rising drought stress, the amount of proline improved. Outcomes revealed that Az+AMF treatments decreased the proline content under well-watered and water deficiency situations. As

a result, the highest proline content ( $47.7 \text{ } \mu\text{g g}^{-1}$ ) was obtained under W3 conditions. This treatment showed 15.8% increases compared to the control treatment ( $40.9 \text{ } \mu\text{g g}^{-1}$ ).

### Auxin

As shown in the results of Table 6, the interaction between treatments on IAA content was significant. IAA content of the *S. hortensis* plants was reduced in W2 and W3 stress situations, while we achieved a higher IAA content in all treatments inoculated with Az+AMF.

### Essential Oil

The result of our study showed plants inoculated with any of the bio-fertilizers alone or together improved the quantity of essence percentage under all irrigation conditions. Plants

**Table 5.** Comparison of two-year means of chlorophylls and carotenoid contents of *Satureja hortensis* by different bio-fertilizers and SA treatments under different irrigation levels.

Treatment		Chlorophyll a (mg g <sup>-1</sup> )	Chlorophyll b (mg g <sup>-1</sup> )	Carotenoid (mg g <sup>-1</sup> )		
W1	Bio-fertilizers	SA (mM)				
	Non-inoculation	Control	0.5 <i>d.f</i>	0.38 <i>e.g</i>	0.25 <i>d.f</i>	
		0.6	0.51 <i>c.e</i>	0.4 <i>d.f</i>	0.25 <i>d.f</i>	
	Azotobacter (Az)	0	0.55 <i>b.d</i>	0.41 <i>c.e</i>	0.27 <i>c.e</i>	
		0.6	0.56 <i>a.c</i>	0.43 <i>c.d</i>	0.27 <i>c.e</i>	
	Mycorrhiza (AMF)	0	0.56 <i>a.c</i>	0.43 <i>c.d</i>	0.28 <i>c.d</i>	
		0.6	0.58 <i>ab</i>	0.45 <i>bc</i>	0.30 <i>bc</i>	
	Co-inoculation with Az+AMF	0	0.6 <i>ab</i>	0.48 <i>ab</i>	0.33 <i>ab</i>	
		0.6	0.61 <i>a</i>	0.5 <i>a</i>	0.35 <i>a</i>	
	W2	Non-inoculation	Control	0.43 <i>g.j</i>	0.33 <i>h.j</i>	0.19 <i>gh</i>
0.6			0.45 <i>f.i</i>	0.33 <i>h.j</i>	0.19 <i>gh</i>	
Azotobacter (Az)		0	0.45 <i>f.i</i>	0.35 <i>g.i</i>	0.2 <i>gh</i>	
		0.6	0.46 <i>e.h</i>	0.35 <i>g.i</i>	0.21 <i>f.g</i>	
Mycorrhiza (AMF)		0	0.48 <i>e.g</i>	0.35 <i>g.i</i>	0.22 <i>f.g</i>	
		0.6	0.48 <i>e.g</i>	0.36 <i>f.h</i>	0.23 <i>e.g</i>	
Co-inoculation with Az+AMF		0	0.48 <i>e.g</i>	0.36 <i>f.h</i>	0.23 <i>e.g</i>	
		0.6	0.5 <i>d.f</i>	0.38 <i>e.g</i>	0.25 <i>d.f</i>	
W3		Non-inoculation	Control	0.33 <i>k</i>	0.23 <i>l</i>	0.13 <i>i</i>
			0.6	0.38 <i>j.k</i>	0.25 <i>l</i>	0.13 <i>i</i>
	Azotobacter (Az)	0	0.38 <i>jk</i>	0.25 <i>l</i>	0.14 <i>i</i>	
		0.6	0.38 <i>jk</i>	0.26 <i>kl</i>	0.15 <i>i</i>	
	Mycorrhiza (AMF)	0	0.4 <i>ij</i>	0.3 <i>jk</i>	0.15 <i>i</i>	
		0.6	0.4 <i>ij</i>	0.31 <i>ij</i>	0.16 <i>hi</i>	
	Co-inoculation with Az+AMF	0	0.4 <i>ij</i>	0.31 <i>ij</i>	0.17 <i>hi</i>	
		0.6	0.41 <i>h.j</i>	0.33 <i>h.j</i>	0.17 <i>hi</i>	

Means followed by the same letter in each column are not significantly different according to the LSD test (p=0.05). Control: W1 (Field capacity); *Medium stress*: W2 (6.5 atm); *Severe stress*: W3 (10 atm); SA: Salicylic acid.

**Table 6.** Comparison of two-year means of proline and auxin (IAA) of *Satureja hortensis* by different bio-fertilizers and SA treatments under different irrigation levels.

Treatment		Proline (µg g <sup>-1</sup> FW)			IAA (µg g <sup>-1</sup> FW)		
Bio-fertilizers	SA (mM)	W1	W2	W3	W1	W2	W3
Non-inoculation	Control	40.9 <i>c</i>	45.5 <i>b</i>	47.7 <i>a</i>	0.85 <i>d.f</i>	0.82 <i>fg</i>	0.80 <i>g</i>
	0.6	40.6 <i>c</i>	44.3 <i>b</i>	45.1 <i>b</i>	0.87 <i>c.e</i>	0.85 <i>d.f</i>	0.83 <i>e.g</i>
Azotobacter (Az)	0	35.2 <i>de</i>	36.5 <i>d</i>	40.2 <i>c</i>	0.89 <i>a.d</i>	0.87 <i>c.e</i>	0.83 <i>e.g</i>
	0.6	33.9 <i>ef</i>	35.8 <i>d</i>	39.5 <i>c</i>	0.90 <i>a.d</i>	0.88 <i>b.d</i>	0.85 <i>d.f</i>
Mycorrhiza (AMF)	0	30.1 <i>hi</i>	31.4 <i>gh</i>	33.8 <i>ef</i>	0.90 <i>a.d</i>	0.89 <i>a.d</i>	0.87 <i>c.e</i>
	0.6	28.8 <i>lj</i>	30.3 <i>gh</i>	32.7 <i>fg</i>	0.93 <i>ab</i>	0.90 <i>a.d</i>	0.89 <i>a.d</i>
Co-inoculation with Az+AMF	0	25.5 <i>kl</i>	27.0 <i>jk</i>	28.7 <i>ij</i>	0.93 <i>ab</i>	0.92 <i>a.c</i>	0.90 <i>a.d</i>
	0.6	22.1 <i>n</i>	23.3 <i>mn</i>	24.4 <i>lm</i>	0.95 <i>a</i>	0.93 <i>ab</i>	0.92 <i>a.c</i>

Means followed by the same letter in each column are not significantly different according to the LSD test (p=0.05). Control: W1 (Field capacity); *Medium stress*: W2 (6.5 atm); *Severe stress*: W3 (10 atm); SA: Salicylic acid.

sprayed with the SA and inoculated with Az+AMF showed the highest percentage of essence 29.2%, 29.7% and 30.7%, respectively under well-watered and stress conditions (W2, W3) compared to control. However, the application of SA with every of Az, AMF, or by their combination significantly enhanced the percentage of the essence under all of the irrigation levels compared to the plants treated with SA alone. Therefore, the highest percentage of essence (1.8 v/w) was induced by spraying 0.6 mM of SA+Az+AMF together as inoculation at W3 drought (Figure 1).

### Thymol Content

Results of the analysis of the data showed that the effect of drought stress, fertilizers Az and AMF, spraying of SA and their interaction on Thymol content was significant. Plants inoculated with any one of the bio-fertilizers alone or together, their Thymol content has been statistically increased compared to the control treatment. Drought stress increased the content of thymol. The W3 drought conditions enhanced the content of thymol by 20.5% compared to control. However, the application of Az, AMF, or their combination showed an increased Thymol content under all irrigation regimes. Furthermore, SA spray increased the content of Thymol 16.4%, 15% and 5.6%, respectively at W1, W2 and W3 levels of irrigation, however, this increase was not significant in the W3 irrigation level. Also, SA had a significant effect on Thymol content in non-inoculated and inoculated plants with either the combination of Az+AMF, just Az, or just AMF in all irrigation treatments. Based on the mean comparison, the highest Thymol content (4.71%) was obtained by the combination treatment (Az+AMF + SA) at W3 drought and the lowest (3.5%) was in untreated plants (control) in W1 irrigation level (Figure 2). Thymol Content Results of the analysis of the data showed that the effect of drought stress, fertilizers Az and AMF, spraying of SA and their interaction on Thymol content was significant. Plants inoculated with any one of the bio-fertilizers alone or together, their Thymol content has been statistically increased compared to the control treatment. Drought stress increased the content of thymol. The W3 drought conditions enhanced the content of thymol by 20.5% compared to control. However, the application of Az, AMF, or their combination showed an increased Thymol content under all irrigation regimes. Furthermore, SA spray increased the content of Thymol 16.4%, 15% and 5.6%, respectively at W1, W2 and W3 levels of irrigation, however, this increase was not significant in the W3 irrigation level. Also, SA had a significant effect on Thymol content in non-inoculated and inoculated plants with either the combination of Az+AMF, just Az, or just AMF in all irrigation treatments. Based on the mean comparison, the highest Thymol content (4.71%) was obtained by the combination treatment (Az+AMF + SA) at W3 drought and the lowest (3.5%) was in untreated plants (control) in W1 irrigation level (Figure 2).

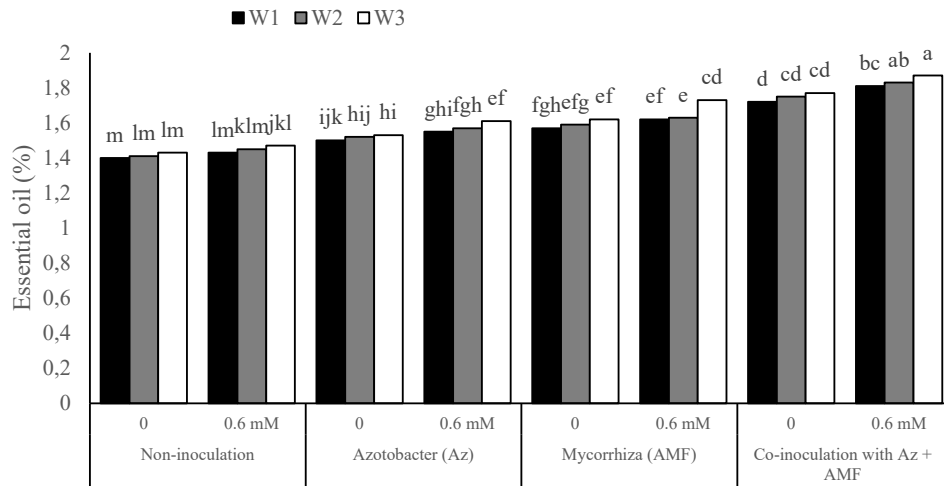
### Carvacrol Content

The results presented in (Figure 3) show significant effects of the irrigation treatments and inoculated with Az+AMF, as drought stress W3 increased carvacrol content 77.1%. As well as plants treated with Az, AMF and the combination of Az+AMF had greater carvacrol content in all irrigation levels W1, W2 and W3 compared with control. Foliar application of SA in non-inoculated plants under W1 irrigation treatment was not statistically significant on carvacrol content, while spraying SA revealed significant enhancement under W2 and W3 conditions. However, under all irrigation treatments, carvacrol content in plants treated with either the combination of SA and Az+AMF increased. Therefore, the highest carvacrol content (38.5%) was achieved in plants inoculated with the Az+AMF+SA under W3 drought stress.

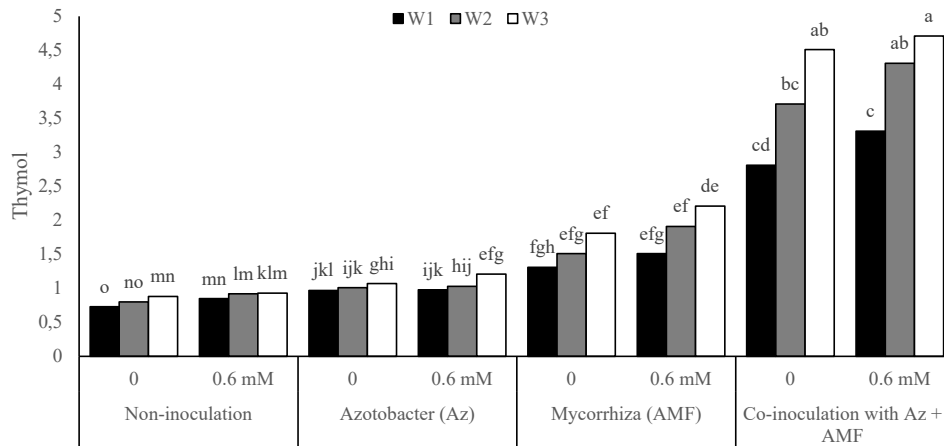
### DISCUSSION

Drought stress had adverse effects on the studied traits of the *S. hortensis* medicinal plant, the application of SA and microorganisms improved these adverse effects of stress. Drought stress reduced the morphological characteristics of the *S. hortensis* medicinal plant. It reported the drought stress diminished RDW and ADW in two *Thymus* species but, inoculation with AMF in low and intense drought stress enhanced the *T. daenensis* species root and shoot dry weight.<sup>12</sup> The influence of drought stress on decreasing the ADW and RDW of plants can be related to that water shortage, lowers the absorption, transferring, and utilization of nutrients, which results in a decline in carbon storage and biomass.<sup>13</sup> It has been reported that the seedlings of valerian inoculated with AMF, Az, and combination of Az+AMF had higher ADW and RDW under good and deficit irrigation conditions than the corresponding non-inoculation seedlings that is in line with this result.<sup>14</sup>

The treatment with bio-fertilizers can counteract the drought stress influences on plant production, particularly at severe drought stress. It is recognized as a positive impact of bio-fertilizers on improving plants' nutritional conditions under stressful environments conditions. Plant growth promoting *Rhizobacteria* have a key role in stimulating the nitrogen uptake and the effectiveness of it in the functioning of photosynthesis and plant growth.<sup>15</sup> It was found that the use of PGPR increased microbial activity because they can produce an exo-polysaccharide, which leads to improved soil physical and chemical conditions such as soil structure, soil aggregation, and soil penetrance following improved soil moisture-holding capacity.<sup>16</sup> It reported improvement of the components of yield and productivity in wheat using the application of PGPR (soil application) alongside SA (foliar spraying) that might be by collaboration with IAA and/or cytokinin synthesis, the stimulation of cell division, and photosynthesis.<sup>17</sup> It has been reported in the plant (*Valeriana officinalis* L.) that rising drought stress



**Figure 1.** Comparison of two-year means of essential oil *Satureja hortensis* by different bio-fertilizers and SA treatments under different irrigation levels. The letters a-m and f indicate that the same letter in each column are not significantly different according to the LSD test ( $p=0.05$ ). Control: W1 (Field capacity); Medium stress: W2 (6.5 atm); Severe stress: W3 (10 atm).

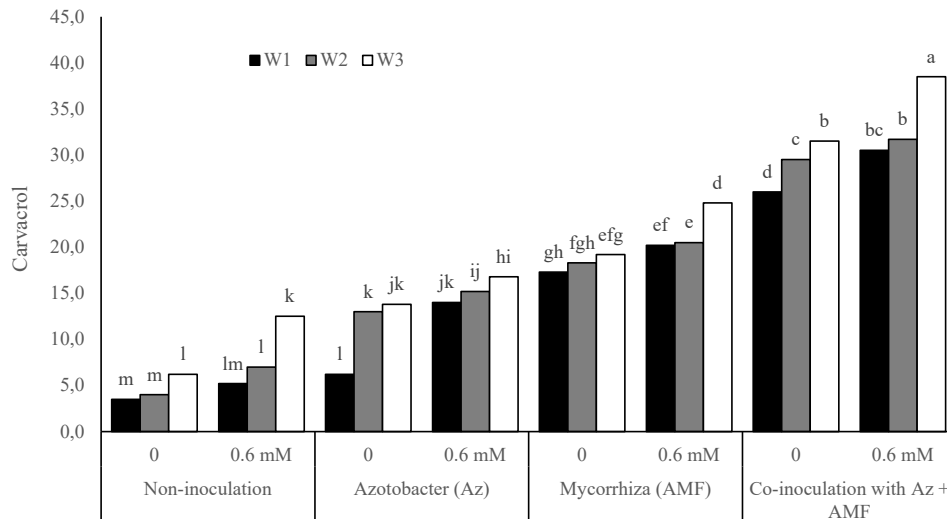


**Figure 2.** Comparison of two-year means of thymol content oil *Satureja hortensis* by different bio-fertilizers and SA treatments under different irrigation levels. The letters a-m indicate that the same letter in each column are not significantly different according to the LSD test ( $p=0.05$ ). Control: W1 (Field capacity); Medium stress: W2 (6.5 atm); Severe stress: W3 (10 atm).

caused decreasing RDW, while bio-fertilizers enhancement the RDW than in the control (without bio-fertilizers). The PGPR stimulated the root growth by improving the nutrient conditions, increasing microbial activity, and influencing other useful symbiotic relationships.<sup>18</sup> It has been reported that the plant (*Scutellaria integrifolia L.*) inoculation with AMF can cause an impressive root growth and increment the power of the plant to overcome difficult conditions such as phosphorus deficiency.<sup>19</sup> Furthermore, increased RDW of the marjoram plant inoculated with bacteria was attributed to increment lateral roots and root nutrients sorption capacity.<sup>4</sup>

Some of the PGPR, which produce *Rhizobiotoxin* via diminishing ethylene production in the plants, enhanced root growth.<sup>20</sup> The proper ratio between nitrogen and phosphorus improves root yield too, and has a useful result on plant growth.

Since the role of Az has been proven in incrementing the solvability of phosphorus from inorganic insoluble compounds, thus, Az can provide a correct level between nitrogen and phosphorus by producing suitable hormones or decreasing ethylene. It can lead to increment root and plant growth.<sup>21</sup> Foliar spray of SA leads to stimulation of root and shoot growth, and as well as strengthened the effect of PGPR on root and shoot growth.<sup>22</sup> Therefore, PGPRs can sustain plant grow under drought stress circumstances. SA, by cooperation in absorption and translocation of essential elements in the plant, caused an increasing plant growth.<sup>23</sup> Besides, foliar spray of SA acts as a cofactor in adjusting the physiological attributes, thus enhancing leaf water content and photosynthetic processes that lead to improved root hairs performance to uptake water and raise plant growth. As a result, it was observed that the application of PGPR with



**Figure 3.** Comparison of two-year means of carvacrol content *Satureja hortensis* by different bio-fertilizers and SA treatments under different irrigation levels. The letters a-m indicate that the same letter in each column are not significantly different according to the LSD test ( $p=0.05$ ). Control: W1 (Field capacity); *Medium stress*: W2 (6.5 atm); *Severe stress*: W3 (10 atm).

SA was effective in alleviating the detrimental effects of water deficit and improving the nutritional situation of plants.<sup>24</sup>

Decreased chlorophyll content under the water deficit condition agrees with other findings.<sup>24</sup> The reduction of chlorophyll a and b concentration may be related to the oxidative burst induced through drought stress, which can decompose these pigments via producing oxygen radicals in cells.<sup>25</sup> About this context, it was reported that application of the PGPR, SA, or their combination in wheat plants mitigated significantly injurious impacts of water deficiency.<sup>24</sup> In plants inoculated with PGPR, SA helped to improve the physiological attributes and photosynthetic activity via raised  $CO_2$  assimilation rates because of enhanced stomata conductance, RWC and photosynthetic pigment concentrations under water shortage.<sup>26</sup> Besides, increased chlorophyll concentration in leaves using PGPR alone or with SA could be related to higher accessibility of nutrients and improved organic matter in the Rhizosphere.<sup>23</sup>

Carotenoid concentration enhancement under water deficiency, in addition to protecting the photosynthetic apparatus, probably improved the cells' defensive system, therewith decreasing the destruction induced via oxidative stress.<sup>27</sup> On this subject, a reduction was seen in carotenoid contents in the thymus species under drought stress conditions,<sup>12</sup> but AMF with inoculation increased its contents, which is in line with our result. PGPRs could stimulate the manufacture of carotenoids via activating the plastidial methylerythritol phosphate (MEP) pathway as the precursor for the synthesis of carotenoids.<sup>28</sup> Thus, enhancing the carotenoid concentration stimulates defence mechanisms activated with these PGPRs to ameliorate plant endurance to stress status.<sup>29</sup>

The use of bio-fertilizers in severe drought stress can be more

efficient in reducing proline accumulation, in comparison with non-treated plants.<sup>14</sup> Proline acts as an essential signalling part against drought stress to stimulate mitochondria performing and change cell replication, increasing the expression of special recovery genes related to drought stress.<sup>30</sup> Increasing proline content helps to sustain membrane structure by protecting the cell redox potential and diminishing the reactive oxygen species (ROS) level through reducing lipids peroxidation.<sup>31</sup>

It has been revealed that *T. aestivum* that has a higher potential for accumulate proline shows higher percentages of endurance.<sup>32</sup> Also, the lowest proline content ( $22.1 \mu\text{g g}^{-1}$ ) was related to treatment inoculation with Az+AMF+SA. This treatment showed 45.9% decreases compared to the control. A similar observation reported that water stress statistically enhanced proline in two *Thymus* species but, all treatments inoculated with AMF resulted in reduced proline in every level of water stress.<sup>12</sup> The results of other research studies stated that plants treated with the combination of PGPR and SA significantly decreased the proline accumulation and brought the amounts near to the irrigation control treatment.<sup>33</sup> Although the *S. hortensis* plants were in water deficiency conditions (W2) and treated with Az+AMF or combination (Az+AMF+SA) did not show statistically significant differences regarding proline content compared to W1 treatments that were similar with the Hafez et al.<sup>24</sup> results. Besides, application SA on plants under stress conditions and inoculation with Az+AMF caused significant decreases of proline than non-application of SA ( $27$  and  $28.7 \mu\text{g g}^{-1}$ ). The Synergistic effects between PGPR and SA decreased the proline accumulation under water shortage situations due to the osmotic regulation, scavenging ROS and sustaining the integrity of subcellular constructions in plant cells, moderating of the adverse effects of water shortage.<sup>34</sup>

Lowering IAA content under stress may result from diminished IAA synthesis or a raise in the destruction of IAA by stimulating the activity of the oxidase enzyme.<sup>35</sup> However, PG-PRs with leak phytohormone in the soil can moderate the endogenous levels of phytohormone IAA.<sup>1</sup> Results exhibited that with rising drought stress levels, the IAA content decreased, which was similar to the previous report by Khan, et al.<sup>33</sup> The highest content of IAA ( $0.95 \mu\text{g g}^{-1}$  FW) was obtained with the use of Az+AMF and SA under irrigation W1 conditions, and the lowest content of this trait ( $0.80 \mu\text{g g}^{-1}$  FW) was related to the treatment of non-inoculation under W3 irrigation condition. Khan et al.<sup>33</sup> reported that spraying of SA was also efficient and improved the IAA content in both the shoot and rhizosphere. The application PGPR, SA, and their combined treatment raised the IAA significantly.<sup>33</sup> When plants were inoculated with AZ+AMF, AMF alone, and with SA, Az+SA under stress conditions showed no significant difference compared to plants under the W1 conditions. All the treatments have ameliorative results, but the treatment with SA exhibited a lessened influence in this context, which could be due to the fundamental difference between the PGPR and SA in the biosynthesis or modulation of phytohormones. In general, IAA production is due to the direct operation of PGPR on crops, that enhances the number of root and absorption surface area of the plant. Therefore, under drought stress follows efficient absorption of nutrients and water by plant roots.<sup>36</sup> High levels of IAA are produced via the intermediate indole-pyruvic acid pathway.<sup>37</sup> The presence of the ipdC gene in the bacteria gives it the capacity to provide enough contents of IAA that could be utilized for plant growth increment.<sup>38</sup>

Previous studies have proved that carvacrol, thymol, and their precursors, p-cymene, and - terpinene are the main components of the *S. hortensis* oil.<sup>39</sup> As well as the concentrations of carvacrol and thymol in Iranian accessions of *S. hortensis* are deficient. Although the essential oil content and its composition in *S. hortensis* is genetically controlled, but variations in phytochemical characters have different origins.<sup>40</sup> Biosynthesis of essential oil components is relevant to producing valuable terpenes that can be considered a defensive response to different stresses.<sup>41</sup> It has been reported that environmental factors such as water stress and inoculation with biofertilizers could significantly influence the biosynthetic pathway and accumulation of natural compounds. As well as was demonstrated that with the use of AMF or rhizobacteria, the production of valuable terpenes in the plant would also be altered.<sup>4</sup> Mohammadi et al.<sup>42</sup> reported that inoculation of *S. hortensis* with certain *P. fluorescens* Migula strains can significantly increase the plant biomass and some essential oil yields under water stress conditions.

## CONCLUSION

The findings of this work demonstrated that the percentage and composition of the essential oil in *S. hortensis* increased significantly under W2 and W3 treatments, while decreased plant FW and DW, chlorophylls and carotenoid contents, and IAA. Application of these rhizobacteria and fungi in soil and spraying SA improved the growth and tolerance of plants under stress by increasing proline, carvacrol, and thymol. The improved growth in response to biofertilizers inoculation at each level of irrigation could be ascribed to the biosynthesis IAA, thereby regulating root development and defence system metabolism to improve drought-tolerance.

**Peer Review:** Externally peer-reviewed.

**Author Contributions:** Conception/Design of Study- P.K., M.G.; Data Acquisition- H.R.T.M., M.N., H.L., M.G.; Data Analysis/Interpretation- P.K., M.G., M.N.; Drafting Manuscript- P.K., M.G., H.R.T.M.; Critical Revision of Manuscript- H.R.T.M., M.N., H.L., M.G.; Final Approval and Accountability- M.G., P.K., H.R.T.M., M.N., H.R.L.

**Conflict of Interest:** Authors declared no conflict of interest related to this article.

**Financial Disclosure:** Authors declared no financial support.

## ORCID IDs of the authors

Mahmood Ghojavand	0000-0001-7336-0988
Porang Kasraei	0000-0001-5831-6604
Hamid Reza Tohidi Moghadam	0000-0002-9759-9886
Mohammad Nasri	0000-0003-2352-3966
Hamid Reza Larijani	0000-0002-4010-5304

## REFERENCES

- Achard P, Gusti A, Cheminant S, et al. Gibberellin signaling controls cell proliferation rate in Arabidopsis. *Curr Protoc.* 2009;19(14):1188-1193.
- Anjum S, Wang L, Farooq M, Khan I, Xue L. Methyl jasmonate induced alteration in lipid peroxidation, antioxidative defence system and yield in soybean under drought. *J Agron Crop Sci.* 2011a;197(4):296-301.
- Elewa TA, Sadak MS, Saad AM. Proline treatment improves physiological responses in quinoa plants under drought stress. *Biol Res.* 2017;14(1):21-33.
- Banchio E, Bogino PC, Zygadlo J, Giordano W. Plant growth promoting rhizobacteria improve growth and essential oil yield in *Origanum majorana* L. *Biochem Syst Ecol.* 2008;36(10):766-771.
- Smith SE, Facelli E, Pope S. Plant performance in stressful environments: interpreting new and established knowledge of the roles of arbuscular mycorrhizas. *Plant and Soil.* 2010;326:3-20.
- Brundrett MC, Tedersoo L. Evolutionary history of mycorrhizal symbioses and global host plant diversity. *New Phytol.* 2018;220(4):1108-1115.
- Bakry B, El-Hariri D, Sadak M, El-Bassiouny H. Drought stress



- mitigation by foliar application of salicylic acid in two linseed varieties grown under newly reclaimed sandy soil. *J Appl Sci Res.* 2012;8(7):3503-3514.
8. Lichtenthaler HK, Buschmann C. Chlorophylls and carotenoids: Measurement and characterization by UV-VIS spectroscopy. *Curr Protoc Food Anal Chem.* 2001;1:F4-3. doi.org/10.1002/0471142913.faf0403s01.
  9. Pang YX, Fan ZW, Wang D, et al. External application of the volatile oil from *Blumea balsamifera* may be safe for liver-A study on its chemical composition and hepatotoxicity. *Molecules* 2014;19:18479–18492.
  10. He Y, Oyaizu H, Suzuki S. Indole-3-acetic acid production in *Pseudomonas fluorescens* HP72 and its association with suppression of creeping bentgrass brown patch. *Curr Microbiol.* 2002;47:138–143.
  11. Bates LS, Waldren RP, Teare ID. Rapid determination of free proline for water-stress studies. *Plant Soil.* 1973;39:205.
  12. Arpanahi AA, Feizian M, Mehdipourian G, Khojasteh DN. Arbuscular mycorrhizal fungi inoculation improve essential oil and physiological parameters and nutritional values of *Thymus daenensis* Celak and *Thymus vulgaris* L. under normal and drought stress conditions. *Eur J Biol.* 2020;100:103217.
  13. Hu Y, Schmidhalter U. Drought and salinity: A comparison of their effects on mineral nutrition of plants. *J Plant Nutr Soil Sci.* 2005;168:541–549.
  14. Javan Gholiloo M, Yarnia M, Ghorttpeh AH. Evaluating effects of drought stress and bio-fertilizer on quantitative and qualitative traits of valerian (*Valeriana officinalis* L.). *J Plant Nutr.* 2019;42(13):1417-1429.
  15. Kader M, Mian, M. Hoque, M. Effects of Azotobacter inoculant on the yield and nitrogen uptake by wheat. *J Biol Sci.* 2002;2(4):259-261.
  16. Kasim WA, Osman ME, Omar MN, Abd El-Daim IA, Bejai S, Meijer J. Control of drought stress in wheat using plant-growth-promoting bacteria. *J Plant Growth Regul.* 2013;32(1):122-130.
  17. Asl KK, Hatami M. Application of zeolite and bacterial fertilizers modulates physiological performance and essential oil production in dragonhead under different irrigation regimes. *Acta Physiol Plant.* 2019;41(1):17.https://doi.org/10.1007/s11738-018-2801-x.
  18. Vessey JK. Plant growth promoting rhizobacteria as biofertilizers. *Plant and Soil.* 2003;255:571-586.
  19. Joshee N, Mentreddy S, Yadav AK. Mycorrhizal fungi and growth and development of micropropagated *Scutellaria integrifolia* plants. *Ind Crops Prod.* 2007;25(2):169-177.
  20. Schippers B, Bakker A, Bakker P, Van Peer R. Beneficial and deleterious effects of HCN-producing pseudomonads on rhizosphere interactions. *Plant and Soil.* 1990;129(1):75-83.
  21. Copetta A, Lingua G, Berta G. Effects of three AM fungi on growth, distribution of glandular hairs, and essential oil production in *Ocimum basilicum* L. var. Genovese. *Mycorrhiza.* 2006;16(7):485-494.
  22. Hafez E, Gharib H. Effect of exogenous application of ascorbic acid on physiological and biochemical characteristics of wheat under water stress. *Int J Plant Prod.* 2016;10(4):579-596.
  23. Khan N, Bano A, Babar MA. The root growth of wheat plants, the water conservation and fertility status of sandy soils influenced by plant growth promoting rhizobacteria. *Symbiosis.* 2017;72(3):195-205.
  24. Hafez E, Omara AED, Ahmed A. The coupling effects of plant growth promoting rhizobacteria and salicylic acid on physiological modifications, yield traits, and productivity of wheat under water deficient conditions. *Agron.* 2019;9(9):524.
  25. Anjum SA, Xie X-Y, Wang L-C, Saleem MF, Man C, Lei W. Morphological, physiological and biochemical responses of plants to drought stress. *Afr J Agric Res.* 2011b;6(9):2026-2032.
  26. Hafez EM, Ragab AY, Kobata T. Water-use efficiency and ammonium-N source applied of wheat under irrigated and desiccated conditions. *Int J Plant Soil Sci.* 2014;3(10):1302-1316.
  27. Ramel F, Birtic S, Ginies C, Soubigou-Taconnat L, Triantaphyllidès C, Havaux M. Carotenoid oxidation products are stress signals that mediate gene responses to singlet oxygen in plants. *Proc Natl Acad Sci.*2012;109(14):5535-5540.
  28. Baslam M, Esteban R, García-Plazaola JI, Goicoechea N. Effectiveness of arbuscular mycorrhizal fungi (AMF) for inducing the accumulation of major carotenoids, chlorophylls and tocopherol in green and red leaf lettuces. *Appl Microbiol Biotechnol.* 2013;97(7):3119-3128.
  29. Kamali S, Mehraban A. Nitroxin and arbuscular mycorrhizal fungi alleviate negative effects of drought stress on Sorghum bicolor yield through improving physiological and biochemical characteristics. *Plant Signaling Behav.* 2020;15(11):1813998.
  30. Jayant KS, Sarangi S. Effect of drought stress on proline accumulation in peanut genotypes. *Int J Adv Res.* 2014;2(10):301-309.
  31. Shinde S, Villamor JG, Lin W, Sharma S, Verslues PE. Proline coordination with fatty acid synthesis and redox metabolism of chloroplast and mitochondria. *Plant Physiol.* 2016;172(2):1074-1088.
  32. Zhou W, Li Y, Zhao B-C, et al. Overexpression of TaSTRG gene improves salt and drought tolerance in rice. *J Plant Physiol.* 2009;166(15):1660-1671.
  33. Khan N, Bano A, Curá JA. Role of beneficial microorganisms and salicylic acid in improving rainfed agriculture and future food safety. *Microorg.* 2020;8(7):1018.
  34. Hafez E, Seleiman M. Response of barley quality traits, yield and antioxidant enzymes to water-stress and chemical inducers. *Int J Plant Prod.* 2017;11(4):477-490.
  35. Muhammad N, Hakim Quraishi U, Chaudhary HJ, Munis MFH. Indole-3-acetic acid induces biochemical and physiological changes in wheat under drought stress conditions. *Philipp Agric Sci.* 2016;99:19-24.
  36. Vacheron J, Desbrosses G, Bouffaud M-L, et al. Plant growth-promoting rhizobacteria and root system functioning. *Fron Plant Sci.* 2013;4:356. https://doi.org/10.3389/fpls.2013.00356.
  37. Ahmed A, Hasnain S. Auxins as one of the factors of plant growth improvement by plant growth promoting rhizobacteria. *Pol J Microbiol.* 2014;63(3):261-266.
  38. Rosier A, Medeiros FH, Bais HP. Defining plant growth promoting rhizobacteria molecular and biochemical networks in beneficial plant-microbe interactions. *Plant and Soil.* 2018;428(1-2):35-55.
  39. Vernet P, Gouyon R, Valdeyron G. Genetic control of the oil content in *Thymus vulgaris* L: A case of polymorphism in a biosynthetic chain. *Genetica.* 1986;69(3):227-231.
  40. Pank F, Pfefferkorn A, Kruger H. Evaluation of a summer savory collection (*Satureja hortensis* L.) with regard to morphology, precocity, yield components and essential oil and carvacrol content, *Zeitschrift Fur Arznei Und Gewurzpflanzen.* 2004;p.72.
  41. Selmar D, Kleinwächter M. Stress enhances the synthesis of secondary plant products: the impact of stress-related over-reduction on the accumulation of natural products. *Plant and Cell Physiol.* 2013;54(6):817-826.

42. Mohammadi H, Dashi R, Farzaneh M, Parviz L, Hashempour H. Effects of beneficial root pseudomonas on morphological, physiological, and phytochemical characteristics of *Satureja hortensis* (*Lamiaceae*) under water stress. *Braz J Biol.* 2017;40(1): 41-48.

**How cite this article**

Ghojavand M, Kasraei P, Moghadam HRT, Nasri M, Larijani HR. Effects of Salicylic Acid and Microorganisms on Morphological and Physiological Characteristics (*Satureja hortensis* L.) under Drought Stress. *Eur J Biol* 2023;82(1): 12-22. DOI: 10.26650/EurJBiol.2023.1196479

# Evaluation of Oxidative Protein Damage in Patients with Type 1 and 2 Diabetes Mellitus in Bangladesh

Sanjeda Tamanna<sup>1</sup>,  Rocky Sheikh<sup>1</sup>,  Taslimul Jannat<sup>1</sup>,  Laila Noor Islam<sup>1</sup> 

<sup>1</sup>University of Dhaka, Department of Biochemistry and Molecular Biology, Dhaka-1000, Bangladesh

## ABSTRACT

**Objective:** Oxidative stress (OS) has been linked to the development and progression of diabetes mellitus (DM). Although maintaining the redox status of protein is crucial for proper cellular function, proteins are likely to be damaged by OS. Therefore, the present study aimed to evaluate oxidative protein damage (OPD) in patients with DM.

**Materials and Methods:** A total of 160 participants were recruited, of whom 16 were patients with type 1 DM (T1DM), 84 were patients with type 2 DM (T2DM), and 60 were healthy control subjects. The activities of NADPH oxidase (NOX) and myeloperoxidase (MPO); total oxidative stress (TOS), ferric reducing ability of plasma (FRAP), oxidative stress index (OSI); serum albumin; OPD markers-total thiols (T-SH), protein carbonyls (PCO), and advanced oxidation protein products (AOPP) were assessed.

**Results:** The activities of serum NOX and MPO were significantly higher in both DM groups compared to controls. Significantly higher TOS and OSI and lower FRAP values were observed in both DM groups than in controls ( $p < 0.001$ , for all). In patients, the levels of albumin and T-SH were significantly lower, but PCO was significantly elevated, while AOPP was higher in T1DM and significantly elevated in T2DM compared to controls. Correlation analyses between these parameters linked hyperglycemia with enhanced NOX, MPO and AOPP, and decreased FRAP and T-SH in diabetic patients. Further, significant correlations of albumin with T-SH and AOPP suggested an association of OS with hypoalbuminemia.

**Conclusion:** These findings highlight that hyperglycemia induces enhanced OS and consequent protein damage in both T1DM and T2DM patients.

**Keywords:** Oxidative protein damage, Advanced oxidation protein products, Total thiols, Ferric reducing ability of plasma, Type 1 diabetes mellitus, Type 2 diabetes mellitus

## INTRODUCTION

Diabetes is characterized by chronic hyperglycemia associated with damage, dysfunction, and failure of different organs, which consequently manifest various complications.<sup>1</sup> One of the major mechanisms underlying the onset of diabetes and latter diabetic complications is oxidative stress (OS), an imbalance between free radical generation and the antioxidant defense systems.<sup>2</sup> OS plays a pivotal role in the autoimmune destruction of pancreatic  $\beta$ -cells in type 1 diabetes mellitus (T1DM) and in type 2 diabetes mellitus (T2DM), which can cause insulin resistance.<sup>3</sup>

Hyperglycemia can augment the activity of reactive oxygen species (ROS)-generating enzymes such as nicotinamide adenine dinucleotide phosphate (NADPH) oxidase (NOX) and

myeloperoxidase (MPO).<sup>4,5</sup> The higher activity of NOX as a major source of ROS has been implicated in the pathophysiology of diabetic vascular disease and diabetic nephropathy.<sup>6</sup> The heme enzyme MPO utilizes hydrogen peroxide to oxidize chloride and generates oxidants, hypochlorous acids (HOCl). These oxidants can modify cellular macromolecules, leading to damage of tissues.<sup>7</sup> There is growing evidence that MPO is associated with insulin resistance and inflammation.<sup>8</sup> Analysis of MPO activity in diabetic patients provides a way to assess both OS and cardiovascular disease (CVD) risk considering its involvement in the pathophysiology of the latter.<sup>9</sup>

Higher levels of ROS cause peroxidation of lipids, amino acids, peptides, and proteins with the resultant production of hydroperoxides.<sup>10</sup> These hydroperoxides have been measured as total oxidative stress (TOS) marker in diabetes.<sup>11</sup> The ferric

**Corresponding Author:** Laila Noor Islam E-mail: laila@du.ac.bd

Submitted: 17.05.2023 • Revision Requested: 22.05.2023 • Last Revision Received: 26.05.2023 • Accepted: 07.06.2023



This article is licensed under a Creative Commons Attribution-NonCommercial 4.0 International License (CC BY-NC 4.0)

reducing ability of plasma (FRAP) manifests the total antioxidant capacity (TAC) based on the cumulative actions of total antioxidants in plasma to inhibit the oxidative effects of ROS. Furthermore, the oxidative stress index (OSI), a ratio of TOS to TAC, might more accurately index oxidant/antioxidant imbalance in diabetic patients.<sup>12</sup>

Albumin is a powerful extracellular antioxidant which contributes more than 70% to the free radical-trapping activity of blood plasma.<sup>13</sup> The conformation of albumin is altered in OS, allowing its thiol groups to be oxidized and decreased in number. The assessment of plasma total thiol (T-SH) levels reliably indicates excessive free radical generation in the body.<sup>14</sup> Protein carbonyls (PCO) are formed when proteins undergo oxidative damage when ROS react with the side chains of certain amino acid residues in proteins including lysine, arginine, proline, and threonine.<sup>15</sup> A novel protein oxidation marker is advanced oxidation protein products (AOPP), which correspond to highly oxidized proteins, especially albumin, and are formed from reactions of MPO-derived chlorinated oxidants and proteins. They include oxidatively modified protein aggregates by disulfide bridges and/or tyrosine cross-linking.<sup>16</sup>

The maintenance of the protein redox state is crucial for cell function. Increased aggregation, fragmentation, distortion of secondary and tertiary structures, susceptibility to proteolysis, and reduction in normal function might result from changes in protein conformations brought on by ROS attack.<sup>17</sup> Therefore, this study was designed to evaluate the oxidative damage to proteins by the analysis of albumin, T-SH, PCO and AOPP markers together with the investigation of NOX and MPO activities and levels of TOS, FRAP and OSI in diabetic patients and compare these findings with a non-diabetic control group.

## MATERIALS AND METHODS

### Study Design

This study was approved by the Ethical Review Committee of the Faculty of Biological Sciences, University of Dhaka, Bangladesh (Ref. No. 108 /Biol. Sci. /2020-2021), and the Diabetic Association of Bangladesh. The study was conducted from January 2021 to May 2022. All the participants gave their informed consent before being enrolled in the study.

A total of 160 subjects were enrolled, of whom 100 were diabetics, comprising 16 T1DM and 84 T2DM patients; the remaining 60 were non-diabetic controls. The patients were randomly approached from the outpatient department of the Bangladesh Institute of Research and Rehabilitation in Diabetes, Endocrine and Metabolic Disorders (BIRDEM) General Hospital. They were previously diagnosed with diabetes and expert physicians distinguished T1DM and T2DM according to the criteria of the American Diabetes Association.<sup>18</sup> The control group was randomly selected from the local community. The study included participants aged 20-50 years and excluded

those having CVD and/or nephropathy. Participants suffering from any condition known to cause OS were excluded from the study to avoid false positive results.

### Data and Sample Collection

The general health information of the participants including age, gender, height, weight, blood pressure, fasting plasma glucose (FPG), glycosylated hemoglobin HbA1c (%), disease duration, family history of diabetes, smoking status, hypertension, diabetic complications, and medications were recorded. Blood samples were collected, and the plasma and serum were separated, collected in small aliquots, and stored at  $-20^{\circ}\text{C}$  until analyzed.

### Assay Procedures

Serum NOX activity was measured using the method established by Reusch and Burger, as detailed previously.<sup>19,20</sup> Serum MPO activity was determined by Bradley et al.'s method<sup>21</sup>. The detailed procedure has been described elsewhere.<sup>22</sup> A modified free oxygen radical test was used to assess the level of plasma TOS and the result was expressed as mmol/L of  $\text{H}_2\text{O}_2$  equivalents.<sup>11</sup> The total antioxidant capacity (TAC) was determined by the FRAP assay, as detailed in a recent study.<sup>23,24</sup> The OSI was determined by the ratio of TOS to TAC<sup>12</sup>, and expressed in arbitrary units (AU), according to the following formula:  $\text{OSI (AU)} = \text{TOS} / \text{TAC}$ .

### Determination of Oxidative Protein Damage

The serum albumin level was estimated using the bromocresol green (BCG) method, as detailed previously.<sup>25,26</sup> The level of T-SH in plasma was measured by Hu's method.<sup>14</sup> The plasma PCO content was quantified by the 2,4-dinitrophenylhydrazine method described by Levine et al.<sup>27</sup> Serum AOPP levels were determined using the method of Witko-Sarsat et al.<sup>16</sup>, with slight modifications. In brief, 300  $\mu\text{L}$  diluted serum (1/10 in phosphate buffer saline) or chloramine T trihydrate (Merck) standard was mixed with 150  $\mu\text{L}$  of acetic acid and 75  $\mu\text{L}$  potassium iodide. The absorbance of the reaction mixture was read after 2 minutes at 340 nm. AOPP concentrations were expressed as  $\mu\text{M}$  chloramine T equivalents.

### Statistical Analyses

Statistical analysis and graphical presentation of the data were performed using GraphPad Prism (version 8.0.1, GraphPad Software, USA). Statistical significance of differences between the values of the continuous variables in the three groups (T1DM, T2DM and controls) was assessed by one-way ANOVA (Analysis of Variance) with post-hoc Games-Howell's multiple comparisons test. For each parameter, the mean  $\pm$  SD

values were computed. The chi squared test was used to compare categorical variables. Spearman's correlation was conducted to evaluate the correlation between variables. The results were considered significant when  $p$  value was  $<0.05$ .

## RESULTS

### Baseline Characteristics of the Studied Subjects

A comparison of the baseline characteristics of the studied subjects has been presented in Table 1. It was found that both the T1DM and T2DM patients had significantly higher FPG levels compared to the controls ( $p<0.05$  and  $p<0.001$ , respectively), FPG among the three groups was significantly different ( $p<0.001$ , one-way ANOVA), while the level between T1DM and T2DM patients did not differ significantly. The mean disease duration of the T1DM and T2DM patients were  $12.8 \pm 9.4$  and  $4.8 \pm 3.7$  years, respectively.

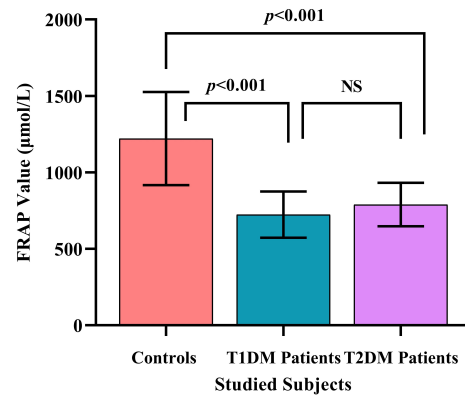
Statistical analyses of the values in the three groups showed family history of diabetes was significantly higher among the diabetics ( $p<0.01$ , Table 1), but a pairwise analysis revealed that compared to the controls, the family history of diabetes was significantly associated with the development of diabetes in T2DM patients only ( $\chi^2 = 12.5$ ,  $p<0.001$ ). On the other hand, there was no significant relationship between hypertension or smoking with the risk of developing diabetes. Among all patients, the number of diabetics taking oral hypoglycemic drug, insulin injection, or both were 24, 37, and 33, respectively, and 8 had retinopathy, 9 had neuropathy, and 11 had both complications.

### Comparison of NOX, MPO, TOS, FRAP and OSI

It was found that the mean activities of the oxidase enzymes NOX and MPO were significantly higher in both T1DM and T2DM patients compared to control subjects (NOX:  $p<0.01$  and  $p<0.001$ , respectively; MPO:  $p<0.001$ , both), while the activities between the T1DM and T2DM patients did not differ significantly (Table 2). Similarly, the mean TOS values in both T1DM and T2DM patients were significantly elevated compared to controls ( $p<0.001$ , both) (Table 2), and no significant difference was found between the DM groups. The mean FRAP value in the control subjects was  $1221.1 \pm 305.0 \mu\text{mol/L}$ , and in the T1DM and T2DM patients were  $723.6 \pm 150.9 \mu\text{mol/L}$  and  $789.6 \pm 142.1 \mu\text{mol/L}$ , respectively, which were significantly lower ( $p<0.001$ , both) (Figure 1). The mean OSI values were significantly elevated in both types of DM patients compared to the controls ( $p<0.001$ , both) (Table 2). The OSI values between the DM groups were not significantly different.

### Evaluation of Oxidative Protein Damage

The mean serum albumin levels in the T1DM and T2DM patients were  $41.0 \pm 10.0 \text{ g/L}$  and  $45.0 \pm 6.0 \text{ g/L}$ , respectively,



**Figure 1.** Comparison of the ferric reducing ability of plasma (FRAP) values between the studied subjects. Both types of diabetic patients had significantly lower FRAP values compared to the controls. There was no significant difference between the FRAP values of T1DM and T2DM patients.

which were significantly lower than  $51.0 \pm 7.0 \text{ g/L}$  in the controls ( $p<0.01$  and  $p<0.001$ , respectively). The albumin levels in T1DM and T2DM patients were not significantly different. The mean T-SH concentration in the control subjects was  $472.7 \pm 61.5 \mu\text{M}$ , and the corresponding values in the T1DM and T2DM patients were  $301.1 \pm 139.2 \mu\text{M}$  and  $323.6 \pm 132.7 \mu\text{M}$ , respectively, which were significantly lower ( $p<0.001$ , both).

Investigation of PCO showed significantly higher values in both T1DM and T2DM patients compared to controls ( $p<0.01$ , both), and the mean values were  $2.2 \pm 0.5$ ,  $2.1 \pm 0.8$  and  $1.6 \pm 0.8 \text{ nmol/mg}$ , respectively (Figure 2). The mean AOPP levels in the controls, T1DM, and T2DM patients were  $441.6 \pm 215.7$ ,  $605.7 \pm 235.6$ , and  $624.3 \pm 233.1 \mu\text{M}$  chloramine T equivalents, respectively (Figure 3). Statistical analyses revealed that the T2DM patients had significantly elevated AOPP levels compared to the controls ( $p<0.001$ ) but the level in T1DM patients was not significantly elevated ( $p=0.053$ ).

### Correlations Between Different Parameters

Spearman correlation analyses between different parameters of the pooled DM patients and control subjects have been presented in Table 3. There was a significant negative correlation between AOPP and albumin ( $p=0.006$ ) (Figure 4a) and a significant positive correlation between OSI and FPG ( $p=0.004$ ) (Figure 4b) in DM patients, which were not found in controls. In DM patients, NOX and MPO each showed significant positive correlations with FPG ( $p=0.003$  and  $p=0.049$ , respectively), and a significant negative correlation was found between FRAP and FPG ( $p<0.001$ ). No such significant correlations were observed in controls. A significant positive correlation was found between TOS and OSI in both DM patients and controls ( $p<0.001$ , both). The patients showed significant positive correlations of T-SH with albumin ( $p=0.001$ ), and NOX with OSI ( $p=0.027$ ). Further, AOPP significantly correlated with NOX in controls

**Table 1.** Comparison of baseline characteristics of the control subjects, T1DM and T2DM patients.

Variables	Controls (N=60)	T1DM (N=16)	T2DM (N=84)	Statistics (p-value)
Gender (M/F) (%)	80/20	94/6	90/10	0.128*
Age (years)	38.5 ± 6.0	34.4 ± 8.0	38.7 ± 4.8	0.075 <sup>‡</sup>
FPG (mmol/L)	5.2 ± 0.3	10.1 ± 6.3	10.3 ± 4.5	< 0.001 <sup>‡</sup>
HbA1c (%)	-	11.7 ± 2.0	8.7 ± 2.8	NA
BMI (kg/m <sup>2</sup> )	25.5 ± 3.7	23.2 ± 2.9	24.5 ± 3.0	0.061 <sup>‡</sup>
SBP (mmHg)	128.7 ± 12.0	130.0 ± 16.0	132.0 ± 19.5	0.512 <sup>‡</sup>
DBP (mmHg)	88.2 ± 10.4	94.3 ± 19.7	92.6 ± 11.0	0.217 <sup>‡</sup>
Family history of DM: positive/negative (%)	34/66	50/50	65/35	< 0.01*
Hypertension (%)	40	40	44	0.945*
Smoking status: current/ex-smokers/non-smokers (%)	18/2/80	25/13/62	17/11/72	0.336*

T1DM, type 1 diabetes mellitus; T2DM, type 2 diabetes mellitus; M, male; F, female; FPG, fasting plasma glucose; HbA1c, glycosylated hemoglobin; NA, not applicable; BMI, body mass index; SBP, systolic blood pressure; DBP, diastolic blood pressure; \*, p-value of chi-square test; <sup>‡</sup>, p-value of one-way ANOVA (analysis of variance).

**Table 2.** Comparison of NOX and MPO activities, and TOS and OSI values between the control subjects, T1DM and T2DM patients.

Parameters	Controls	T1DM	T2DM	p-value (ANOVA Post-hoc)	
				Control vs. T1DM	Control vs. T2DM
NOX (U/L)	6.3 ± 1.8	9.5 ± 2.8	11.3 ± 3.2	<0.01	<0.001
MPO (U/L)	45.8 ± 12.7	58.6 ± 10.2	64.5 ± 11.3	<0.001	<0.001
TOS (mmol/L)	11.4 ± 2.3	16.3 ± 3.7	15.0 ± 4.0	<0.001	<0.001
OSI (AU)	10.1 ± 3.6	24.0 ± 9.2	20.6 ± 7.0	<0.001	<0.001

T1DM, type 1 diabetes mellitus; T2DM, type 2 diabetes mellitus; NOX, NADPH oxidase; MPO, myeloperoxidase; TOS, total oxidative stress; OSI, oxidative stress index; ANOVA, analysis of variance; U/L, unit per liter; mmol/L, millimole per liter; AU, arbitrary units.

(p=0.007), but this correlation was not significant in DM patients.

## DISCUSSION

This study investigated OPD in patients with diabetes mellitus by assessing activities of NOX and MPO, and levels of oxidative stress (OS) along with OPD markers, and compared the findings with a control group. The study enrolled younger patients of 20 to 50 years to avoid additional OS caused by older age-related diabetic complications. Both the T1DM and T2DM patients had significantly higher FPG levels compared to the controls. The family history of diabetes among first-degree relatives was found to be associated with the incident risk of T2DM in patients, which was in line with a previous study.<sup>28</sup> No such significant association was found in T1DM patients. The reason could be the small number of T1DM patients in this

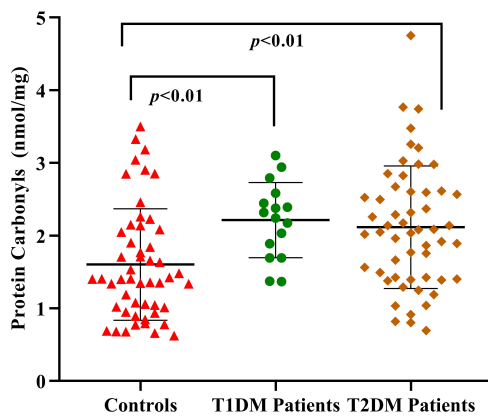
study, and also the incident risk of T2DM was more associated with family history than T1DM was.<sup>18</sup> Therefore, this finding suggests that family history could be used as an important tool for identifying the people at risk of developing diabetes.

This study demonstrated significantly higher NOX activities in both DM patient groups compared to the controls, and a significant positive association was observed between FPG and NOX in diabetic patients. These findings support a previous study showing hyperglycemia-induced higher NOX activity in T2DM patients and a positive correlation between glucose levels and p22phox expression, a critical component of NOX activation.<sup>4</sup> The current findings of significantly higher MPO activities in both types of DM patients were consistent with previous findings in T1DM and T2DM patients.<sup>5,29</sup> The latter study further reported enhanced levels of ROS including HOCl in the cultured peripheral blood mononuclear cells of T2DM

**Table 3.** Spearman correlation analysis between different parameters in diabetic patients and control subjects.

Correlation of parameters	Spearman correlation coefficient, $\rho$	<i>p</i> -value
<b>Diabetic Patients</b>		
FPG-NOX	0.428	0.003
FPG-MPO	0.236	0.049
FPG-OSI	0.325	0.004
FPG-FRAP	-0.693	<0.001
Duration of DM-FRAP	-0.324	0.003
TOS-OSI	0.766	<0.001
FRAP-OSI	-0.580	<0.001
NOX-OSI	0.378	0.027
T-SH-Albumin	0.377	0.001
AOPP-Albumin	-0.327	0.006
AOPP-NOX	0.181	0.229
<b>Control subjects</b>		
AOPP-NOX	0.379	0.007
TOS-OSI	0.508	<0.001
FRAP-OSI	-0.728	<0.001

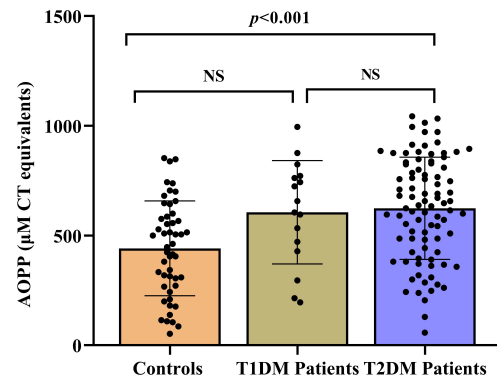
DM, diabetes mellitus; FPG, fasting plasma glucose; NOX, NADPH oxidase; MPO, myeloperoxidase; TOS, total oxidative stress; FRAP, ferric reducing ability of plasma; OSI, oxidative stress index; T-SH, total thiol; AOPP, advanced oxidation protein products.



**Figure 2.** Comparisons of the protein carbonyls (PCO) levels in the studied subjects. Both types of diabetic patients had significantly higher PCO levels compared to the controls. There was no significant difference between the PCO levels of T1DM and T2DM patients.

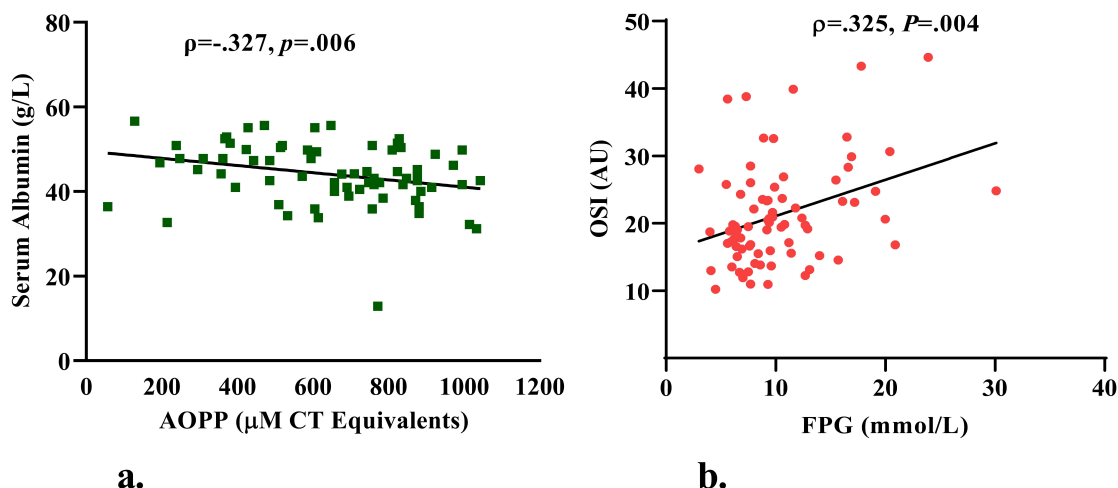
patients in higher glucose condition.<sup>5</sup> Interestingly, the present study also found a significant positive correlation between FPG and MPO in diabetic patients. The enhanced activities of these two enzymes and their associations with FPG corroborate the involvement of hyperglycemia in the increased generation of ROS and higher OS in diabetes.

The present study demonstrated that both types of diabetic patients had significantly higher TOS levels than the controls,



**Figure 3.** Comparisons of the advanced oxidation protein products (AOPP) levels in  $\mu\text{M}$  Chloramine T (CT) equivalents between the studied subjects. The T2DM patients had significantly higher AOPP levels than the controls.

which was consistent with previous findings.<sup>11,30</sup> Elevated TOS levels provide pronounced evidence of oxidative damage in diabetic patients. This study further showed that the FRAP values were significantly lower in both types of diabetic patients, which confirmed existing studies reporting lower FRAP values in patients with DM.<sup>31,32</sup> Furthermore, there were significant negative correlations of FRAP with FPG and duration of diabetes. Similar findings were reported in other studies that validated the current observations.<sup>32,33</sup> These findings indicated that the exogenous pool of total antioxidants was depleted gradually by



**Figure 4.** Spearman correlation analyses showed a significant negative correlation between advanced oxidation protein products (AOPP) and serum albumin (a), and a significant positive correlation of oxidative stress index (OSI) with fasting plasma glucose (FPG) (b) in diabetic patients (T1DM + T2DM).

the increased oxidants, resulting from hyperglycemia, leading to disturbed redox balance in plasma and the progression of diabetes.

The current study showed significantly higher OSI values in both types of DM patients, which suggests a greater intensity of OS. Accordingly, OSI was positively associated with TOS, and FPG, and negatively with FRAP. The significant increase of OSI in diabetic patients and its association with FPG were in accordance with previous findings.<sup>12</sup> The association of OSI with NOX and FPG highlighted OSI as a promising marker to evaluate oxidant/antioxidant imbalance and further indicated linkage of hyperglycemia with OS. The current findings of significantly lower levels of serum albumin in both types of DM patients corroborated a similar observation in diabetic patients.<sup>34</sup> Previous studies reported an association of hypoalbuminemia with an increased risk of ketosis in patients with T2DM.<sup>35</sup>

The present study found significantly elevated PCO and AOPP, and significantly lower T-SH levels in T2DM patients. The T1DM patients demonstrated significantly higher PCO, but the AOPP levels were slightly elevated without any significant difference from controls, while the T-SH levels were significantly lower. Overall, these findings are in accordance with those reported by previous investigators.<sup>31,36–38</sup> Taken together, the present study explored the effects of hyperglycemia-induced ROS generating enzymes/oxidants and evaluated subsequent deleterious damage to proteins in both types of diabetic patients.

The most important findings of the present study include significant positive and negative correlations of albumin in diabetic patients with two OPD markers, T-SH and AOPP, respectively. The most compelling explanation of these correlations

could be that extremely oxidative conditions modify albumin through irreversible oxidations of its cysteine-34 residue and hence lessen thiol levels; AOPP are known to be oxidized albumin products in aggregate or monomeric forms<sup>16</sup>, therefore, oxidative modifications of albumin may lead to underestimation of total albumin concentrations by the conventional bromocresol green assay method, which may be the reason for inverse correlation with AOPP. The interpretation that protein oxidation might interfere with albumin measurement was supported by previous studies.<sup>39</sup>

The present study showed a noteworthy finding in a significant positive correlation between AOPP and NOX in control subjects. Growing evidence demonstrated that AOPP might be not only a marker of oxidant-mediated protein damage, but also a potential inducer of oxidative stress and inflammation by activating neutrophils, monocytes, and T lymphocytes.<sup>40</sup> A previous study reported that AOPP mediates the activation of NOX to induce ROS generation in human endothelial cells.<sup>41</sup> These studies indirectly supported the correlation of AOPP with NOX.

Finally, there were at least two potential limitations to this investigation. The first limitation concerned the small sample size, particularly since the number of T1DM patients was extremely low. Due to the lower prevalence of T1DM, stringent inclusion criteria and the need to perform the analysis on fresh samples, it was difficult to collect a large number of samples. The second limitation was that the analysis was performed on patients, the majority of whom were on some form of anti-diabetic treatment, which might play a role in subduing some of their oxidative stress and represent a partial result. Despite these limitations, the significant findings of this study on oxidative protein damage in patients with T1DM and T2DM could



be used as a reference for future studies with larger sample size, considering the significance of the measured parameters, and also taking into account the use of anti-diabetic treatment.

## CONCLUSION

The present study showed increased activities of oxidative enzymes NOX and MPO and decreased FRAP levels, reflecting disturbances between ROS and antioxidants in patients with diabetes mellitus. Increased levels of TOS and OPD markers indicate damage of cellular macromolecules in diabetic patients and draw attention to future intervention studies concerning the development of secondary diabetic complications. The correlations of parameters with FPG observed in this study showed hyperglycemia triggering both the excessive burden of oxidants and the declined FRAP levels in diabetic patients. This study sheds light on the concerted mechanism connecting the activity of oxidative enzymes and oxidant mediated damage of proteins. To the best of our knowledge, no previous study focused simultaneously on the activity of oxidative enzymes and OPD markers in both T1DM and T2DM patients. Finally, this study showed an interesting association of a novel OPD marker, AOPP, with NOX.

**Acknowledgements:** The authors wish to thank Professor Dr. M. Sawkat Hassan, Director, Laboratory Services, and Mr. Md. Nayeemul Islam Khan, Principal Scientific Officer, Clinical Biochemistry Laboratory of the BIRDEM General Hospital for their kind cooperation in collecting samples from patients. The authors wish to thank all participants of this study.

**Peer Review:** Externally peer-reviewed.

**Author Contributions:** Conception/Design of Study- L.N.I., S.T.; Data Acquisition- S.T., R.S., T.J.; Data Analysis/Interpretation- S.T., R.S., T.J., L.N.I.; Drafting Manuscript- S.T.; Critical Revision of Manuscript- L.N.I., S.T., R.S., T.J.; Final Approval and Accountability- L.N.I., S.T., R.S., T.J.

**Conflict of Interest:** Authors declared no conflict of interest.

**Financial Disclosure:** Authors declared no financial support.

## ORCID IDs of the authors

Sanjeda Tamanna	0000-0002-3871-6245
Rocky Sheikh	0000-0001-9611-1554
Taslumul Jannat	0000-0002-7600-2884
Laila Noor Islam	0000-0001-8832-8737

## REFERENCES

- Forbes JM, Cooper ME. Mechanisms of diabetic complications. *Physiol Rev.* 2013; 93(1):137-188.
- Maiese K. New insights for oxidative stress and diabetes mellitus. *Oxid Med Cell Longev.* 2015;87596.
- Yaribeygi H, Sathyapalan T, Atkin SL, Sahebkar A. Molecular mechanisms linking oxidative stress and diabetes mellitus. *Oxid Med Cell Longev.* 2020;8609213.
- Huang X, Sun M, Li D, et al. Augmented NADPH oxidase activity and p22phox expression in monocytes underlie oxidative stress of patients with type 2 diabetes mellitus. *Diabetes Res Clin Pract.* 2011;91(3):371-380.
- Ghoshal K, Das S, Aich K, Goswami S, Chowdhury S, Bhattacharyya M. A novel sensor to estimate the prevalence of hypochlorous (HOCl) toxicity in individuals with type 2 diabetes and dyslipidemia. *Clin Chim Acta.* 2016;458:144-153.
- Lambeth JD. Nox enzymes, ROS, and chronic disease: an example of antagonistic pleiotropy. *Free Radic Biol Med.* 2007;43(3):332-347.
- García AG, Rodríguez MR, Alonso CG, Ochoa DYR, Aguilar CA. Myeloperoxidase is associated with insulin resistance and inflammation in overweight subjects with first-degree relatives with type 2 diabetes mellitus. *Diabetes Metab J.* 2015;39(1):59-65.
- Khan AA, Alsahli MA, Rahmani AH. Myeloperoxidase as an active disease biomarker: Recent biochemical and pathological perspectives. *Med Sci (Basel).* 2018;6(2):33.
- Ndrepepa G. Myeloperoxidase - A bridge linking inflammation and oxidative stress with cardiovascular disease. *Clin Chim Acta.* 2019;493:36-51.
- Davies MJ. Protein oxidation and peroxidation. *Biochem J.* 2016;473(7):805-825.
- Saha P, Banerjee P, Auddya L, et al. Simple modified colorimetric methods for assay of total oxidative stress and antioxidant defense in plasma: Study in diabetic patients. *Arch Med.* 2015; 7(5):1-7.
- Boyacı I, Yiğitbaşı T, Ankaralı H. Is oxidative stress a consequence of hyperglycemia? Or is hyperglycemia the consequence of oxidative stress? Or are both caused by insulin resistance? *Int Arch Endocrinol Clin Res.* 2021;7(1):023.
- Sitar ME, Aydın S, Çakatay U. Human serum albumin and its relation with oxidative stress. *Clin Lab.* 2013;59(9-10):945-952.
- Hu ML. Measurement of protein thiol groups and glutathione in plasma. *Methods Enzymol.* 1994;233:380-385.
- Dalle-Donne I, Rossi R, Giustarini D, Milzani A, Colombo R. Protein carbonyl groups as biomarkers of oxidative stress. *Clin Chim Acta.* 2003;329(1-2):23-38.
- Witko-Sarsat V, Friedlander M, Capeillère-Blandin C, et al. Advanced oxidation protein products as a novel marker of oxidative stress in uremia. *Kidney Int.* 1996;49(5):1304-1313.
- Höhn A, Jung T, Grune T. Pathophysiological importance of aggregated damaged proteins. *Free Radic Biol Med.* 2014;71:70-89.
- American Diabetes Association. 2. Classification and diagnosis of diabetes: Standards of medical care in diabetes-2021. *Diabetes Care.* 2021;44(Suppl 1):15-33.
- Reusch VM Jr, Burger MM. Distribution of marker enzymes between mesosomal and protoplast membranes. *J Biol Chem.* 1974;249(16):5337-5345.
- Ferdausi N, Anik MEK, Binti NN, Islam LN. Oxidase enzyme activities and their correlations with antioxidative stress biomarkers in patients with acute coronary syndrome in Bangladesh. *World J Cardiovasc Dis.* 2020;10(4): 163-177.
- Bradley PP, Priebat DA, Christensen RD, Rothstein G. Measurement of cutaneous inflammation: estimation of neutrophil content with an enzyme marker. *J Invest Dermatol.* 1982;78(3):206-209.
- Choudhury TZ, Kamruzzaman M, Islam LN. Investigation of the

- cellular and soluble markers of inflammation for the assessment of cardiovascular risk in patients with acute coronary syndrome in Bangladesh. *Int J Electron Healthc.* 2019;11(1): 67-80.
23. Benzie IF, Strain JJ. The ferric reducing ability of plasma (FRAP) as a measure of "antioxidant power": the FRAP assay. *Anal Biochem.* 1996;239(1):70-76.
  24. Haque R, Hafiz FB, Habib MA, Radeen KR, Islam LN. Role of complete blood count, antioxidants, and total antioxidant capacity in the pathophysiology of acute coronary syndrome. *Afr J Bio Sci.* 2022;4(1):37-47.
  25. Rodkey FL. Direct spectrophotometric determination of albumin in human serum. *Clin Chem.* 1965;11(4):478-487.
  26. Binti NN, Ferdausi N, Anik MEK, Islam LN. Association of albumin, fibrinogen, and modified proteins with acute coronary syndrome. *PLOS One.* 2022;17(7):e0271882. doi:10.1371/journal.pone.0271882
  27. Levine RL, Garland D, Oliver CN, et al. Determination of carbonyl content in oxidatively modified proteins. *Methods Enzymol.* 1990;186:464-478.
  28. Geetha A, Gopalakrishnan S, Umadevi R. Study on the impact of family history of diabetes among type 2 diabetes mellitus patients in an urban area of Kancheepuram district, Tamil Nadu. *Int J Community Med Public Health.* 2017;4(11):4151-4156.
  29. Savu O, Serafinceanu C, Grajdeanu IV, Iosif L, Gaman L, Stoian I. Paraoxonase lactonase activity, inflammation and antioxidant status in plasma of patients with type 1 diabetes mellitus. *J Int Med Res.* 2014;42(2):523-529.
  30. Marra G, Cotroneo P, Pitocco D, et al. Early increase of oxidative stress and reduced antioxidant defenses in patients with uncomplicated type 1 diabetes: a case for gender difference. *Diabetes Care.* 2002;25(2):370-375.
  31. Fatima N, Faisal SM, Zubair S, et al. Role of pro-inflammatory cytokines and biochemical markers in the pathogenesis of type 1 diabetes: Correlation with age and glycemic condition in diabetic human subjects. *PLOS One.* 2016;11(8):e0161548. doi:10.1371/journal.pone.0161548
  32. Siddique MAH, Tamannaa Z, Kamaluddin SM, et al. Total antioxidant status in newly-diagnosed type II diabetes patients in Bangladeshi population. *J Mol Pathophysiol.* 2014;5(1):5-9.
  33. Al-Deen ZMM, Ajeena IA. Study of total antioxidant capacity in patients with diabetic peripheral neuropathy. *Med J Babylon.* 2015;12(1):192-201.
  34. Rehman A, Zamir S, Bhatti A, Jan SS, Ali S, Wazir F. Evaluation of albuminuria, total plasma proteins, and serum albumin in diabetics. *Gomal J Med Sci.* 2012;10(2):198-200.
  35. Cheng PC, Hsu SR, Cheng YC. Association between serum albumin concentration and ketosis risk in hospitalized individuals with type 2 diabetes mellitus. *J Diabetes Res.* 2016;1269706.
  36. Bansal S, Chawla D, Siddarth M, Banerjee BD, Madhu SV, Tripathi AK. A study on serum advanced glycation end products and its association with oxidative stress and paraoxonase activity in type 2 diabetic patients with vascular complications. *Clin Biochem.* 2013;46(1-2):109-114.
  37. Kalousová M, Fialová L, Skrha J, et al. Oxidative stress, inflammation and autoimmune reaction in type 1 and type 2 diabetes mellitus. *Prague Med Rep.* 2004;105(1):21-28.
  38. Ates I, Kaplan M, Yuksel M, et al. Determination of thiol/disulphide homeostasis in type 1 diabetes mellitus and the factors associated with thiol oxidation. *Endocrine.* 2016;51(1):47-51.
  39. Michelis R, Kristal B, Snitkovsky T, Sela S. Oxidative modifications impair albumin quantification. *Biochem Biophys Res Commun.* 2010;401(1):137-142.
  40. Witko-Sarsat V, Gausson V, Nguyen AT, et al. AOPP-induced activation of human neutrophil and monocyte oxidative metabolism: a potential target for N-acetylcysteine treatment in dialysis patients. *Kidney Int.* 2003;64(1):82-91.
  41. Yuan F, Liu SX, Tian JW. Advanced oxidation protein products induce reactive oxygen species production in endothelial cells. *Di Yi Jun Yi Da Xue Xue Bao.* 2004;24(12):1350-1352.

### How cite this article

Tamanna S, Sheikh R, Jannat T, Islam LN. Evaluation of Oxidative Protein Damage in Patients with Type 1 and 2 Diabetes Mellitus in Bangladesh. *Eur J Biol* 2023;82(1): 23-30. DOI: 10.26650/EurJBiol.2023.1298202

# Morphological and Biochemical Investigation of the Protective Effects of *Panax ginseng* on Methotrexate-Induced Testicular Damage

Fatma Bedia Karakaya-Cimen<sup>1,2,3</sup>,  Caglar Macit<sup>4</sup>,  Guzin Goksun Sivas<sup>5</sup>,   
Tugba Tunali Akbay<sup>5</sup>,  Goksel Sener<sup>6</sup>,  Feriha Ercan<sup>2</sup> 

<sup>1</sup>Marmara University, Institute of Health Sciences, Department of Histology and Embryology, Istanbul, Turkiye

<sup>2</sup>Marmara University, School of Medicine, Department of Histology and Embryology, Istanbul, Turkiye

<sup>3</sup>Bezmialem Vakif University, School of Medicine, Department of Histology and Embryology, Istanbul, Turkiye

<sup>4</sup>Istanbul Medipol University, School of Pharmacy, Department of Pharmacology, Istanbul, Turkiye

<sup>5</sup>Marmara University, Faculty of Dentistry, Basic Medical Sciences, Department of Basic Health Sciences, Istanbul, Turkiye

<sup>6</sup>Fenerbahce University, School of Pharmacy, Department of Pharmacology, Istanbul, Turkiye

## ABSTRACT

**Objective:** Methotrexate (MTX) is a chemotherapeutic agent that causes testicular toxicity used in the cure of various types of cancer. The anti-oxidant and anti-cancer effects of *Panax ginseng* (PxG) have been reported in both experimental and clinical studies. This study aims to examine the healing effect of PxG on testicular damage induced by MTX.

**Materials and Methods:** Sprague Dawley male rats (8-week-olds) were used in the study. A single dose of MTX dissolved in saline (20 mg/kg) was given to MTX and MTX+PxG groups by intraperitoneal injection. PxG dissolved in saline (100 mg/kg) was given by orogastric gavage once a day for 5 days to the MTX+PxG group. Saline was given to the control and MTX groups orally during the experiments. After decapitation, the testis samples were obtained. Seminiferous tubules and basement membrane were evaluated histopathologically. Seminiferous tubule diameter and germinal epithelium thickness were measured. Furthermore, oxidative stress parameters such as malondialdehyde, glutathione, superoxide dismutase, and glutathione-S-transferase were measured.

**Results:** MTX treatment caused seminiferous tubule degeneration with a decrease in Johnsen's score, the seminiferous tubule's diameter, and the germinal epithelium's thickness. Parallel with the histopathological results increased testicular oxidative stress with an increase in malondialdehyde level and a decrease of endogenous anti-oxidant activity with a decrease in glutathione level and glutathione-S-transferase and superoxide dismutase activities. PxG treatment improved these histological and biochemical parameters in MTX-induced testis cytotoxicity.

**Conclusion:** MTX treatment causes testicular damage via the oxidative processes. PxG treatment ameliorates MTX-induced testicular damage by inhibiting oxidative stress.

**Keywords:** Methotrexate, *Panax ginseng*, testis, oxidative stress

## INTRODUCTION

Methotrexate (MTX) is a folate antagonist often used in various types of cancer such as osteosarcoma, acute lymphoblastic leukemia, head and neck tumors, and inflammatory processes such as rheumatoid arthritis, psoriatic arthritis, and systemic lupus erythematosus.<sup>1–4</sup> It has been shown to have toxic effects on the bone marrow, liver, lung, kidney, intestine, central nervous system, and gonads, and also cause drug toxicity leading to chronic testicular damage.<sup>1–7</sup> Therefore, numerous studies have been conducted on the prevention of testicular damage caused by MTX. It has been shown that MTX reduces testicular sperm

count and motility, causes DNA damage in sperm, atrophy in seminiferous tubules, and apoptosis in spermatocytes, these damages are related to an increase of reactive oxygen species (ROS).<sup>3–4</sup> Therefore, anti-oxidant-containing compounds may help the protection of testis against the harmful effects of MTX-induced oxidative stress.<sup>3–8</sup>

In recent studies, various antioxidants have been used to decrease the side effects associated with MTX application.<sup>2,4,6–10</sup> *Panax ginseng* (PxG) a powerful anti-oxidant belonging to the Araliaceae family, is a medicinal herb, widely used especially in Southeast Asia.<sup>9</sup> PxG contains ginsenosides, saponins, non-

**Corresponding Author:** Feriha Ercan E-mail: eferiha@hotmail.com; fercan@marmara.edu.tr

Submitted: 27.01.2023 • Revision Requested: 11.05.2023 • Last Revision Received: 22.05.2023 • Accepted: 24.05.2023



This article is licensed under a Creative Commons Attribution-NonCommercial 4.0 International License (CC BY-NC 4.0)

saponins, oils, phytosterols, polysaccharides, vitamins, minerals, enzymes, and organic acids.<sup>11-12</sup> The pharmacological effects of PxG have been demonstrated in the cardiovascular, immune, endocrine, and central nervous systems.<sup>13</sup> PxG and its components have also shown anti-diabetic, anti-hypertensive, anti-inflammatory, anti-tumor, anti-apoptotic, anti-stress, and anti-aging properties.<sup>13-15</sup> In addition, Ginseng extract protects the testicular and erectile function.<sup>16-17</sup> It has been shown to stimulate spermatogenesis, increase sperm survival rate, motility, and quality, and prevent erectile dysfunction in animal models.<sup>17</sup> It has been also noted that anti-oxidant, anti-apoptotic effects of PxG on cisplatin-induced testicular toxicity.<sup>18</sup>

It aimed to investigate the anti-oxidant effects of PxG extract on MTX-induced testicular damage in rats in this study. Testicular histopathological damage was evaluated using histopathological Johnsen's score. Testicular oxidative damage was evaluated by estimating malondialdehyde (MDA) and glutathione (GSH) levels and glutathione *S* transferase (GST), and superoxide dismutase (SOD) activities using biochemical methods.

## MATERIALS AND METHODS

### Experimental Animals

Sprague Dawley male rats (8-week-olds, 250-300 gr) were obtained from the İstanbul Medeniyet University, Science and Advanced Technologies Research Center (BİLTAM), Laboratory Animal Care Unit. During the study, they were kept in a laboratory environment with ventilation (air exchange 18 h/h), 12 h light/dark cycle, humidity (50-60%), and temperature (23-25°C). The rats accessed food and water *ad libitum*. This study was confirmed by The Animal Care and Ethical Committee for Experimental Animals at Marmara University (37.2022.mar).

### Experimental Groups

Animals were randomly divided into three groups (n=8 in each group) as control, MTX, and MTX+PxG. A single dose of MTX dissolved in saline (20 mg/kg) was applied to MTX<sup>19</sup> and MTX+PxG groups by intraperitoneal injection. PxG dissolved in saline (100 mg/kg) was given orally once a day for 5 days to the MTX+PxG group.<sup>20,21</sup> Saline was given by orogastric gavage to the control and MTX groups during the experiment. PxG was purchased from "Naturel Kimya" by Casel İlaç Sanayi and kindly donated to us. Animals were decapitated under light ether anesthesia, and testes were obtained at the end of the experiment for histological and biochemical investigations.

### Light Microscopic Preparation

Testis samples were fixed with 10% formalin and processed for the routine paraffin embedding method. Paraffin sections

(4  $\mu$ m in thickness) were stained with hematoxylin and eosin (H&E) for histopathological investigation, and periodic acid Schiff (PAS) reaction for investigation of basement membrane and examined under an Olympus BX51 (Tokyo, Japan) photomicroscope. In each H&E-stained section, the diameter of seminiferous tubules and thickness of germinal epithelium were measured using Image J (NIH-USA) program in 20 seminiferous tubules. Also, these tubules were evaluated histopathologically using Johnsen's scoring criteria as follows: 10: Full spermatogenesis; 9: Slightly disturbed spermatogenesis and many spermatozoa; 8: A few spermatozoa; 6: A few spermatids; 5: Many spermatocytes, but the absence of spermatozoa or spermatids; 4: A few spermatocytes; 3: Only spermatogonia; 2: Only Sertoli cells and absence of germinal cells; 1: Absence of germinal epithelium.<sup>22,23</sup> According to these criteria, using a scale ranging seminiferous tubules was scored from ten (complete full spermatogenesis) to one (absence of germinal epithelium). In PAS-stained sections, PAS-positive staining intensity of basement membrane was scored semiquantitatively as follows: 3: strong; 2: moderate; 1: weak, and 0: absence.

### Measurement of MDA and GSH Levels, GST, and SOD Activities

Testis tissue homogenates in physiological saline were prepared using a glass homogenizer. The cooling process during homogenization was done by immersing a glass homogenizer into a beaker containing ice. Tissue homogenates were then centrifuged at 3000xg for 10 min. The supernatant samples were used for the measurement of MDA and GSH levels, and GST and SOD activities.<sup>24-27</sup>

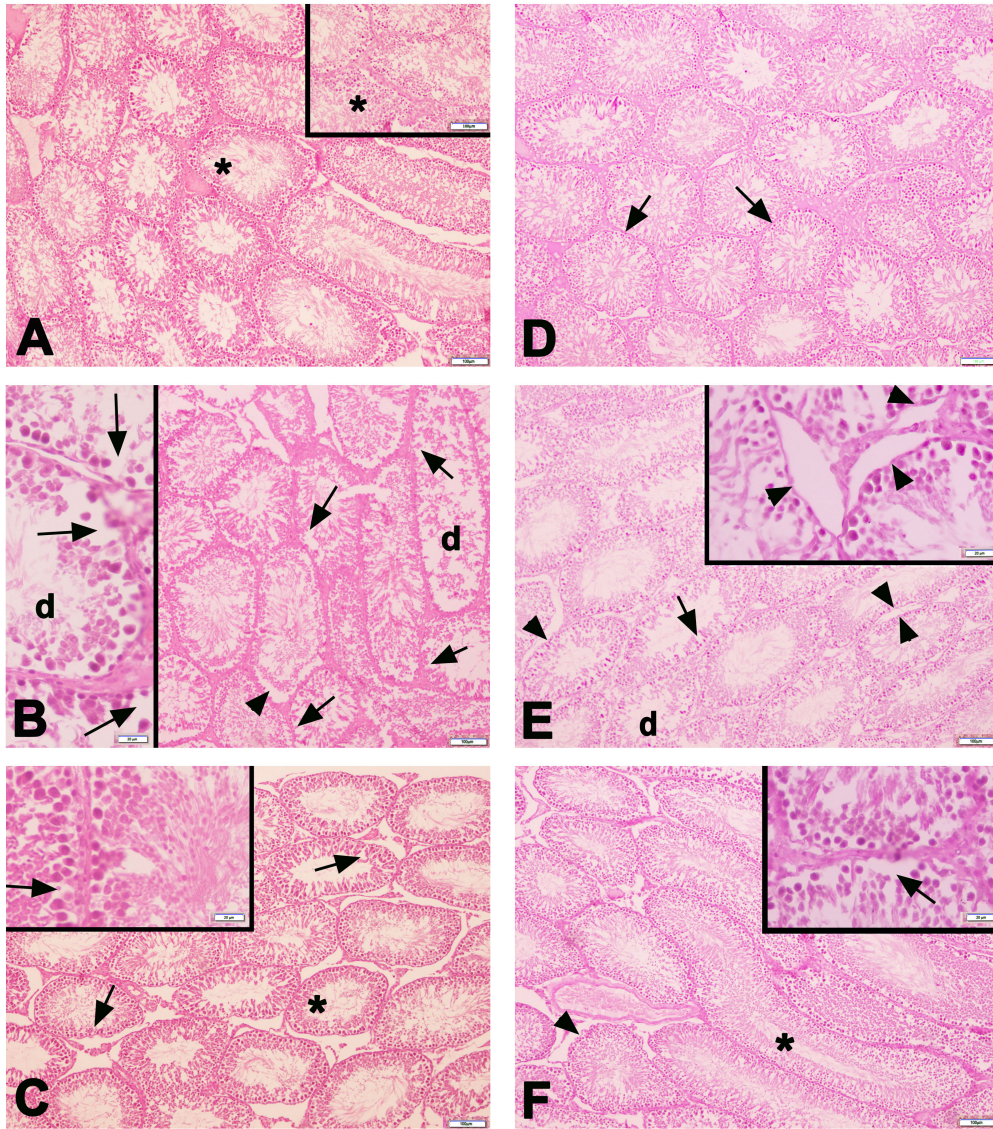
### Statistical Analysis

The histological and biochemical analyses were done by the researchers who were blinded to the experimental groups. One-way analysis of variance was used for analysis of the data and Tukey's multiple comparisons test was used to determine the differences between groups. The results were expressed as mean  $\pm$  standard deviation (SD). Analysis was estimated by Graph Pad Prism Version 8.0 (Graph Pad Software, San Diego, USA). A  $p < 0.05$  level was considered significant.

## RESULTS

### Histopathological Results

In the control group, basement membrane contours and germinal epithelial arrangement of the seminiferous tubules were normal, and a large number of sperm were seen in the seminiferous tubule lumen. In the MTX group, dilatations in the tubule epithelium, a decrease in the germinal cell line, basement membrane irregularity, and extensive dilatations between



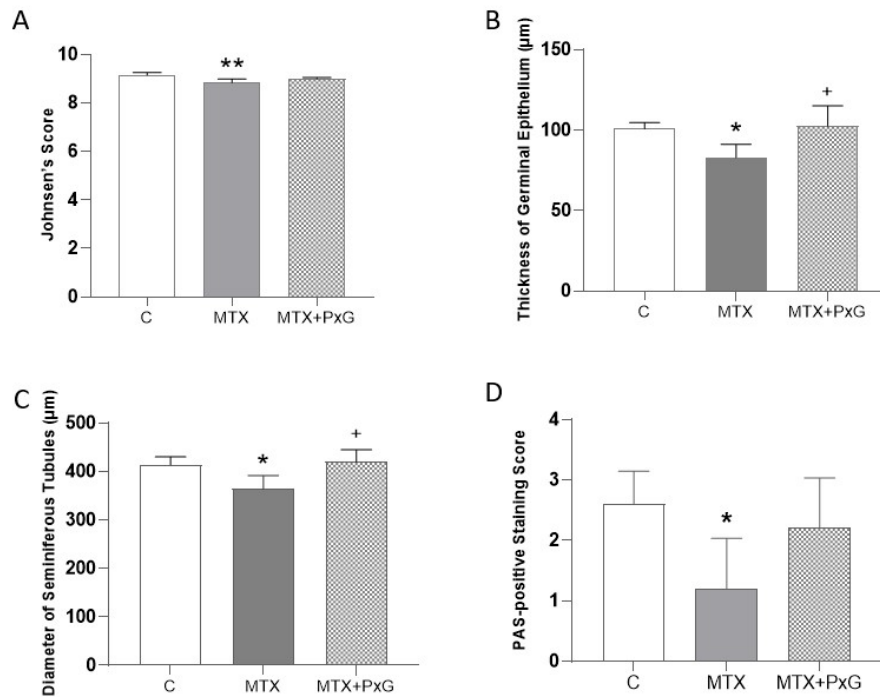
**Figure 1.** Representative light micrographs of testis samples are seen in the experimental groups. Normal seminiferous tubules morphology (\*) with regular PAS-positive basement membrane (arrow) is seen in the control group (A, D). Dilatations (arrow) among the germinal epithelial cells, degenerated tubules (d), and PAS-positive stained irregular basement membrane (arrowhead) are observed in the MTX group (B, E). Numerous quite regular seminiferous tubules morphology (\*) and some degenerated seminiferous tubules with germinal epithelial dilatation (arrow) and PAS-positive stained irregular basement membrane (arrowhead), are seen in the MTX+PxG group (C, F). A-C: H&E staining, D-F: PAS staining. Scale bar: 100  $\mu\text{m}$ , insets: 20  $\mu\text{m}$ .

the seminiferous tubules and degenerated tubule structures were observed. Although dilatations in the seminiferous tubules and irregularities in the germinal epithelium were detected in some places, numerous quite regular seminiferous tubules were seen in the MTX+PxG group (Figure 1). Histopathological Johnsen's score ( $p < 0.01$ ), the thickness of germinal epithelium ( $p < 0.05$ ), the diameter of seminiferous tubules ( $p < 0.05$ ), and PAS-positive staining intensity score of basement membrane ( $p < 0.05$ ) were decreased in the MTX group compared to the control group. Thickness of germinal epithelium ( $p < 0.05$ ), and diameter of seminiferous tubules ( $p < 0.05$ ) were increased in the MTX+PxG group compared to the MTX group. Although

the histopathological Johnsen's score and PAS-positive staining intensity of the basement membrane tended to increase, no statistical significance was found between these groups (Figure 2).

#### MDA and GSH Levels and GST and SOD Activities Results

Testis MDA level ( $p < 0.001$ ) increased, and GSH level ( $p < 0.01$ ) and GST ( $p < 0.001$ ) and SOD ( $p < 0.001$ ) activities reduced in the MTX group in comparison with the control group. The administration of PxG to the MTX group significantly reduced testis



**Figure 2.** Johnsen's histopathological score (A), the thickness of germinal epithelium (B), the diameter of seminiferous tubules (C), and the PAS-positive staining intensity score of basement membrane (D) are seen in the experimental groups. \*  $p < 0.05$  and \*\* $p < 0.01$  compared to control group. +  $p < 0.05$  compared to the MTX group.

MDA level ( $p < 0.001$ ) while increasing GSH level ( $p < 0.05$ ), and GST ( $p < 0.001$ ) and SOD ( $p < 0.01$ ) activities (Figure 3).

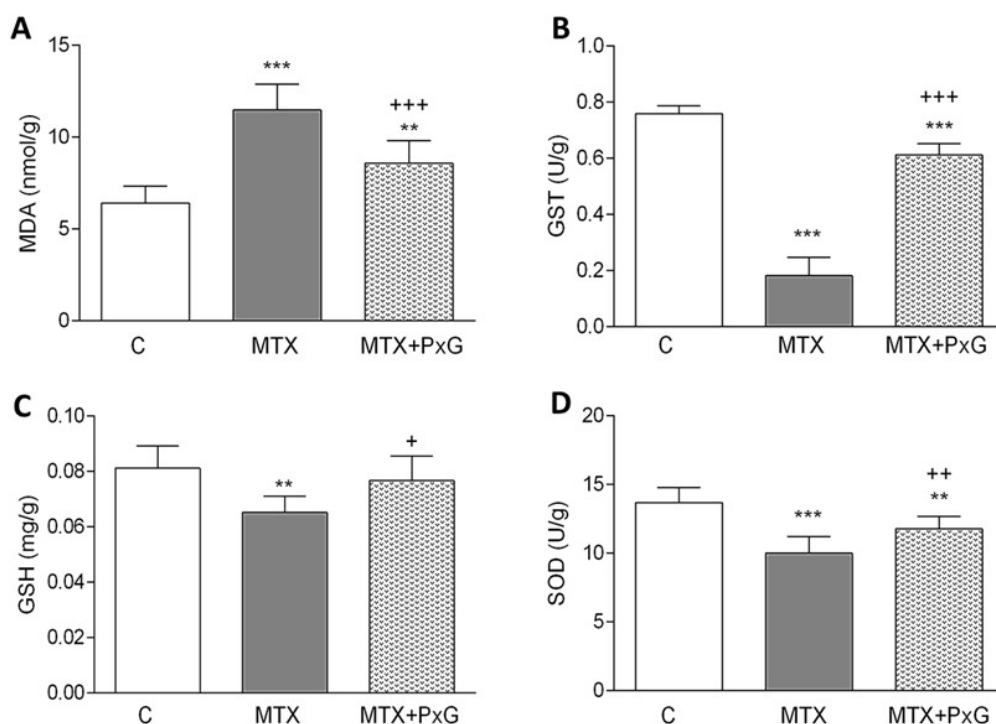
## DISCUSSION

In this study, attenuating effects of PxG on MTX-induced testicular injury were shown by histological and biochemical techniques. The findings of this study showed that MTX treatment led to seminiferous tubule degeneration with a decrease in seminiferous tubule diameter, germinal epithelial thickness, PAS-positive staining intensity of basement membrane, and histopathological Johnsen's score. Parallel with the histopathological results, it was determined that the testicular oxidative stress increased with the increase in MDA level and the endogenous anti-oxidant activity decreased with the decrease in the GSH level and GST and SOD activities.

Free radicals and lipid peroxidation are the two leading factors in MTX-induced testicular pathology.<sup>28</sup> Intensive production of free radicals results in increased lipid peroxidation. Lipid peroxidation also leads to the oxidation of polyunsaturated fatty acids.<sup>29</sup> Testicular toxicity is a serious side effect of MTX.<sup>6–8</sup> The testis, in particular, is highly sensitive to oxidative injury because of containing high polyunsaturated fatty acids. Oxidative stress is a major pathogenic factor of MTX-induced testicular damage. MTX is not capable of redox but

indirectly contributes to the generation of oxidative stress. The oxidation/anti-oxidant balance is inhibited by external stimuli, thus increasing the level of ROS.<sup>4</sup> The increase in ROS disrupts the functioning of the male genital system, leading to infertility. For this reason, antioxidants are needed to preserve the body from oxidative stress injury.<sup>30</sup> Vardi et al<sup>7</sup> revealed that MTX reduces the effectiveness of the anti-oxidant enzyme system and causes destructive changes in the testicles by making cells vulnerable to the harmful effects of ROS. In this study, PxG extract administration ameliorated the MTX-induced testis damage. It is thought that the reason for this improvement is the increase in the anti-oxidant capacity of the testicular tissue with the application of PxG extract and the decrease in oxidative damage in the testicular tissue, which is also reflected in the histological results.

In recent years, PxG's anti-oxidant and anti-cancer effects, as well as its effects on improving immunity, energy, and sexuality and fighting cardiovascular diseases, diabetes, and neurological diseases have been investigated in both experimental and clinical studies.<sup>13,15</sup> The positive effects of the use of PxG on testicular morphology, sperm parameters, reproductive functions, and libido have been demonstrated in various damages.<sup>31,32</sup> Several modern medicines originate from traditional medicines.<sup>33</sup> Ginseng is used in clinical settings all over the world<sup>34</sup> and holds promise for the development of new therapeutic agents.<sup>35</sup> For



**Figure 3.** Testicular MDA (A), GST (B), GSH (C), and SOD (D) levels are seen in the experimental groups. \*\* $p < 0.01$  and \*\*\*  $p < 0.001$  compared to control group. +  $p < 0.05$ , ++  $p < 0.01$  and +++  $p < 0.001$  compared to MTX group.

this reason, in this study, the therapeutic effects of PxG against testicular damage caused by MTX application were examined histologically and biochemically.

MTX causes cellular and mitochondrial glutathione depletion by altering the redox properties of the cell resulting in a dose-dependent increase in peroxide levels, which confers immunosuppressive properties to MTX.<sup>36</sup> Oxidative stress injury results from an imbalance between oxidants and antioxidants and leads to many cytopathological alterations. MTX toxicity causes free radical formation and lipid peroxidation resulting from oxidative cellular damage.<sup>37</sup> It also suppresses antioxidants and increases oxidant levels in various tissues.<sup>38</sup> It has been reported that MTX administration causes severe degeneration of seminiferous tubules with epithelial vacuolization, desquamation, decrease in spermatogenic cells, increase number of apoptotic cells, and separation of germinal epithelium from the basement membrane and alteration in sperm parameters.<sup>6</sup> In the pilocarpine-induced temporal lobe epilepsy model, ginseng application improved seminiferous tubule morphological disorders and decrease sperm count that occurs with epilepsy.<sup>9</sup> It was reported that PxG treatment ameliorated cisplatin-induced testicular damage via inhibiting oxidative stress formation.<sup>18</sup> In another study investigating the effect of ginseng on testicular damage caused by aging, it was reported that ginseng application improved the morphological deteriorations that occur with aging.<sup>39</sup> Parallel with these find-

ings, degenerated seminiferous tubules with dilatation in the germinal epithelium, decrease in germ cell number and germinal epithelium thickness, basement membrane irregularity with decrease of PAS-positive staining intensity were observed in the MTX group. PxG application improved these histopathological damages thanks to its anti-oxidant properties.

## CONCLUSION

Based on the histological and biochemical findings of this study, MTX administration caused degeneration in seminiferous tubules with dilatation among the germinal epithelial cells and irregular basement membrane and decrease of PAS-positive staining intensity, germinal epithelium thickness, Johnsen's score, decreased endogenous GSH level, GST and SOD activities and increased MDA level in rat testis. PxG treatment ameliorated MTX-induced testicular damage by inhibiting oxidative stress through its anti-oxidant properties.

**Ethics Committee Approval:** This study was approved by The Animal Care and Ethical Committee for Experimental Animals at Marmara University (37.2022.mar).

**Informed Consent:** Written consent was obtained from the participants.

**Author Contributions:** Conception/Design of Study- C.M., G.S., F.E.; Data Acquisition- F.B.K.C., C.M., G.G.S., T.T.A.,

G.S., F.E.; Data Analysis/Interpretation- F.B.K.C., C.M., G.G.S., T.T.A., G.S., F.E.; Drafting Manuscript- F.B.K., F.E.; Critical Revision of Manuscript- F.B.K.C., T.T.A., G.S., F.E.; Final Approval and Accountability- F.B.K.C., C.M., G.G.S., T.T.A., G.S., F.E.

**Conflict of Interest:** Authors declared no conflict of interest.

**Financial Disclosure:** This study was financially supported by Marmara University, Scientific Research Project Committee (TDK-2020-10047).

#### ORCID IDs of the authors

Fatma Bedia Karakaya-Cimen	0000-0001-6054-0752
Caglar Macit	0000-0002-5532-2395
Guzin Goksun Sivas	0000-0001-7347-490X
Tugba Tunali Akbay	0000-0002-2091-9298
Goksel Sener	0000-0001-7444-6193
Feriha Ercan	0000-0003-2339-5669

#### REFERENCES

- Hamed KM, Dighriri IM, Baomar AF, et al. Overview of Methotrexate Toxicity: A Comprehensive Literature Review. *Cureus*. 2022;14(9):e29518. doi:10.7759/cureus.29518
- Bleyer WA. Methotrexate: clinical pharmacology, current status and therapeutic guidelines. *Cancer Treat Rev*. 1977;4(2):87-101.
- Pinar N, Cakirca G, Ozgur T, Kaplan M. The protective effects of alpha lipoic acid on methotrexate induced testis injury in rats. *Biomed Pharmacother*. 2018;97:1486-1492.
- Wang Y, Zhao TT, Zhao HY, Wang H. Melatonin protects methotrexate-induced testicular injury in rats. *Eur Rev Med Pharmacol Sci*. 2018;22(21):7517-7525.
- Abdelhameed RFA, Fattah SA, Mehanna ET, et al. Zymo-Albuside A: New Saponin from *Zygophyllum album* L. with significant antioxidant, anti-inflammatory and antiapoptotic effects against methotrexate-induced testicular damage. *Int J Mol Sci*. 2022;23(18):10799. doi:10.3390/ijms231810799
- Kanpalta F, Ozbeyli D, Sen A, Cevik O, Sener G, Ercan F. Bitter melon (*Momordica charantia*) fruit extract ameliorates methotrexate-induced reproductive toxicity in male rats. *Marmara Med J*. 2021;34(3):222-228.
- Vardi N, Parlakpınar H, Ates B, Cetin A, Otlu A. Antiapoptotic and antioxidant effects of beta-carotene against methotrexate-induced testicular injury. *Fertil Steril*. 2009;92(6):2028-2033.
- Armagan A, Uzar E, Uz E, et al. Caffeic acid phenethyl ester modulates methotrexate-induced oxidative stress in testes of rat. *Hum Exp Toxicol*. 2008;27(7):547-552.
- Ganjkhani M, Nourozi S, Bigonah R, Rostami A, Shokri S. Ameliorating impacts of ginseng on the apoptosis of spermatogenic cells and sperm quality in temporal lobe epilepsy rat model treated with valproate. *Andrologia*. 2019;51(9):e13348. doi: 10.1111/and.13348.
- Padmanabhan S, Tripathi DN, Vikram A, Ramarao P, Jena GB. Methotrexate-induced cytotoxicity and genotoxicity in germ cells of mice: intervention of folic and folinic acid. *Mutat Res*. 2009;673(1):43-52.
- Ernst E. Panax ginseng: an overview of the clinical evidence. *J Ginseng Res*. 2010;34(4):259-263.
- Ratan ZA, Haidere MF, Hong YH, et al. Pharmacological potential of ginseng and its major component ginsenosides. *J Ginseng Res*. 2021;45(2):199-210.
- Liu CX, Xiao PG. Recent advances on ginseng research in China. *J Ethnopharmacol*. 1992;36(1):27-38.
- Lu J-M, Yao Q, Chen C. Ginseng compounds: an update on their molecular mechanisms and medical applications. *Curr Vasc Pharmacol*. 2009;7(3):293-302.
- Yue PY, Mak NK, Cheng YK, et al. Pharmacogenomics and the Yin/Yang actions of ginseng: anti-tumor, angiomodulating and steroid-like activities of ginsenosides. *Chin Med*. 2007;2:6. doi: 10.1186/1749-8546-2-6.
- Kim W, Hwang S, Lee H, Song H, Kim S. Panax ginseng protects the testis against 2,3,7,8-tetrachlorodibenzo-p-dioxin induced testicular damage in guinea pigs. *BJU Int*. 1999;83(7):842-849.
- Wanderley MI, Saraiva KL, Cesar Vieira JS, Peixoto CA, Udrisar DP. Foetal exposure to Panax ginseng extract reverts the effects of prenatal dexamethasone in the synthesis of testosterone by Leydig cells of the adult rat. *Int J Exp Pathol*. 2013;94(3):230-240.
- Aslan E, Kumalar K, Güzel H, Demirel HH, Çelik S, Pektaş MB. Effects of Panax ginseng on cisplatin-induced testicular damage of rats. *Ant J Bot*. 2021;5(1):37-43.
- Uzar E, Sahin O, Koyuncuoglu HR, et al. The activity of adenosine deaminase and the level of nitric oxide in spinal cord of methotrexate administered rats: protective effect of caffeic acid phenethyl ester. *Toxicology*. 2006;218(2-3):125-133.
- Qiao C, Den R, Kudo K, et al. Ginseng enhances contextual fear conditioning and neurogenesis in rats. *Neurosci Res*. 2005;51(1):31-38.
- Koşmaz K, Durhan A, Şenlikçi A, et al. Evaluation of the protective effect of Red Ginseng on lipid profile, endothelial and oxidative damage after splenectomy in rats. *Arch Clin Exp Med*. 2021;6(2):43-49.
- Johnsen SG. Testicular biopsy score count—a method for registration of spermatogenesis in human testes: normal values and results in 335 hypogonadal males. *Hormones*. 1970;1(1):2-25.
- Elmas MA, Ozakpınar OB, Kolgazi M, Sener G, Arbak S, Ercan F. Exercise improves testicular morphology and oxidative stress parameters in rats with testicular damage induced by a high-fat diet. *Andrologia*. 2022;54(11):e14600. doi:10.1111/and.14600.
- Fujii S, Dale GL, Beutler E. Glutathione-dependent protection against oxidative damage of the human red cell membrane. *Blood*. 1984;63(5):1096-1101.
- Habig WH, Jakoby WB. Assays for differentiation of glutathione S-Transferases. *Methods Enzymol*. 1981;77:398-405.
- Ledwozyw A, Michalak J, Stepień A, Kadziółka A. The relationship between plasma triglycerides, cholesterol, total lipids and lipid peroxidation products during human atherosclerosis. *Clin Chim Acta*. 1986;155(3):275-283.
- Mylroie AA, Collins H, Umbles C, Kyle J. Erythrocyte superoxide dismutase activity and other parameters of copper status in rats ingesting lead acetate. *Toxicol Appl Pharmacol*. 1986;82(3):512-520.
- Tracey WR, Linden J, Peach MJ, Johns RA. Comparison of spectrophotometric and biological assays for nitric oxide (NO) and endothelium-derived relaxing factor (EDRF): nonspecificity of the diazotization reaction for NO and failure to detect EDRF. *J Pharmacol Exp Ther*. 1990;252(3):922-928.
- Rikans LE, Hornbrook KR. Lipid peroxidation, antioxidant pro-



- tection and aging. *Biochim Biophys Acta*. 1997;1362(2-3):116-127.
30. Koroglu KM, Cevik O, Sener G, Ercan F. Apocynin alleviates cisplatin-induced testicular cytotoxicity by regulating oxidative stress and apoptosis in rats. *Andrologia*. 2019;51(4):e13227. doi:10.1111/and.13227.
  31. Leung KW, Wong AS. Ginseng and male reproductive function. *Spermatogenesis*. 2013;3(3):e26391. doi:10.4161/spmg.26391.
  32. Sanad NH, Abbas HR, Yaseen AA, Habeeb IA, Alsalam HA. Hormonal, histological, and comparative study of the effect of pure ginseng on testicular function in the breeding/non-breeding season of rams in Basrah. *Arch Razi Inst*. 2021;76(5):1519-1535.
  33. Thomford NE, Senthebane DA, Rowe A, et al. Natural products for drug discovery in the 21st century: Innovations for novel drug discovery. *Int J Mol Sci*. 2018;19(6):1578.
  34. He Y, Yang J, Lv Y, et al. A Review of Ginseng Clinical Trials Registered in the WHO international clinical trials registry platform. *Biomed Res Int*. 2018;2018:1843142. doi:10.1155/2018/1843142.
  35. Wee JJ, Mee Park K, Chung AS. Biological activities of Ginseng and its application to human health. In: Benzie IFF, Wachtel-Galor S, eds. *Herbal Medicine: Biomolecular and Clinical Aspects*. 2nd ed. 2011.
  36. Phillips DC, Woollard KJ, Griffiths HR. The anti-inflammatory actions of methotrexate are critically dependent upon the production of reactive oxygen species. *Br J Pharmacol*. 2003;138(3):501-511.
  37. Helal MG, Said E. Tranilast attenuates methotrexate-induced renal and hepatic toxicities: Role of apoptosis-induced tissue proliferation. *J Biochem Mol Toxicol*. 2020;34(5):e22466. doi:10.1002/jbt.22466.
  38. Montasser AOS, Saleh H, Ahmed-Farid OA, Saad A, Marie MS. Protective effects of *Balanites aegyptiaca* extract, melatonin and ursodeoxycholic acid against hepatotoxicity induced by methotrexate in male rats. *Asian Pac J Trop Med*. 2017;10(6):557-565.
  39. Won YJ, Kim BK, Shin YK, et al. Pectinase-treated *Panax ginseng* extract (GINST) rescues testicular dysfunction in aged rats via redox-modulating proteins. *Exp Gerontol*. 2014;53:57-66.

### How cite this article

Karakaya-Cimen FB, Macit C, Goksun Sivas G, Tunali Akbay T, Sener G, Ercan F. Morphological and Biochemical Investigation of the Protective Effects of *Panax ginseng* on Methotrexate-Induced Testicular Damage. *Eur J Biol* 2023;82(1): 31-37. DOI: 10.26650/EurJBiol.2023.1271825

# Anti-Bacterial, Anti-Mycobacterial and Anti-Fungal Properties of *Punica granatum* as Natural Dye

Pinar Guner<sup>1</sup>,  Tulin Askun<sup>1</sup> 

<sup>1</sup>University of Balikesir, Faculty of Sciences and Arts, Biology, Cagis Campus, Balikesir, Turkiye

## ABSTRACT

**Objective:** This study aimed to determine the anti-mycobacterial, anti-bacterial, and anti-fungal effects of dry/fresh pomegranate peel ethanol/methanol extracts, and the dyeing performance and antimicrobial effects of dyed fabric samples with pomegranate peel ethanol extract.

**Materials and Methods:** Anti-mycobacterial activity against *Mycobacterium tuberculosis* H37Ra/H37Rv and two-clinical *M. tuberculosis* strains, and anti-bacterial activity against eight bacteria (*Bacillus cereus*, *Staphylococcus aureus*, *Salmonella typhimurium*, *Pseudomonas aeruginosa*, *Klebsiella pneumonia*, *Proteus vulgaris*, Methicillin-resistant *Staphylococcus aureus* and *Escherichia coli*) and anti-fungal activity against five fungal pathogens (*Candida albicans*, *Aspergillus flavus*, *Aspergillus ochraceus*, *Aspergillus niger*, *Fusarium proliferatum*) were determined by microplate assay. The anti-microbial activity of dyed fabric samples (30/ 1 Rib and single jersey 100% cotton) as well as their coloring properties, were investigated using the parallel streak method (AATCC 147).

**Results:** Extracts showed the anti-mycobacterial efficacy between MIC 7.81-31.25 µg/ml and MBC 31.25-250 µg/ml, respectively against four strains of *M. tuberculosis*. Also, each extract showed anti-bacterial activity between MIC 0.97-62.50 µg/ml and MBC 7.81-250 µg/ml and anti-fungal activity between MIC 31.25-125 µg/ml and MBC 125-250 µg/ml. While control and mordanting of fabric samples did not show any inhibition zones, significant anti-microbial activity against *S. aureus* was obtained after dyeing using dry peel on fabric samples without mordant.

**Conclusion:** These findings provide valuable information for future applications of natural dyes in textiles. The anti-mycobacterial, anti-fungal, and anti-bacterial properties of pomegranate could be significant in developing a model for drug design.

**Keywords:** Anti-microbial activity, Coloring Properties, Natural Dye, Pomegranate, *Punica granatum*

## INTRODUCTION

Pomegranate fruit, which has an important place in human history, is one of the oldest cultivated agricultural products. It is known that the homeland of the pomegranate is the Mediterranean, western Asia, and Iran, and today it is grown in the USA (California and Arizona), Argentina, China, Afghanistan, India, Arabia, Chile, and northern Mexico.<sup>1,2</sup> The pomegranate is the most important plant belonging to the family Punicaceae. The name of the pomegranate is derived from *Malum granatum*, which means "granular apple" in Latin.<sup>1</sup> *Punica granatum* has multiple spiny branches and the leaves are elliptic; the edible fruit is a berry with seeds and pulp produced from the ovary of a white or red single flower.<sup>3</sup> 50% of the pomegranate consist of the edible part and 50% of the peel (Fawole and Opara).<sup>4</sup>

Throughout history, diseases and infections have been a

great concern for humans.<sup>5</sup> For this reason, natural substances such as pomegranate have been added to medicines, foods, and textiles.<sup>6</sup> Pomegranate can be used in various products such as drugs, dye, pomegranate molasses and sour syrup, juice, preserves, vinegar, citric acid, and animal feed, used in the production of seed oils, and used as a refreshing additive.<sup>7</sup> All the parts of the pomegranate, from the bark to the flower, have been used for treatment by many nations since ancient times.<sup>8</sup> Pomegranate peel's properties are important and contain cures for and protection from cardiovascular disease, diabetes, cancers, erectile dysfunction, and dental problems.<sup>9</sup> The peel of *P. granatum* is used in the treatment of genital infections, mastitis, folliculitis, acne, piles, allergic dermatitis, tympanitis, scald, dysentery, and diarrhea.<sup>10</sup> In classical usage, the bark and rind fruits are used for tanning and as a vermifuge, especially for cold and cough.<sup>11</sup> In addition, *P. granatum* has some biological

Corresponding Author: Tulin Aşkun E-mail: taskun@balikesir.edu.tr

Submitted: 19.01.2023 • Revision Requested: 04.04.2023 • Last Revision Received: 26.05.2023 • Accepted: 27.05.2023



This article is licensed under a Creative Commons Attribution-NonCommercial 4.0 International License (CC BY-NC 4.0)

properties such as anti-oxidant,<sup>12,13</sup> anti-atherosclerotic,<sup>14,15</sup> anti-bacterial<sup>16,17</sup> and anti-viral<sup>10</sup> activities. According to the literature, pomegranate has great therapeutic effects, due to its anti-oxidant and anti-tumor capacity, using different extracts from different parts of the plant.<sup>18</sup> These biological activities are due to the presence of bioactive compounds called "Tanins." The main function of tannins is plant defense against microorganisms and animal attacks, due to their astringent capacity and ability to create compound with proteins and polysaccharides.<sup>19–21</sup> The components of *P. granatum* contain pelargonidin, cyanidin, delphinidin, gallic acid, ellagic acid, gallic acid and sitosterol, whose therapeutical properties are known.<sup>22,23</sup> In addition, in the studies, it was determined that pomegranate peel extracts showed an inhibitory effect, especially against Gram-positive bacteria, namely *Propionibacterium acnes*, *Staphylococcus aureus*,<sup>24</sup> and *Bacillus subtilis*.<sup>25</sup> In the literature, it has been determined that methanol extracts of pomegranate peel are effective on *Shigella dysenteriae* serotype 2, *Salmonella typhimurium*,<sup>26</sup> and *Escherichia coli*.<sup>27</sup> In anti-fungal activity studies, methanol extracts of pomegranate peel were tested against *Penicillium expansum*, *Penicillium digitatum* and *Botrytis cinerea* and at the end of the 20-hour incubation period, it was observed that the viability of the conidia decreased compared to the control.<sup>28</sup> In another study, it was determined that pomegranate peel extracts showed higher anti-mycobacterial activity (MIC 64–1024/ml) than potable fruit juice (MIC 256–>1024g/ml).<sup>29</sup> Furthermore, pomegranate peel has important biological properties that have anti-inflammatory (activation of white blood cells, the release of immune system chemicals) and anti-allergic effects.<sup>30</sup>

Synthetic dyes are used in many industries, such as textile, rubber, paper, plastic, leather, food, pharmaceutical, petrochemical, dyestuffs, and cosmetics. The release of synthetic dyes into the environment causes environmental pollution and many health problems.<sup>31</sup> Today, water pollution caused by non-biodegradable colored wastes of textile dyes is one of the leading environmental problems in the world.<sup>32</sup> For this reason, in textile dyeing natural dyes are preferred to synthetic dyes.<sup>33,34</sup> In traditional dyeing, organic photoprotective agents, such as some natural dyes, are applied to silk, cotton, and wool fabrics.<sup>35,36</sup> Although synthetic fibers are preferred more in dyeing, natural fibers such as cotton are mostly used in traditional natural dyeing. Natural fibers can be dyed with natural dyes with the help of a metallizing agent.<sup>37</sup> Natural dyes do not cause an allergic reaction and are not toxic to people and the environment.<sup>38,39</sup> The pomegranate peel is an anti-microbial product containing significant amounts of phenolic compounds, tannins, and pellets.<sup>20</sup> The major dyeing factor in the pomegranate peel is granatone, which is N-methyl granatone found in alkaloid form. This compound in the pomegranate provides the coloring property.<sup>40</sup> A color scale consisting of different shades of yellow, brown, and black is ob-

tained from fabrics dyed with pomegranate peel.<sup>41</sup> In this study, the anti-mycobacterial, anti-bacterial, and anti-fungal activities of ethanol and methanol extracts of pomegranate (*P. granatum*) peels, which are considered natural waste, were determined. In addition, this study investigates the anti-bacterial activity of the treated and control fabric samples that were examined as per standard AATCC-147 methods (Parallel Streak Method).

## MATERIALS AND METHODS

### Preparation of Extracts

Pomegranate was collected from Balıkesir (2013), and identification of the plant was made by Prof. Dr. Güldam Tümen and Fatih Satıl. The plant used in the study is kept in the herbarium of the Biology Department of Balıkesir University (Herbarium Number: FS1566). The dried and fresh pomegranate peels were cut into small pieces and weighed. For the extraction, the dry and fresh pomegranate peels (100 g) were added to ethanol (1000 ml) and methanol (1000 ml) extracts at 25 °C for two weeks. They were extracted separately. As a result of the extraction, four different extracts were obtained: dry pomegranate peel ethanol, dry pomegranate peel methanol, fresh pomegranate peel ethanol, and fresh pomegranate peel methanol. The extracts were filtered through filter paper and evaporated with a rotary evaporator. The extracts were preserved at -20 °C.<sup>42–44</sup> The schematic diagram of the experimental sections is given in Figure 1.

### Microorganisms

The eight strains of bacteria used were *Bacillus cereus* (BC, ATCC 10876), *Staphylococcus aureus* (SA, ATCC 538), *Salmonella typhimurium* (ST, ATCC 14028), *Pseudomonas aeruginosa* (PA, ATCC 27853), *Klebsiella pneumonia* (KP, ATCC 31488), *Proteus vulgaris* (PV, ATCC 6897), Methicillin-resistant *Staphylococcus aureus* (MRSA, ATCC 33592), and *Escherichia coli* (EC, ATCC 8739). The stock culture was maintained on a Nutrient agar (NA) medium at 4 °C in the refrigerator. Five fungal pathogens, *Candida albicans* (CA, ATCC10239), *Aspergillus flavus* Link (AF, TA41-17), *Aspergillus ochraceus* K. Wilh (AO, MUCL 39534), *Aspergillus niger* van Tiegh (AN, TA47-3), and *Fusarium proliferatum* (FP, Matsushima, Nirenberg, TA18-2), were used. The stock culture was maintained on Malt Extract Agar (MEA) medium at -20 °C. We investigated the anti-mycobacterial activities of the extracts against four tuberculosis strains (MT-H37Ra, MT-H37Rv, and two clinical isolates) by MPBA.

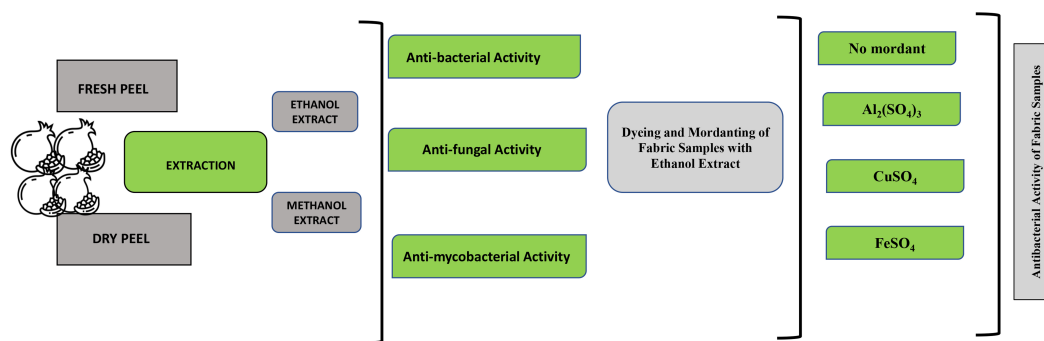


Figure 1. Schematic diagram of the experimental sections.

### Preparation of Bacterial and Fungal Cultures

The samples were weighed; their weight was found to be 0.5 g. They were solubilized within 5 ml DMSO to prepare the main stock. The stock solution concentration was 50 mg/mL. All stock solutions were stored in a deep freeze at  $-20^{\circ}\text{C}$ . To prepare 10 mL (500  $\mu\text{g}/\text{ml}$  concentration) of solution, 0.10 ml of stock solution was taken and 9.90 mL of DMSO was added. Therefore, the final solution concentrations were 500  $\mu\text{g}/\text{ml}$ . The range of working solution concentrations was between 250 and 0.12  $\mu\text{g}/\text{ml}$ . In vitro anti-bacterial activity efficiency was established by using MHA (Mueller Hinton Agar) and MHB (Mueller Hinton Broth), and anti-fungal activity assays SDA (Sabouraud Dextrose Agar) and SDB (Sabouraud Dextrose Broth). Anti-mycobacterial assays used were M7H9B (Middlebrook 7H9 Broth, Becton & Dickinson) and M7H10A (Middlebrook 7H10 Agar, Becton & Dickinson).

### Anti-Bacterial and Anti-Fungal Sensitivity Assays

#### Minimum Inhibitory Concentration Assay (MIC)

MIC determination for anti-bacterial and anti-fungal tests was carried out according to "Methods for Dilution Antimicrobial Susceptibility Tests, Approved Standards" for fungi<sup>45</sup> and bacteria.<sup>46</sup> In this study, the negative control well contains no organisms, while the positive control well contains organisms. Final concentrations in the wells ranged from 0.12  $\mu\text{g}/\text{ml}$  to 250  $\mu\text{g}/\text{ml}$ . For the incubation of all microplates, 24-48 h at  $37^{\circ}\text{C}$  for bacteria and 72 h at  $28^{\circ}\text{C}$  for fungi were selected. Anti-bacterial and anti-fungal activity tests were performed in three series. Then, Tiazolyl Blue Tetrazolium Bromide (TBTB, 20  $\mu\text{l}$ , Sigma) was added to the wells and incubated at  $37^{\circ}\text{C}$  for an additional 4 h. The color change in the solution was investigated. After the indicator dye turned pink, indicating positive bacteria growth, TBTB solution was added to the other wells.

### Minimum Bactericidal Concentration Assay (MBC) and Minimum Fungicidal Concentration Assay (MFC)

For MBC/MFC determination, the inoculum was taken from the MIC wells and higher concentration wells and then added to wells containing fresh and sterile SDA for fungi and MHB for bacteria. The plates were incubated at  $37^{\circ}\text{C}$  for bacteria and  $28^{\circ}\text{C}$  for fungi. Color change in positive and negative control wells was checked with a TBTB indicator. The lowest concentration without bacterial and fungal growth was accepted as MBC/MFC.

### Preparation of Mycobacterial Inocula and Anti-mycobacterial Activity Test

For susceptibility tests of *M. tuberculosis*, the MGIT guideline and National Committee for Clinical Laboratory Standards (NCCLS) were used.<sup>46-48</sup> For the production of *M. tuberculosis* strains incubated at  $37^{\circ}\text{C}$ , 7H9 Broth Base (4 ml), OADC (oleic acid, albumin, dextrose, and catalase) supplement (0.5 ml), and the antibiotic mixture of PANTA (polymyxin-B, amphotericin-B, nalidixic acid, trimethoprim, and azlocillin) (0.1 ml) were used. In the mycobacterial activity of pomegranate extract in the test using Microplate Presto Blue Assay (MPBA), 198  $\mu\text{l}$  of M7H9B and 2  $\mu\text{l}$  of extract were added to the first column of each row then 100  $\mu\text{l}$  of the medium was added to the other wells. Afterwards, 20  $\mu\text{l}$  of inoculum was added to the wells and each microplate was incubated at  $37^{\circ}\text{C}$  for 5 days. The experiments also included positive and negative controls. The final extract concentration was in the range of 0.12-250  $\mu\text{g}/\text{ml}$ . Anti-mycobacterial activity tests were performed in three series. After incubation, the results were evaluated with 20  $\mu\text{l}$  of Presto blue (Invitrogen, Life Technologies) solution.

In the evaluation, the blue color in the well means no growth, and the pink color means positive growth. The MIC was determined as the lowest concentration at which the color did not turn pink and gave a negative result. To determine the MBC, 20  $\mu\text{l}$  of the solution was taken from the non-growth wells and transferred to a new plate, and 80  $\mu\text{l}$  of freshly modified

M7H9B was added. The plates were incubated at 37 °C. Color change in positive and negative control wells was checked with Presto blue indicator. The lowest concentration without bacterial growth was accepted as MBC.

### Anti-Bacterial Activity of Textile Materials

The Parallel Streak Method<sup>49</sup> (AATCC Test Method 147-2011) is applied quickly and easily to determine the anti-bacterial activity of anti-microbial agents that can spread on treated textile materials. If a diffusible anti-microbial agent has anti-bacterial activity, a zone of inhibition is formed; this means that there is no growth of a microorganism on the surface of an agar medium near the boundaries of the sample placed in direct contact with the agar surface. Two strains of bacteria used were SA (ATCC 538) and KP (ATCC 31488). The stock culture was maintained on an NA at 4 °C in the refrigerators. Control and dyed fabric samples (non-sterile, (30/ 1 Rib and single jersey 100 % cotton) were cut by hand or with a die. Rectangular specimens cut 25 × 50 mm were recommended. The amount of bacterial inoculum was prepared using 0.5 McFarland standard (MF;  $1.5 \times 10^8$  CFU/ml). The bacterial inoculum was prepared by transferring 1.0 ml of a 24 h nutrient broth culture into 9.0 ml of sterile distilled water. During the application, five strips of 6 cm in length at 10 mm intervals were drawn on the surface of the NA using a loopful of diluted inoculum. Test specimens were placed along the five inoculation lines with gentle pressure to make contact with the agar surface. All petri dishes were incubated at 37 °C for 18-24 h.<sup>50</sup> It was examined whether there was a growth interruption and a clear inhibition zone along the inoculum lines in the incubation plates. The mean width of the line and the inhibition zone on both sides of the test samples were measured and the calculation was made using the formula:

$$W = (T - D)/2.$$

W = width of the net inhibition zone in mm

T = total diameter of test specimen and net area in mm

D = diameter of the test specimen in mm

## RESULTS

The pomegranate peel was successfully extracted using a rotary evaporator. All assays were performed using a microdilution method. Each extract showed anti-bacterial activity between 0.97-62.50 /ml as MICs and 7.81-250 g/ml as MBCs, and anti-fungal activity between 31.25-125 g/ml and 125-250 g/ml as MIC and MFC, respectively. The methanol extract of dry pomegranate peels exhibited the most significant activity, with a MIC value of 0.97 g/ml, and the ethanol extract of dry pomegranate exhibited a MIC value of 1.95 g/ml against *K. pneumonia*. The pomegranate peel ethanol extract exhibited the most significant activity against *A. flavus* and

*A. ochraceous* with a MIC value of 62.5 g/ml. It was also determined that the pomegranate extract was found to be effective against *C. albicans* (MIC 31.25- 62.5 g/ml) (Table1).

We also demonstrated the anti-mycobacterial activities of extracts against MT-H37Ra, MT- H37Rv, and two clinical isolates by myco-bactericidal activity test using the MPBA. The anti-mycobacterial activity of dry and fresh pomegranate extracts (ethanol and methanol) as MIC and MBC ( $\mu\text{g/ml}$ ) are shown in Table 2. Each extract showed anti-mycobacterial efficacy between MIC 7.81-31.25  $\mu\text{g/ml}$  and MBC 31.25-250  $\mu\text{g/ml}$  against four strains of *M. tuberculosis*. The extract of peels exhibited the most significant activity against MT-H37Ra and MT-H37Rv with a MIC value of 7.81  $\mu\text{g/ml}$  and 31.25  $\mu\text{g/ml}$ , respectively.

As a result of dyeing with pomegranate peel extract, a color scale ranging from dark brown to yellow was obtained. CIE color coordinates are given in Table 3.

The anti-microbial efficacy of the treated and control fabric samples was determined by the parallel streak method (AATCC 147). The extent of anti-microbial activity was measured and recorded, and the zone of inhibition of the anti-microbial activity of the dyed and control fabric samples against two pathogens is shown in Figure 1. In this study, we used two factors for measuring the inhibition zone method: the anti-microbial activity of the samples against the microorganism, and the capability of the anti-microbial agent to diffuse into the agar. In this way, fabric samples acquire anti-microbial activity by gaining bactericidal (killing bacteria) or bacteriostatic (reducing bacterial growth and development) properties (Figure 2).

The fabric samples dyed with fresh and dry pomegranate peel extract and placed in the agar surface were monitored after 24 hours. The effect of the anti-microbial agents diffused into the agar was examined from under the plate as an inhibition zone or no growth. Whereas the control fabric sample and mordanted fabric samples did not show any zone of inhibition, the fabric samples dyed with dry pomegranate peel showed better anti-bacterial activity against *S. aureus* (16 mm). The results are shown in Figure 3.

## DISCUSSION

The results of the anti-microbial activities of methanol and ethanol extracts revealed that both extracts had an inhibitory effect on test microorganisms. The results of MIC and MBC indicated that the pomegranate extract had a great ability to prevent the growth of bacteria, fungi, and mycobacteria. The best inhibitory concentrations of fresh and dry peel ethanolic extracts were observed on *K. pneumoniae* (1.95  $\mu\text{g/ml}$ ), *E. coli* (62.5  $\mu\text{g/ml}$ ), and *C. albicans* (31.25  $\mu\text{g/ml}$ ). Also, the fresh and dry peel methanol extracts showed an inhibitory effect on *S. aureus* (1.95  $\mu\text{g/ml}$ ), *E. coli* (62.5  $\mu\text{g/ml}$ ), and *B. cereus* (7.81  $\mu\text{g/ml}$ ). In addition, the inhibitory concentrations of dry

**Table 1.** Anti-bacterial and anti-fungal activity of pomegranate extracts ( $\mu\text{g/mL}$ ).

	Anti-bacterial and Anti-fungal Activity ( $\mu\text{g/mL}$ )							
	MIC	MBC/MFC	MIC	MBC/MFC	MIC	MBC/MFC	MIC	MBC/MFC
	DP-E		DP-M		FP-E		FP-M	
<i>S. aureus</i>	7.81	15.62	1.95	15.62	3.90	250	1.95	1.95
<i>K. pneumoniae</i>	1.95	250	0.97	250	1.95	250	1.95	1.95
<i>E. coli</i>	62.5	250	62.5	250	62.5	250	62.5	62.5
<i>B. cereus</i>	7.81	250	7.81	125	7.81	250	7.81	7.81
<i>S. typhimurium</i>	62.5	250	62.5	250	62.5	250	125	125
<i>P. vulgaris</i>	15.62	62.5	15.62	125	7.81	7.81	15.62	15.62
<i>P. aeruginosa</i>	62.5	125	62.5	125	62.5	125	62.5	62.5
MRSA	31.25	250	62.5	250	15.62	250	7.81	7.81
<i>C. albicans</i>	31.25	125	62.5	125	31.25	125	31.25	250
<i>A. flavus</i>	62.5	250	125	250	62.5	250	125	250
<i>A. niger</i>	125	125	125	250	62.5	125	125	250
<i>A. ochraceus</i>	62.5	125	62.5	125	125	125	125	250
<i>F. proliferatum</i>	125	125	125	250	125	125	125	125

MIC: Minimum Inhibition Concentration; MBC/MFC: Minimum bactericidal/fungicidal concentration; DP-E: Dry pomegranate ethanol extract; DP-M: Dry pomegranate methanol extract; FP-E: Fresh pomegranate ethanol extract; FP-M: Fresh pomegranate methanol extract

**Table 2.** Anti-mycobacterial activity of pomegranate extracts ( $\mu\text{g/ml}$ ).








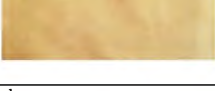
	Anti-mycobacterial activity ( $\mu\text{g/mL}$ )							
	H37Ra		H37Rv		Strain 1		Strain 2	
	MIC	MBC	MIC	MBC	MIC	MBC	MIC	MBC
DP-E	15.62	125	31.25	125	31.25	250	31.25	31.25
DP-M	7.81	62.5	31.25	125	31.25	250	31.25	31.25
FP-E	15.62	125	31.25	125	31.25	250	15.62	31.25
FP-M	15.62	62.5	15.62	125	31.25	250	31.25	31.25
	Standard drugs							
INH	0.13	1.04	0.52	1.04	0.52	1.04	0.52	4.16
RIF	0.64	5.12	0.32	2.56	0.64	0.64	5.12	10.24

INH: Isoniazid; RIF: Rifampicin; DP-E: Dry pomegranate ethanol extract; DP-M: Dry pomegranate methanol extract; FP-E: Fresh pomegranate ethanol extract; FP-M: Fresh pomegranate methanol extract

peel ethanolic extracts belonged to MRSA, *C. albicans* and *A. flavus* (31.25  $\mu\text{g/ml}$ ), and dry peel methanolic extracts (62.50  $\mu\text{g/ml}$ ). It can be concluded that the ethanolic solvent is more

effective than the methanolic in reacting with components and ingredients of the pomegranate extract due to an increase in the release of active substances from the plant, and enhancing con-

**Table 3.** Fabric samples dyed with fresh and dry pomegranate peel with and without mordants.

Sample Name	Mordant	Pom. Peel Amount (%)	Obtained Color	CIE color coordinates		
				L*	a*	b*
FPP-1	No mordant	100		55.1	7.4	9.4
DPP-1	No mordant	100		77.0	2.6	8.9
FPP-2	Al <sub>2</sub> (SO <sub>4</sub> ) <sub>3</sub>	100		70.4	3.5	17.9
DPP-2	Al <sub>2</sub> (SO <sub>4</sub> ) <sub>3</sub>	100		87.4	1.9	-2.1
FPP-3	CuSO <sub>4</sub>	100		52.1	14.7	52.2
DPP-3	CuSO <sub>4</sub>	100		76.1	5.7	2.1
FPP-4	FeSO <sub>4</sub>	100		58.4	8.0	11.4
DPP-4	FeSO <sub>4</sub>	100		67.8	3.8	14.1

DPP: Dry pomegranate peel; FPP: Fresh pomegranate peel

centrations of these substances in ethanolic extract compared to methanolic extract is more effective.<sup>52</sup>

Pomegranate has a strong inhibitory effect against many microorganisms (Gram-negative and Gram-positive bacteria, filamentous fungi, and mold) and a broad spectrum of anti-microbial action. Although different parts of the pomegranate (peels, leaf seeds) showed various anti-microbial activities with different extracts, many scientists stated that the anti-microbial activity of the pomegranate peel was stronger than the other parts, and the anti-microbial activity of the peel was dependent on the total flavonoid and tannin content.<sup>53</sup> The anti-microbial activity of pomegranate peel was also shown by Ismail et al.<sup>54</sup> against bacteria and fungi. Ali et al.<sup>55</sup> showed that pomegranate peel extracts inhibited the growth of *S. aureus* (Gram-positive) and *Salmonella* (Gram-negative). In their research, they investigated the effectiveness of extracts of the different parts of pomegranate (skin, seed, juice, and whole fruit) against seven bacteria: *B. coagulans*, *B. cereus*, *B. subtilis*, *S. aureus*, *E. coli*, *K. pneumoniae*, and *P. aeruginosa*. The highest effect

was seen in the pomegranate peel.<sup>56</sup> Other works based on the anti-fungal activity of pomegranate and some researchers<sup>57</sup> showed that the peel of pomegranate was the most efficient for inhibiting *C. albicans* growth. In addition, the anti-fungal activity of pomegranate against mycelial fungi has been determined in many studies.<sup>58</sup> Glazer et al., demonstrated the anti-fungal effects of pomegranate peel extracts against *Stemphylium botryosum*, *Alternaria alternata*, and *Fusarium species*.<sup>59</sup>

Phenolic compounds and their derivatives are important compounds in the defense system of plants, and many pathogenic microorganisms have a deterrent effect on their development. Where plant-derived anti-microbial agents come to the fore, cessation of microorganism growth and subsequent prevention of a secondary infection are expected features.<sup>60</sup> It has been reported that pomegranate peel contains many important active anti-fungal compounds, such as punicalagin, castagalagin, granatin, catechin, gallo catechin, kaempferol, and quercetin.<sup>61-64</sup>

In our study, the anti-mycobacterial activities of pomegranate peel extracts were tested on reference and patient strains. The

## Mechanism Anti-bacterial Activity: Comparison of dyed and undyed fabric samples

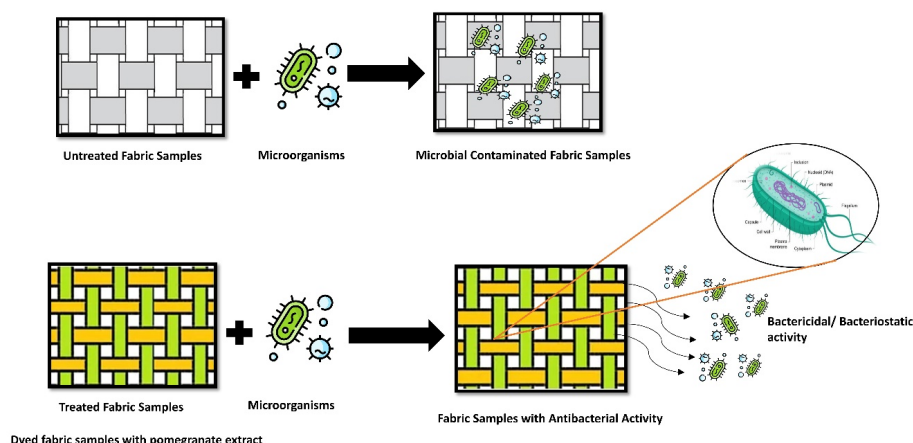


Figure 2. A mechanism between fabric samples and pomegranate extract.

extract of dried peel methanol extract exhibited the most significant activity against MT-H37Ra, with an MIC value of  $7.81 \mu\text{g/ml}$ , and fresh methanol peel extract exhibited the most significant activity against MT-H37Rv, with an MIC value of  $15.62 \mu\text{g/ml}$ . When the anti-mycobacterial activity of ethanol and methanol extracts was compared, it was found that methanol extract showed higher activity than ethanol on reference strains. This study is the first report describing the anti-mycobacterial activity of pomegranate peel in different forms (fresh/dry) and extracts (ethanol/methanol) against reference and patient strains. Another study evaluated the inhibitory effect of alcoholic extracts of *Berberis vulgaris*, *Rosa canina*, *Peganum harmala*, *P. granatum*, *Digitalis sp.*, and *Citrus lemon* on *Mycobacterium* isolates. The findings indicated that extracts of *P. harmala*, *P. granatum*, *Digitalis sp.*, and *C. lemon* exhibited inhibitory effects against non-MDR bacteria at various doses, with *P. granatum* showing the maximum inhibition zone ( $19.5 \text{ mm}$ ) against isoniazid and rifampin-resistant isolates.<sup>65</sup> The results we obtained in our study are consistent with the anti-mycobacterial activity results of these studies.

Since textile products are organic, fibrous, and absorbent materials, they offer suitable conditions for microorganisms during human contact and exposure to atmospheric dirt. For these reasons, there is increasing interest in the development of textile materials that inhibit the growth of microorganisms.<sup>51</sup> Various mineral particles and organic compounds were evaluated as anti-microbial additives for textiles.<sup>66</sup> Investigations have revealed that pomegranate could be used as a natural alternative to synthetic bactericidal materials against different microbial pathogens. The pomegranate peel extract contains a higher amount of phenolic content than the pulp and thus demonstrates superior anti-bacterial activity.<sup>67</sup> There are studies in the literature for fabrics to gain anti-bacterial properties

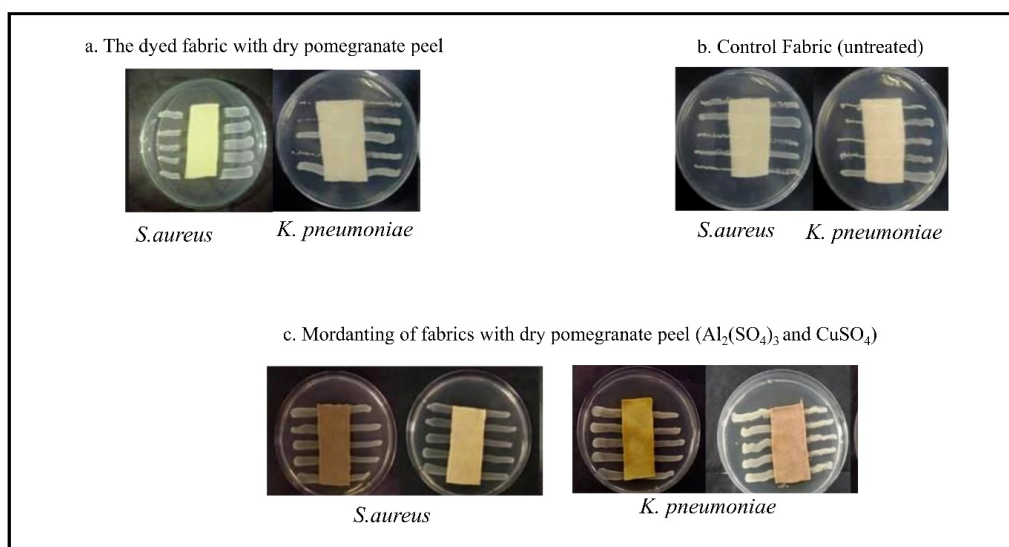
by utilizing the high number of phenolic substances contained in the pomegranate peel.

Ul-Islam et. al,<sup>68</sup> aimed to develop low-cost bacterial cellulose-based anti-bacterial composite with pomegranate (*P. granatum L.*) peel extract for potential biomedical applications. Field-emission scanning electron microscopic (FE-SEM) observation showed a nanofibrous and microporous morphology of pristine bacterial cellulose and confirmed the development of bacterial cellulose-pomegranate peel composite. The bacterial cellulose-pomegranate peel composite exhibited better reswelling capabilities than pristine bacterial cellulose after three consecutive re-wetting cycles. The bacterial cellulose-pomegranate peel composite showed good anti-microbial activity against *S. aureus* (Gram-positive). The findings of this study indicate that bacterial cellulose-pomegranate peel composite could be a promising anti-bacterial wound dressing material.

Another study reports the simultaneous coloring, anti-oxidant activity, and anti-microbial activity of cotton fabrics dyed using silver nanoparticles (AgNPs) and pomegranate peel extract. During the reaction, hydroxyl groups present in pomegranate peel-tannins served to interact with silver ions, subsequently reducing them to AgNPs. The formation of AgNPs, and subsequently their deposition on the surface of cotton, was characterized by UV-visible spectroscopy, transmission electron microscopy (TEM), scanning electron microscopy (SEM), energy disperse X-ray (EDX) line, and ICP-MS analysis. It was determined that cotton fabrics dyed with this combination exhibited an effective anti-bacterial activity.<sup>69</sup>

As a result of dyeing with pomegranate peel extract, a color scale was obtained ranging from dark brown to yellow. The anti-microbial efficacy of the treated and untreated fabric sample





**Figure 3.** Assessment of anti-bacterial activity of the treated and untreated fabric samples.

was determined by the parallel streak method (AATCC 147). In our study, the fabric sample dyed with dry pomegranate peel showed better anti-bacterial activity against *S. aureus*. Regarding biological activities known in the literature, anti-bacterial natural dyes have gained in importance in recent years. There is the use of anti-microbial compounds, especially from natural sources<sup>70,71</sup>, including pomegranate polyphenols, and they may show appropriate anti-microbial activity due to the presence of broad-spectrum antibiotic compounds in this plant.<sup>72</sup> *S. aureus* (SA) is the main cause of infections in hospitals.<sup>73</sup> The use of textile products with anti-microbial activity in clinical and medical applications also has advantages, such as reducing the transmission of infection by bacteria<sup>74</sup> and non-toxicity in contact with human skin.<sup>75</sup> In recent years, measures to protect textile products from microorganisms and their toxins have increased.<sup>76</sup> Therefore, anti-microbial textiles have become important in terms of protection and are promising in this respect.<sup>77,78</sup>

These findings provide valuable information for future applications of natural dyes in textiles. The anti-mycobacterial, anti-fungal, and anti-bacterial properties of pomegranate could be significant in developing a model for drug design. Fabrics coated with natural anti-microbial agents derived from plants can have anti-microbial properties, making them ideal for use in textiles. Furthermore, due to their environmentally friendly and non-toxic nature, these natural anti-microbial materials are still promising candidates for textile applications.

**Peer Review:** Externally peer-reviewed.

**Author Contributions:** Conception/Design of study: T.A., P.G.; Data Acquisition: T.A., P.G.; Data Analysis/Interpretation: T.A., P.G.; Drafting Manuscript: P.G.; Critical Revision of Manuscript: T.A., P.G.; Final Approval and Accountability: T.A., P.G.; Technical or Material Support: T.A.; Supervision: T.A.. All authors have read and agreed to the published version of the manuscript.

**Conflict of Interest:** Authors declared no conflict of interest.

**Financial Disclosure:** Authors declared no financial support.

#### ORCID IDs of the authors

Pinar Guner 0000-0001-6922-7009  
Tulin Askun 0000-0002-2700-1965

#### REFERENCES

1. El Barnossi A, Moussaid F, Iraqi Housseini A. Tangerine, banana, and pomegranate peels valorization for a sustainable environment: A review. *Biotechnol Rep.* 2021;29.
2. Gündoğdu M, Yılmaz H, Canan İ, Nar ( *Punica granatum L.*) Çeşit ve Genotiplerin Fizikokimyasal Karakterizasyonu. *IJAWS.* 2015;1(2):57-65.
3. Egharevba HO, Kunle OF. Preliminary phytochemical and proximate analysis of the leaves of *Piliostigma thionningii* (Schumach.) Milne-Redhead. *Ethnobot Leaflets.* 2010;14:570-577.
4. Fawole OA, Opara UL. Harvest discrimination of pomegranate fruit: Postharvest quality changes and relationships between instrumental and sensory attributes during shelf life. *J Food Sci.* 2013;78(8).

5. Gupta D, Khare SK, Laha A. Antimicrobial properties of natural dyes against Gram-negative bacteria. *Color Technol.* 2004;120:167–171.
6. Onar N, Aksit A, Sen Y, Mutlu M. Antimicrobial, UV-protective and self-cleaning properties of cotton fabrics coated by dip-coating and solvothermal coating methods. *Fibers Polym.* 2011;12:461–470.
7. Malviya S, Jha A, Hettiarachchy N. Antioxidant and antibacterial potential of pomegranate peel extracts. *J Food Sci Technol.* 2014; 51:4132–4137.
8. Jayaprakasha GK, Negi PS, Jena BS. Antimicrobial activities of Pomegranates. In Pomegranates, ed. CRC press. FL, USA: Boca Raton, Inc; 2006:167-168.
9. Bassiri-Jahromi S. *Punica granatum* (Pomegranate) activity in health promotion and cancer prevention. *Oncol Rev.* 2018;12(1):345.
10. Zhang J, Zhan, B, Yao X, Gao Y, Shong J. Antiviral activity of tannin from the pericarp of *Punica granatum* L. against genital Herpes virus *in vitro*. *Zhongguo Zhong yao za zhi.* 1995;20(9):556-576.
11. Vijayanand S, Hemapriya J. In vitro antibacterial efficacy of peel and seed extracts of *Punica granatum* L. against selected bacterial strains. *Int J Microbiol Res.* 2011;1(4):231-234.
12. Parmar HS, Kar A. Medicinal values of fruit pericarp from *Citrus sinensis*, *Punica granatum* and *Musa paradisiaca* with respect to alterations in tissue lipid peroxidation and serum concentration of glucose, insulin and thyroid hormones. *J Med Food.* 2008;11(2):376-381.
13. Heber D, Seeram NP, Wyatt H, Henning SM, Zhang Y. Safety and antioxidant activity of a pomegranate ellagitannin-enriched polyphenol dietary supplement in overweight individuals with increased waist size. *J Agric Food Chem.* 2007;55:10050-10054.
14. Parmar HS, Kar A. Protective role of *Citrus sinensis*, *Musa paradisiaca* and *Punica granatum* pericarp against diet-induced atherosclerosis and thyroid dysfunctions in rats. *Nutr Res.* 2007;27(11):710-718.
15. Aviram A, Rosenblat M, Gaitini Aviram M, et al. Pomegranate juice consumption for 3 years by patients with carotid artery stenosis reduces common carotid intima-media thickness, blood pressure and LDL oxidation. *Clin Nutr.* 2004;23:423-433.
16. Naz S, Siddiqi R, Ahmad S, Rasool SA, Sayeed SA. Antibacterial activity directed isolation of compounds from *Punica granatum*. *J Food Sci.* 2007;72(9):M341-M345.
17. Braga LC, Shupp JW, Cummings C, et al. Pomegranate extract inhibits *Staphylococcus aureus* growth and subsequent enterotoxin production. *J Ethnopharmacol.* 2005;96(1-2):335-339.
18. Zhang L, Fu Q, Zhang Y. Composition of anthocyanins in pomegranate flowers and their antioxidant activity. *Food Chem.* 2011;127:1444–1449.
19. Aguilera-Carbo A, Augur C, Prado-Barragan LA, Favela-Torres E, Aguilar CN. Microbial production of ellagic acid and biodegradation of ellagitannins. *Appl Microbiol Biotechnol.* 2008;78:189–199.
20. Prashanth D, Asha M, Amit A. Antibacterial activity of *Punica granatum*. *Fitoterapia.* 2001;72:171–173.
21. Tiwari HC, Singh P, Mishra PK, Shrivastava P. Evaluation of various techniques for extraction of natural colorants from pomegranate rind ultrasonic and enzyme assisted extraction. *IJFTR.* 2010;35:272-276.
22. Kandyli P, Kokkinomagoulos E. Food applications and potential health benefits of pomegranate and its derivatives. *Foods.* 2020;9(2):122.
23. Lansky EP, Newman RA. *Punica granatum* (Pomegranate) and its potential for prevention of treatment of inflammation and cancer. *J Ethnopharmacol.* 2007;109:177-206.
24. Panichayupakaranant P, Tewtrakul S, Yuenyongsawad S. Antibacterial, anti-inflammatory, and anti-allergic activities of standardized pomegranate rind extract. *Food Chem.* 2010;123: 400–403.
25. Turkyilmaz, M. Anthocyanin and organic acid profiles of pomegranate (*Punica granatum* L.) juices from registered varieties in Turkey. *Int J Food Sci Technol.* 2013;48:2086–2095.
26. Smaoui S, Hlima H, Ben Mtibaa AC, et al. Pomegranate peel as phenolic compounds source: Advanced analytical strategies and practical use in meat products. *Meat Sci.* 2019;158.
27. Juneja VK, Cadavez V, Gonzales-Barron U, Mukhopadhyay S, Friedman M. Effect of pomegranate powder on the heat inactivation of *Escherichia coli* O104: H4 in ground chicken. *Food Control.* 2016;70:26–34.
28. Li Destri Nicosia MG, Pangallo S, Raphael G, et al. Control of postharvest fungal rots on citrus fruit and sweet cherries using a pomegranate peel extract. *Postharvest Biol Technol.* 2016;114: 54–61.
29. Diganta D, Ratnamala R, Banasri H. Antimicrobial activity of pomegranate fruit constituents against drug-resistant *Mycobacterium tuberculosis* and b-lactamase producing *Klebsiella pneumoniae*. *Pharm Biol.* 2015;53(10):1474–1480.
30. Olukunle JO, Adenubi OT, Oladele GM, Sogebi EA, Oguntoke PC. Studies on the anti-inflammatory and analgesic properties of *Jatropha curcas* leaf extract. *Acta Vet Brno.* 2011;80:259–262.
31. Crini G. Non-conventional low-cost adsorbents for dye removal: A review. *Bioresource Technol.* 2006;97: 1061-1085.
32. Forgacs E, Cserháti T, Oros G. Removal of synthetic dyes from wastewaters: A review. *Environ Int.* 2004;30(7):953-971.
33. Hou XL, Chen XZ, Cheng YX, Xu HL, Chen LF. Dyeing and UV-protection properties of water extracts from orange peel. *J Clean Prod.* 2013;52:410-419.
34. Hosseinneshad M, Gharanjig K, Razani N, et al. Green miles in dyeing technology: Metal-rich pumpkin extracts in aid of natural dyes. *Environ Sci Pollut Res.* 2022;29:50608–50616.
35. Gong K, Pan Y, Rather LJ, Wang W, Zhou Q, Li TZ. Natural pigment during flora leaf senescence and its application in dyeing and UV protection finish of silk and wool a case study of *Cinnamomum camphora*. *Dyes Pigm.* 2019;166:114–121.
36. Jose S, Pandit P, Pandey R. Chickpea husk—a potential agro waste for coloration and functional finishing of textiles, *Ind Crop Prod.* 2019;142:111833.
37. Otaviano BTH, Sannomiya M, Soares de Lima F, et al. Pomegranate peel extract and zinc oxide as a source of natural dye and functional material for textile fibers aiming for photoprotective properties. *Mater Chem Phys.* 2023;(293):126766.
38. Barhanpurkar S, Bhat P, Kumar A, Purwar R, professor A. Studies of Banana SAP used as mordant for natural dye. *Int J Text Eng Process.* 2015;1(4):2395-3578.
39. Zhou Y, Yang ZY, Tang RC. Facile and green preparation of bioactive and UV protective silk materials using the extract from red radish (*Raphanus sativus* L.) through adsorption technique. *Arab J Chem.* 2020;13:3276–3285.
40. Goodarzian H, Ekrami E. Wool dyeing with extracted dye from pomegranate (*Punica granatum*) peel. *World Appl Sci J.* 2010;8(11):1387-1389.
41. Kulkarni SS, Gokhale AV, Bodake UM, Pathade GR. Cotton dyeing with natural dye extracted from Pomegranate

- (*Punica granatum*) peel. *Univers. J Environ Res Technol.* 2011;1(2):135-139.
42. Albu S, Joyce E, Paniwnyk L, Lorimer JP, Mason TJ. Potential for the use of ultrasound in the extraction of antioxidants from *Rosmarinus officinalis* for the food and pharmaceutical industry. *Ultrason Sonochem.* 2004;1(3):261–265.
  43. Barkhordari P, Bazargani-Gilani B. Effect of apple peel extract and zein coating enriched with ginger essential oil on the shelf life of chicken thigh meat. *J Food Meas Charact.* 2021;15(3):2727–2742.
  44. Pan Y, Wang K, Huang S, et al. Antioxidant activity of microwave-assisted extract of longan (*Dimocarpus longan Lour.*) peel. *Food Chem.* 2008;106(3):1264–1270.
  45. National Committee for Clinical Laboratory Standards (NCCLS). National Committee for Clinical Laboratory Standards. Reference Methods for broth dilution antifungal susceptibility testing of filamentous fungi. Approved Standard. Second Edition NCCLS document M38-A2. Wayne, Pennsylvania, 2008;28(16):1-29.
  46. National Committee for Clinical Laboratory Standards (NCCLS). National Committee for Clinical Laboratory Standards. Methods for Dilution Antimicrobial Susceptibility Tests for Bacteria That Grow Edition Aerobically; Approved Standard. Seventh Edition NCCLS Document M7-A7., Wayne, Pennsylvania, 2006;26(2):1-16.
  47. Becton Dickinson and Company Newsletter BD. Bactec MGIT 960 SIRE kit now FDA-cleared for susceptibility testing of *Mycobacterium tuberculosis*. *Microbiology News & Ideas.* 2002;13: 4-4.
  48. National Committee for Clinical Laboratory Standards (NCCLS). Susceptibility Testing of *Mycobacteria*, *Nocardiae*, and Other Aerobic Actinomycetes; Approved Standard. NCCLS document M24-A [ISBN 1-56238-500-3]. NCCLS, 940 West Valley Road, Suite 1400, Wayne, Pennsylvania 19087-1898 USA, 2003.
  49. AATCC Test Method 147-2004, Antibacterial activity assessment of textile materials: Parallel streak method. AATCC Technical Manual, American Association of Textile Chemists and Colorists, Research Triangle Park, NC. 2008.
  50. Bahtiyari Mİ, Benli H, Yavaş A. Printing of wool and cotton fabrics with natural dyes. *Asian J Chem.* 2008;25(6):3220-3224
  51. de Oliveira CRS, Mulinari J, Batistell MA, Augusto Ulson de Souza A, Selene Maria de Arruda Guelli Ulson de Souza. Antimicrobial effect of cotton fabric functionalized with a kaolinite-titania nano-hybrid composite. *Mater Chem Phys.* 2023;295:127078.
  52. Hajimohammadi NJR, Gharbani P, Mehrizad A. Antibacterial activity of *Punica granatum* L. and *Areca nut* (P.A) combined extracts against some food born pathogenic bacteria. *Saudi J Biol Sci.* 2022;1730-1736.
  53. Casquete R, Castro SM, Martín A, Ruíz-Moyano S, Saraiva J. Evaluation of the effect of high pressure on total phenolic content, antioxidant and antimicrobial activity of citrus peels. *Innov Food Sci Emerg Technol.* 2015;31:37–44.
  54. Ismail T, Akhtar S, Sestili P, Riaz M, Ismail A. Antioxidant, antimicrobial and urease inhibitory activities of phenolics-rich pomegranate peel hydro-alcoholic extracts. *J Food Biochem.* 2016;40(4):550–558.
  55. Ali A, Chen Y, Liu H, et al. Starch-based antimicrobial films functionalized by pomegranate peel. *Int J Biol Macromol.* 2019;129:1120–1126.
  56. Dahham, BSS, Ali MN, Tabassum H, Khan M. Studies on antibacterial and antifungal activity of pomegranate (*Punica granatum* L.). *AEJAES.* 2010;9(3):273–281.
  57. Tayel AA, El-Tras WF. Anticandidal activity of pomegranate peel extract aerosol as an applicable sanitizing method. *Mycoses.* 2010;53(2):117-122.
  58. Shuhua Q, Hongyun, Yanning Z. Inhibitory effects of *Punica granatum* peel extracts on *Botrytis cinerea*. *J Plant Dis Prot.* 2010; 36 (1):148-150.
  59. Glazer I, Masaphy S, Marciano P, et al. Partial identification of antifungal compounds from *Punica granatum* peel extracts. *J Agric Food. Chem.* 2012;60 (19):4841-4848.
  60. Farag MA, Al-Mahdy DA, Salah El Dine R, Fahmy S, Yassi A. Structure activity relationships of antimicrobial gallic acid derivatives from pomegranate and acacia fruit extracts against potato bacterial wilt pathogen. *Chem Biodivers.* 2015;12 (6): 955-962.
  61. Wang R, Ding Y, Liu R, Xiang L, Du L. Pomegranate: Constituents, bioactivities and pharmacokinetics. *Fruit, Vegetable Cereal Sci Biotechn.* 2010;4 (2), 77-87.
  62. Prakash CVS, Prakash I. Bioactive chemical constituents from pomegranate (*Punica granatum*) juice, seed and peel - a review. *Int J Res in Chem Environt.* 2011;1 (1), 1-18.
  63. Nahar PP, Driscoll MV, Li L, Slitt AL, Seeram NP. Phenolic mediated antiinflammatory properties of a maple syrup extract in RAW 264.7 murine macrophages. *J Func Foods.* 2014; 6:126-136.
  64. Amyrgialaki E, Makris DP, Mauromoustakos A, Kefalas P. Optimisation of the extraction of pomegranate (*Punica granatum*) husk phenolics using water/ethanol solvent systems and response surface methodology. *Ind Crops Pro.* 2014;59:216-222.
  65. Kardan Yamchi J, Mahboubi M, Kazemian H, Hamzelou G, Feizabadi MM. The chemical composition and antimycobacterial activities of *Trachyspermum copticum* and *Pelargonium graveolens* essential oils. *Recent Pat Antiinfect Drug Discov.* 2020;15(1):68-74. doi:10.2174/1574891X14666191028113321
  66. Yang F, Wang A. Recent researches on antimicrobial nanocomposite and hybrid materials based on sepiolite and palygorskite. *Appl Clay Sci.* 2022; 219: 106454. doi: 10.1016/j.clay.2022.106454.
  67. Gozlekçi S, Saraçoğlu O, Onursal E, Ozgen M. Total phenolic distribution of juice, peel, and seed extracts of four pomegranate cultivars. *Pharmacogn Mag.* 2011;7:161. doi: 10.4103/0973-1296.80681 .
  68. Ul-Islam M, Alhajaim W, Fatima A, et al. Development of low-cost bacterial cellulose-pomegranate peel extract-based antibacterial composite for potential biomedical applications. *Int J Bio. Macromol.* 2023;231:123269.
  69. Ul-Islam S, Butola BS, Gupta A, Roy A. Multifunctional finishing of cellulosic fabric via facile, rapid in-situ green synthesis of AgNPs using pomegranate peel extract biomolecules. *Sustainable Chem Pharm.* 2019;12:100135.
  70. Ibrahim N, El-Gamal A, Gouda M, Mahrous F. A new approach for natural dyeing and functional finishing of cotton cellulose. *Carbohydr Polym.* 2010;82:1205–1211. doi: 10.1016/j.carbpol.2010.06.054
  71. Singh R, Jain A, Panwar S, Gupta D, Khare S. Antimicrobial activity of some natural dyes. *Dyes Pigm.* 2005; 66:99–102
  72. Mahmood MA, Al-Dhaher ZA, AL-Mizraqchi AS. Antimicrobial activity of aqueous extracts of pomegranate, sumac, sage, anise, hand bull tongue, thyme, cloves, lemon and mint against some food-borne pathogens. *Iraqi J Vet Med.* 2010; 34(2):85–94. doi:10.30539/iraqjvm.v34i2.635.
  73. Sanbhal N, Ma Y, Sun G, Li Y, Peerzada M, Wang L. Preparation and characterization of antibacterial polypropylene

- meshes with covalently incorporated  $\beta$ -cyclodextrins and captured antimicrobial agent for hernia repair. *Polymers*. 2018;10:58. doi:10.3390/polym10010058.
74. Sun G. Antibacterial textile materials for medical applications. *Mater Sci Eng*. 2011;360–375.
75. Simoncic B, Tomsic B. Structures of novel antimicrobial agents for textiles: A review. *Text Res J*. 2010;80:1721–1737.
76. Al-Zoreky N. Antimicrobial activity of pomegranate (*Punica granatum* L.) fruit peels. *Int J Food Microbiol*. 2009;134:244–248.
77. Ismail T, Sestili P, Akhtar S. Pomegranate peel and fruit extracts: a review of potential anti-inflammatory and anti-infective effects. *J Ethnopharmacol*. 2012;143:397–405.
78. Kim ND, Mehda R, Weiping Y, Ishak N, Talia L. Chemopreventive and adjuvant therapeutic potential of pomegranate (*Punica granatum*) for human breast cancer. *Breast Cancer Res Treat*. 2002;71:203–217.

### How cite this article

Guner P, Askun T. Anti-Bacterial, Anti-Mycobacterial and Anti-Fungal Properties of *Punica granatum* as Natural Dye. *Eur J Biol* 2023;82(1): 38-48. DOI: 10.26650/Eur-JBiol.2023.1239283

# The Senescence Program is Reduced in Proteasome Inhibitor Bortezomib-Resistant PC3 Prostate Cancer Cell Line

Ertan Kanbur<sup>1,2,3</sup>,  Semih Seker<sup>4</sup>,  Ferah Budak<sup>3</sup>,  Azmi Yerlikaya<sup>4</sup> 

<sup>1</sup>Nanothera Lab, Drug Application and Research Center (ERFARMA), Erciyes University, Kayseri, Türkiye

<sup>2</sup>Clinical Engineering Research and Implementation Center (ERKAM), Erciyes University, Türkiye

<sup>3</sup>Department of Immunology, Faculty of Medicine, Bursa Uludağ University, Bursa, Türkiye

<sup>4</sup>Kutahya Health Sciences University, Faculty of Medicine, Department of Medical Biology, Kutahya, Türkiye

## ABSTRACT

**Objective:** Senescence may act as an antitumor mechanism by preventing the proliferation of cancer cells. Here we investigated the hypothesis that PC3 prostate cancer cells resistant to bortezomib respond differently to proteasomal inhibition with respect to induction of the senescence program as compared to the parental cells.

**Materials and Methods:** The degree of senescence was measured by  $\beta$ -galactosidase activity and the level of senescence-associated p16 INK4a by Western blotting after treatment of cells with varying concentrations of bortezomib. In addition, the senescence-associated secretory phenotype was analyzed by Human Cytokine Antibody Array.

**Results:** It is reported that the basal level of senescence was lower in resistant cells compared to non-resistant cells. It was found that the basal level of the senescence marker p16 INK4a was lower in bortezomib-resistant cells than in parent non-resistant cells. Moreover, p16 INK4a was significantly reduced in both cells under conditions of 100 nM bortezomib treatment, a finding suggesting that the reduced senescence after proteasomal inhibition was likely due to the reduced levels of p16 INK4a. Finally, it is reported here for the first time that basal levels of the proteins NAP2, FGF-6, MIP-3 $\alpha$ , and PARC are significantly increased in the resistant cells compared to the parental cells.

**Conclusion:** Overall, the results suggest that inhibition of senescence may play an important function in the development of resistance to bortezomib.

**Keywords:** Bortezomib, cancer, prostate, proteasome, p16 INK4a, senescence

## INTRODUCTION

Senescence, also known as cellular aging, is a dynamic cellular program that restricts the proliferation of old or damaged cells.<sup>1,2</sup> Characteristic features of senescent cells include the absence of proliferation markers and expression of the senescence-induced  $\beta$ -galactosidase.<sup>3</sup> Recent studies show that senescence is a highly stable cell cycle arrest and can be induced *in vitro* or *in vivo* in actively proliferating cells in response to proliferative stress or DNA damage.<sup>2,4</sup> Senescence stimuli also include oncogenic stress, ionizing agents, reactive oxygen species, and chemotherapeutic agents.<sup>4,5</sup> Because senescence can function as an antitumor mechanism, the integrity of the senescence program can also significantly affect cancer development and treatment outcomes.<sup>2</sup> In the absence of simple molecular or biochemical assays, there are few studies investigating the mechanism of senescence. Moreover, some of the

detected senescence markers are not specific to the senescence program; for example, upregulation of certain cyclin-dependent kinase inhibitors (CDKi) also occurs in quiescent cells.<sup>4,6</sup> Interestingly, several viral oncogenes (SV40 large T antigen, HPV E6, and E7 proteins) are known to bypass the cellular senescence program by inactivating the tumor suppressor genes p53 and Rb.<sup>7,8</sup> However, it is very interesting to note that in the presence and stimulation of p53 and p16 INK4a proteins, it has been observed that the Ras oncogene stimulates the senescence response, which has been defined as oncogene-induced senescence.<sup>9</sup> Examination of the Ras signal transduction pathway suggests that the Raf/MEK/MAPK cascade is involved in stimulating the senescence program.<sup>10</sup> These results suggest that induction of the same pathway under different cellular conditions can stimulate not only cellular transformation but also the senescence program. The studies in Ras-expressing senes-

**Corresponding Author:** Azmi Yerlikaya **E-mail:** azmi.yerlikaya@ksbu.edu.tr

**Submitted:** 21.01.2023 • **Revision Requested:** 17.04.2023 • **Last Revision Received:** 24.05.2023 • **Accepted:** 31.05.2023



This article is licensed under a Creative Commons Attribution-NonCommercial 4.0 International License (CC BY-NC 4.0)

cent cells have shown that target proteins of the ERK/MAPK pathway are degraded during the induction of senescence. Detailed analyzes have also shown that the degradation of many of these proteins is mediated by the proteasomal pathway.<sup>11,12</sup> These results indicate that the ubiquitin-mediated proteasomal pathway, a selective protein degradation pathway in eukaryotic cells, is also actively involved in the senescence program. In addition, many *in vivo* and *in vitro* studies have shown that inhibitors of the ubiquitin-proteasomal pathway prevent malignant cell proliferation.<sup>13–15</sup>

The proteasome inhibitor bortezomib is currently used in clinics to treat hematologic tumors (e.g., multiple myeloma).<sup>16,17</sup> Our previous studies have also shown that the proteasome inhibitor bortezomib is a promising chemotherapeutic agent against cells of solid tumors (e.g., prostate and breast cancer), and has significantly lower IC<sub>50</sub> values compared with commonly used chemotherapeutic agents (e.g., 5-fluorouracil, cisplatin, and etoposide).<sup>18,19</sup> However, as observed with many chemotherapeutic agents, resistance mechanisms to bortezomib develop during the course of treatment.<sup>20</sup> To elucidate the resistance mechanisms, we developed a bortezomib-resistant PC3 prostate cancer cell as a model cell line by gradually increasing the bortezomib concentration. The results showed that bortezomib-resistant PC3 cells were approximately 4.3-fold more resistant to bortezomib compared with the parent cells.<sup>21</sup> As mentioned previously, it is also known that the senescence response may play an important role in chemotherapy resistance.<sup>22</sup> It is known that the molecular pathways and causes of cancer and the senescence program also interact and overlap considerably.<sup>23</sup> Therefore, the main purpose of this research was to accurately describe the potential role of senescence mechanisms in the development of resistance to the proteasome inhibitor bortezomib. We first decided to investigate whether there was a differential response in the induction of senescence between parental and bortezomib-resistant cells. Although induction of senescence appears to be a barrier to malignant transformation, recent studies suggest that senescence induction also has tumor-progressive potential because of the senescence-associated secretory phenotype, which contains more than 40 secretory factors (e.g., IL-6, IL-8 and MMP-1).<sup>24–27</sup> Indeed, this is the first time that the senescence program has been reported to be reduced in both nonresistant and resistant cells in response to bortezomib treatment. In addition, basal levels of the proteins NAP-2, FGF-6, MIP-3 $\alpha$ , and PARC are significantly increased in untreated bortezomib-resistant PC3 cells compared with untreated parental cells. Upon exposure to 100 nM bortezomib, the expression of NAP-2, FGF-6, MIP-3 $\alpha$ , and PARC proteins was significantly increased in the resistant cells compared with bortezomib-treated parental cells.

## MATERIALS AND METHODS

### Reagents

Cell culture reagents were purchased from Sigma-Aldrich (Steinheim, Germany). The protein assay dye was from BioRad, and the human cytokine antibody array was purchased from Abcam (Cambridge, UK). Senescence-associated  $\beta$ -galactosidase staining reagents were purchased from Cell Signaling Technology. The authenticity of the PC3 prostate cancer cell line (ATCC Cat# CRL-1435)<sup>28</sup> was verified by loss of the normal Y chromosome using RT-PCR with Applied Biosystem Quantifiler™ Trio DNA Quantitation Kit (Cat# 4482910), optimized, and validated as part of a complete DNA testing system targeting Y chromosome. Y-chromosome amplification results were analyzed using HID RT-PCR Analysis Software-Version 1.2.

### Cell Lines

Bortezomib-resistant cells were developed as described in a previous study using a stepwise dose-escalation method, a common method for developing cell lines resistant to chemotherapeutic agents to achieve high fold resistance.<sup>21,29</sup>

### Measurement of $\beta$ -Galactosidase Activity

Senescence-associated  $\beta$ -galactosidase staining kit (Cat# 9860, Cell Signaling Technology) was used to measure  $\beta$ -galactosidase activity at pH 6.0. PC3-P and PC3-R cells were seeded in 6-well plates at 50,000 cells per well. Cells were grown to a logarithmic phase and treated with isotonic water, 10 nM, and 100 nM bortezomib for 48 h. Bortezomib concentrations were selected based on our previous IC<sub>50</sub> determinations with IC<sub>50</sub> values of 71 nM in 4T1 cells, 2.5 nM in B16F10 cells, and 53.4 nM in PC3 cells.<sup>18,30</sup> All agents and solutions were prepared and applied according to the manufacturer's protocol. After treatment with the drug, the medium was removed from all wells, and the cells were washed once with PBS. After washing, 1X fixative solution was added to each well, and the cells were fixed for 15 min at room temperature. After the washing steps, 1 ml of  $\beta$ -gal staining solution was added, and the plates were sealed and incubated overnight at 37°C in a CO<sub>2</sub>-free incubator. The developing blue color was photographed under an inverted microscope and at 200X magnification. Senescence-associated  $\beta$ -gal activity (%) was calculated using the following formula: SA- $\beta$ -gal (%) = (# of stained cells/total # of cells in the field of view) x 100

### Western Blotting

Western blotting experiment was performed as described previously.<sup>31,32</sup> Briefly, cells were seeded in 6-well plates at 200,000 cells per well. Then, cells were grown to a logarithmic

**Table 1.** Human cytokine antibody array map. The array is used for the concurrent detection of 60 human cytokine levels in the resistant and parental cells. POS – Positive control; NEG – Negative control; BLANK – No antibody.

	A	E	C	D	E	F	G	H	I	J	K	L	M	N
1.	Pos	Pos	Neg	Neg	Blank	Angio genin	BDNF	BLC	BMP-4	BMP-6	CKpS-1	CNTF	EGF	Eotaxin
2.	Pos	Pos	Neg	Neg	Blank	Angio genin	BDNF	BLC	BMP-4	BMP-6	CKpS-1	CNTF	EGF	Eotaxin
3.	Eotaxin-2	Eotaxin-3	FGF-6	FGF-7	Flt-3 Ligand	Fractalkine	GCP-2	GDNF	GM-CSF	1-309	IFN- $\gamma$	IGFBP-1	IGFBP-2	IGFBP-4
4.	Eotaxin-2	Eotaxin-3	FGF-6	FGF-7	Flt-3 Ligand	Fractalkine	GCP-2	GDNF	GM-CSF	1-309	IFN- $\gamma$	IGFBP-1	IGFBP-2	IGFBP-4
5.	IGF-1	IL-10	IL-13	IL-15	IL-16	IL-1 $\alpha$	IL-1 $\beta$	IL-1ra	IL-2	IL-3	IL-4	IL-5	IL-6	IL-7
6.	IGF-1	IL-10	IL-13	IL-15	IL-16	IL-1 $\alpha$	IL-1 $\beta$	IL-1ra	IL-2	IL-3	IL-4	IL-5	IL-6	IL-7
7.	Leptin	LIGHT	MCP-1	MCP-2	MCP-3	MCP-4	M-CSF	MDC	MIG	MIP-1 $\delta$	MEP-3 $\alpha$	NAP-2	NT-3	PARC
8	Leptin	LIGHT	MCP-1	MCP-2	MCP-3	MCP-4	M-CSF	MDC	MIG	MIP-1 $\delta$	MEP-3 $\alpha$	NAP-2	NT-3	PARC
9.	PDGF-BB	RAMTES	SCF	SDF-1	TARC	TGF- $\beta$ 1	TGF- $\beta$ 3	TNF- $\alpha$	TNF- $\beta$	Blank	Blank	Blank	Blank	POS
10.	PDGF-BB	EANTES	SCF	SDF-1	TARC	TGF- $\beta$ 1	TGF- $\beta$ 3	TNF- $\alpha$	TNF- $\beta$	Blank	Blank	Blank	Blank	POS

mic phase and treated with 10 nM and 100 nM bortezomib or isotonic solution for 24 and 48 h. Cells were lysed with RIPA buffer (Cat# R0278, Sigma-Aldrich) containing a 1X protease inhibitor cocktail (Cat# sc-29131). Quantification of protein amount was performed using the Bradford assay.<sup>33</sup> Equal amounts of protein (35  $\mu$ g) were separated using 10% SDS-PAGE and then transferred to PVDF membranes (Cat# 1704156) using a Bio-Rad Trans-Blot Turbo Transfer System. Membranes were exposed to rabbit monoclonal anti-p16 INK4a (1:1000 dilution, Cat# 80772) or rabbit monoclonal anti-MMP-1 (1:1000 dilution, Cat# 54376). To determine equal protein loading, membranes were re-probed with anti- $\beta$ -actin rabbit antibody (1:3000, Cat# ab8227, Abcam). After incubation with the primary antibody, an anti-rabbit HP-conjugated secondary antibody (1:3000, Cat# 7074) was added for 1 h in TBS-T. Membranes were incubated with LumiGLO reagent (Cat# 7072), and protein bands were visualized using a Bio-Rad ChemiDoc Imaging System. Protein bands were quantified after background correction using the Image J program. Graphs and statistical analyzes were obtained with the GraphPad Prism 5 program.

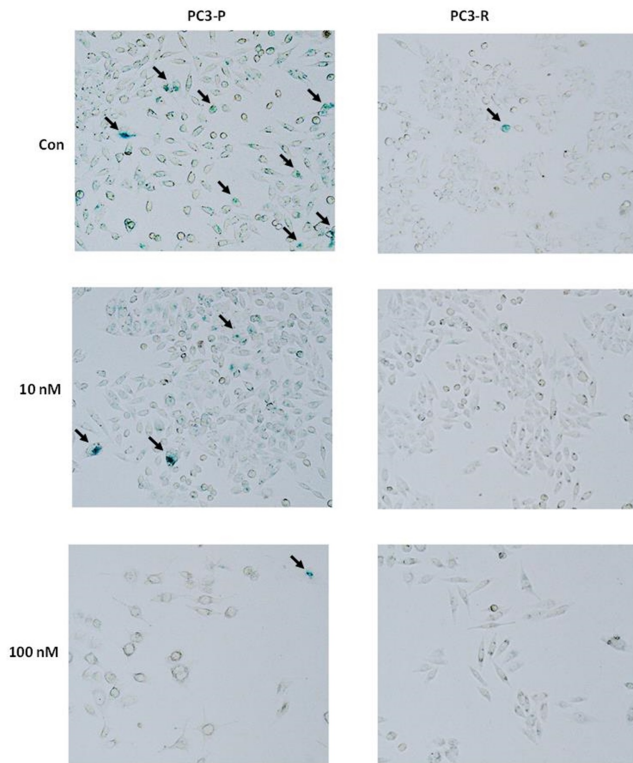
### Analysis of Human Cytokine Array

Changes in the levels of cytokines were analyzed using the Human Cytokine Antibody Array (Cat# ab169817, Abcam), which detects the expression of 60 different cytokines (Table 1).<sup>34</sup> First, PC3-P and PC3-R cells were seeded in 6-well plates at 100,000 cells per well. At a confluence level of approximately 70%, cells were treated with isotonic water (vehicle for bortezomib, control group) or 100 nM bortezomib for 24 h. After treatment, cells were washed with PBS and homogenized with a lysis buffer for protein extraction. Experimental steps were then performed according to the manufacturer's instructions. Briefly, after each membrane was placed in an 8-well plate, they were incubated with 1 ml of 1X blocking buffer containing 200  $\mu$ g protein at room temperature for 2 h. After incubation, the membranes were washed 3X with wash buffer I and 2X with wash buffer II. After washing, membranes were

incubated with a biotinylated antibody cocktail (1 ml) for 2 h. After extensive washing, membranes were treated with 1X HP-conjugated streptavidin for 2 h. Then, the membranes were treated with the detection buffer (500  $\mu$ l) for 2 min (250  $\mu$ l each of buffers C and B, mixed in a 1:1 ratio). Finally, the membranes were exposed to Kodak BioMax X-ray film in a darkroom. Quantification of individual protein spots was performed using the Image J program after background correction. Statistical analyzes were performed with GraphPad Prism 5.0 using One-way ANOVA and Bonferroni's post hoc test.

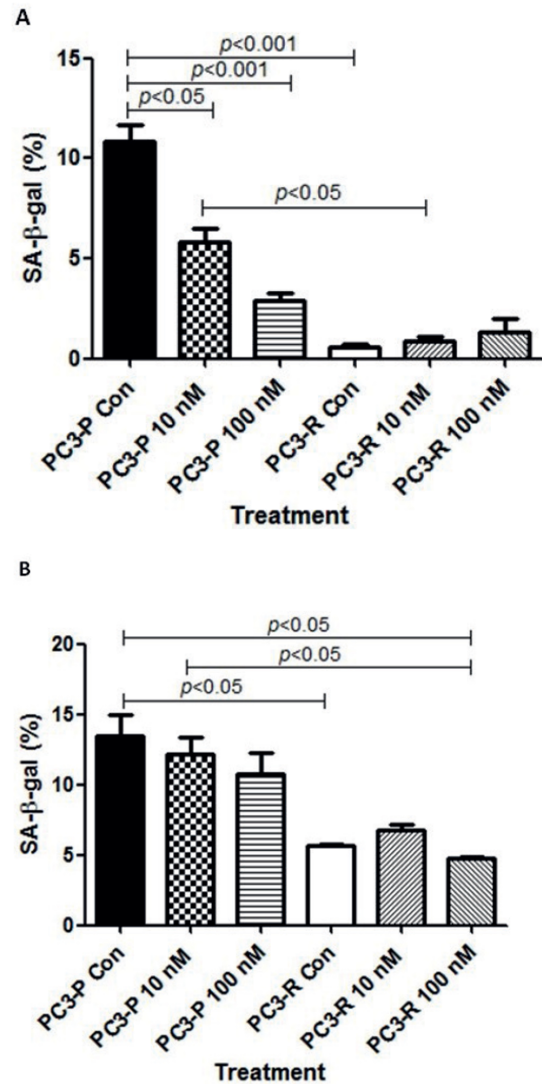
### RESULTS

In our previous studies, we found that resistance to the proteasome inhibitor bortezomib in PC3 prostate cancer cells was not due to upregulation of the mature form of the proteasome subunit beta type-5 (PSMB5), the heat shock protein HSP70, or the multidrug resistance (MDR) transporters.<sup>21,31</sup> Because it is also known that an incomplete and heterogeneous senescence response may play a key role in chemotherapy resistance and produce more tumor-aggressive variants<sup>22,35</sup> we first wanted to investigate whether the senescence program is involved in the mechanism of bortezomib resistance. As shown in Figures 1 and 2A, SA- $\beta$ -gal activity (as inferred from the number of blue-stained cells) was significantly higher in PC3-P cells compared with PC3-R cells ( $p < 0.001$ ) after 48 h of bortezomib exposure. Interestingly, SA- $\beta$ -gal activity was significantly decreased in parental PC3-P cells after 10 nM and 100 nM bortezomib concentrations ( $p < 0.05$ ,  $p < 0.001$ , respectively) (Figure 2A). Since the basal level of SA- $\beta$ -gal activity was significantly lower in the resistant PC3-R cells, the dose-response effect was not observed in these cells (Figure 2A). These results suggest that the resistant cells may be less susceptible to induction of the senescence program. To confirm these results, we then treated the cells with the same concentrations of bortezomib for a relatively short period of time (i.e., 24 h). As shown in Figure 2B, SA- $\beta$ -gal activity was again significantly lower in untreated resistant PC3-R cells compared with untreated parental PC3-P cells ( $p < 0.05$ ). Senescence-associated  $\beta$ -gal activity in 100



**Figure 1.** Determination of the level of senescence in parental PC3-P and resistant PC3-R cells. SA- $\beta$ -gal activity assay was used to determine the senescent cells at pH 6.0. The photographs were taken under an inverted microscope at 200X magnification. The cells were treated with isotonic water, 10 nM or 100 nM bortezomib for 48 h.

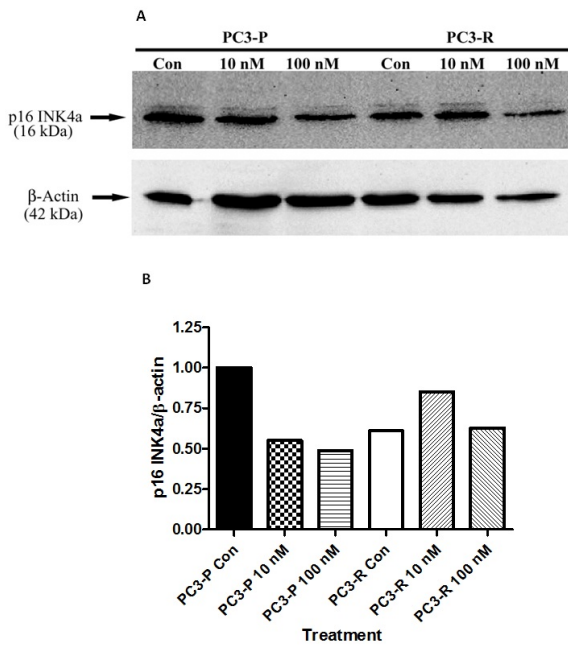
nM bortezomib-treated resistant PC3-R cells was also significantly lower compared with untreated PC3-P ( $p < 0.05$ ) or 10 nM bortezomib-treated PC3-P cells ( $p < 0.05$ ) (Figure 2B). We next examined the expression of the classic senescence marker p16 INK4a, as well as the expression of matrix metalloproteinase-1 (MMP-1), the abnormal expression of which has been associated with age-related diseases.<sup>36</sup> As shown in Figures 3A and B, although the expression of p16 INK4a was decreased in PC3-P cells after bortezomib treatment, there was no significant decrease in expression in PC3-R cells after 24 h of treatment compared with untreated PC3-R cells. A similar observation was made for the level of MMP-1 in both cells (Figures 4A and B). Interestingly, the basal level of p16 INK4a was approximately 40% lower in untreated PC3-R cells than in untreated PC3-P cells. After 48 h of treatment, both p16 INK4a and MMP-1 levels were significantly reduced in PC3-P and PC3-R cells after 100 nM bortezomib exposure (Figures 5A and B). Again, the basal level of p16 INK4a in untreated PC3-R cells was less than 50% compared with untreated PC3-P cells, a result consistent with the reduced SA- $\beta$ -gal activity in untreated PC3-R cells. Finally, the Human Cytokine Antibody Array Kit was used to examine the changes in cytokine profiles in PC3-P and PC3-R cells after 48 h of treatment with 100 nM bortezomib. The 60 different cytokines detected are shown in Table 1. Bone mor-



**Figure 2.** A) Quantitation of the level of senescence in parental PC3-P and resistant PC3-R cells after 48 h of bortezomib treatment. B) The analysis of the level of senescence in parental PC3-P and resistant PC3-R cells after 24 h of bortezomib treatment. The results are presented as means  $\pm$  SEM ( $n = 3$ ). The groups were compared using one-way ANOVA with Bonferroni multiple comparison post-test. PC3-P, the parental PC3 cell; and PC3-R, bortezomib-resistant PC3 cell.

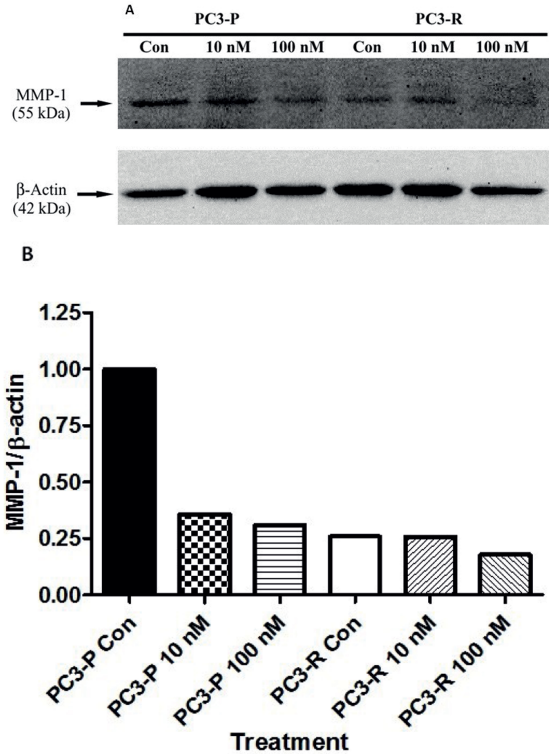
phogenetic proteins (BMPs) are involved in the development of bone formation as well as cell growth and apoptosis.<sup>37</sup> As shown in Figures 6 and 7, BMP-4 was decreased in PC3-P cells exposed to 100 nM bortezomib, whereas BMP-6 was decreased in both PC3-P and PC3-R cells after inhibition of the proteasome by 100 nM bortezomib. Interestingly, the basal level of BMP-6 was significantly higher in untreated PC3-R cells than in untreated parental cells ( $p < 0.05$ ). Similarly, CK  $\beta$  8-1 [a CC chemokine that induces cell-cycle progression<sup>38</sup>] and ciliary neurotrophic factor (CNTF) were decreased in response to treatment with 100 nM bortezomib in both PC3-P and PC3-R cells (Figures 6 and 7). As shown in Figure 7, the basal level of CNTF was significantly higher in untreated PC3-R cells com-





**Figure 3.** A) Examination of p16 INK4a protein in PC3-P and PC3-R prostate cells after 24 h of bortezomib treatment. Both cell lines were treated with 10 nM and 100 nM bortezomib for 24 h; the control cells were treated with isotonic water. 35 μg of protein was separated by 12% SDS-PAGE. Rabbit polyclonal anti-p16 INK4a antibodies were used for loading controls. B) Quantification of Western blot results is seen in Figure 3A. p16 INK4a expression levels were normalized with β-actin levels.

pared with untreated PC3-P cells, a result similar to that of BMP-6 described above. The levels of EGF and eotaxin proteins were also decreased in PC3-P cells after treatment with 100 nM bortezomib, with no significant effect on PC3-R cells (Figures 6 and 7). IGFBP-2 levels were reduced in both PC3-P and PC3-R cells after treatment with 100 nM bortezomib ( $p < 0.05$ ), but IGFBP-1 was reduced only in PC3-P cells after inhibition of the proteasome by bortezomib. IFN-γ (a dimerized soluble cytokine) was also significantly decreased in PC3-P cells after 100 nM bortezomib exposure ( $p < 0.05$ ). Although its level appeared to be reduced in the resistant cells, no significant changes were detected after statistical analysis (Figure 7). On the other hand, basal levels of FGF-6, MIP-3α, NAP-2 and PARC proteins were significantly higher in untreated PC3-R cells than in untreated PC3-P cells ( $p < 0.05$  in all cases, Figures 6 and 8). After exposure to 100 nM bortezomib, the expression of FGF-6, MIP-3α, NAP-2, and PARC proteins was similar and significantly higher in PC3-R cells than in PC3-P cells treated with 100 nM bortezomib ( $p < 0.05$  in all cases, Figure 8). The levels of eotaxin 3, IGF-1, MIP-1δ, NT-3, MCP-1, and MCP-4 were significantly increased in the resistant cells treated with 100 nM bortezomib compared to the untreated PC3-R cells as well as compared to the PC3-P cells treated with 100 nM bortezomib (Figure 8). No statistically significant differences in the expression levels of the other proteins shown on the cytokine

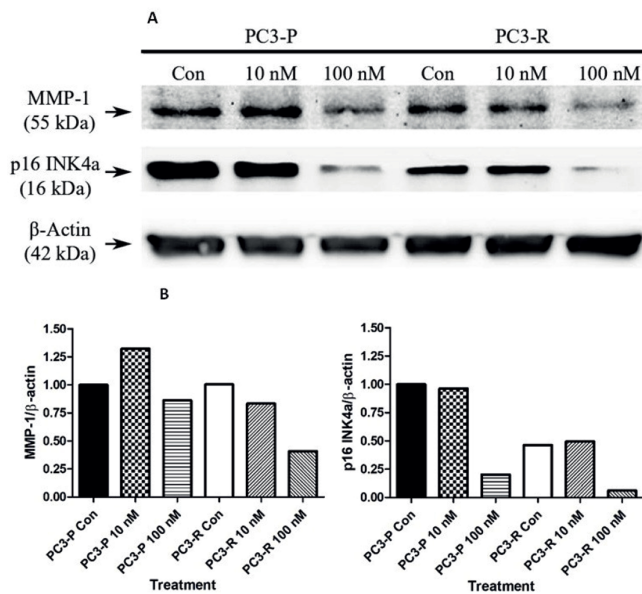


**Figure 4.** A) Examination of MMP-1 protein in PC3-P and PC3-R prostate cell lines after 24 h of bortezomib treatment. Both cell lines were treated with 10 nM and 100 nM bortezomib for 24 h; the control cells were treated with isotonic water. 35 μg of protein was separated by SDS-PAGE. Rabbit polyclonal anti-MMP-1 antibodies were used for loading controls. B) Quantification of Western blot results seen in Figure 4A. MMP-1 expression levels were normalized with β-actin levels. The result is representative of two experiments, each run in duplicate.

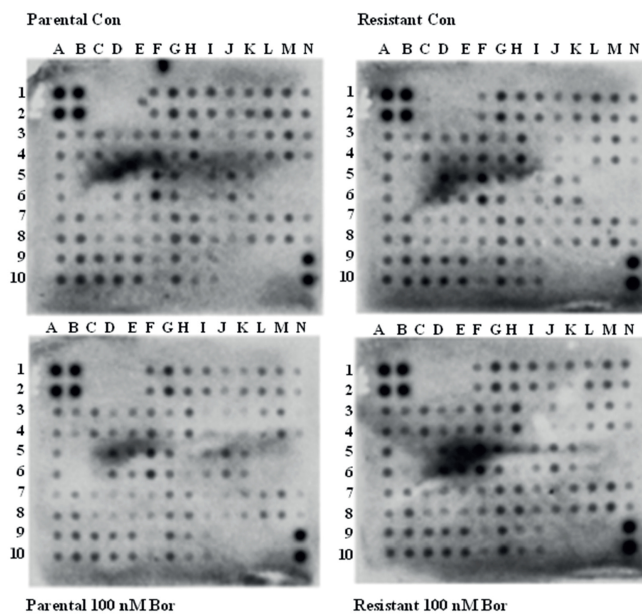
array were detected between the experimental groups (Table 1 and Figure 6).

## DISCUSSION

In the current study, we investigated whether there was a differential response in the degree of senescence program between parental and bortezomib-resistant cells after treatment with different concentrations of bortezomib. Previous studies have shown that bortezomib has both senescence-promoting and -inhibiting effects.<sup>39,40</sup> For example, Krwtowski et al reported that bortezomib caused a time-dependent increase in the senescence of normal fibroblasts, an effect that was particularly observed under hypoxic conditions.<sup>40</sup> On the other hand, exposure of rituximab-resistant cell lines (RRCL) derived from Raji cells (a continuous human cell line of hematopoietic origin) to bortezomib resulted in varying degrees of senescence inhibition and induced cell cycle arrest in G2-M phase associated with mitotic catastrophe.<sup>39</sup> Here, we showed for the first time that the degree of senescence was lower in bortezomib-resistant PC3 cells compared with parent cells treated with different doses of bortezomib at 24 or 48 h. These results suggest that the



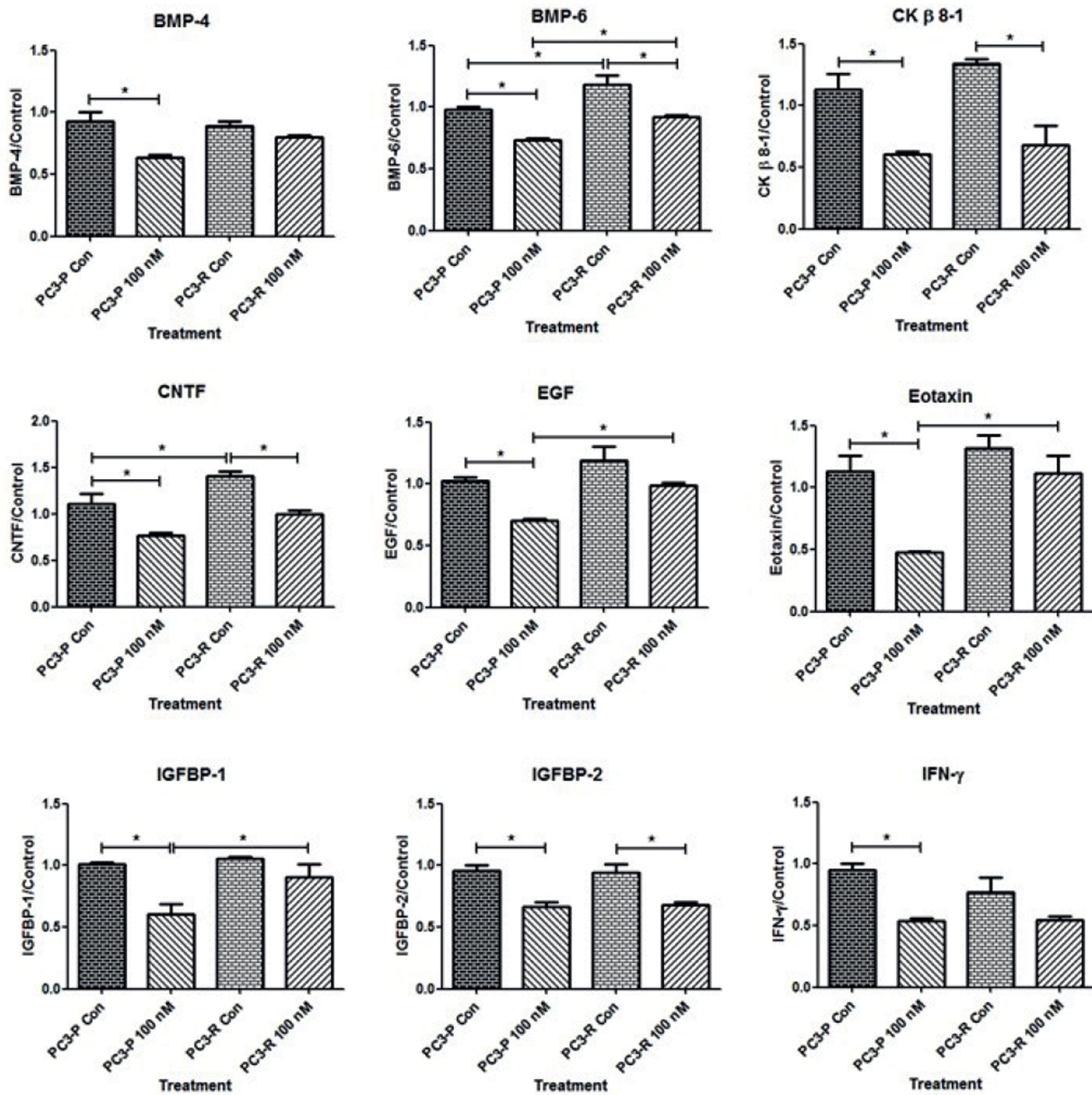
**Figure 5.** Analyses of MMP-1 and p16 INK4a proteins in PC3-P and PC3-R prostate cell lines after 48 h of bortezomib treatment. Both cell lines were treated with 10 nM and 100 nM bortezomib for 48 h; the control cells were treated with isotonic water. 35  $\mu$ g of protein was separated by 12% SDS-PAGE. Rabbit polyclonal anti- $\beta$ -actin antibodies were used for loading controls. B) Quantification of the level of MMP-1 and p16 INK4a seen in Figure 5A. MMP-1 (left panel) and p16 INK4a (right panel) expression levels were normalized with  $\beta$ -actin levels.



**Figure 6.** Cytokine array analysis in PC3-P and PC3-R prostate cell lines. Cytokine profiles were visualized by a Bio-Rad ChemiDoc Imaging System. The cells were treated with 100 nM bortezomib for 48 h; the control cells were treated with isotonic water.

inability to induce senescence may be a critical factor in resistance to chemotherapeutic agents, particularly bortezomib. p16 INK4a is a tumor suppressor and is also known to be re-

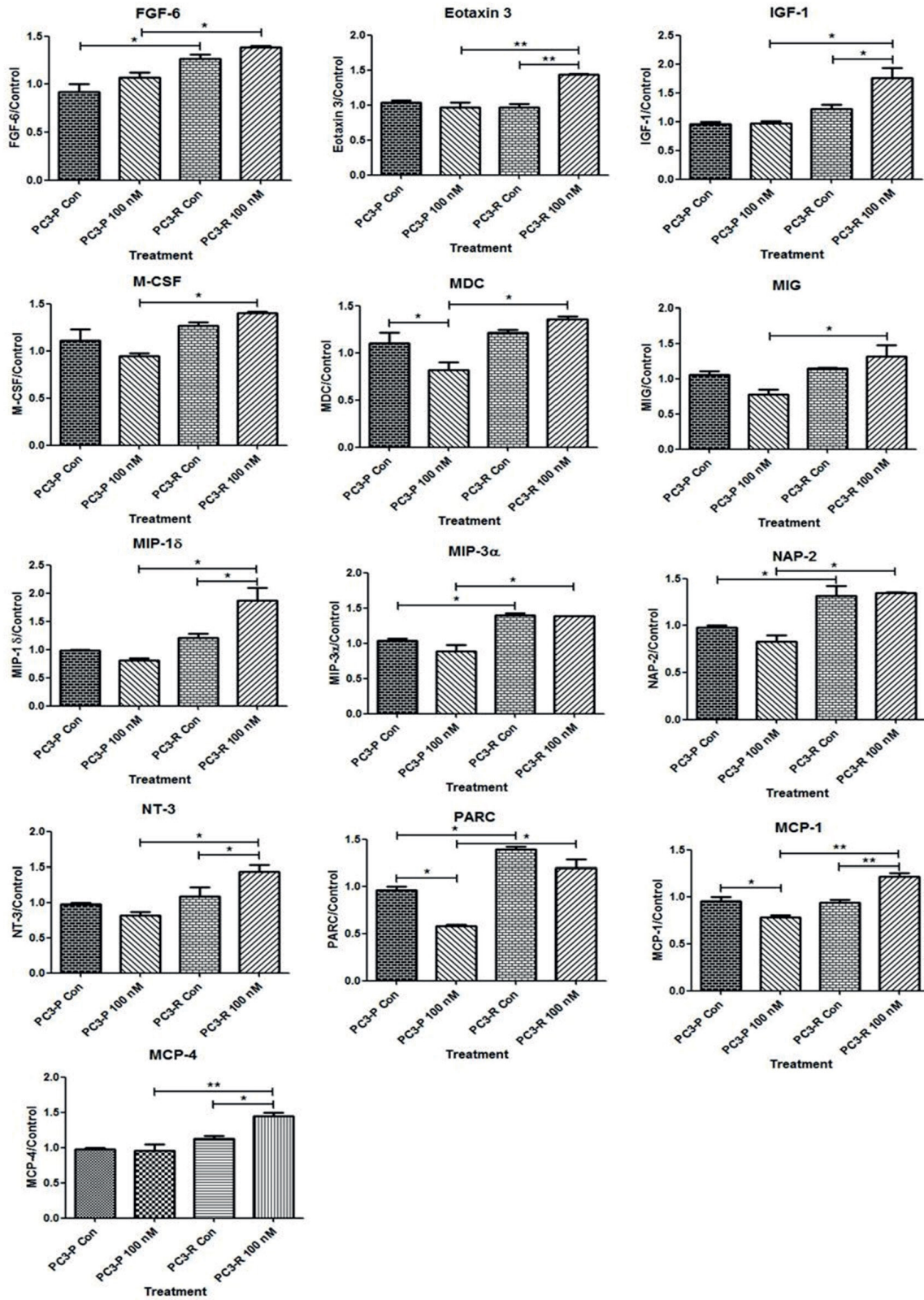
quired for the induction of senescence. In fact, it is probably the best-known biomarker for cellular senescence.<sup>41</sup> MMP-1 is also known to be associated with many age-associated disease pathologies and tumor progression and metastasis.<sup>36</sup> Therefore, we examined p16 INK4a and MMP-1 expressions by Western blot analysis to elucidate the mechanism of senescence in cells resistant to bortezomib. Consistent with the results shown in Figures 1 and 2, the basal level of p16 INK4a was lower in the resistant cells compared with the parental cells. Moreover, 100 nM bortezomib exposure decreased the expression of p16 INK4a in both cells, suggesting that the reduction in senescence after 100 nM bortezomib treatment may be due to the decreased expression of p16 INK4a. To the best of our knowledge, this is the first study to indicate that p16 INK4a expression is reduced in response to bortezomib exposure and thus is not degraded in a proteasomal-dependent manner. To further investigate the mechanisms leading to bortezomib resistance and the changes in the senescence program, the expression levels of 60 different cytokines were analyzed after treatment of parental and resistant cells with 100 nM bortezomib. BMP-4 protein was significantly reduced in parental cells treated with 100 nM bortezomib. It has been previously reported that the BMP-4 signaling pathway can induce senescence and downregulate the growth of A549 lung cancer cells.<sup>42</sup> IFN- $\gamma$  was also reduced in parental cells treated with 100 nM bortezomib. A previous study reported that IFN- $\gamma$  and TNF are able to induce stable growth arrest, which is similar to senescence in cancer cells.<sup>43</sup> In light of these previous studies, it can be concluded that the reduction in senescence in the parental cells after bortezomib treatment may be due to the decreased expression of BMP-4 and IFN- $\gamma$ . On the other hand, the only cytokines detected in higher expression in the resistant cells compared with the parental cells were NAP-2 (also called CXCL7), FGF-6, MIP-3 $\alpha$ , and PARC. NAP-2 is able to interact with both core and linker histones and transfer histones to DNA templates.<sup>44</sup> Previous studies have shown that NAP-2 plays a central role in mediating the interaction of mesenchymal stem cells (MSCs) with cancer stem cells (CSCs) and in maintaining increased numbers of CSCs in the tumor.<sup>45,46</sup> NAP-2 also forms a complex with the epidermal growth factor receptor (EGFR), activating the EGFR signaling pathway.<sup>47</sup> It is therefore critical for tumor cell proliferation and survival; indeed, it is associated with highly metastatic lesions and aggressive prostate cancer.<sup>48,49</sup> Thus, it is proposed here that NAP-2 may also play an important role in resistance to the proteasome inhibitor bortezomib, as well as in reduced senescence in resistant cells. FGF is known to promote self-renewing proliferation and inhibit cellular senescence<sup>50</sup>, a finding that supports the observations presented here. Shang et al reported that MIP-3 $\alpha$  is among the seven cytokines that consistently induce senescence in HUVECs.<sup>51</sup> Although this result seems to dispute the findings presented here regarding the expression level of MIP-3 $\alpha$ , the conflicting observations could be due to the cell-specific effects. Moreover, the effects observed in different cells may certainly be caused by the combinations of



**Figure 7.** Graphical representations of cytokines with reduced levels between the experimental groups. The results are presented as means  $\pm$ SD (n = 2). To determine the statistical significance, One-way ANOVA and Bonferroni's post hoc tests were applied using GraphPad Prism 5 program. \*represents p<0.05, \*\*represents p<0.01.

cytokines induced under certain conditions. Nevertheless, the results presented here provide important insights into the regulatory mechanisms of MIP-3 $\alpha$  and other cytokines that are down- or up-regulated under proteasomal inhibition. There is limited information on the regulation and expression of PARC (also known as CCL18) under different circumstances. In one of these rare studies, Struyf et al reported that serum levels of PARC/CCL18 are elevated in childhood acute lymphoblastic leukemia and thus may represent a novel leukemia marker.<sup>52</sup> Therefore, this study provides crucial information not only on the regulatory mechanism of PARC under inhibition of the

ubiquitin-proteasome pathway, but also on the possible role of the PARC protein in the development of resistance to proteasomal inhibitors as well as in the induction of senescence.



**Figure 8.** Graphical representations of cytokines with increased levels between the experimental groups. The results are means  $\pm$ SD (n = 2). One-way ANOVA and Bonferroni's post hoc tests were performed using GraphPad Prism 5 program. \*represents  $p < 0.05$ , \*\*represents  $p < 0.01$ .

## CONCLUSION

In summary, as discussed in detail above, it is well known that there are many conflicting studies on the role of senescence in tumor progression. In addition, there are few studies on the potential role of senescence in the development of resistance to chemotherapeutic agents, particularly the proteasome inhibitor bortezomib. Interestingly, the results presented here suggest that the basal level of senescence is decreased in bortezomib-resistant cells compared with parental cells. Furthermore, the experimental data suggest that senescence is downregulated in response to different concentrations of bortezomib in both resistant and nonresistant cells. In light of the data presented here, it is anticipated that a detailed investigation of the mechanisms of senescence, as well as the cytokines studied here, may provide further insight for the development of novel therapeutic targets and mechanisms for cancer cells resistant to common chemotherapeutic agents, particularly the proteasome inhibitor bortezomib.

**Acknowledgements:** We would like to acknowledge the financial support by the Scientific Research Projects Coordination Unit of Kutahya Health Sciences University with Grant No. TSA-2021-56.

**Ethics Committee Approval:** The study was approved by Kutahya Health Sciences University Non-invasive Clinical Research Ethics Committee with 2020-17/01 number.

**Informed Consent:** Written consent was obtained from the participants.

**Peer Review:** Externally peer-reviewed.

**Author Contributions:** Conception/Design of Study- A.Y., E.K., S.S., F.B.; Data Acquisition- A.Y., E.K., S.S.; Data Analysis/Interpretation- A.Y., E.K., S.S., F.B.; Drafting Manuscript- A.Y., E.K., S.S., F.B.; Critical Revision of Manuscript- A.Y., E.K., S.S., F.B.; Final Approval and Accountability- A.Y., E.K., S.S., F.B.

**Conflict of Interest:** Authors declared no conflict of interest.

**Financial Disclosure:** Authors declared no financial support.

## ORCID IDs of the authors

Ertan Kanbur	0000-0001-8399-8942
Semih Seker	0000-0002-8957-2050
Ferah Budak	0000-0001-7625-9148
Azmi Yerlikaya	0000-0002-0678-0701

## REFERENCES

- Herranz N, Gil J. Mechanisms and functions of cellular senescence. *J Clin Invest.* 2018;128(4):1238-1246.
- Kumari R, Jat P. Mechanisms of cellular senescence: cell cycle arrest and senescence associated secretory phenotype. *Front Cell Dev Biol.* 2021 9:645593. doi: 10.3389/fcell.2021.645593
- Hanahan D, Weinberg RA. Hallmarks of cancer: the next generation. *Cell.* 2011;144(5):646-674.
- Bolden JE, Lowe SW. Cellular Senescence. In: *The Molecular Basis of Cancer.* 4th edn. Edited by Mendelsohn J, Gray JW, Howley PM, Israel MA, Thompson CB. Philadelphia, PA: Elsevier Inc. 2014;229-238.
- Liu XL, Ding J, Meng LH. Oncogene-induced senescence: a double edged sword in cancer. *Acta Pharmacol Sin.* 2018;39(10):1553-1558.
- Schwarze SR, Shi Y, Fu VX, Watson PA, Jarrard DF. Role of cyclin-dependent kinase inhibitors in the growth arrest at senescence in human prostate epithelial and uroepithelial cells. *Oncogene.* 2001;20(57):8184-8192.
- Land H, Parada LF, Weinberg RA. Tumorigenic conversion of primary embryo fibroblasts requires at least two cooperating oncogenes. *Nature.* 1983;304(5927): 596-602.
- Shay JW, Pereira-Smith OM, Wright WE. A role for both RB and p53 in the regulation of human cellular senescence. *Exp Cell Res.* 1991;196(1):33-39.
- Serrano M, Lin AW, McCurrach ME, Beach D, Lowe SW. Oncogenic ras provokes premature cell senescence associated with accumulation of p53 and p16INK4a. *Cell.* 1997;88(5):593-602
- Lin AW, Barradas M, Stone JC, van Aelst L, Serrano M, Lowe SW. Premature senescence involving p53 and p16 is activated in response to constitutive MEK/MAPK mitogenic signaling. *Genes Dev.* 1998;12(19):3008-3019.
- Deschenes-Simard X, Gaumont-Leclerc MF, Bourdeau V, et al. Tumor suppressor activity of the ERK/MAPK pathway by promoting selective protein degradation. *Genes Dev.* 2013;27(8):900-915.
- Deschenes-Simard X, Lessard F, Gaumont-Leclerc MF, Bardeesy N, Ferbeyre G. Cellular senescence and protein degradation: breaking down cancer. *Cell Cycle.* 2014;13(12):1840-1858.
- Hilt W, Wolf DH. Proteasomes: Destruction as a programme. *Trends Biochem Sc.* 1996;21(3):96-102.
- Leestemaker Y, Ovaas H. Tools to investigate the ubiquitin proteasome system. *Discov Today Technol.* 2017;26:25-31.
- Wu WK, Cho CH, Lee CW, et al. Proteasome inhibition: a new therapeutic strategy to cancer treatment. *Cancer Lett.* 2010;293(1):15-22.
- Robak P, Robak T. Bortezomib for the treatment of hematologic malignancies: 15 Years Later. *Drugs R D.* 2019;19(2):73-92.
- Yerlikaya A, Yontem M. The significance of ubiquitin proteasome pathway in cancer development. *Recent Pat Anticancer Drug Discov.* 2013;8(3):298-309.
- Aras B, Yerlikaya A. Bortezomib and etoposide combinations exert synergistic effects on the human prostate cancer cell line PC-3. *Oncol Lett.* 2016;11(5):3179-3184.
- Yerlikaya A, Altikat S, Irmak R, Cavga FZ, Kocacan SA, Boyaci I. Effect of bortezomib in combination with cisplatin and 5-fluorouracil on 4T1 breast cancer cells. *Mol Med Rep.* 2013;8(1):277-281.
- Yerlikaya A, Kanbur E. The ubiquitin-proteasome pathway and resistance mechanisms developed against the proteasomal inhibitors in cancer cells. *Curr Drug Targets.* 2020;21(13):1313-1325.
- Yerlikaya A, Okur E. An investigation of the mechanisms underlying the proteasome inhibitor bortezomib resistance in PC3 prostate cancer cell line. *Cytotechnology.* 2020;72(1):121-130.
- Guillon J, Petit C, Toutain B, Guette C, Lelievre E, Coqueret O. Chemotherapy-induced senescence, an adaptive mech-

- anism driving resistance and tumor heterogeneity. *Cell Cycle* 2019;18(19):2385-2397.
23. Wyld L, Bellantuono I, Tchkonja T, et al. Senescence and cancer: a review of clinical implications of senescence and senotherapies. *Cancers*. 2020;12(8). doi: 10.3390/cancers12082134
  24. Coppe JP, Patil CK, Rodier F, et al. A human-like senescence-associated secretory phenotype is conserved in mouse cells dependent on physiological oxygen. *PLoS One*. 2010;5(2):e9188. doi: 10.1371/journal.pone.0009188.
  25. Hinds P, Pietruska J. Senescence and tumor suppression. *F1000Res*. 2017;6:2121. doi: 10.12688/f1000research.11671.1.
  26. Kuilman T, Michaloglou C, Vredeveld LC, et al. Oncogene-induced senescence relayed by an interleukin-dependent inflammatory network. *Cell*. 2008;133(6):1019-1031.
  27. Sapochnik M, Fuertes M, Arzt E. Programmed cell senescence: role of IL-6 in the pituitary. *J Mol Endocrinol*. 2017;58(4):241-253.
  28. Bairoch A. The UniProt database, a cell-line knowledge resource. *J Biomol Tech*. 2018;29(2):25-38.
  29. McDermott M, Eustace AJ, Busschots S, et al. In vitro development of chemotherapy and targeted therapy drug-resistant cancer cell lines: a practical guide with case studies. *Front Oncol*. 2014;4:40. doi: 10.3389/fonc.2014.00040.
  30. Yerlikaya A, Erin N. Differential sensitivity of breast cancer and melanoma cells to proteasome inhibitor Velcade. *Int J Mol Med*. 2008;22(6):817-823.
  31. Kanbur E, Baykal AT, Yerlikaya A. Molecular analysis of cell survival and death pathways in the proteasome inhibitor bortezomib-resistant PC3 prostate cancer cell line. *Medical Oncol*. 2021;38(9):112. doi: 10.1007/s12032-021-01563-1.
  32. Yerlikaya A, Dokudur H. Investigation of the eIF2alpha phosphorylation mechanism in response to proteasome inhibition in melanoma and breast cancer cells. *Mol Biol (Mosk)*. 2010;44(5):859-866.
  33. Bradford MM. A rapid and sensitive method for the quantitation of microgram quantities of protein utilizing the principle of protein-dye binding. *Anal Biochem*. 1976;72:248-254.
  34. Park HH, Kim H, Park SY, et al. RIPK3 activation induces TRIM28 derepression in cancer cells and enhances the anti-tumor microenvironment. *Mol Cancer*. 2021;20(1):107. doi: 10.1186/s12943-021-01399-3.
  35. Yang L, Fang J, Chen J. Tumor cell senescence response produces aggressive variants. *Cell Death Discov*. 2017;3:17049. doi: 10.1038/cddiscovery.2017.49.
  36. Dasgupta J, Kar S, Liu R, Joseph J, Kalyanaraman B, Remington SJ, et al. Reactive oxygen species control senescence-associated matrix metalloproteinase-1 through c-Jun-N-terminal kinase. *J Cell Physiol*. 2010;225(1):52-62.
  37. Wang RN, Green J, Wang Z, et al. Bone Morphogenetic Protein (BMP) signaling in development and human diseases. *Genes Dis*. 2014;1(1):87-105.
  38. Kim J, Kim YS, Ko J. CKbeta8/CCL23 and its isoform CKbeta8-1 induce up-regulation of cyclins via the G(i)/G(o) protein/PLC/PKCdelta/ERK leading to cell-cycle progression. *Cytokine*. 2010;50(1):42-49.
  39. Gu JJ, Kaufman GP, Mavis C, Czuczman MS, Hernandez-Ilizaliturri FJ. Mitotic catastrophe and cell cycle arrest are alternative cell death pathways executed by bortezomib in rituximab resistant B-cell lymphoma cells. *Oncotarget*. 2017;8(8):12741-12753.
  40. Kretowski R, Borzym-Kluczyk M, Cechowska-Pasko M. Hypoxia enhances the senescence effect of bortezomib—the proteasome inhibitor—on human skin fibroblasts. *Biomed Res Int*. 2014;196249. doi: 10.1155/2014/196249.
  41. Marcoux S, Le ON, Langlois-Pelletier C, et al. Expression of the senescence marker p16INK4a in skin biopsies of acute lymphoblastic leukemia survivors: a pilot study. *Radiat Oncol*. 2013;8:252. doi: 10.1186/1748-717X-8-252.
  42. Buckley S, Shi W, Driscoll B, Ferrario A, Anderson K, Warburton D. BMP4 signaling induces senescence and modulates the oncogenic phenotype of A549 lung adenocarcinoma cells. *Am J Physiol Lung Cell Mol Physiol*. 2004;286(1):81-86.
  43. Braumuller H, Wieder T, Brenner E, et al. T-helper-1-cell cytokines drive cancer into senescence. *Nature*. 2013;494(7437):361-365.
  44. Rodriguez P, Pelletier J, Price GB, Zannis-Hadjopoulos M. NAP-2: Histone chaperone function and phosphorylation state through the cell cycle. *J Mol Biol*. 2000;298(2):225-238.
  45. Guo F, Long L, Wang J, et al. Insights on CXCR2 chemokine receptor 2 in breast cancer: An emerging target for oncotherapy. *Oncology Lett*. 2019;18(6):5699-5708.
  46. Liu S, Ginestier C, Ou SJ, et al. Breast cancer stem cells are regulated by mesenchymal stem cells through cytokine networks. *Cancer Res* 2011;71(2):614-624.
  47. Liu Q, Li A, Tian Y, et al. The CXCL8-CXCR1/2 pathways in cancer. *Cytokine Growth Factor Rev*. 2016;31:61-71.
  48. Rani A, Dasgupta P, Murphy JJ. Prostate cancer: the role of inflammation and chemokines. *Am J Pathol* 2019;189(11):2119-2137.
  49. Salazar N, Castellan M, Shirodkar SS, Lokeshwar BL. Chemokines and chemokine receptors as promoters of prostate cancer growth and progression. *Crit Rev Eukaryot Gene Expr*. 2013; 23(1): 77-91.
  50. Coutu DL, Galipeau J. Roles of FGF signaling in stem cell self-renewal, senescence and aging. *Aging (Albany NY)*. 2011;3(10):920-933.
  51. Shang D, Sun D, Shi C, Xu J, Shen M, Hu X, et al. Activation of epidermal growth factor receptor signaling mediates cellular senescence induced by certain pro-inflammatory cytokines. *Aging Cell* 2020;19(5):e13145. doi: 10.1111/ace1.13145
  52. Struyf S, Schutyser E, Gouwy M, Gijssbers K, Proost P, Benoit Y, et al. PARC/CCL18 is a plasma CC chemokine with increased levels in childhood acute lymphoblastic leukemia. *Am J Pathol* 2003;163(5):2065-2075.

### How to cite this article

Kanbur E, Seker S, Budak F, Yerlikaya A. The Senescence Program is Reduced in Proteasome Inhibitor Bortezomib-Resistant PC3 Prostate Cancer Cell Line. *Eur J Biol* 2023;82(1): 49-58. DOI: 10.26650/EurJBiol.2023.11240253

# Morphological and Molecular Identification of *Trichoderma* Isolates Used as Biocontrol Agents by DNA Barcoding

Yuksel Gezgin<sup>1,2</sup>,  Gulce Guralp<sup>3</sup>,  Ayse Bercin Barlas<sup>4,5</sup>,  Rengin Eltem<sup>2</sup> 

<sup>1</sup>Ege University, Faculty of Medicine, Molecular Medicine Laboratory, İzmir, Türkiye

<sup>2</sup>Ege University, Faculty of Engineering, Department of Bioengineering, İzmir, Türkiye

<sup>3</sup>Sabancı University, Faculty of Engineering and Natural Sciences, Molecular Biology Genetics and Bioengineering Program, İstanbul, Türkiye

<sup>4</sup>Dokuz Eylül University, İzmir International Biomedicine and Genome Institute, İzmir, Türkiye

<sup>5</sup>İzmir Biomedicine and Genome Center, İzmir, Türkiye

## ABSTRACT

**Objective:** *Trichoderma* genus are environmentally friendly, targeted biocontrol agents used in organic agriculture. Currently, due to the increasing number of organic farming practices, *Trichoderma* species form a good market as commercial biocontrol agents. This study aims to make morphological and molecular identification of *Trichoderma* isolates, which were found to be potential biocontrol agents against plant pathogenic fungi, and to perform phylogenetic diversity analyses of these species using different bioinformatics tools.

**Materials and Methods:** Two different gene regions (the nuclear ribosomal internal transcribed spacer (ITS) and translation elongation factor 1 (EF) were used for molecular identification of *Trichoderma* isolates in this study. Polymerase Chain Reaction (PCR) related regions were amplified and sequenced using primers specific to these gene regions. Following molecular identifications based on these two different gene regions, phylogenetic trees were drawn and polymorphic regions in the nucleotide sequences of these genes were determined.

**Results:** As a result of the study, *Trichoderma* isolates were determined as *T. citrinoviride* Bissett and *T. atroviride* P. Karst. at the species level. This study not only provides essential information about the biodiversity of *Trichoderma* species, which is a biocontrol agent, but also allows the design of new species-specific primers based on the polymorphic regions of both species.

**Conclusion:** It will be possible to make fast and low-cost molecular identification independent of sequence analysis by using primers unique to these species in the future.

**Keywords:** *T. citrinoviride*, *T. atroviride*, BLAST, TrichOKEY, TrichoBLAST, targeted biocontrol agents, DNA barcoding

## INTRODUCTION

*Trichoderma* genus are recognized as environmentally friendly, targeted biocontrol agents. For this reason, there are extensive studies on the biology of *Trichoderma* species, their enzyme production and their use in different biotechnological fields.<sup>1–10</sup> Due to the importance of the *Trichoderma* genus in the biological control of plant diseases, it is crucial to identify the species in this genus correctly.

Morphological identification of *Trichoderma* species is based on a number of parameters, such as colony colors, characteristics and growth rates, sporulation degree, sclerotic formation, color of mycelium and spores.<sup>11</sup> Colors ranging from white to green are observed in different *Trichoderma* species. Growth

culture used, inoculation technique and incubation conditions may affect morphological characteristics.<sup>12–15</sup> Commonly used parameters in microscopic observations are the conidiophore character, conidiophore branching and the shape of the conidium (spore). However, the fact that some species have similar morphology and similar cultural characteristics is not sufficient for a clear and precise definition of the species belonging to the *Trichoderma* genus.<sup>15,16</sup> For this reason, morphological methods should be used together with molecular techniques. Today, molecular techniques have proven to be extremely important in the taxonomy of fungi, and the application of these techniques has led to the re-evaluation of many types.<sup>15–18</sup> For this reason, precise, accurate, rapid identification and classification of the species in the *Trichoderma* genus are still the subjects of intense

Corresponding Author: Yuksel Gezgin E-mail: yukselgezgin@gmail.com

Submitted: 07.04.2023 • Revision Requested: 02.05.2023 • Last Revision Received: 02.06.2023 • Accepted: 05.06.2023



This article is licensed under a Creative Commons Attribution-NonCommercial 4.0 International License (CC BY-NC 4.0)

study.<sup>19–22</sup> New *Trichoderma* species isolated from different geographical regions are on the increase and new nucleotide sequences of these new species have been obtained.<sup>23–25</sup> The Nuclear Ribosomal Internal Transcribed Spacer (ITS) is the most reliable gene region used for species-level identification of *Trichoderma*. Differences between closely related species can be detected using this gene region. In addition to this gene, The Translation Elongation Factor 1 (EF) gene is also used in the identification of species and it reflects the differences between closely related species. Studies show that most of the species-level definitions are made clearly and accurately by using the ITS and EF1 gene regions together.<sup>26,27</sup> In this study, mycelial production was carried out in liquid cultures of 11 *Trichoderma* isolates, which were determined to be biological control agents isolated from local sources. Then, genomic DNA isolation from these mycelia, followed by Polymerase Chain Reaction (PCR) and sequencing studies were performed. Nucleotide sequences were compared using different bioinformatics tools (BLAST, TrichOKEY, TrichoBLAST). Differences were determined by phylogenetic analyses and molecular identifications were carried out at the species level.

## MATERIALS AND METHODS

### Fungal Isolates

All *Trichoderma* spp. were isolated from the lumbering industry in Turkey. The soil dilution plating method was used for the isolation of *Trichoderma* spp. The diluted samples were directly plated onto Rose Bengal Chloramphenicol agar as a selective medium. After 6 days of incubation at 28°C, fungal colonies were transferred to "Malt Extract Agar (MEA)" and "Potato Dextrose Agar (PDA)" slants and they were stored +4°C for further investigations.<sup>28–30</sup>

### Activation and Cultivation of *Trichoderma* Isolates

In order to activate a total of 11 *Trichoderma* isolates, three-point sowing was performed on MEA and PDA media stored in MEA slanted agar at +4 °C in the host mold collection. The cultivated petri dishes were incubated at 28 °C for 3–5 days and observed at 24-hour intervals during this time.

### Morphological and Microscopic Characterization

In order to make the morphological and microscopic characterization of *Trichoderma* spp. in the study, they were cultivated in "MEA" and "PDA" media and incubated at 28°C for one week. For observation, the microscopic slides were stained with trypan blue. *Trichoderma* hyphae, clamydospores, spores and phialides were observed with the OLYMPUS BX53 light microscope.<sup>30–32</sup>

## Molecular Analysis

### Liquid Culture Production

In order to produce *Trichoderma* spp. in liquid culture and to obtain mycelia, spore solution of each isolate was prepared initially. 0.1% Tween 80 was used for the homogeneous spore solution. Tween 80 was added to cover the surface of the media containing the spores of the activated *Trichoderma* isolates, and the spores were gently scraped from the surface with the help of an L baguette and taken into previously numbered sterile glass tubes with caps. For liquid culture production, 1% of the prepared spore solutions were inoculated into 250 ml flasks containing 50 ml MEB. They were then incubated for 4 days in a shaker at 28 °C and 120 rpm. During this time, pellet/mycelia formation was observed at 24-hour intervals.

### Genomic DNA Extraction

Mycelia obtained as a result of liquid culture production were separated from the production medium by using filtration under aseptic conditions and then they were used for genomic DNA isolation. In this study, the manual genomic DNA isolation method was modified and used.<sup>33</sup> Polymerase Chain Reaction Amplification: PCR studies were performed for two different gene regions (ITS and EF gene). GeneMark 5X PCR Dye Master Mix II (GeneMark, Taiwan) was used for PCR. The primer pairs of the ITS and EF gene regions used in the study and the base sequences of these primers are as follows, respectively: ITS-V9G-F (TTACGTCCCTGCCCTTTGTA) and ITS-LS266-R (GCATTCCTCCAAACAACACTCGACTC), EF1-728F-F-Tric (CATCGAGAAGTTCGAGAAGG) and TEF- 1-LLerev-R-Tric (AACTTGCAGGCAATGTGG).<sup>34–36</sup> The PCR condition used is 94 °C 3 min for ITS gene region, [94 °C 30sec, 58 °C 30sec, 72°C 1.5 min] (35 cycles), 72 °C 5min, 4 °C and 94 °C 3min for EF gene region, [94 °C 30 sec, 59 °C 1 min, 74 °C 50 sec] (35 cycles), 74 °C 7 min, 4 °C. PCR products obtained in the studies were purified using the Invitrogen Pure Link Quick Gel Extraction Kit (Invitrogen, USA). Genomic DNA and PCR products were run on 1% and 2% agarose gel, respectively. The bands were then visualized on the G-BOX gel imaging device (G-Box Syngene, UK).

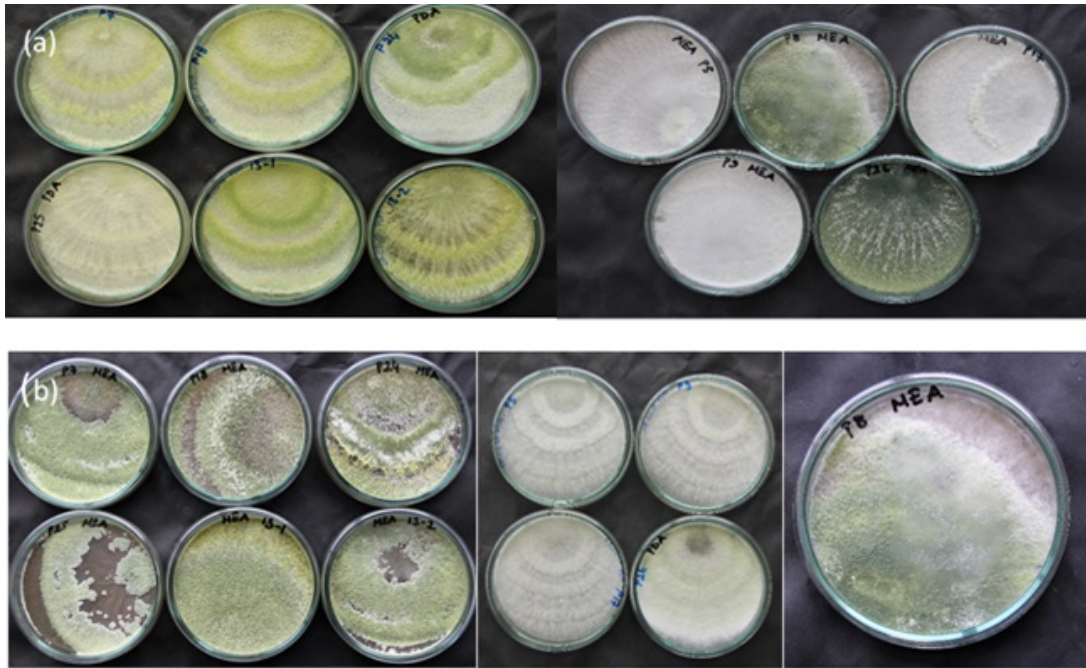
### Sequence Analysis

PCR products of the ITS and EF gene regions of each isolate were sent to REFGEN Biotechnology Limited Company (Ankara) for sequence analysis.

### Bioinformatics Studies

The similarity percentages of the base sequences belonging to both different gene regions were determined using the NCBI





**Figure 1.** (a) The growth and sporulation on PDA medium and (b) MEA medium of *Trichoderma* species (*T. citrinoviride* P7, P13-1, P13-2, P18, P24, P25 and *T. atroviride* P5, P8, P9, P17, P26).

(National Center of Biotechnology Information) database programs BLAST (<http://www.blast.ncbi.nlm.nih.gov>), TrichOKEY (an oligonucleotide barcode for *Hypocrea* and *Trichoderma*) and TrichoBLAST (a sequence similarity search tool for *Hypocrea* and *Trichoderma*) and an accession number was received.<sup>37–39</sup> DNA sequences were aligned using Molecular Evolutionary Genetics Analysis Version X (MEGA X).<sup>40,41</sup> ClusterW program and conserved regions between species were determined by comparing with each other.<sup>42</sup> In addition, polymorphic areas belonging to two different gene regions were identified and gene motifs were determined. Phylogenetic trees were constructed with 1000 replication Bootstrap analysis using the Maximum Likelihood (GTR + G) method in MEGA X: Molecular Evolutionary Genetics Analysis Version X.

## RESULTS

As a result of the study, *Trichoderma* isolates, which were isolated from the lumbering industry were determined as *T. citrinoviride* and *T. atroviride* at the species level.

### Morphological and Microscopic Characterization of *Trichoderma* Isolates

*T. citrinoviride* species showed faster growth when compared to *T. atroviride* species (Figures 1a and 1b).

When *Trichoderma* species were compared in terms of growth and sporulation, MEA medium was found to be better

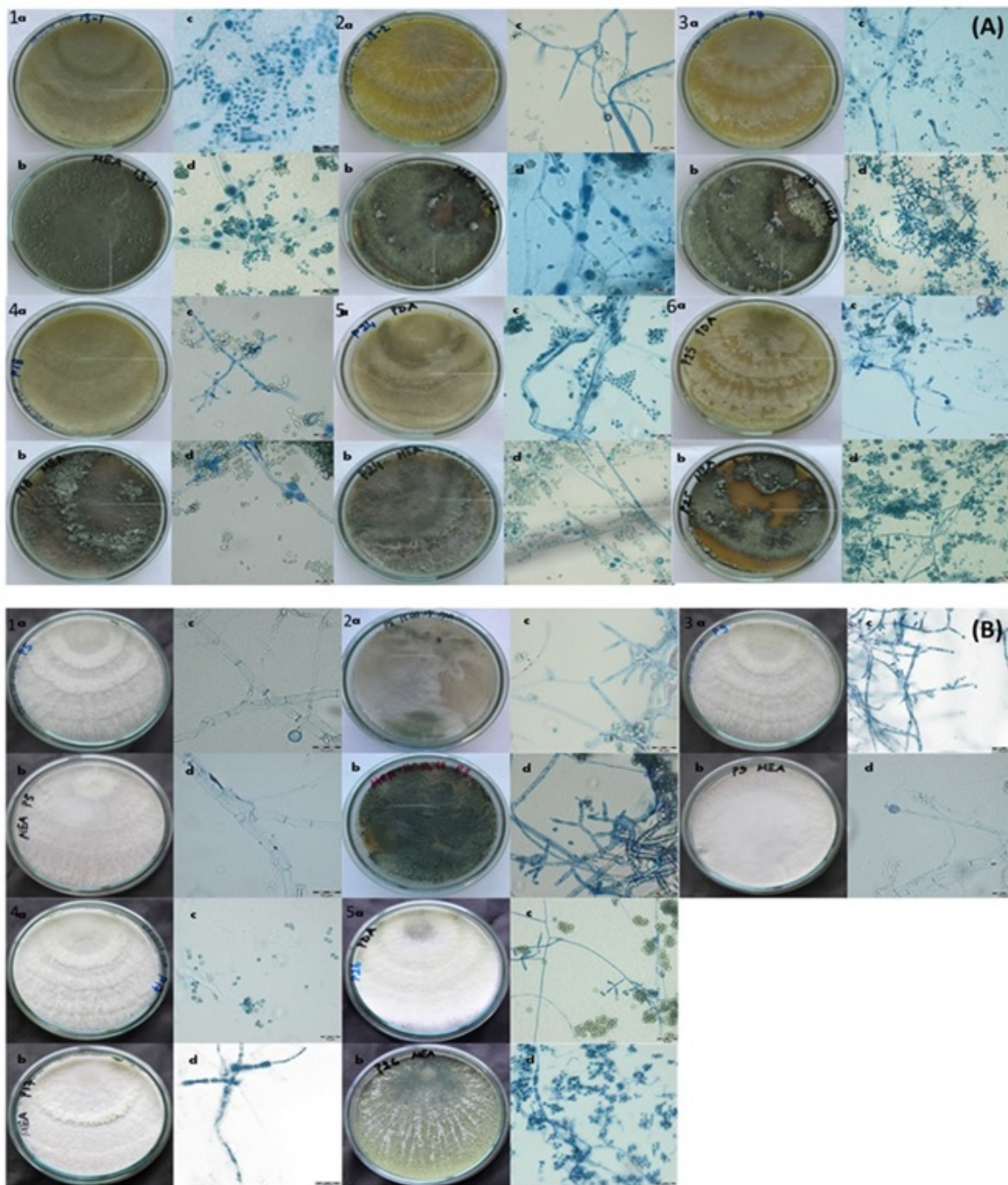
than the PDA medium (Figures 2A and 2B). Morphological and microscopic views of all isolates are given in Figure 2. The color of the colonies varied from light green to dark green. However, colony characteristics were not sufficient for the identification of the species level. Colonies of *T. citrinoviride* became light greenish and all characteristics are shown in Figure 1. Green conidia were dispersed on the whole plate. Mature cultures of *T. atroviride* were developed from white to green pigmentation (Figure 1). Morphology of the spores and sporulating structures of the *Trichoderma* isolates were more or less similar.

### Molecular Identification of *Trichoderma* Isolates

Two different gene regions (ITS and EF) were used for molecular identification of *Trichoderma* isolates in this study. The binding temperatures of both gene regions were determined as the first step. As a result of PCR studies, the binding temperature was determined as 58 °C for the ITS gene region and 59 °C for the TEF gene region. PCR products with a length of approximately 1000 bp for the ITS gene region (Figure 3a) were obtained. If it belonged to the EF gene region, PCR with a length of approximately 1400-1500 bp products were obtained (Figures 3b and 3c). Figures 3a, 3b and 3c show the single band image of the PCR products obtained as a result of PCR.

### Bioinformatics Studies

The nucleotide sequences of both gene regions were compared using the BLAST, TrichOKEY and TrichoBLAST bioinfor-



**Figure 2.** (A) Morphological and microscopic characterization of *T. citrinoviride* (P7, P13-1, P13-2, P18, P24 and P25). (B) Morphological and microscopic characterization of *T. atroviride* isolates P5, P8, P9, P17 ve P26.

matics tools and the percentages of similarity were determined (Table 1).<sup>37–39</sup>

As a result of the analyses made accordingly, the isolates were determined as *T. atroviride* and *T. citrinoviride*. Sequences of both gene regions for all species were registered in NCBI-GenBank and their accession numbers were obtained (Table 2).

By comparing base sequences in *T. atroviride* and *T. citrinoviride* species, polymorphic areas were identified at the gene level and gene motifs belonging to two different gene regions were determined for both species. Table 3 reflects the bases that differ between the two species in bold.

In order to compare phylogenetic similarities, *H. schweinitzii* CBS 818.91 (Accession no: Z31013, 647 bp) and *Hypocrea atroviridis* strain NBRC 8436 (Accession no: JN943354, 1144

**Table 1.** Molecular identification of *Trichoderma* isolates by using BLAST, TrichOKEY, TrichoBLAST and the calculating the similarity percentages of *ITS* and *EF* gene regions of species.

Isolate names	Gene	NCBI/BLAST		TrichOKEY	TrichoBLAST	
		Similarity (%)	Species	Species	Species	
P5	<i>ITS</i>	99	<i>T. atroviride</i>	<i>T. atroviride</i>	-	
P8		99	<i>T. atroviride</i>	<i>T. atroviride</i>	-	
P9		99	<i>T. atroviride</i>	<i>T. atroviride</i>	-	
P17		99	<i>T. atroviride</i>	<i>T. atroviride</i>	-	
P26		99	<i>T. atroviride</i>	<i>T. atroviride</i>	-	
P7		99	<i>T. citrinoviride</i>	<i>T. citrinoviride</i>	-	
P13-1		100	<i>T. citrinoviride</i>	<i>T. citrinoviride</i>	-	
P13-2		99	<i>T. citrinoviride</i>	<i>T. citrinoviride</i>	-	
P18		99	<i>T. citrinoviride</i>	<i>T. citrinoviride</i>	-	
P24		99	<i>T. citrinoviride</i>	<i>T. citrinoviride</i>	-	
P25		99	<i>T. citrinoviride</i>	<i>T. citrinoviride</i>	-	
P5		<i>EF</i>	99	<i>T. atroviride</i>	-	<i>T. atroviride</i>
P8			99	<i>T. atroviride</i>	-	<i>T. atroviride</i>
P9			99	<i>T. atroviride</i>	-	<i>T. atroviride</i>
P17			99	<i>T. atroviride</i>	-	<i>T. atroviride</i>
P26	99		<i>T. atroviride</i>	-	<i>T. atroviride</i>	
P7	99		<i>T. citrinoviride</i>	-	<i>T. citrinoviride</i>	
P13-1	99		<i>T. citrinoviride</i>	-	<i>T. citrinoviride</i>	
P13-2	99		<i>T. citrinoviride</i>	-	<i>T. citrinoviride</i>	
P18	99		<i>T. citrinoviride</i>	-	<i>T. citrinoviride</i>	
P24	99		<i>T. citrinoviride</i>	-	<i>T. citrinoviride</i>	
P25	100		<i>T. citrinoviride</i>	-	<i>T. citrinoviride</i>	

bp) registered in GenBank were selected for the *ITS* gene region.<sup>43,44</sup> In addition, *T. harzianum* strain CBS 226.95 (Accession no: AF057606, 548 bp) was used in the analyses since it is an outgroup located outside the species in this study.<sup>45</sup> In order to compare phylogenetic similarities, the *T. atroviride* strain CBS 693.94 (Accession no: KJ786838.1, 1249 bp), and *T. citrinoviride* strain DAOM 139758 (Accession no: EU338334.1, 619 bp) registered in GenBank, were selected for the *EF* gene region.<sup>2,46</sup> In addition, the *T. harzianum* strain CBS 226.95 (Accession no: AY605833.1, 534 bp) was used in the analyses since it is also an outgroup located outside the species in the present study.<sup>47</sup> Numbers on the phylogenetic tree indicate Bootstrap values (Figure 4). Looking at the trees

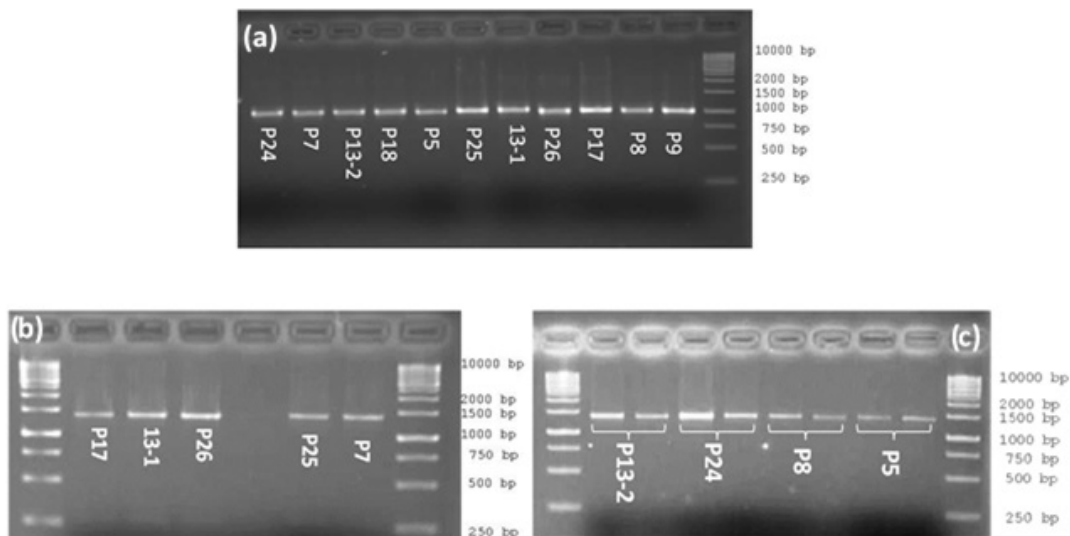
in Figure 4, it is seen that there is a clear distinction between *T. atroviride* and *T. citrinoviride* species for both gene regions. As a result, the amplicon lengths and accession numbers obtained using primers specific to the *ITS* and *EF* gene region of *Trichoderma* species are also presented in Table 4.

## DISCUSSION

*Trichoderma* spp. have been known for quite a long time and the species within this genus are wide. However, there has been considerable confusion about the identification of different species. In the past, identification of various strains was mainly based on morphological methods. However, today, molecular identi-

**Table 2.** Accession numbers of ITS and EF gene regions of *Trichoderma* spp species in this study.

Species	Isolates names	Genbank Accession Number	
		ITS Gene	EF Gene
<i>T. atroviride</i>	P5	MG972794	MH393753
<i>T. atroviride</i>	P8	MG972795	MH393751
<i>T. atroviride</i>	P9	MG972796	MH393750
<i>T. atroviride</i>	P17	MG972797	MH393749
<i>T. atroviride</i>	P26	MG972798	MH393752
<i>T. citrinoviride</i>	P7	MG972799	MH393744
<i>T. citrinoviride</i>	P13-1	MG972800	MH393747
<i>T. citrinoviride</i>	P13-2	MG972801	MH393748
<i>T. citrinoviride</i>	P18	MG972802	MH393745
<i>T. citrinoviride</i>	P24	MG972803	MH393743
<i>T. citrinoviride</i>	P25	MG972804	MH393746



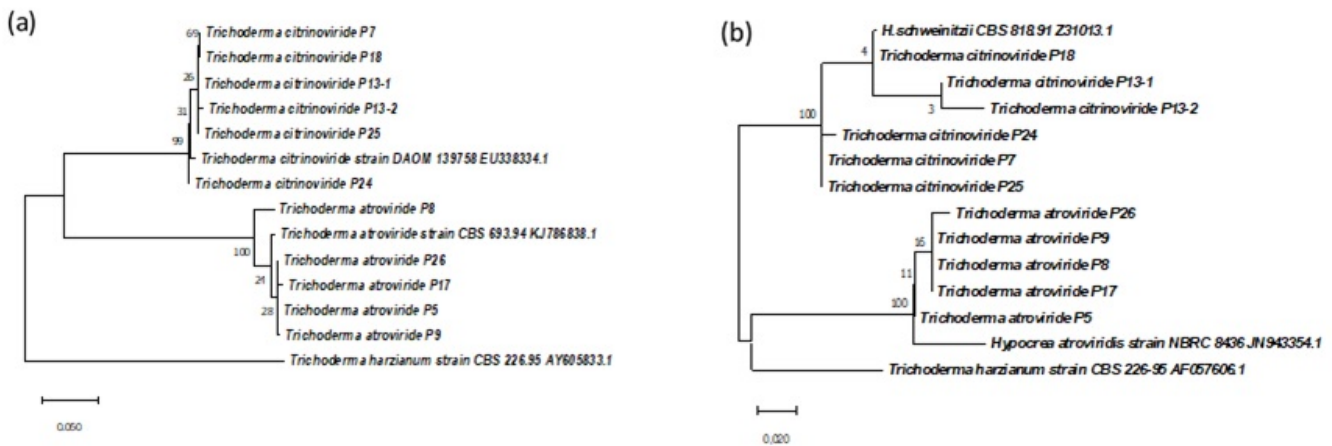
**Figure 3.** (a) PCR was performed by using (ITS-fw and ITS-rev) primers to amplify ITS region. PCR products that is averagely 1000 bp in length are showed. (b and c) PCR was carried out by using (EF1-728F-F-Tric and TEF -1-LLerev-R-Tric) primers to amplify EF region PCR products which are 1400-1500 bp in length were obtained from *Trichoderma* isolates. 1 kb DNA Ladder (Fermentas SM03131) was used.

fication techniques are preferred, enabling the analysis of the multilocus gene sequences of ITS, TEF-1 $\alpha$  and Calmodulin (Cal), to differentiate between different strains.<sup>20-22</sup> The differences between the sequences of the conserved gene regions of

different species serve as DNA barcodes for the species. These barcodes emerge as a method based on the use of protected DNA regions for the determination of biological diversity and species, and provide a clear distinction at the species level.

**Table 3.** The determined gene motifs in ITS and EF gene of *Trichoderma* species and the comparison of base differences in this gene. The different base was displayed in bold to show the base difference in the conserved region in both species.

Gene	Base	<i>Trichoderma</i> species	
		<i>T. atroviride</i> motifs	<i>T. citrinoviride</i> motifs
<i>ITS</i>	61-80	AGGTGGGCAA CTACCACTCA	AGGTGGGCAA CCACCACTCA
	191-210	CAATGTGAAC CATAACAAAC	CAATGTGAAC <b>G</b> TTACCAATC
	221-240	GCGGGG <b>T</b> CAC - - GCCCCGGG	GCGGGATT <b>C</b> T CTGCCCCGGG
	241-260	TGCGTCGCAG CCCCGGA <b>A</b> CC	CGCGTCGCAG CCCCGGAT <b>C</b> CC
	261-280	<b>A</b> - - GGCGCC GCCGGAG <b>G</b> GA	<b>C</b> ATGGCGCC GCCGGAG <b>G</b> AC
	281-300	CCAACCAAAC TCTTTTCTGT	CAACTCAAAC TCTTTTTTCT
	301-320	<b>A</b> GTCCCC - - - - - TCG	<b>C</b> TCCGTC <b>G</b> CG GCCTAC <b>G</b> TCG
	321-340	CGGACGTTAT TTCTTACAGC	CGGCTCTGTT TTATTTTT <b>T</b> GC
	341-360	TCTGAGC - - - - -	TCTGAGC <b>C</b> TT TCTCG <b>G</b> CGAC
	361-380	- - - - - <b>AA</b> AAATTCAAAA	<b>C</b> CTAGCGGGC GTCTCGAAAA
<i>EF</i>	252-270	GTACTCAAT TGCATCGTCT	GCACTCGTC CGGTCATCA
	271-290	TCTCCATCTC TGTGTGGTTC	TCACTGCAGC TGTAT - - TTC
	291-310	<b>A</b> TTGTGCTAA TCATGCTCA	<b>G</b> CGATGCTAA CCATCTTCC
	311-330	ATCAATAGGA AGCCGCCGAG	<b>C</b> TTAACAGGA AGCCGCCGAA
	341-360	GTTCTTTCAA GTATGCGTGG	GTTCCCTCAA GTATGCGTGG
	391-410	CGTGGTATCA CCATCGACAT	CGTGGCATCA CCATCGACAT
	461-480	TG <b>T</b> TTTCGCT TTTCTCATT	TGTGGATCCA TTGCTCACC
	481-500	GATACT <b>T</b> GGA GACCAAGATT	<b>G</b> CGTCT <b>T</b> TC GGACACGGCA
	501-520	CTAACGT <b>G</b> CC GCTCTGTAGA	CTAACGAT <b>C</b> CCGC - ACAGA
	521-540	CGCTCCCGGT CACCGTGATT	CGCTCCCGGC CACCGTGACT
571-590	AGGCTGACTG CGCTATCCTG	AGGCCGACTG CGCTATTCTC	
591-610	ATTATCGCTG CCGTACTGG	ATCATTGCCG CCGTACTGG	



**Figure 4.** (a) Phylogenetic trees based on partial EF sequence data (b) ITS sequence data of *Trichoderma* species.

Both morphological and multi-gene-based molecular identification of *Trichoderma* isolates were performed in this study.

As a result of the comparative analyses of the sequences of two different gene regions (ITS, EF) amplified by PCR on genomic

**Table 4.** The comparison of ITS and EF gene regions of different *Trichoderma* spp.

Gene	Primer	Amplicon length (bp)	Accession number	Species
ITS	ITS-V9G-F ve ITS-LS266-R	848	MG972794,	<i>T. atroviride</i>
		880	MG972795,	
		899	MG972796,	
		933	MG972797,	
		912	MG972798	
	ITS-V9G-F ve ITS-LS266-R	536	MG972799,	<i>T. citrinoviride</i>
		902	MG972800,	
		773	MG972801,	
		725	MG972802,	
		798	MG972803,	
688	MG972804			
ITS-1- ALR0	548	AF057606	<i>T. harzianum</i> strain CBS 226.95	
SR6R & 5.8S -5.8SR & LR1- ITS s (ITS-1 & ITS-2)	621	Z48811	<i>T. harzianum /atroviride</i>	
ITS 6 ve ITS 4 primerleri	605	KJ786740	<i>T. atroviride</i> strain TRS31	
EF, TEF1 $\alpha$	EF 1-728F-F-Tric-TEF -1-LLerev-R-Tric	754	MH393749,	<i>T. atroviride</i>
		785	MH393750,	
		598	MH393751,	
		696	MH393752,	
	EF 1-728F-F-Tric-TEF -1-LLerev-R-Tric	704	MH393753	<i>T. citrinoviride</i>
		600	MH393743,	
		696	MH393744,	
		680	MH393745,	
		527	MH393746,	
		780	MH393747,	
716	MH393748			
EF 1-728F TEF1-LLerev	1019	KP008873	<i>T. harzianum</i>	
EF 728M EF2	1026	KP008948	<i>Trichoderma</i> sp. TRS4	
	1026	KP008949	<i>Trichoderma</i> sp. TRS29	
	1026	KP008950	<i>Trichoderma</i> sp. TRS33	
	488	KT275197	<i>T. harzianum</i>	
	488	KT275198	<i>T. harzianum</i>	
488	KT275199	<i>T. harzianum</i>		

DNA, the isolates were successfully identified on a species basis as *T. citrinoviride* (n=6) and *T. atroviride* (n=5).

The ITS gene region is one of the most reliable genes used for species-level identification. By comparing the sequences of its gene region with the sequences registered in the NCBI GenBank, *Trichoderma* isolates can be identified at the species level with a high percentage of homology. However, some sequences in the NCBI GenBank are stored under the name from which the strain was originally obtained, not the name by which the strain was later identified. In addition, the high similarity of the base sequences as well as the intraspecific variability

of the sequence should be known. Even though it is known that a particular strain may exhibit, such as 1% nucleotide (nt) variation, this may not be the case for the entire sequence and the nt's at some positions do not change. For the accurate identification of *Hypocrea/Trichoderma* members on the basis of species and eliminating the problems mentioned, the publicly available TrichoBLAST database was developed, powered by sequence identification and similarity tools.<sup>39</sup> This database distinguishes most species using sequences from the TEF-1 $\alpha$  gene region used in taxonomic and phylogenetic studies.<sup>48</sup> In the same year, TrichOKey version 1.0 was published, the first

fungal oligonucleotide barcode database for the identification of *Hypocrea* and *Trichoderma* species.<sup>38</sup> They have mentioned that the GenBank database contains sequences of many mis-named and misidentified *Trichoderma* isolates.<sup>38</sup> Therefore, they formed the publicly available TrichOKEY database, which specifically compares only the ICH1 and ITS1 gene sequences for the reliability of the results and the correct identification of *Trichoderma* species.<sup>49</sup> The program provides an online opportunity for rapid molecular identification of an isolate at genus, division, and species levels based on the diagnostic combination of several oligonucleotides (pronounced markers) specifically nested within ITS1 and -2. However, identification based on sequences from the gene ITS region sometimes fails to distinguish closely related taxa as more than one species can share the same ITS genotype. For this reason, the base sequences of the ITS and EF gene regions in the present study were compared using different bioinformatics tools (BLAST, TrichOKEY, TrichoBLAST) and differences between species were determined by phylogenetic analyses (Table 3).

In line with the findings obtained in the study, these two gene regions can be used together for molecular identification of *Trichoderma* species. The amplicon lengths and accession numbers obtained using primers specific to the ITS and EF gene region of different *Trichoderma* species are presented in Table 4.

Today, PCR-based molecular techniques/new strategies are required for rapid, accurate and low-cost sequence-independent identification of *Trichoderma* species. There are limited studies on this subject. One of these studies was carried out by and PCR-based molecular identifications were performed by designing new primers specific to the TEF1 gene region for two *Trichoderma* species (*T. citrinoviride* and *T. reesei*).<sup>50</sup>

Conserved and polymorphic regions of ITS and EF gene regions of *T. atroviride* and *T. citrinoviride* species in the present study are shown in Table 3.

## CONCLUSION

In the light of the data obtained, new species-specific primers can be designed based on different base regions between the two species. With the guidance of these species-specific primers/DNA Barcode, PCR-based molecular identification will be possible and fast and inexpensive methods will be developed independent of sequence analysis.

**Acknowledgment::** This study is supported by Ege University Scientific Research Projects Coordination Unit. Project Number: 15-MÜH-059

**Peer Review::** Externally peer-reviewed.

**Author Contributions::** Conception/Design of Study- Y.G., R.E.; Data Acquisition- Y.G., G.G., A.B.B.; Data Analysis/Interpretation- Y.G., G.G., A.B.B.; Drafting Manuscript- Y.G.; Critical Revision of Manuscript- ; Final Approval and Accountability- Y.G., G.G., A.B.B., R.E.

**Conflict of Interest::** Authors declared no conflict of interest.

**Financial Disclosure::** Authors declared no financial support.

## ORCID IDs of the authors

Yuksel Gezgin	0000-0001-5812-1882
Gulce Guralp	0000-0001-7628-4001
Ayşe Bercin Barlas	0000-0003-3100-9553
Rengin Eltem	0000-0002-0642-7676

## REFERENCES

- Degenkolb T, Gräfenhan T, Nirenberg HI, Gams W, Brückner H. *Trichoderma brevicompactum* complex: rich source of novel and recurrent plant-protective polypeptide antibiotics (peptaibiotics). *J Agric Food Chem*. 2006; 54(19): 7047-7061.
- Degenkolb T, Dieckmann R, Nielsen KF, et al. The *Trichoderma brevicompactum* clade: a separate lineage with new species, new peptaibiotics, and mycotoxins. *Mycol Prog*. 2008a; 7(3):177-219.
- Degenkolb T, Von Doehren H, Nielsen KF, Samuels GJ, Brückner H. Recent advances and future prospects in peptaibiotics, hydrophobin, and mycotoxin research, and their importance for chemotaxonomy of *Trichoderma* and *Hypocrea*. *Chem Biodivers*. 2008b; 5(5):671-680.
- Maral D, Sozer S, Gezgin Y, et al. Evaluation of the properties of *Trichoderma* sp. isolates as a biocontrol agent and biofertilizer. *Environ Eng Manag J*. 2012; 11(3): S154.
- Sargin S, Gezgin Y, Eltem R, Vardar FA. Micropropagule production from *Trichoderma harzianum* EGE-K38 using solid-state fermentation and a comparative study for drying methods. *Turk J Biol*. 2013; 37(2):139-146.
- Gezgin Y, Gül DM, Şenşatar SS, Kara CU, Sargin S, Sukan FV. Evaluation of *Trichoderma atroviride* and *Trichoderma citrinoviride* growth profiles and their potentials as biocontrol agent and biofertilizer. *Turkish J Biochem*. 2020; 45(2):163-175.
- Sharma A, Arya SK, Singh J, et al. Prospects of chitinase in sustainable farming and modern biotechnology: An update on recent progress and challenges. *Biotechnol Genet Eng Rev*. 2023; 1-31.
- Lyubenova A, Rusanova M, Nikolova M, Slavov SB. Plant extracts and *Trichoderma* spp: possibilities for implementation in agriculture as biopesticides. *Biotechnol Biotechnol Equip*. 2023; 37(1):159-166.
- Salem SS. A mini review on green nanotechnology and its development in biological effects. *Arch Microbiol*. 2023; 205(4):128. <https://doi.org/10.1007/s00203-023-03467-2>.
- Barakat I, Chtaina N, El Kamli T, Grappin P, El Guilli M, Ezzahiri

- B. Bioactivity of *Trichoderma harzianum* A peptaibols against *Zymoseptoria tritici* causal agent of septoria leaf blotch of wheat. *J Plant Prot Res.* 2023; 63(1):59-67.
11. John NS, Anjanadevi IP, Nath VS, et al. Characterization of *Trichoderma* isolates against *Sclerotium rolfsii*, the collar rot pathogen of *Amorphophallus*—A polyphasic approach. *Biol Control.* 2015; 90:164-172.
  12. Chaverri P, Samuels GJ. *Hypocrea/Trichoderma* (ascomycota, hypocreales, hypocreaceae): species with green ascospores. Netherlands, N.L.: Centraalbureau voor Schimmelcultures (CBS); 2003: p1-35.
  13. Jaklitsch WM. European species of *Hypocrea* Part I. The green-spored species *Stud Mycol.* 2009; 63:1-91.
  14. Jaklitsch WM. European species of *Hypocrea* part II: species with hyaline ascospores. *Fungal Divers.* 2011; 48(1):1-250.
  15. Savitha MJ, Sriram S. Morphological and molecular identification of *Trichoderma* isolates with biocontrol potential against *Phytophthora blight* in red pepper. *Pest Manage Horticult Ecosyst.* 2015; 21(2):194-202.
  16. Siddiquee S. Morphology-based characterization of *Trichoderma* species. In: Practical handbook of the biology and molecular diversity of *Trichoderma* species from tropical regions. Fungal biology. Switzerland, C.H.: Springer International Publishing; 2017:41-73.
  17. Dou K, Lu Z, Wu Q. MIST: A multilocus identification system for *Trichoderma*. *Appl Environ Microbiol.* 2020; 86(18): e01532-20. <https://doi.org/10.1128/AEM.01532-20>.
  18. Saravanakumar K, Yu C, Dou K, Wang M, Li Y, Chen J. Biodiversity of *Trichoderma* community in the tidal flats and wetland of southeastern China. *PLoS One.* 2016; 11(12): e0168020. <https://doi.org/10.1371/journal.pone.0168020>.
  19. Srivastava M, Shahid M, Pandey S, et al. *Trichoderma* genome to genomics: A review. *J Data Min Genom Proteom.* 2014; 5(162). <https://doi.org/10.4172/2153-0602.1000162>.
  20. Kubicek CP, Steindorff AS, Chenthamara K, et al. Evolution and comparative genomics of the most common *Trichoderma* species. *BMC Genom.* 2019; 20:1-24.
  21. Kamil D, Prameela Devi T, Choudhary SP, Das A, Kumar A. Genome-mediated methods to unravel the native biogeographical diversity and biosynthetic potential of *Trichoderma* for plant health. In Fungal diversity, ecology and control management, In: Rajpal VR, Singh I, Navi SS, eds. Fungal diversity, ecology and control management. Fungal biology, Singapore: SG: Springer Nature Singapore, 2022:109-124.
  22. Maheshwary NP, Naik BG, Chittaragi A, Morpho-molecular characterization, diversity analysis and antagonistic activity of *Trichoderma* isolates against predominant soil born pathogens. *Indian Phytopathol.* 2022; 75(4): 1009-1020.
  23. Gal-Hemed I, Atanasova L, Komon-Zelazowska M, Druzhinina IS, Viterbo A, Yarden O. Marine isolates of *Trichoderma* spp. as potential halotolerant agents of biological control for arid-zone agriculture. *J Appl Environ Microbiol.* 2011; 77(15):5100-5109.
  24. Samuels GJ, Ismaiel A, Mulaw TB, et al., The Longibrachiatum Clade of *Trichoderma*: a revision with new species. *Fungal Divers.* 2012; 55(1):77-108.
  25. Oskiera M, Szczech M, Bartoszewski G. Molecular identification of *Trichoderma* strains collected to develop plant growth-promoting and biocontrol agents. *J Horticult Res.* 2015; 23(1): 75–86.
  26. Kullnig-Gradinger CM, Szakacs G, Kubicek CP. Phylogeny and evolution of the genus *Trichoderma*: a multigene approach. *Mycol Res.* 2002; 106(7):757-767.
  27. Anees M, Tronsmo A, Edel-Hermann V, Hjeljord LG, Héraud C, Steinberg C. Characterization of field isolates of *Trichoderma* antagonistic against *Rhizoctonia solani*. *Fungal Biol.* 2010; 114(9):691-701.
  28. Elad Y, Chet I, Henis Y. A selective medium for improving quantitative isolation of *Trichoderma* spp. from soil. *Phytoparasitica.* 1981; 9:59-67.
  29. Howell CR. Selective isolation from soil and separation in vitro of P and Q strains of *Trichoderma virens* with differential media. *Mycologia.* 1999; 91(6): 930-934.
  30. Gams W, Bissett J. Morphology and identification of *Trichoderma* and *Gliocladium*. In: *Trichoderma and Gliocladium* Volume 1, Basic biology, taxonomy and genetics. Eds. Kubicek CP, Harman GE, Bristol, BS: Taylor and Francis Ltd, Inc; 2002; 3-31.
  31. Samuels GJ. *Trichoderma*: A review of biology and systematics of the genus. *Mycol Res.* 1996; 100(8):923-935.
  32. Jaklitsch WM, Voglmayr H. Biodiversity of *Trichoderma* (*Hypocreaceae*) in Southern Europe and Macaronesia. *Stud Mycol.* 2015; 80:1-87.
  33. Liu D, Coloe S, Baird R, Pedersen J. Rapid mini-preparation of fungal DNA for PCR. *J Clin Microbiol.* 2000; 38(1):471-471.
  34. Van den Ende AH, De Hoog GS. Variability and molecular diagnostics of the neurotropic species *Cladophialophora bantiana*. *Stud Mycol.* 1999; 43:151-162.
  35. Carbone I, Kohn LM. A method for designing primer sets for speciation studies in filamentous ascomycetes. *Mycologia.* 1999; 91(3):553-556.
  36. Jaklitsch WM, Komon M, Kubicek CP, Druzhinina IS. *Hypocrea voglmayrii* sp. nov. from the Austrian Alps represents a new phylogenetic clade in *Hypocrea/Trichoderma*. *Mycologia.* 2005; 97(6):1365-1378.
  37. The Basic Local Alignment Search Tool (BLAST) website, <https://blast.ncbi.nlm.nih.gov/Blast.cgi>. Accessed May 03, 2023.
  38. Druzhinina IS, Kopchinskiy AG, Komoń M, Bissett J, Szakacs G, Kubicek CP. An oligonucleotide barcode for species identification in *Trichoderma* and *Hypocrea*. *Fungal Genet Biol.* 2005; 42(10):813-828.
  39. Kopchinskiy A, Komoń M, Kubicek CP, Druzhinina IS. TrichoBLAST: A multilocus database for *Trichoderma* and *Hypocrea* identifications. *Mycol Res.* 2005; 109(6):658-660.
  40. Tamura K, Nei M. Estimation of the number of nucleotide substitutions in the control region of mitochondrial DNA in humans and chimpanzees. *Mol Biol Evol.* 1993; 10(3):512-526.
  41. Kumar S, Stecher G, Li M, Knyaz C, Tamura K. MEGA X: Molecular evolutionary genetics analysis across computing platforms. *Mol Biol Evol.* 2018; 35(6):1547-1549.
  42. Thompson JD, Higgins DG, Gibson TJ. CLUSTAL W: Improving the sensitivity of progressive multiple sequence alignment through sequence weighting, position-specific gap penalties and weight matrix choice. *Nucleic Acids Res.* 1994; 22(22):4673-4680.
  43. Kuhls K, Lieckfeldt E, Samuels GJ, et al. Molecular evidence that the asexual industrial fungus *Trichoderma reesei* is a clonal derivative of the ascomycete *Hypocrea jecorina*. *Proc Natl Acad Sci.* 1996; 93(15):7755-7760.
  44. Schoch CL, Seifert KA, Huhndorf S, et al. Nuclear ribosomal internal transcribed spacer (ITS) region as a universal DNA barcode marker for Fungi. *Proc Natl Acad Sci.* 2012; 109(16):6241-6246.
  45. Ospina-Giraldo MD, Royse DJ, Chen X, Romaine CP. Molecular



- phylogenetic analyses of biological control strains of *Trichoderma harzianum* and other biotypes of *Trichoderma* spp. associated with mushroom green mold. *Phytopathology*. 1999; 89(4):308-313.
46. Skoneczny D, Oskiera M, Szczech M, Bartoszewski G. Genetic diversity of *Trichoderma atroviride* strains collected in Poland and identification of loci useful in detection of within-species diversity. *Folia Microbiol*. 2015; 60(4):297-307.
  47. Druzhinina IS, Kubicek CP, Komoń-Zelazowska M, Mulaw TB, Bissett J. The *Trichoderma harzianum* demon: Complex speciation history resulting in coexistence of hypothetical biological species, recent agamospecies and numerous relict lineages. *BMC Ecol Evol*. 2010; 10(1):1-4.
  48. Hageskal G, Vrålstad T, Knutsen AK, Skaar ID. Exploring the species diversity of *Trichoderma* in Norwegian drinking water systems by DNA barcoding. *Mol Ecol Resour*. 2008; 8(6):1178-1188.
  49. Fahmi AI, Eissa RA, El-Halfawi KA, Hamza HA, Helwa MS. Identification of *Trichoderma* spp. by DNA barcode and screening for cellulolytic activity. *J Microb Biochem Technol*. 2016; 8(3):202-209.
  50. Saroj DB, Dengeti SN, Aher S, Gupta AK. A rapid, one step molecular identification of *Trichoderma citrinoviride* and *Trichoderma reesei*. *World J Microbiol Biotechnol*. 2015; 31(6):995-999.

#### How cite this article

Gezgin Y, Guralp G, Bercin Barlas A, Eltem R. Morphological and Molecular Identification of *Trichoderma* Isolates Used as Biocontrol Agents by DNA Barcoding. *Eur J Biol* 2023;82(1): 59-69. DOI: 10.26650/EurJBiol.2023.1279151

# Screening of Antibiotics Biodegradability from Wastewater

Saim Souhila<sup>1</sup>,  Mokrani Slimane<sup>2</sup>,  Isabel Martínez-Alcalá<sup>3</sup>,  Ramazan Erenler<sup>4</sup> 

<sup>1</sup>Natural and Life Sciences, Biology Department, University of Mustapha Stambouli, Geo-Environment and Spaces Development Laboratory, Mascara, Algeria

<sup>2</sup>University of Mustapha Stambouli, Faculty of Natural and Life Sciences, Department of Agronomy, Laboratory of Research on Biological and Geomantic Systems, Mascara, Algeria

<sup>3</sup>Universidad Católica de Murcia (UCAM). HiTech, Sport & Health Innovation Hub. Av. Andres Hernandez Ros, Murcia, Spain.

<sup>4</sup>Igdir University, Faculty of Health Science, Department of Chemistry, Research Laboratory Practice and Research Center, Igdir, Turkiye

## ABSTRACT

**Objective:** One of the sources of environment antibiotics contamination is wastewater treatment plants (WWTPs), there by constituting a global public health risk. This present study aimed to investigate the biodegradability of antibiotics and antiseptics and highlights the biodegradation of Ciprofloxacin as a sole carbon source by a bacterium isolated from the sludge "El Kouwaer," WWTP located in Mascara.

**Materials and Methods:** In the present study, biodegradability of some antibiotics and antiseptic were tested at 50 mg/l concentration through active sludge microorganisms by Manometric Respirometry Method (OECD 301F). Further analysis of 16S rRNA gene sequencing used to identify MK4 strain isolated from the sludge. Furthermore, ATR-FTIR spectroscopy was conducted in order to identify its biodegradation in the presence of different carbon sources and LCMS/MS spectrometry were used to identify the metabolite degradation.

**Results:** Our Results revealed that four antibiotics tested were readily biodegradable (60%) as Ciprofloxacin, Doxycycline, Amoxicillin, Ampicillin, and Penicillin. Conversely, other was not readily biodegradable, such as Azithromycin (36.11%), Cephalexin (36.20%), and Metronidazole (33.33%). Meanwhile, the remaining antibiotics under examination were degraded, with Sulfamethoxazole (25.75%), Clarithromycin (25.36%), and Nifuroxazide (16.33%) recording degradation. Ciprofloxacin was chosen to represent the most biodegraded antibiotic. Based on 16S rRNA gene, MK4 strain was related to *Klebsiella oxytoca* (99.99%). ATR-FTIR revealed that the strain *K. oxytoca* MK4 caused changes in the structure of the Ciprofloxacin, in the presence of various sources of carbon, with varying effects on bacterial growth and biodegradation.

**Conclusion:** In this study, the identified strain *K. oxytoca* MK4 facilitated the degradation of Ciprofloxacin.

**Keywords:** Wastewater, antibiotic, antiseptics, biodegradability, ATR-FTIR spectroscopy, LCMS/MS metabolites.

## INTRODUCTION

Antibiotics represent a widely-used pharmaceutical product, used for treating humans.<sup>1</sup> The metabolism of antibiotics in the human body is slight and they are excreted through urine and feces. Then, they are transmitted to sewage treatment plants where there is no effective removal by conventional biological treatments, and they reach the aquatic environment as emerging and persistent micro-pollutants processes.<sup>2</sup> Similar to penicillins, some antibiotics have rapid degradation, while others, such as Ciprofloxacin (CIP), tylosin, and tetracyclines, exhibit different degradation rates or behaviors. CIP and oxolinic acid are known to be relatively persistent in water.<sup>3</sup> Thus, it seems that wastewater treatment plants are major reservoirs of antibiotic-resistant

bacteria which are transmitted into aquatic environments.<sup>4</sup> The European Water Framework Directive included many antibiotic groups in the "watch-list".<sup>5</sup> The challenge is to remove antibiotics from wastewater treatment plants (WWTPs), as documented in multiple studies.<sup>6</sup> As a result, significant parts of these substances tend to accumulate in active sludge<sup>7</sup>, particularly in systems with anaerobic digestion where they have a lack treatment.<sup>8</sup> Among the commonly used antibiotics, amoxicillin, trimethoprim, and CIP are frequently detected at high levels in both soil and water environments.<sup>9</sup> Studies and data have indicated that biodegradation<sup>10</sup> is among the range of methods that have been proven effective in eliminating various types of antibiotics in WWTPs.<sup>10</sup> The removal of antibiotics by microbial biodegradation in sewage sludge and aquatic environ-

**Corresponding Author:** Saim Souhila **E-mail:** saim.souhila@univ-mascara.dz

**Submitted:** 19.05.2023 • **Revision Requested:** 01.06.2023 • **Last Revision Received:** 05.06.2023 • **Accepted:** 19.06.2023



This article is licensed under a Creative Commons Attribution-NonCommercial 4.0 International License (CC BY-NC 4.0)

ments was reported to be an important elimination process.<sup>11</sup> During sludge treatment, between 0-40% of CIP by biodegradation was found.<sup>12,13</sup> Unfortunately, a significant quantity of CIP remained present in the digested sludge found in wastewater treatment plants, indicating its persistence.<sup>14</sup> The microbial community structure involved in the degradation of CIP has not been reported yet.<sup>3,15</sup>

The biodegradability test is a screening method used to evaluate the biodegradability or mineralization potential of chemicals based on predefined criteria.<sup>16</sup> The focus of this work was to examine the biodegradability of some antibiotic compounds to predict their fate in biological systems treating wastewater using the OECD 310 guideline. The assessment of the biodegradability of specific antibiotics and antiseptics was conducted. In 28-day manometric respirometry tests, the percentages of biodegradation of the targeted compound (CIP) were computed. CIP was selected as a representative of fluoroquinolones due to its extensive usage as an antibiotic in most regions across the globe. The main goals of the present study were to isolate and identify the predominant indigenous bacterial cultures from effluent wastewater, to evaluate their ability to biodegrade CIP in the presence of various carbon sources, and to assess their impact on bacterial growth and biodegradation. Additionally, the degradation pathways were analyzed by utilizing the Attenuated total reflectance-Fourier transform infrared spectroscopy (ATR-FTIR) technique to determine structural changes. Additionally, the objective of the present study is to identify the metabolites or transformation products that are generated during the biodegradation process.

## MATERIALS AND METHODS

### Sample Collection

The wastewater treatment plant "El Kouwaer", the subject of the current study, is located 3.2 km from the Mascara department and 361 km from Algiers in the Kouwaer area (35°23'02.6"N 0°08'36.4" E). Two kinds of samples (wastewater influent and effluent) were taken every month from June 2019 to May 2020. Also, for the biodegradability test, a total of nine samples of activated sludge were collected from the aeration tank of a WWTP. During the same day, the samples collected were transported to the laboratory using sterile bottles at 4°C and analyzed.<sup>17</sup>

### Preparation of Activated Sludge Samples

Samples of activated sludge underwent some preparations such as keeping them to settle for 1 h until the supernatant was drawn off. Then, the activated sludge samples were subjected to a series of steps, including washing once, centrifugation, and resuspension in Mineral salt medium MMSM.<sup>18</sup>

## Physico-Chemical Analysis of Wastewater Samples

Physico-chemical parameters of wastewater samples were measured for pH, temperatures (air and water temperatures) and dissolved oxygen, and also, pollution indicators: Biological oxygen demand (BOD<sub>5</sub>) and Chemical oxygen demand (COD).<sup>19,20</sup> The BOD<sub>5</sub>/COD ratio was calculated. Results were compared with those obtained in Algeria.<sup>19</sup>

## Biodegradability Evaluation

### Manometric Respirometry Test

A Manometric respirometry test (MRT, OECD 301F) was performed using 300 ml of sterile mineral medium<sup>18</sup> containing each of the tested compounds (10 antibiotics and 01 antiseptic) and inoculated with 0.5 ml of inoculum (activated sludge) and 20 drops per liter of nitrification inhibitor *N-allylthiourea* used to selectively inhibit nitritation and nitratation bacteria. The mixtures formed were kept in sterile BOD bottles at 30°C±1 during 28 days under constant agitation 150 tr/min.<sup>18</sup> Automatic analyzer (System OxiTop® OC100, Germany) was used daily to measure the aerobic biodegradation.<sup>21</sup>

### BOD<sub>28</sub> Determination

BOD after 28 days was calculated according to OECD (1992) guidelines. Mean replicate values for each batch were calculated daily from collected data (equation 1).

$$\text{BOD} = \frac{\text{O}_2 \text{ mg/L substance absorption} - \text{O}_2 \text{ mg/l blanc absorption}}{\text{mg/L test substance}} \text{ mg/l} \dots \dots \dots (1)$$

### Percentage of Biodegradation

Percentage of biodegradation of 10 antibiotics and 01 antiseptic was determined by measuring the quantity of oxygen consumed by the inoculums used. This value was adjusted by deducting the oxygen consumption of the blank, and expressed as percentage of the theoretical oxygen demand (ThOD) as shown in equation 2.<sup>18</sup>

$$\text{Biodegradation (\%)} = \left[ \frac{\text{DBO}}{\text{ThOD}} \right] \times 100 \dots \dots \dots (2)$$

Where: BOD: Biochemical Oxygen Demand of the compound (mg/l) after 14 days or 28 days. ThOD: Theoretical Oxygen Demand required to completely oxidize the compound (mg/L)

Theoretical Oxygen Demand (ThOD) was calculated at the end of the experiment according to equation 3 (OECD, 1992).

$$\text{ThOD} = \frac{16 \left[ 2c + 0.5(h - cl - 3n) + 3s + \left(\frac{5}{2}\right)p + 0.5na - \right] \text{mg/mg}}{\text{MW}} \dots \dots \dots (3)$$

In terms of biodegradation of the test compounds, OECD (18) stipulates that for a compound to be classified as having passed for ready biodegradability, it should have attained 60% of ThOD, within a period of 10 days after oxygen consumption reached 10%.

Further, CIP was selected to represent the most widely used and mostly biodegraded. Thus, it was chosen for the isolation and identification of predominant indigenous bacterial cultures from effluent wastewater able to degrade CIP.

### Ciprofloxacin Degradation Bacteria

#### Isolation

The process used for acclimating and enriching microorganisms was the same as described in the studies of Liyanage & Manage.<sup>22,23</sup> In an Erlenmeyer flask, a mixture was prepared containing 50 ml of sample (activated sludge) and CIP at a final concentration of 60 mg/l. Then, the volume was finalized with sterile water up to 100 ml, and incubated at 28 °C±1/14 days under agitation at 100 rpm. After that, resistant bacteria were inoculated in a Luira Broh medium containing 60 mg/l of CIP to isolate, and the medium was incubated at 28°C/3 days.<sup>22,23</sup> The enriched culture was plated onto Mineral salt medium agar plates supplemented with 20 mg/l of CIP. The isolated colonies that grew on the plates were purified and assessed for their capability to degrade CIP. Among them, a specific strain named MK4 exhibited the ability to degrade CIP, and was chosen for subsequent investigation.

#### Molecular Identification of Ciprofloxacin Resistance Bacteria

The Bacterial Genome DNA Extraction Kit (Nucleospin de Macherey-Nagelen) was used to extract Genomic DNA. The 16S rRNA amplified fragment of approximately 1465 bases using two primers 27 F/1492 R; forward (5'AGAGTTTGATCCTGGCTCAG-3') and reverse (5'TACGGYTACCTTGTTACGACTT-3').<sup>24</sup> DNA sequences were analyzed with the Basic Local Alignment Search Tool at the National Center for Biotechnology Information website (NCBI, <http://www.ncbi.nlm.nih.gov/>).<sup>25</sup> The phylogenetic tree was constructed using the MEGA 11 software.<sup>26</sup>

The optimal tree is shown using the Neighbor-Joining method inferred the evolutionary history.<sup>27</sup> The bootstrap test, with a specified number of replicates (in this case, 100), is used to assess the robustness of the phylogenetic tree.<sup>28</sup> Using the Maximum Composite Likelihood method, the evolutionary distances were computed.<sup>29</sup> All positions with less than 5% site coverage were eliminated, i.e., fewer than 95% alignment gaps, missing

data, and ambiguous bases were allowed at any position (partial deletion option). There were a total of 1467 positions in the final dataset.

### Ciprofloxacin Biodegradation Test

In order to test effect ciprofloxacin concentration on biodegradation, resistant bacteria were transferred to 5 ml of Luira Broh broth supplemented with CIP at different concentrations (5 mg/l, 2.5 mg/l, 1.25 mg/l, 0.625 mg/l, 0.312 mg/l, 0.15mg/l) and incubated at 28°C/24 h. Then, centrifugation was performed and turbidity was adjusted to (OD=0.35) at a wavelength of 590 nm.<sup>23</sup> 150 µl of bacterial suspension was inoculated into microplate and incubated at 28°C. Absorbance was measured by ELISA microplate at 595 nm during 0, 24 and 48 experimental hours.<sup>23</sup>

### Effect of Organic Substrate on Growth and Biodegradability

In order to determine best organic substrate affecting the most biodegraded antibiotic by strain MK4 biodegradability of the antibiotic at a concentration of 5 mg/ml exposed to different carbone sources (glucose, sodium acetate, and sucrose) was realized in erlenmeyer flasks containing 50 ml of MMSM medium and inoculated with bacterial suspension (3.0%), and incubated at 30 °C. The effect of sodium acetate was used as control. Bacterial growth and biodegradability were measured at the different specific time points (0, 24, 48 h).<sup>30</sup>

### ATR- FTIR Analysis

After 14 days of incubation period, ATR- FTIR spectral was used to analyze the structural properties of degradation product in each sample.<sup>31</sup> The sample containing CIP, strain MK4 and carbone sources (glucose, sodium acetate and sucrose) prepared as described previously was analyzed by ATR-FTIR technique. A scanning range from 400 to 4000 nm was performed using the ATR-FTIR instrument (Cary 63). The obtained analytical spectrum was compared to a library of reference spectra to identify the specific functional groups present in the samples.

### Potential Intermediates of Ciprofloxacin Biodegradation

The approach described by author Pan et al.<sup>32</sup> was used for the samples collected from the biodegradation experiment. Ultra-performance liquid chromatography tandem mass spectrometry with a MS QQQ Mass spectrometer was utilized to analyze the intermediate metabolites from CIP biodegradation. Prior to conducting chemical analysis, liquid samples underwent filtration using a 0.22-µm nylon membrane. The LC/MS/MS analysis was performed using 6400 Series Triple Quadrupole with an electrospray ionization source employed for the identification of CIP and its biodegradation intermediates. A Column Comp

(G1316A) C18 column (150 mm×2.1 mm, 3  $\mu$ m) was utilized, and the mobile phase consisted of solvent A (ultrapure water with acetonitrile). Samples were injected with a volume of 50  $\mu$ l, and the column oven temperature was maintained 0.8°C.

### Statistical Analysis

In this study, the significant difference ( $P < 0.05$ ) in the CIP biodegradation and growth bacteria was determined using analysis of variance (ANOVA) to check the significant difference ( $P < 0.05$ ) in the CIP biodegradation under the conditions of different nutrients.

## RESULTS

### Physico-Chemical Analysis of Wastewater Samples

Physical parameters including temperature (air and water)<sub>2</sub>, pH, and oxygen dissolved of the influent and effluent wastewater samples were recorded (Figure 1).

#### Temperature

Results of analysis conducted on water samples showed that wastewater temperature was close to ambient temperature representing significant values ranging between ( $T = 8.79^\circ\text{C}$ ) and ( $T = 17^\circ\text{C}$ ). However, unregistered air temperature values varied from ( $T = 13^\circ\text{C}$ ) and ( $T = 23^\circ\text{C}$ ).

#### pH

A range pH value of influent water samples was between 7.5 and 10.22. Likewise, pH of effluent average 7.91 and 10.25. Those measures were close to neutral or alcalin pH.

#### Oxygen

Monthly change of oxygen in wastewater (influent and effluent) showed the presence of significant amounts, varying between 0.30 mg/l to 4.19 mg/l. There was a trend between atmospheric temperature and microbial oxygen uptake; experiments received in summer showed highest value uptake of 4.19 mg/l, however, the lowest value of 2.98 mg/l correspond to February 2020, which was the winter season.

### Pollution Indicators

#### Chemical Oxygen Demand

COD values unregistered of influent wastewater ranged from 175 mg O<sub>2</sub>/l to 1480 mg O<sub>2</sub>/l (Figure 2). On the other hand, COD of effluent wastewater recorded were much lower; they varied between 56 mg O<sub>2</sub>/l and 368 mg O<sub>2</sub>/l

#### Biological Oxygen Demand

BOD<sub>5</sub> values of influent samples varied between 150 mg/l to 900 mg/l (Figure 2). Whereas, reduction in BOD<sub>5</sub> content of effluent wastewater was observed ranging between 5 mg O<sub>2</sub>/l and 65 mg O<sub>2</sub>/l.

#### BOD<sub>5</sub>/COD Ratio

To characterize the nature of the effluent, the ratio of BOD<sub>5</sub>/COD was used (Figure 3). COD and BOD<sub>5</sub> are parameters to quantification of the biodegradable or non-biodegradable polluting load of the inoculum. The ratio BOD<sub>5</sub>/COD used as an index of biodegradability in water, as it gives an initial estimate of the biodegradability of the material organic from our effluents. The BOD<sub>5</sub>/COD ratio value was between 2 and 3 for the samples taken, which indicates that it is moderately loaded with biodegradable organic matter. But, the BOD<sub>5</sub>/COD ratio of some sample was less than 2, which indicates that the effluent this time is lightly loaded with inorganic matter.

### Biodegradability Evaluation

#### BOD<sub>28</sub> Determination

All substances tested showed varied BOD values during 28 days (Figure 4). BOD<sub>28</sub> values for different antibiotic compounds varied from the lowest 3.1 mg/L for nifuroxazide mg/l, whereas, the highest registered value 186.34 mg/l for CIP before 10 days, followed by penicillin and doxycillin after 14 days. The BOD<sub>28</sub> values for the negative control (inoculum in mineral medium) recorded was between 1.24 mg/l to 6.2 mg/l. The BOD<sub>28</sub> value for the positive control batch (sodium acetate in mineral medium) unregistered was between 39.06 mg/l to 57.66 mg/l.

#### Percentage of Biodegradation

Percentage of biodegradation revealed that some antibiotic compounds were highly biodegraded within 14 days of incubation. Then, biodegradation increased after 28 days. While, for other antibiotic substances, the highest biodegradation was achieved within 28 days (Figure 5). All the experiments demonstrated the percentage degradation of the reference compound (Sodium acetate) at a concentration of 50 mg/l, ranging from 82.05% within 14 days to as high as 189.75% within 28 days. These results indicate that the reference compound achieved ready biodegradation after 28 days. Out of following 11 antibiotics, three were considered as readily biodegradable (biodegradability above the threshold of 60%) including ciprofloxacin (138.33%), doxycillin (66.66%), and penicillin (54.23%) at 14 days. Other antibiotics, such as cephalixin (36.20%), azithromycin (36.11%), metronidazol (33.33%), (25.75%) clarithromycin (25.36%), and nifruaxid (16.36%) were moderate or low-degradable.

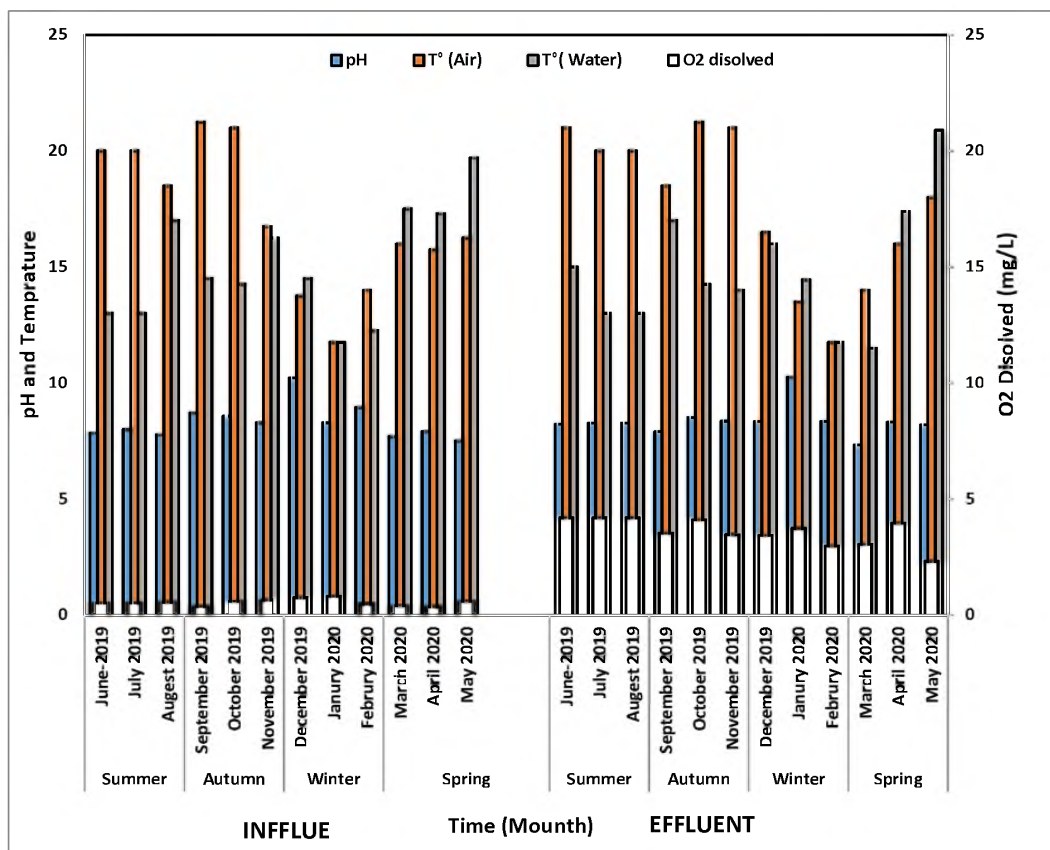


Figure 1. Physico-chemical parameters of wastewater samples.

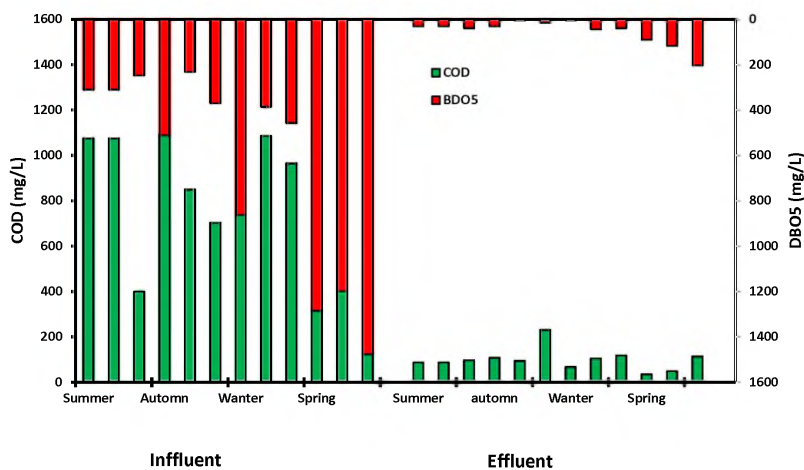


Figure 2. Pollution parameters of wastewater samples.

### Ciprofloxacin Degrading Bacteria

#### Identification

Morphological analysis revealed that the MK4 strain (MK474159.1) was Gram-negative and rod shaped (Figures

6B and C), forming on a GN medium incubated at 30°C/24 h. Phylogenetic analysis of 16S rRNA gene sequence indicated that it belongs to the *Klebsiella oxytoca* species. The MK4 strain showed a high level of homology (99% of similarity) at 85% with the *K. oxytoca* HE650838 and *K. oxytoca* AY150697

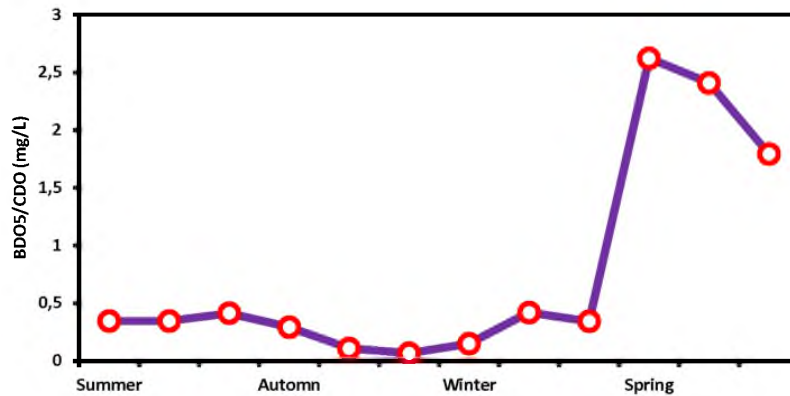


Figure 3. BOD<sub>5</sub>/COD ratio of wastewater samples.

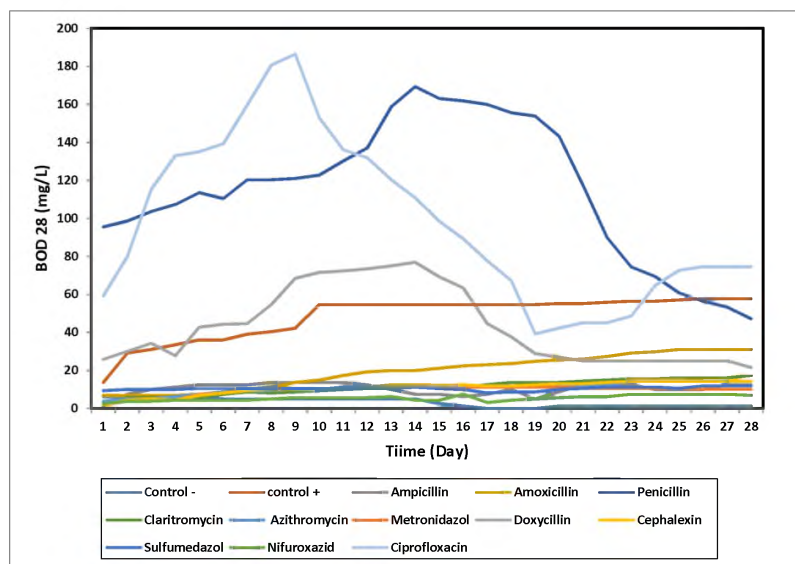


Figure 4. BOD<sub>28</sub> of antibiotic compounds analysis.

strains. A detailed phylogenetic analysis of the strain's placement is illustrated in Figure 6A.

#### Effect of Ciproflaxin Concentration on Biodegradation

In this part of study, the MK4 strain was adopted as a model bacterium to assess the biodegradation of CIP. Figure 7 illustrates the growth curves of the MK4 strain in various concentrations of CIP. In the control group (without CIP), the growth curve displayed a decline due to the absence of carbon and energy sources in the medium. Growth of the MK4 strain in different concentrations of CIP showed that maximal growth was observed within 24 h; then, growth decrease at the end of 48 h when the CIP concentration was less than C3=1.25 mg/l. Higher than C4=0.625 mg/l, the maximal bacterial growth was observed at 24 h, then decreased at the end of incubation at

48 h. Growth of strain MK4 in the control group, showed no variation at 24 and 48 h (Figure 8). The highest growth of the MK4 strain was observed at concentrations C5, C4 and C6 during 24 h, showing optical densities of 3.711; 3.302; 2.967, respectively.

#### Effect of Organic Substrate on Growth and Biodegradability

In order to determine the best organic substrate for CIP degradation by MK4 strain, different carbon sources were tested on bacterial growth. Growth of the MK4 strain was significantly increased in the presence of the three carbon sources tested including glucose sodium acetate, and sucrose (Figure 9). The highest bacterial growth was observed for sucrose (OD=0.5248) at 24 h, then decreased at 48 h, rep-

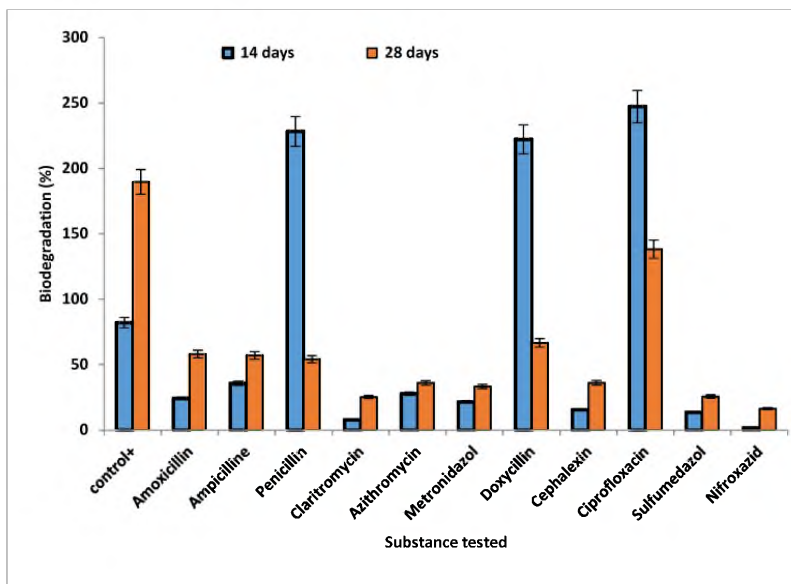


Figure 5. Percentage of biodegradation (%) of antibiotic substances.

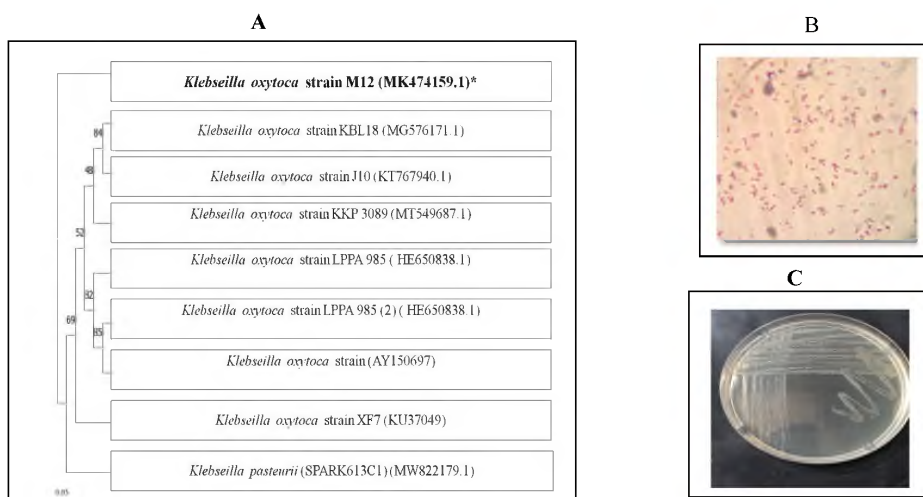


Figure 6. Macroscopic, microscopic and phylogenetic analysis by neighbor-joining method based on 16S rRNA gene sequence of MK4 strain and related strains (A: phylogenetic tree MK4; B: Microscopic characteristics of MK4 strain; C: Macroscopic characteristics of MK4 strain).

resenting OD=0.162. For glucose and acetate, respectively, growth increased from OD=0.2961 and OD= 0.207 at 24, to OD=0.2869 and OD=0.3907 at 48 h. In these conditions, comparable growth of the MK4 strain was observed in the cultures that were fed with CIP and carbone sources, with no significant difference ( $p > 0.05$ ) between them.

### ATR-FTIR Analysis

All spectra of (CIP+Glu) at T=0 h, T=24 h, and T=48 h in (Figure 9) showed the same peaks indicating the presence of same function. Function O-H is visible approximately at 311

$\text{cm}^{-1}$ , 2729  $\text{cm}^{-1}$ , 2509  $\text{cm}^{-1}$  and a peak at 2346  $\text{cm}^{-1}$  is characteristic of the  $\text{C}\equiv\text{N}$  nitrile group. Additionally, a peak at 1704  $\text{cm}^{-1}$  is characteristic of the  $\text{C}=\text{O}$  ketone group, indicating a change of the pyridazine and quinolone rings.

Infrared spectra of CIP samples revealed different functions of substances produced in the presence of various carbone sources: glucose (GLU), sucrose (sac) and sodium acetate (acetate), at T=0, T=24 h, T=48 h (Figure 9). Comparison result of samples (CIP+acetate) at T0 and (CIP+sac) at T0, (CIP+sac) at T24h (Figure 9) with standard spectrum revealed same peaks at 3267  $\text{cm}^{-1}$ , indicating the presence of (O-H) hydroxyl in carboxyl group, and vibrations absorption at 1634



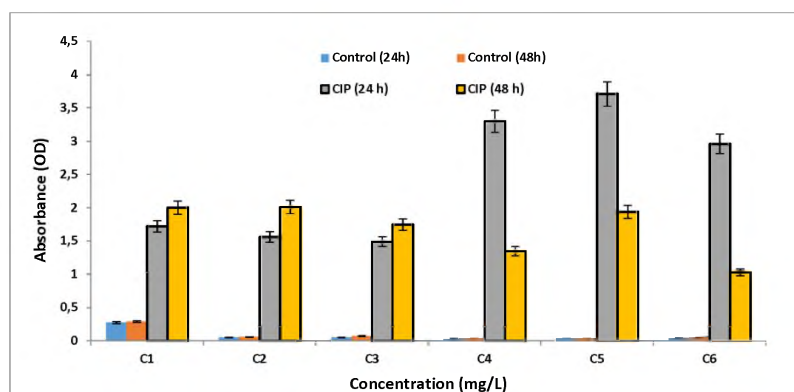


Figure 7. Impact of ciprofloxacin concentration on growth of the MK4 strain.

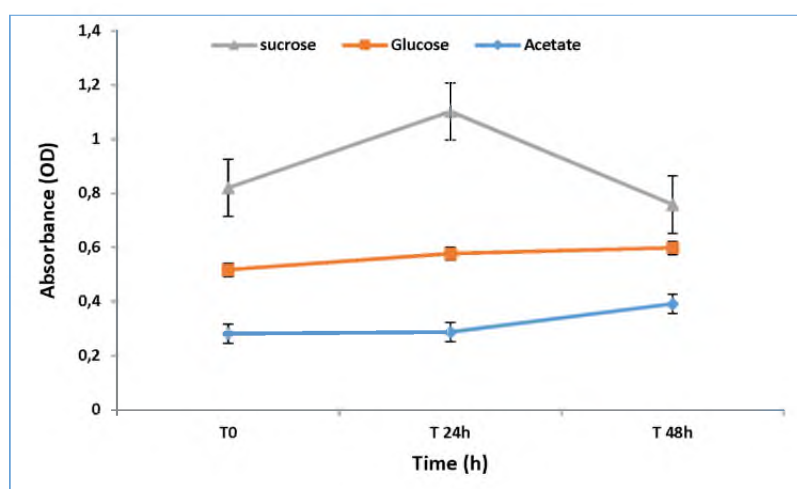


Figure 8. Impact of ciprofloxacin concentration on growth of the MK4 strain.

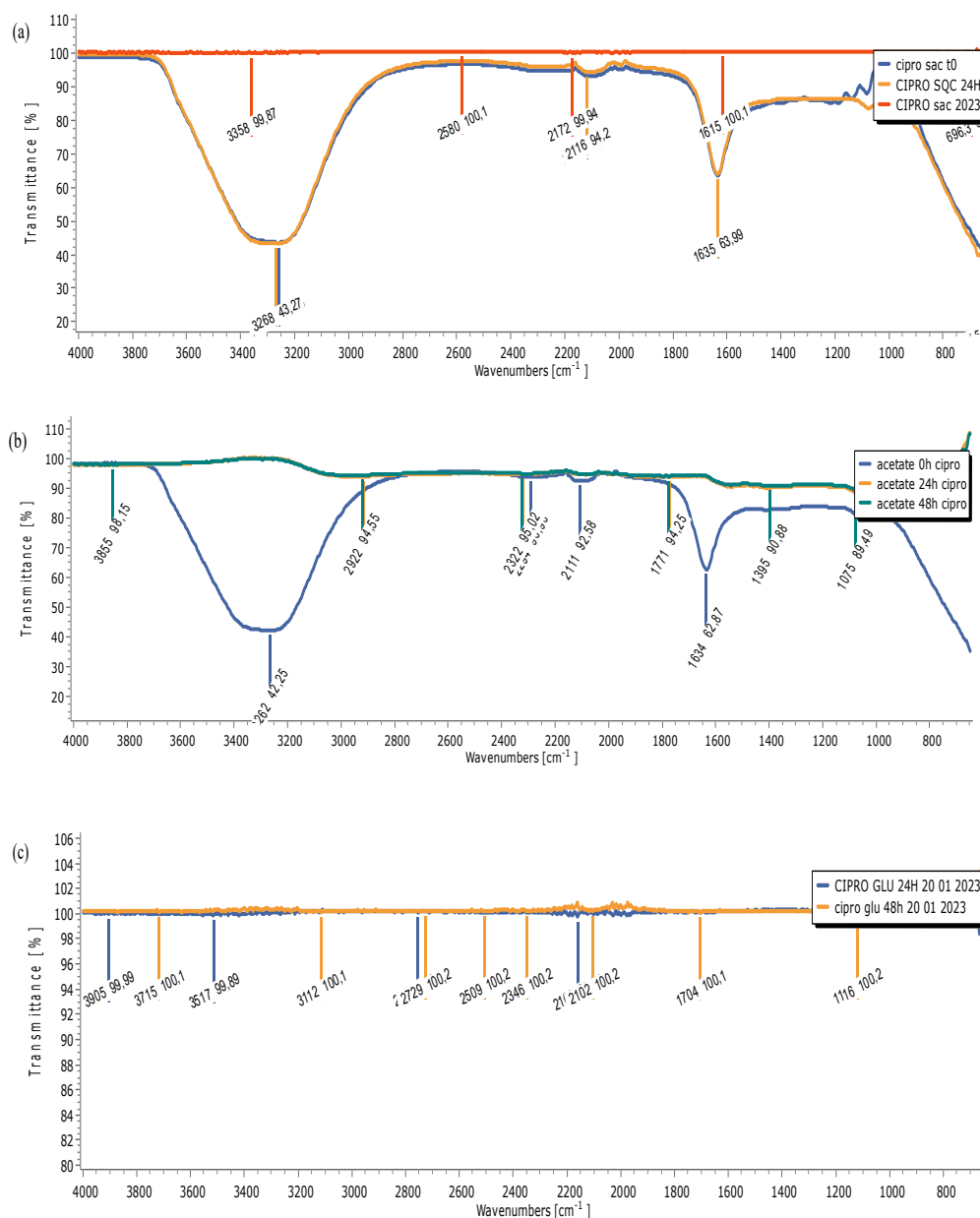
$\text{cm}^{-1}$  and  $2111 \text{ cm}^{-1}$  were attributed to  $\text{C}=\text{C}$  function while peaks were  $1075 \text{ cm}^{-1}$  and  $1184 \text{ cm}^{-1}$  are characteristic of the  $\text{C}-\text{F}$  stretching function. Results analysis of (CIP+ acetate) at T24 and T48h, (Figure 9 a), showed that all peaks disappear while other peaks at  $2921 \text{ cm}^{-1}$ ,  $1396 \text{ cm}^{-1}$  and  $1075 \text{ cm}^{-1}$  were detected. Peaks of the spectrum (CIP+ sac) at 48 h in the (Figure 9 b) revealed the presence of band at  $2172 \text{ cm}^{-1}$ , indicating the stretching of  $-\text{H}$  in alkynes, while a peak at  $1615 \text{ cm}^{-1}$  is indicative of symmetric stretching of  $\text{C}-\text{C}=\text{C}$  in alkanes, which is a characteristic feature of this functional group.

All spectra of (CIP+Glu) at T=0 h, T=24 h, and T=48 h in (Figure 9c) showed the same peaks indicating the presence of same function. Function O-H is visible approximately at  $3112 \text{ cm}^{-1}$ ,  $2729 \text{ cm}^{-1}$ ,  $2509 \text{ cm}^{-1}$  and a peak at  $2346 \text{ cm}^{-1}$  is characteristic of the  $\text{C}\equiv\text{N}$  nitrile group. Additionally, a peak at  $1704 \text{ cm}^{-1}$  is characteristic of the  $\text{C}=\text{O}$  ketone group, indicating a change of the pyridazine and quinolone rings.

Taken together, current findings suggest that the MK4 strain resulted in the decomposition and conversion of the aforementioned groups or components of CIP. At T=0 h and T=24 h, the ATR-FTIR spectra obtained with sodium acetate and sucrose had some degree of similarity, indicating the presence of the same function groups. After T=48 h, the ATR-FTIR spectra of the three carbone sources (sucrose, glucose and sodium acetate) were different, meaning the presence of variable functions.

#### Potential Intermediates of Ciprofloxacin Biodegradation

After 14 days of acclimatization of the sample added microbiota, LC/MS/MS analysis was employed to identify the biodegradation products of CIP. The major intermediate compound was produced by the MK4 strain during the degradation, which had been cultivated with CIP for 14 days. In contrast, the absence of any peaks in the negative control (without microorganisms) corresponds to the absence of these particular metabolites. The suggested configurations of CIP intermediates



**Figure 9.** ATR-FTIR analysis of CIP degradation (a) in presence of sodium acetate; (b) in presence of sucrose; (c) in presence of glucose.

were derived from the analysis of the overall ion chromatogram and information previously documented in publications by Girardi et al.<sup>33</sup> Additionally, the ChemBioDraw Ultra software was employed in this process.

Figure 10 displays the protonated molecules [M-H]<sup>+</sup> of the intermediate metabolites. In order to confirm the structures more accurately, the protonated molecules of the major intermediate metabolites were chosen for production analysis. Based on the identified products, four potential degradation pathways were proposed, as illustrated in Figure 10. Initially, the elimination of the piperazine through desethylation of the piperazine substituent and hydroxylation from CIP led to the formation of

the first intermediate metabolite, named CIP-A1, which can be identified as C<sub>13</sub>H<sub>10</sub>FN<sub>3</sub>O<sub>3</sub>, and it exhibits (280.8 m/z) mass-of-charge. Through the subsequent elimination of the amino group (-NH<sub>2</sub>) from the benzene ring of CIP-A1, an intermediate metabolite was generated, named CIP-A2, at a mass-to-charge of 193.9 m/z, and it is identified as C<sub>10</sub>H<sub>9</sub>NO<sub>3</sub>. Additionally, at a mass-to-charge ratio at 162.9 m/z, another metabolite was formed and derived from CIP-A1, named (CIP-B), which is C<sub>7</sub>H<sub>7</sub>FN<sub>2</sub>O<sub>2</sub>. Furthermore, the introduction of an OH group onto the benzene ring of CIP resulted in the creation of CIP-C, which was identified as C<sub>17</sub>H<sub>19</sub>FN<sub>3</sub>O<sub>4</sub> and displays a mass-to-charge ratio at 342.9 m/z.

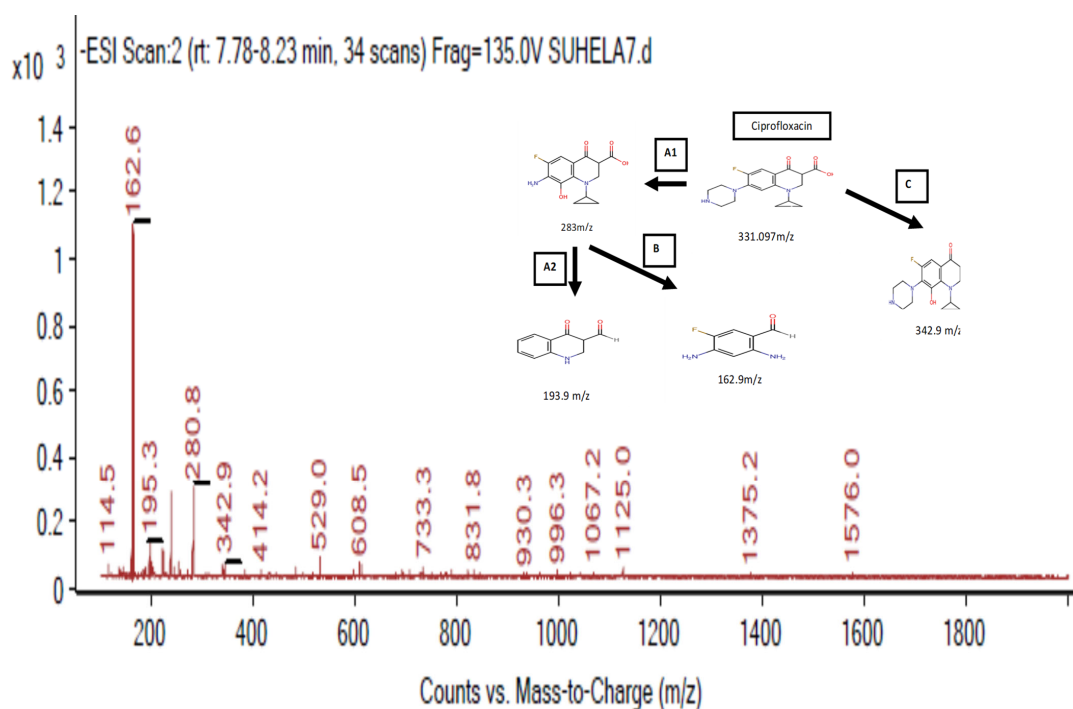


Figure 10. Proposed chemical structure of intermediate products of CIP by LC-MS/MS.

## DISCUSSION

Assessing the biodegradability of some antiseptic and antibiotic compounds in wastewater to predict their fate in biological systems seems of great importance as an ecofriendly elimination of environment pollution. Current findings revealed that air and water temperatures of WWTP varied between 8.79 to 23°C. The variation of temperature depends on time of sampling, and the different processing stages of WWTP. Temperature directly influences the development of microorganisms present in wastewater. It is one of the most important ecological factors for sludge function and the purification activity by microorganisms.<sup>34</sup>

Neutral to basic pH of wastewater samples: influent (7.5-10.22), and effluent (7.91-10.25), can be explained by the presence of chemicals of the El Kouyer station. In accordance with the FAO<sup>35</sup>, the pH levels fall within the typical range of 6.5 to 8.4. Many authors mentioned that wastewater pH depends on the stage of treatment.<sup>36</sup>

Monthly change of oxygen in wastewater (influent and effluent) of the El Kouyer station varied between 0.30 mg/l to 4.19 mg/l. This change is due to the differences in oxygen consumption, limiting of microbial respiration, and is attributed to the seasonal temperature variations.<sup>37,38</sup>

The current study indicated that COD of wastewater was reduced from: influent samples (175 mg O<sub>2</sub>/l to 1480 mg O<sub>2</sub>/l) to effluent samples (56 mg O<sub>2</sub>/l and 368 mg O<sub>2</sub>/l). They were ob-

tained with treated water in compliance with Algerian discharge standards (120 mg O<sub>2</sub>/l).<sup>19</sup>

The decrease of BOD<sub>5</sub> values of influent samples (150 mg/l-900 mg/l) to effluent wastewater (5 mg O<sub>2</sub>/l-65 mg O<sub>2</sub>/l) indicates that WWTP eliminates the maximum rate of biodegradable organic pollution. Also, high BOD<sub>5</sub> levels, implying the effect of microbial oxygen demand, cause hypoxia conditions for the aquatic flora.<sup>39</sup>

In order to characterize the nature of the effluent, the ratio of BOD<sub>5</sub>/COD was calculated. According to Bechac et al.<sup>40</sup>, the ratio in question remains within the normal range of 1 to 3. Abdouni et al.<sup>41</sup> stated that this ratio depends on the nature and origin of sewage which can be domestic or industrial. It is associated with the growth of abundant bacteria and a decrease in the oxygen ratio after the oxygen is consumed by the microorganisms.<sup>42</sup> The observed differences in BOD<sub>5</sub> values can be due to the variations in seasonal temperature changes which may affect microbial respiration.<sup>37,38</sup> Another possible reason for the relatively low blank BOD<sub>5</sub> could be an insufficient amount of inoculum, as suggested by Kümmerer et al.<sup>43</sup> and Seyfried et al.<sup>44</sup> These studies mentioned that the high inoculum had a positive effect on biodegradation experiments, leading to a reduction in the lag phase and an enhanced representation of competent degraders.

Several antibiotics were tested for their biodegradability in our study. These were classified as readily biodegradable to persistent or recalcitrant in the environment by ECHA.<sup>45</sup> In

a comparison of our results with the guidelines OECD<sup>18</sup> and the studies of Painter<sup>36</sup> and O'Malley<sup>46</sup>, the tested reference compound sodium acetate exhibited rapid and complete degradation with a percentage of 82.05% via MRT within 14 days. The biodegradation of the reference compound must be rapid (14 days) and reach at least 60% of degradation. Guziłowska-Tic and Tic<sup>47</sup> reported 83.33% degradation of sodium acetate using MRT on the 14th day at a concentration of 100 mg/L. Bergheim et al.<sup>48</sup> and Piętka-Ottlik et al.<sup>49</sup> demonstrated 78% biodegradation of sodium acetate within 14 days but at a concentration of 30 mg/l.

In order to characterize the nature of the effluent, the ratio of BOD<sub>5</sub>/COD was calculated. According to Abdouni et al.<sup>41</sup>, this ratio depends on the nature and origin of sewage which can be domestic or industrial. It is associated with the growth of abundant bacteria and a decrease in the oxygen ratio after the oxygen is consumed by the microorganisms.<sup>42</sup> The observed differences in BOD<sub>5</sub> values can be due to the variations in seasonal temperature changes which may affect microbial respiration.<sup>37,38</sup> Another possible reason for the relatively low blank BOD<sub>5</sub> could be an insufficient amount of inoculum, as suggested by Kümmerer et al.<sup>43</sup> and Seyfried et al.<sup>44</sup> These studies mentioned that the high inoculum had a positive effect on biodegradation experiments, leading to a reduction in the lag phase and an enhanced representation of competent degraders.

The process of antibiotic compounds was found to be low for most of them.<sup>50</sup> Al-Ahmad et al.<sup>51</sup> tested the biodegradation ability of penicillin G, CIP, cefotiam, meropenem, and sulfamethoxazole using the closed bottle test. They found that only penicillin G was biodegradable to some degree, with approximately 27% being removed after 28 days, or increase to 35% in 40 days. However, none of the others were readily biodegradable.  $\beta$ -lactam antibiotics were recorded to be highly biodegradable in several studies.<sup>15,52</sup> On the other hand, macrolides seem to be more recalcitrant for biodegradation.<sup>53</sup> While some antibiotics, such as penicillins, have been reported to degrade easily, antibiotics such as CIP, tetracyclines and tylosin have been reported to be more recalcitrant and cause more dispersal in the environment at higher concentrations with their persistence and accumulation in the environment.<sup>54</sup> Li et al.<sup>55</sup> tested 16 antibiotics using both OECD 302 B and OECD 301 B tests, and they found that only benzyl penicillin (penicillin G) was completely mineralized. Kümmerer et al.<sup>43</sup> tested the biodegradability of CIP, ofloxacin, and metronidazole, and found that none of them were biodegraded. The biodegradation assessments of trimethoprim and sulfamethoxazole conducted by Bertelkamp et al.<sup>56</sup> demonstrated that trimethoprim was a biodegradable molecule, but SMX, with zero or very low biodegradability coefficients, was more persistent. According to our results, it was determined that Sulfamethoxazole was degradable (25.75%). Although several researchers have documented varying rates of removal for tetracycline, and some studies indicate that tetracyclines are

not biodegradable, there is a lack of documented evidence regarding their mineralization.<sup>57,58</sup> Gartiser et al.<sup>59</sup> studied the degradation of 17 antibiotics from different antibiotic groups as cephalosporins: (Ceftriaxone, Cefuroxime); B-lactams (Penicillins: Amoxicillin, Benzylpenicillin); macrolides (Clarithromycin, Erythromycin); tetracyclines (Tetracycline, Chlortetracycline) macrolides (Clarithromycin, Erythromycin); quinolones (Ofloxacin); carbapenem (Imipenem); lincosamides (Clindamycin); nitroimidazole (Metronidazole); aminoglycosides (Gentamicin); polyeneantimycotics (Nystatin); sulphonamides (Sulfamethoxazole, Trimethoprim); glycopeptides (Vancomycin, Monensin) by inherent biodegradability test combined with the Zahn-Wellens test in the Closed Bottle Test.<sup>18</sup> By result, all these substances are classified as "readily biodegradable", also in WWTPs and thus have no accumulation in the aquatic bodies.<sup>60</sup> This variation in % of degradation of antibiotics compounds in the present results may be due to some factors such as the nature and source of the inoculum (active sludge or second effluent), and the viability of the inoculum is one of the conditions test. Physical-chemical factors such as pH and temperature can limit or at least slow down microbial activity, and affect the removal efficiency of antibiotics when optimum requirements are not attained.<sup>61</sup> Because of the relation between the atmospheric seasonal temperature and microbial oxygen uptake, the microbial respiration can be limited.<sup>37,38</sup> According to the guideline<sup>18</sup>, when the substance tested exhibits a biodegradation rate of less than 60%, the pH value should remain between pH=6 to pH=8.5. So, it is crucial to maintain pH neutrality as it greatly influences the activity of microbial inoculum.

CIP is a third generation antibiotic of the fluoroquinolone family with a large antibacterial activity.<sup>62</sup> Based on molecular identification with morphological characteristics the CIP degrading bacterial strain was identified as *K. oxytoca*. Chen et al.<sup>63</sup> found that although the strains were present in all water samples, large numbers of them were present in WWTP and activated sludge. Additionally, *K. oxytoca* epidemics are frequently linked to strains that have enzymes which inactivate the antibiotic activity such as carbapenems and extended-spectrum beta-lactamases.<sup>64-67</sup> The resistance mechanisms of *K. oxytoca* may be due to the over-expression of gene coding of the beta-lactamase enzyme or to the presence of multiple copies of beta-lactamase genes. Both of these mechanisms lead to the over-production of beta-lactamase enzymes.<sup>68,69</sup> In addition, some studies have noted that the genomes of several *K. oxytoca* isolates are resistant to other wide antibiotics families, such as tetracycline and fluoroquinolones.<sup>70</sup> Several studies highlighted the potential of *K. oxytoca* as a promising candidate for the biodegradation of antibiotics in wastewater treatment processes. Wang et al.<sup>71</sup> reported enhanced degradation of norfloxacin with a rate of 90% within 72 h. Also, a previous study of Wang<sup>15</sup> found that the *K. oxytoca* HKE-10 strain can degrade CIP at a range of concentration between 0.8 mg/L and 100 mg/L

in 5 days. In the present study, the use of glucose and sodium acetate stimulated bacterial growth and CIP degradation. The *K. oxytoca* MK4 growth increased rapidly in presence of glucose and sodium acetate compared to sucrose. This might suggest that co-metabolism plays a crucial role in eliminating the antibacterial activities of CIP. Thus, those organic substrates were considered the best sources for CIP degradation as they resulted in rapid bacterial growth and an elimination rate of CIP after 24 h incubation. Co-substrates play a dynamic and significant role in the degradation reaction of emerging contaminants. Moreover, previous studies have demonstrated that the presence of easier-to-use substrates, such as sodium acetate and glucose, can enhance the degradation rate of antibiotics.<sup>72,73</sup> In the current study, the presence of another source of carbon and energy favored the bacterial growth and elimination of the CIP, and compared to the negative control. It is well known that an adequate supply of a simple source of carbon and energy stimulates bacterial growth and its co-metabolism. On the other hand, in the presence of a complex carbon source (sucrose), the bacteria may take a long lag phase duration to adapt.

In our study, the ATR-FTIR spectrophotometer provides a distinct and clear view of antibiotic degradation by the *K. oxytoca* MK4 strain in presence of the different sources of carbon. The significative reduction in vibration that corresponds to the piperazine ring, as shown, indicates that various locations on the piperazine ring may have undergone oxidation, and potentially formed carboxy groups. In addition, the displacement of the corresponding bands in the degraded sample, as compared to those in the standard, can be attributed to the existence of metabolites. Based on the results reported by Guo et al.<sup>74</sup>, it can be inferred that the cleavage of the piperazinyl ring can lead to the formation of transformation products. The appearance of two new stretching absorption peaks of C-F ( $1075\text{ cm}^{-1}$ ,  $1185\text{ cm}^{-1}$ ,  $1116\text{ cm}^{-1}$ ) respectively, and other news peaks corresponding to CC, C=O and CN groups, suggests that the CIP antibiotic has undergone changes as a result of bacterial degradation.<sup>75,76</sup> The vibrations observed at ( $1472\text{ cm}^{-1}$ ,  $1628\text{ cm}^{-1}$ ) correspond to the bonds in the benzene ring as well as those in the pyrazine ring. These vibrations were still detectable in the spectrum of *M. luteus* and *B. subtilis* even after the incubation of 14 days as reported by Tan et al.<sup>75</sup> and Yan et al.<sup>76</sup> The spectra for *L. gesseri*, *Enterobacter* sp., and *Bacillus* sp. bacteria closely resembled the degradation products of CIP recorded in previous studies.<sup>77,78</sup> However, it was observed that the products of the quinolone ring structure remained detectable even after the incubation period; this suggests that the piperazinyl ring cleavage may be responsible for the elimination of the antibacterial activity of CIP. Further research may be required to fully comprehend the chemical structure and characteristics of these compounds. Several studies have indicated that the degradation of CIP involves at least two distinct parts of the CIP molecule; the piperazinyl substituents and quinolone moiety.<sup>79,80</sup> These two components can undergo

separate degradation processes during biodegradation and can be subject to biotransformation or degradation by microbial enzymes. The same finding in the study of Wang<sup>15</sup> showed that the *K. oxytoca* HKE-10 strain is capable of efficiently degrading CIP through amide bond hydrolyzed, followed by quinolone degradation via oxidation and ring opening. The degradation of CIP was confirmed by ATR-FITR, which revealed structural changes in both the piperazine ring and the quinolone moiety of the molecule.

The results indicate that the presence of glucose and sodium acetate stimulated bacterial growth and CIP degradation for the first 24 h, compared to sucrose where the bacterium started growing and exhibited a high capability to degrade CIP after 48 h. Pan et al.<sup>32</sup> tested the influence of sodium acetate as a co-substrate and observed approximately 60% of the antibiotic elimination after 5 days. They reported that sodium acetate triggered the bacterial growth and improved the breakdown of CIP. Nguyen et al.<sup>81</sup> recorded degradation of CIP at a level of 80-90% by adsorption on sludge during the treatment of wastewater whose substance is stable. Moreover, the adsorption process is the step that helps the activated sludge system to degrade about 50-% of CIP by anaerobic biodegradation.<sup>82,83</sup> These findings suggest that *K. oxytoca* strain could be a promising candidate for the bioremediation of CIP-contaminated environments, including wastewater treatment plants and polluted soil.

In our study, CIP changed to four products mainly by degradation and hydroxylation of the piperazinyl substitute. Thus, the transformation process of CIP was observed to occur in two regions of the molecule: the piperazinic portion and the quinolone portion by two different reactions: (A) decomposition of piperazinyl substituent; and (B) hydroxylation. The study conducted by Liu et al.<sup>12</sup> discovered that the biological oxidation process carried out by a mixed culture specifically targeted the piperazine ring of CIP. However, the antibiotic quinolone component of CIP remained unchanged and unaffected by the transformation process.

During our study, we observed the biodegradation of CIP and its metabolite CIP-A1. The metabolite CIP-A1 exhibited a protonated molecule signal at  $m/z$  283, which had been previously identified during the biotransformation of CIP using the fungi *Pestalotiopsis guepini*.<sup>78</sup> In addition, we observed the elimination of the amino group ( $-\text{NH}_2$ ) from the benzene ring of CIP-A1, resulting in the formation of CIP-A2, with a molecular weight of 193. This finding aligns with the research conducted by Xiaobin et al.<sup>84</sup> Additionally, we observed the formation of CIP-C, with a molecular weight of 348, which is consistent with previous reports by Alexandrino.<sup>13</sup> In the fact, the FQ such as CIP transformed in natural environments by a consortia of non-characterized microorganisms but not by a single microorganism. For instance, Feng et al.<sup>85</sup> used a consortium isolated from activated sludge which has been used in many CIP biotransformations. Furthermore, the same

biodegradation products of CIP identified as CIP-A and CIP-C were found as the bacterial community responsible for the degradation of CIP by the strains belonging to different genera such as *Stenotrophomonas*, *Phenylobacterium*, *Pseudoxanthomonas*, *Dysgonomonas*, *Ferruginibacter*, and *Leucobacter* in the study reported by Liao.<sup>10</sup> The same metabolite product (CIP-C) in our findings was reported in the study of Wetzstein et al.<sup>86</sup>, showing the biodegradation of CIP by the *Gloeophyllum striatum*, the brown rot fungus. In addition, the metabolite CIP-A is a result of CIP biodegradation by certain fungi.<sup>77,87,88</sup>

The study of Jia et al.<sup>89</sup> investigated the degradation of CIP using a mixture of bacteria, specifically anaerobic sulfate-reducing bacteria such as *Desulfobacter* sp., which were isolated from a sludge system. These bacterial strains were found to produce metabolites known as CIP-A and CIP-C in our study. The formation of these metabolites occurred through a desethylation reaction of the piperazine substituent and the subsequent hydroxylation processes. However, some studies reported the biodegradation of CIP by one strain, as reported by Jung et al.<sup>90</sup> They reported the biotransformation of CIP by an *Escherichia coli* strain which is highly resistant to CIP and isolated from a municipal WWTP. This strain is able to degrade CIP and inactivate certain FQs via acetylating the piperazine ring by the aminoglycoside acetyltransferase enzyme coding in its genome. Also, Pan et al.<sup>32</sup> reported that CIP can be transformed into seven products, and five of them (M2, M3, M4, M7, M16) were also demonstrated in other studies, by the thermophilic bacterium *Thermus* sp. isolated from acclimated sludge.

## CONCLUSION

The biodegradability of antibiotic and antiseptic drugs in wastewater has been thoroughly investigated. The results of this study indicate that some antibiotics tested did not meet the expected levels for biodegradation established according to the OECD 301F guidelines. Therefore, it can be concluded that while certain antibiotic drugs are assumed to be readily biodegradable compounds, some of the tested compounds degrade by less than 20%, rendering them non-biodegradable and potentially persistent. This, in turn, serves as an indicator of the chemicals being potentially persistent. It is noteworthy that, as in the case of ecotoxicity, the biodegradability assessment must be conducted through several independent test runs to take into account the variability in the microbial inoculum. An alternative approach could be the analysis of the taxonomic composition of the inoculum, which can help identify significant variations within the microbial community and identify the microorganisms that are potentially responsible for the transformation process. In this study, a bacterial strain was isolated and identified as *K. oxytoca* MK4, which facilitated the degradation of CIP and the analysis of its transformation products. The ATR-FTIR spectrums used in the analysis showed changes in antibacterial active sites of the antibiotic tested CIP (piper-

azine ring and quinolone part) and confirmed the degradation of CIP by the bacteria isolated. As such, this bacterial strain is a potential candidate for introduction into wastewater effluents to remove CIP in effluent water before discharging into the environment. This research also demonstrated that indigenous bacterial strains enhance biodegradation when added to active sludge. From these results, the gene encoding the CIP degradation by the dominant isolates of active sludge should be investigated via metagenomics, transcriptomics and proteomics.

## Acknowledgements

The authors acknowledge the Ministry of High Education and Scientific Research of Algeria, Laboratory of Geomatics, Ecology and Environment, Department of biology. University of Mustapha Stambouli. Mascara, (ALGERIA), for supporting this work. Also, the sample analysis for ATR-FTIR and LCMS/MS were done at Research Laboratory Practice and Research Center, Iğdır, Türkiye.

## Availability of data and materials

The 16S rRNA gene sequence data of the ciprofloxacin degrading *Klebsiella oxytoca* MK4 deposited to National Centre of Biotechnology Information (NCBI) GenBank with accession number MK474159.1.

**Peer Review:** Externally peer-reviewed.

**Author Contributions:** Conception/Design of Study- S.S.; Data Acquisition- S.S.; Data Analysis/Interpretation- S.S.; Critical Revision of Manuscript- I.M.A.; Final Approval and Accountability- M.S., S.S., I.M.A., R.E.

**Conflict of Interest:** Authors declared no conflict of interest.

**Financial Disclosure:** Authors declared no financial support.

## ORCID IDs of the authors

Saim Souhila	0000-0001-8399-8942
Mokrani Slimane	0000-0003-0664-9241
Isabel Martínez-Alcalá	0000-0002-4109-3253
Ramazan Erenler	0000-0002-0505-3190

## REFERENCES

1. Yang YSO, Kim KH, Kwon EE, Tsang YF. Occurrences and removal of pharmaceuticals and personal care products (PPCPs) in drinking water and water/sewage treatment plants: A review. *Sci Total Environ.* 2017;596-597:303-320.
2. Liu H, Pu C, Yu X, Sun Y, Chen J. Removal of tetracyclines, sulfonamides, and quinolones by industrial-scale composting and anaerobic digestion processes. *Environ Sci Pollut and Environ Monitoring.* 2018;18:313-318.
3. Amorim IS, Moreira AS, Maia ME, Tiritan PM, Castro P. Biodegradation of ofloxacin, norfloxacin, and ciprofloxacin as

- single and mixed substrates by *Labrys portucalensis* F11. *Appl Microbiol Biotechnol.* 2014;98:3181-3190.
4. Kumar A, Pal D. Antibiotic resistance and wastewater: Correlation, impact and critical human health challenges. *J Environ Chem Eng.* 2018;6: 52–58.
  5. Carvalho RN, Ceriani L, Ippolito A, Lettieri T. Development of the first Watch List under the Environmental Quality Standards Directive. EUR–Scientific and Technical Research series 2015 – ISSN 1831-9424-166.
  6. Sabri NA, van Holst S, Schmitt H, et al., Fate of antibiotics and antibiotic resistant genes during conventional and additional treatment technologies in wastewater treatment plants. *Sci Total Environ.* 2020;741:140199.
  7. Sorinolu AJ, Tyagi N, Kumar A, Mariya Munir M. Antibiotic resistance development and human health risks during wastewater reuse and biosolids application in agriculture. *Chemosphere.* 2021; 265:129032.
  8. Aziz A, Sengar A, Basheer F, Farooqi IH, Isa MH. Anaerobic digestion in the elimination of antibiotics and antibiotic-resistant genes from the environment—A comprehensive review. *J Environ Chem Eng.* 2022;10(1):106423.
  9. Kinigopoulou V, Ioannis P, Kalderis D, Anastopoulos I. Microplastics as carriers of inorganic and organic contaminants in the environment: A review of recent progress. *J Mol Liq.* 2022; 350:118580.
  10. Sahlin, S, Larsson JD, Agerstrand M. CIP: EQS Data Overview. In The Department of Environmental Science and Analytical Chemistry (ACES) Report; Stockholms Universitet: Stockholm, Sweden, 2018; p.15.
  11. Dorival-Garcia N, Zafra-Gomez A, Navalon A, Gonzalez J, Vilchez JL. Removal of quinolone antibiotics from wastewaters by sorption and biological degradation in laboratory-scale membrane bioreactors. *Sci Total Environ.* 2013; 442:317–328.
  12. Liu Z, Sun P, Pavlostathis SG, Zhou X, Zhang Y. Adsorption, inhibition, and biotransformation of ciprofloxacin under aerobic conditions. *Bioresour Technol.* 2013;144: 644-651
  13. Alexandrino DA, Mucha AP, Almeida CMR, Gao W, Jia Z, Carvalho MF. Biodegradation of the veterinary antibiotics enrofloxacin and ceftiofur and associated microbial community dynamics. *Sci Total Environ.* 2017;581:3593.
  14. Lima VB, Goulart LA, Rocha RS, Steter JR, Lanza MR. Degradation of antibiotic ciprofloxacin by different AOP systems using electrochemically generated hydrogen peroxide. *Chemosphere.* 2020;125807.
  15. Wang J, Mao D, Mu Q, Luo Y. Fate and proliferation of typical antibiotic resistance genes in five full-scale pharmaceutical wastewater treatment plants. *Sci Total Environ.* 2015;526:366-373.
  16. OECD 310. Ready biodegradability-CO<sub>2</sub> in sealed vessels (Headspace test). 2014
  17. Osińska A, Korzeniewska E, Harnisz M, Niestępski S. The prevalence and characterization of antibiotic-resistant and virulent *Escherichia coli* strains in the municipal wastewater system and their environmental fate. *Sci Total Environ.* 2017; 577: 367-375.
  18. OECD. Guideline for Testing of Chemicals (301 D). Closed Bottle Test. Organisation of Economic Cooperation and Development, Paris. 1992.
  19. Arrêté interministériel fixant la liste des cultures pouvant être irriguées avec des eaux usées épurées du 2 janvier 2012. *Journal Officiel de la République Algérienne (JORADP).* 2012;41:21.
  20. American Public Health Association, Water Pollution Control Federation, Water Environment Federation. Standard methods for the examination of water and wastewater. Washington, D.C., USA: American Public Health Association; 2005.
  21. Brown DM, Hughes CB, Spence M, Bonte M, Whale G. Assessing the suitability of a manometric test system for determining the biodegradability of volatile hydrocarbons. *Chemosphere.* 2018;195:381-389.
  22. Liyanage GY, Pathmalal MM. Risk of prophylactic antibiotics in livestock and poultry farms; a growing problem for human and animal health and for the environment. Proceeding of 2nd Environment and Natural Resources International Conference; 20. 2016; Thailand.
  23. Liyanage GY, Pathmalal MM. Isolation and characterization of oil degrading bacteria from coastal waters and sediments in Sri Lanka. *J Natn Sci Foundation.* 2016; 44(4):351-358.
  24. Heuer H, Krsek M, Baker P, Smalla K, Wellington E. Analysis of actinomycete communities by specific amplification of genes encoding 16S rRNA and gel-electrophoretic separation in denaturing gradients. *Appl Environ Microbiol.* 1997;63:3233-3241.
  25. NCBI (2023) Available from: <http://www.ncbi.nlm.nih.gov/>. Accessed on 22 March 2023.
  26. Tamura K, Stecher G, Kumar S. MEGA 11: Molecular Evolutionary Genetics Analysis Version 11. *Mol Biol Evol.* 2021;38(7):3022-3027.
  27. Saitou N, Nei M. The neighbor-joining method. A new method for reconstructing phylogenetic trees. *Mol Biol Evol.* 1987;4:406-425.
  28. Felsenstein J. Confidence limits on phylogenies: An approach using the bootstrap. *Evolution.* 1985; 39:783-791.
  29. Tamura K, Nei M, Kumar S. Prospects for inferring very large phylogenies by using the neighbor-joining method. *Proc Natl Acad Sci (USA).* 2004;101:11030-11035.
  30. Lan-jia P, Bao-wei Y, Jun L, Xiao-li S, Jian-Hua S. Effect of sodium acetate on ciprofloxacin elimination and microbial community in a sequencing batch reactor. *Chemosphere.* 2017;168:1479-1485.
  31. Wackerlig J, Schirhagl R. Biodegradation of UV absorbers in wastewater using moving bed biofilm reactors. *Water Res.* 2015; 69:1-10.
  32. Pan LJ, Li J, Li CX, Yu GW, Wang Y. Study of ciprofloxacin biodegradation by a *Thermus* sp. isolated from pharmaceutical sludge. *J Hazard Mater.* 2018;343:59-67.
  33. Garland JL, Mills AL. Classification and characterization of heterotrophic microbial communities on the basis of patterns of community level sole-carbon-source utilization. *Appl Environ Microbiol.* 1991; 57(8):2351-2359.
  34. Touyer M, Lashermes G, Baudez, JC. Effect of temperature on the kinetics of organic matter degradation in anaerobic sludge digesters. *Bioresour Technol.* 1998;63(2): 141-147.
  35. FAO, Irrigation with treated wastewater: Operating manual, regional office for the near East and North Africa, Cairo, Egypt, 2003.
  36. Painter HA. Detailed review paper on biodegradability testing (No. 98). Organisation for Economic Co-Operation and Development. 1995.
  37. Nouha K, Yan S, Tyagi RD, Surampalli RY. EPS producing microorganisms from municipal wastewater activated sludge. *Civil Engineering*, 2016.
  38. Xu S, Yao J, Ainiwaer M, Hong Y, Zhang Y. Analysis of bacterial community structure of activated sludge from wastewater

- treatment plants in winter. *Biomed Res Int*. 2018;2018:8278970. doi:10.1155/2018/8278970.
39. Sukumaran M, Rama Murthy V, Raveendran S, et al. Biodiversity of Microbes in Tannery Effluent. *J Ecotoxicol*. 2008.
  40. Bechac JP, Boutin P, Mercier B, Nuer P. Traitements des eaux usées; Eyrolles: Paris, France, 1987.
  41. Abdouni AE, Bouhout S, Merimi I, Hammouti B, Haboubi K. Physicochemical characterization of wastewater from the Al-Hoceima slaughterhouse in Morocco. *Caspian J Environ Sci*. 2021; 19(3):423-429.
  42. Bliefert C, Perraud, D. Mass balances of organic matter and nutrients in the biodegradation of hydrocarbons. *J Hazard Mater*. 2009; 163(2-3): 1185-1192.
  43. Kümmerer K, Al-Ahmad A, Mersch-Sundermann V. Biodegradability of some antibiotics, elimination of the genotoxicity and affection of wastewater bacteria in a simple test. *Chemosphere*. 2000; 40(7):701-710.
  44. Seyfried M, Boschung A, Miffon F, Ohleyer E, Chaintreau A. Elucidation of the upper pathway of alicyclic musk Romandolide® degradation in OECD screening tests with activated sludge. *Environ Sci Pollut Res*. 2014;21(16):9487-9494.
  45. ECHA. Guidance on information requirements and chemical safety assessment 2017; chapter R.11: PBT/vPvB Assessment. Version 4.0, June 2017.
  46. O'Malley LP. Evaluation and modification of the OECD 301F Respirometry biodegradation test method with regards to test substance concentration and inoculum. *Water Air Soil Pollut*. 2006; 177(1-4):251-265.
  47. Guziłowska-Tic K, Tic W. Biodegradation of selected volatile organic compounds in groundwater. *J Ecol Engineering*. 2016; 17(3):145-150.
  48. Bergheim M, Gieré R, Kümmerer K. Biodegradability and ecotoxicity of tramadol, ranitidine, and their photoderivatives in the aquatic environment. *Environ Sci Pollut Res*. 2012;19(1):72-85.
  49. Piętka-Ottlik M, Frąckowiak R, Maliszewska I, Kotwzan B, Wilk KA. Ecotoxicity and biodegradability of antielectrostatic dicephalic cationic surfactants. *Chemosphere*. 2012; 89(9):1103-1111.
  50. Cristóbal-García J, González-Martínez A, Dionysiou DD. Biodegradation of pharmaceutical compounds: A review. *J Hazard Mater*. 2011;167(1-3):355-367.
  51. Al-Ahmad A, Daschner FD, Kümmerer K. Biodegradability of Cefotiam, ciprofloxacin, Meropenem, Penicillin G, and Sulfamethoxazole and inhibition of wastewater bacteria. *Arch Environ Contam Toxicol*. 1999;37:158-163.
  52. Deng Y, Zhang Y, Gao Y, et al. Microbial community compositional analysis for series reactors treating high level antibiotic wastewater. *Environ Sci Technol*. 2012; 46:795-801.
  53. Li L, Guo C, Fan S, et al. Dynamic transport of antibiotics and antibiotic resistance genes under different treatment processes in a typical pharmaceutical wastewater treatment plant. *Environ Sci Pollut Res*. 2018; 25:30191-30198.
  54. Blackwell PA, Kay P, Pemberton EJ, Croxford A. Veterinary medicines in the environment. *Rev Environ Contam Toxicol*. 2007; 180:1-91.
  55. Li H, Helm PA, Metcalfe CD. Sampling in the Great Lakes for pharmaceuticals, personal care products, and endocrine-disrupting substances using the passive polar organic chemical integrative sampler. *Environ Toxicol Chem*. 2010; 29(4):751-762. <https://doi.org/10.1002/ETC>.
  56. Bertelkamp C, Reungoat J, Cornelissen ER, et al. Sorption and biodegradation of organic micropollutants during river bank filtration: A laboratory column study. *Water Res*. 2014; 52:231-241. doi:10.1016/j.watres.2013.10.068
  57. Cetecioglu Z, Bahar I, Meritxell G, Sara Rodriguez-Mozaz, Damia B, Orhan I, Derin O. Biodegradation and reversible inhibitory impact of sulfamethoxazole on the utilization of volatile fatty acids during anaerobic treatment of pharmaceutical industry wastewater. *Sci Total Environ*. 2015; 536:667-674.
  58. Prado B, Seco A, Ferrero L, Fdz-Polanco M. Behaviour of tetracyclines in soils: Mobility, degradation, and interaction with clay fractions. *J Environ Sci Health. Part B*. 2009;44(1):72-83.
  59. Gartiser S, Urich E, Alexy R, Kümmerer K. Ultimate biodegradation and elimination of antibiotics in inherent tests. *Chemosphere*. 2007;67:604-613. doi: 10.1016/j.chemosphere.2006.08.038
  60. Nyholm N. The European system of standardised legal tests for assessing the biodegradability of chemicals. *Environ Toxicol Chem*. 1991;11:1237-1246.
  61. Pepper IL, Charles PG, Terry J. G. Environmental microbiology. Third edition. United States of America. 2015.
  62. Luo Y, Xu L, Rysz M, Wang Y, Zhang H, Alvarez PJ. Occurrence and transport of tetracycline, sulfonamide, quinolone, and macrolide antibiotics in the Haihe River Basin, China. *Environ Sci Technol*. 2011; 45(5):1827-1833.
  63. Chen Y, Zhiping W, Lili L, Hanbin Z, Pin W. Stress-responses of microbial population and activity in activated sludge under long-term ciprofloxacin exposure. *J Environ Manage*. 2021; 281:111896.
  64. Decre D, Burghoffer B, Gautier V, Petit JC, Arlet G. Outbreak of multi-resistant *Klebsiella oxytoca* involving strains with extended-spectrum beta-lactamases and strains with extended-spectrum activity of the chromosomal beta-lactamase. *J Antimicrob Chemother*. 2004;54:881-888.
  65. Lowe C, Willey B, O'Shaughnessy A, et al., Mount Sinai Hospital Infection Control Team. Outbreak of extended-spectrum beta-lactamase-producing *Klebsiella oxytoca* infections associated with contaminated handwashing sinks (1). *Emerg Infect Dis*. 2012; 18:1242-1247.
  66. Schulz-Stubner S, Kniehl E. Transmission of extended-spectrum beta-lactamase *Klebsiella oxytoca* via the breathing circuit of a transport ventilator: root cause analysis and infection control recommendations. *Infect Control Hosp Epidemiol*. 2011;32:828-829.
  67. Zárate MS, Gales AC, Picão RC, Pujol GS, Lanza A, Smayevsky J. Outbreak of OXY-2-producing *Klebsiella oxytoca* in a renal transplant unit. *J Clin Microbiol*. 2008; 46:2099-2101.
  68. Gheorghiu R, Yuan M, Hall LM, Livermore DM. Bases of variation in resistance to beta-lactams in *Klebsiella oxytoca* isolates hyperproducing K1 beta-lactamase. *J Antimicrob Chemother*. 1997;40:533-541.
  69. Paterson DL, Bonomo RA. Extended-spectrum beta-lactamases: a clinical update. *Clin Microbiol Rev*. 2005; 18:657-686.
  70. Brisse S, Verhoef J. Phylogenetic diversity of *Klebsiella pneumoniae* and *Klebsiella oxytoca* clinical isolates revealed by randomly amplified polymorphic DNA, gyrA and parC genes sequencing and automated ribotyping. *Int J Syst Evol Microbiol*. 2001;51:915-924.
  71. Wang Y, Zhang S, Ye J, Huang J, Jiang X. Enhanced degradation of norfloxacin and sulfamethoxazole in aqueous solution by *Klebsiella oxytoca* under aerobic conditions. *Ecotoxicol Environ Saf*. 2020; 201:110843. doi: 10.1016/j.ecoenv.2020.110843



72. Xiong MB, Kurade JR, Kim HS, Roh B, Jeon H. Ciprofloxacin toxicity and its co-metabolic removal by a freshwater microalga *Chlamydomonas mexicana*. *J Hazard Mater*. 2016; 323:212-219.
73. Pan LJ, Tang XD, Li CX, Yu GW, Wang Y. Biodegradation of sulfamethazine by an isolated *Thermophile-Geobacillus* sp. S-07. *World J Microbiol Biotechnol*. 2017;33(5):85. doi:10.1007/s11274-017-2245-2
74. Guo HG, Gao NY, Chu WH, et al., Photochemical degradation of ciprofloxacin in UV and UV/H<sub>2</sub>O<sub>2</sub> process: kinetics, parameters, and products. *Environ Sci Pollut Research*. 2013; 20(5):3202-3213.
75. Tan Z, Tan F, Zhao L, Li J. The Synthesis, characterization and application of ciprofloxacin complexes and its coordination with Copper, Manganese and Zirconium Ions. *J Cryst Process Technol*. 2012;2(02):55
76. Yan SW, Chen HY, Xiao DR, et al. An unprecedented 2D→3D polythreaded metal-lomefloxacin complex assembled from sidearm-containing 2D motifs. *Inorg Chem Commun*. 2012;15: 47-51. DOI: 10.1016/j.inoche.2011.09.036.
77. Prieto A, Möder M, Rodil R, Adrian L, Marco-Urrea E. Degradation of the antibiotics norfloxacin and ciprofloxacin by a white-rot fungus and identification of degradation products. *Biores Technol*. 2011;102(23):10987–10995.
78. Parshikov I, Heinze T, Moody J, Freeman J, Williams A, Sutherland J. The fungus *Pestalotiopsis guepini* as a model for biotransformation of ciprofloxacin and norfloxacin. *App Microbiol Biotechnol*. 2001; 56(3-4):474-477.
79. Dewitte B, Dewulf J, Demeestere K, et al., Ozonation of ciprofloxacin in water: HRMS identification of reaction products and pathways. *Environ Sci Technol*. 2008; 42(13): 4889-4895.
80. Santoke H, Song W, Cooper WJ, Greaves J, Miller GE. Free-radical-induced oxidative and reductive degradation of fluoroquinolone pharmaceuticals: kinetic studies and degradation mechanism. *J Physical Chem A*. 2009;113(27):7846-7851.
81. Nguyen TT, Bui XT, Dang BT, et al., Effect of ciprofloxacin dosages on the performance of sponge membrane bioreactor treating hospital wastewater. *Bioresour Technol*. 2019; 273: 573-580.
82. Polesel F, Lehnberg K, Dott W, Trapp S, Thomas KV, Plósz BG. Factors influencing sorption of ciprofloxacin onto activated sludge: Experimental assessment and modelling implications. *Chemosphere*. 2015;119:105-111.
83. Shokoohi R, Ghobadi N, Godini K, Hadi M, Atashzaban Z. Antibiotic detection in a hospital wastewater and comparison of their removal rate by activated sludge and earthworm-based vermifiltration: Environmental risk assessment. *Process Saf Environ Prot*. 2020;134:169–177.
84. Xiaobin L, Bingxin L, Rusen Z, Yu D, Shuguang X, Baoling Y. Biodegradation of antibiotic ciprofloxacin: Pathways, influential factors, and bacterial community structure. *Environ Sci Pollut Res*. 2016;23:7911-7918.
85. Feng NX, Yu J, Xiang L, et al. Co-metabolic degradation of the antibiotic ciprofloxacin by the enriched bacterial consortium XG and its bacterial community composition. *Sci Total Environ*. 2019;665:41–51.
86. Wetzstein HG, Stadler M, Tichy HV, Dalhoff A, Karl W. Degradation of 650 ciprofloxacin by basidiomycetes and identification of metabolites generated by the brown 651 rot fungus *Gloeophyllum striatum*. *Appl Environ Microb*. 1999;65(4):1556-1563.
87. Wetzstein HG, Schneider J, Karl W. Patterns of metabolites produced from the fluoroquinolone norfloxacin by basidiomycetes indigenous to agricultural sites. *Appl Microbiol Biotechnol*. 2006; 71: 90-100.
88. Čvančarová M, Moeder M, Filipová A, Cajthaml T. Biotransformation of fluoroquinolone antibiotics by ligninolytic fungi—metabolites, enzymes and residual antibacterial activity. *Chemosphere*. 2015; 136:311-320.
89. Jia Y, Khanal SK, Shu H, Zhang H, Chen GH, Lu H. Ciprofloxacin degradation in anaerobic sulfate-reducing bacteria (SRB) sludge system: Mechanism and pathways. *Water Res*. 2018;136:64-74.
90. Jung CM, Heinze TM, Strakosha R, Elkins CA, Sutherland JB. Acetylation of fluoroquinolone antimicrobial agents by an *Escherichia coli* strain isolated from a municipal wastewater treatment plant. *J Appl Microbiol*. 2009; 106(2):564–571.

### How to cite this article

Souhila S, Slimane M, Martínez-Alcalá I, Erenler R. Screening of Antibiotics Biodegradability from Wastewater. *Eur J Biol* 2023;82(1): 70-85. DOI: 10.26650/EurJBiol.2023.1299300

# The Use of Plant Steroids in Viral Disease Treatments: Current Status and Future Perspectives

Pınar Obakan Yerlikaya<sup>1,2</sup>,  Elif Damla Arisan<sup>3</sup>,  Leila Mehdizadehtapeh<sup>4</sup>,  Pınar Uysal-Onganer<sup>5</sup>,   
 Ajda Coker-Gurkan<sup>6</sup> 

<sup>1</sup>Istanbul Medeniyet University, Faculty of Engineering and Natural Sciences, Department of Molecular Biology and Genetics, Istanbul, Turkiye

<sup>2</sup>Istanbul Medeniyet University, Science and Advanced Technology Research Center, Istanbul, Turkiye

<sup>3</sup>Gebze Technical University, Institute of Biotechnology, Kocaeli, Turkiye

<sup>4</sup>Istanbul Sabahattin Zaim University, Department of Food and Nutrition, Halkali Campus, Istanbul, Turkiye

<sup>5</sup>University of Westminster, Cancer Research Group, School of Life Sciences, London, United Kingdom

<sup>6</sup>Marmara University, Faculty of Science and Literature, Department of Biology, Istanbul, Turkiye

## ABSTRACT

Plants have been used for the prevention and treatment of diseases since the early days of humankind and constitute the natural sources of today's modern medicine. Approximately one-quarter of approved drugs are derived from plants. Plant steroids are a group of biologically active secondary metabolites with a  $5\alpha$  and  $5\beta$  gonane carbon skeleton. There is immense chemical diversity in plant steroids due to the side chains, oxidation status of the carbons in the tetracyclic core, and methyl groups. Plant steroids are classified into several groups based on their biological functions and structures, also on their mechanism of biosynthesis. All subtypes have been investigated for their anti-cancer, immunomodulatory, anti-inflammatory, and anti-viral properties. The novel coronavirus disease (COVID-19) is caused by severe acute respiratory syndrome coronavirus (SARS-CoV-2), which carries an RNA genome. An intense effort has been made in terms of effective treatment strategies and vaccine development since it was declared a pandemic. Nucleoside analogs such as favipiravir and remdesivir are used to block RNA-dependent RNA polymerase enzymes. Other strategies including neuraminidase inhibitors, chloroquine, and hydroxychloroquine as immunomodulatory agents, stem cell and cytokine based therapies are being conducted. One part of the therapies against SARS-CoV-2 is focused on the spike (S) protein of the virus that binds to the host receptor, angiotensin-converting enzyme 2 (ACE2). It has been suggested that SARS-CoV-2 S protein has a free fatty acid-binding pocket, and according to molecular simulations, steroids are ligands that bind to this pocket. Therefore, this review summarizes the plant steroid biological actions as well as their anti-viral potential against SARS-CoV-2 infection.

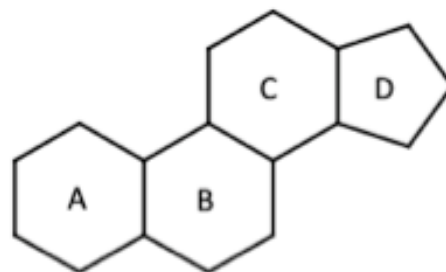
**Keywords:** Plant steroids, anti-viral drug, SARS-CoV-2

## INTRODUCTION

### PLANT STEROIDS AND THEIR BIOLOGICAL ACTIONS

Plant steroids are unique compounds found throughout the plant kingdom, which exert critical physiological effects including plant growth, development, and reproduction. They are also important micronutrients commonly found in a diet<sup>1</sup>. Plant steroids have a definite chemical structure composed of four carbon rings called the steroid nucleus (Figure 1). The nucleus typically contains the tetracyclic  $5\alpha$  or  $5\beta$ -gonane carbon skeleton with methyl substituents at C-10, C-13, and an alkyl side chain at C-17 (Figure 1).

Plant steroids are quite similar to those of well-known an-



**Figure 1.** Plant steroids backbone structure. Created by ChemSpider.

**Corresponding Author:** Pınar Obakan Yerlikaya **E-mail:** pinar.obakan@medeniyet.edu.tr

**Submitted:** 14.06.2022 • **Revision Requested:** 27.10.2022 • **Last Revision Received:** 07.03.2023 • **Accepted:** 15.03.2023



This article is licensed under a Creative Commons Attribution-NonCommercial 4.0 International License (CC BY-NC 4.0)

imal steroids in terms of the regulation of the expression of specific genes and complex physiological processes involved in cell growth and division. The addition of distinct chemical groups at different positions to the nucleus leads to the formation of many types of steroids categorized into seven main groups based on their biological functions, structures, and taxonomic considerations such as brassinosteroids, bufadienolides, cardenolides, cucurbitacins, ecdysteroids, saponins, steroidal alkaloids, and withanolides (Table 1).<sup>2,3</sup>

**Table 1.** Major groups of plant steroids.

Plant steroid group	Examples
Phytosterols	$\beta$ -Sitosterol , campesterol , stigmasterol
Brassinosteroids	Brassinolide , castasterone
Withanolides (withasteroids)	Withanolide A ,withanolides Q
Phytoecdysteroids	20-Hydroxyecdysone
Steroidal alkaloids /glycoalkaloids	Jervine , $\alpha$ -solanine , conessine
Steroidal saponins /sapogenins	Tigogenin,25-Epi-ruiizgenin
Mammalian steroidal hormones	Androstenone , progesterone
Bufadienolides	19-nor bufadienolides
Cardenolides	Quabain
Cucurbitacins	Cucurbitacins(A,B,C,D)
Ecdysteroids	Dacryhainansterone

Along with their important physiological functions within plants, they exhibit pharmacological activities helpful to humankind. Due to the knowledge about the pharmacological activities of these herbs, they are gaining increasing attention all over the world as herbal medicine supplements.<sup>4</sup> The pharmacological actions of these various types of plant steroids indicated that they have growth-promoting, cardiogenic, antimicrobial, anti-tumor, hepatoprotective, anti-fungal, antioxidant, antiinflammatory, and anti-viral roles.<sup>5-8</sup>

### Brassinosteroids

One of the most studied classes of plant steroids is brassinosteroids (BRs). BRs were discovered in 1979 by Grove et al. and have been isolated from the pollen of *Brassica napus*.<sup>9</sup> The most bioactive BR was referred to as brassinolide, followed by castasterone (CS) among more than fifty brassinosteroids identified to date.<sup>10</sup> BRs regulate growth in very low concentrations in plants and have the ability to make impacts on physiological processes (germination, growth, reproductive development, etc), modulation of the antioxidative enzyme cascade and protection from various stress conditions, including drought, heavy metals, herbicidal injury, thermotolerance, and salinity.<sup>11,12</sup> Antigenotoxicity effect of 24-epibrassinolide has been verified employing *Allium cepa* chromosomal aberration assay.<sup>13</sup> *In vitro* analyses in neuronal PC12 mammalian cell line demon-

strated that the potent antioxidant and neuroprotective role of 24-epibrassinolide reduce DNA fragmentation, Bax/Bcl-2 protein rate and cleaved caspase-3 and inhibit the MPP<sup>+</sup>-induced (1-methyl-4-phenylpyridinium) apoptosis in dopaminergic neurons.<sup>14</sup> BRs have numerous impacts on plant physiological processes including germination, growth, reproductive development, and protection from environmental stresses including drought, heavy metals, and salinity.<sup>15</sup> For instance, 24-epibrassinolide (EBR) has been shown to increase thermotolerance of tomato plants via heat-shock proteins.<sup>16</sup> BRs, apart from their well-known roles in the improvement in quality and yield of crops, have been shown to inhibit cancer cell survival and replication of viruses. 28-homocastasterone(homoCS) and EBR were first suggested as nuclear hormone receptor blockers and to cause cell cycle arrest in prostate and breast cancer cells. Recently, Coskun et al showed that EBR can trigger mitochondria-mediated apoptosis in an endoplasmic reticulum stress-inducing manner in prostate and colon cancer cell lines without causing the same effect in normal epithelial cells due to the autophagic induction.<sup>17</sup> Their findings showed that calreticulin alteration, an ER-resident chaperone protein, was the main phenomenon in EBR-induced apoptosis. The anti-angiogenic roles of BRs were also identified. Both EBR and homoCS inhibited the proliferation, adhesion, and migration of HMEC-1/HUVEC endothelial cells.<sup>18,19</sup> BRs were shown to be effective against several disorders apart from cancer, e.g., Alzheimer's and Huntington's Diseases, sexual differentiation disorders, steroid-induced osteoporosis and cataract, hyperadrenocorticism, etc.<sup>20</sup>

### Bufadienolides

Plant steroid subgroups, bufadienolides, and cardenolides, are described as cardiac glycosides because they increase the contractile force of the heart via the inhibition of cardiac Na<sup>+</sup>-K<sup>+</sup>/ATPase.<sup>21,22</sup> They consist of a steroid nucleus bearing a pentadienolide ring at C17 $\beta$ . Bufadienolides and cardenolides containing plants can cause severe toxicity to livestock. Besides, they have a wide range of bioactivities including blood pressure stimulating, immunoregulatory, etc.<sup>23</sup> They also exert cytotoxic effects on HCT116 colon, A549 lung, and HepG2 hepatocellular, A-375a skin, MCF-7 breast cancer cell lines.<sup>23,24</sup> Bufadienolides and cardenolides are also found in other organisms such as *Bufo marinus* and *Chrysolina coeruleans*, Lampyridae, and Colubridae as well as mammalian tissues.<sup>24</sup>

### Cucurbitacins

Cucurbitacins are steroid-like molecules found in the plants of the Cucurbitaceae family, as well as Cruciferae, Rubiaceae, etc. They possess a lanostane skeleton with hydroxy, methyl, and oxo substituents with unsaturation at positions 5 and 23. Their medicinal and toxic properties have been identified. Cer-

tain species-rich in cucurbitacins have been used in traditional medicines against metabolic diseases like diabetes via activating the 5' AMP-activated protein kinase pathway.<sup>25</sup> The anti-tumor, anti-inflammatory, antidiabetic, and immunosuppressant roles of these metabolites were investigated in several studies. The anti-cancer effect of cucurbitacins, such as elatericin A and B, was discovered more than fifty years ago via inhibition of cell proliferation, induction of apoptosis *in vitro*, and tumor growth in tumor-bearing mice. Oi et al cited cucurbitacin as a signal transducer activator of transcription 3 (STAT3 inhibitor and a novel therapeutic agent in osteosarcoma, lung, laryngeal, and breast cancer cell lines.<sup>25,26</sup> Cucurbitacins can inhibit the expression of tumor necrosis factor (TNF) and proinflammatory mediators such as cyclooxygenase-2 to exert an anti-inflammatory effect.<sup>27</sup>

### Phytoecdysteroids

The natural polyhydroxylated plant steroids group, phytoecdysteroids, appears in many plants as toxins for protection against herbivore insects. More than 300 different phytoecdysteroids have been described, and they show a wide distribution in the plant kingdom.<sup>28</sup> Besides, their presence is not restricted to plants, several aquatic plants and fungi also contain ecdysteroids.<sup>29</sup> A broad spectrum of these compounds with medicinal properties in mammals has been described, including antimicrobial, hepatoprotective, hypoglycemic, and hypocholesterolemic. The ecdysteroids have very low toxicity in mice with LD50 approximately 6 g kg<sup>-1</sup> of body mass.<sup>30,31</sup> They have been suggested as skin collagenase inhibitors and accelerators of wound healing. More recently, ecdysteroids isolated from *Vitex doniana* have exhibited antidepressant effect via monoaminergic transmission interference in mice studied by Isohola et al. Besides, the antioxidant and antiproliferative action of phytoecdysteroids have been also reported both *in vitro* and *in vivo* studies.<sup>32,33</sup> The fact that ecdysteroids influence various cellular processes was explained by their Akt/Protein kinase B signaling targeting.<sup>30</sup>

### Saponins

Saponins are a group of plant steroids with a classical steroid nucleus to which sugar groups are attached. They are subdivided into triterpenoid and steroid glycosides. Saponins are used in many applications in the pharmaceutical industry as a starting material for the synthesis of steroidal hormones such as vitamin D and cardioactive glycosides. They are also used as food additives or firefighting foams due to their foaming and surface tension reducing properties,<sup>34</sup> in other words, they are natural surfactants and emulsifiers. Saponins have been proposed for the treatment of diabetes, obesity, and osteoporosis.<sup>35</sup> Their anti-inflammatory, hypocholesterolemic, and immunostimulating roles are also described. They have been sug-

gested as anti-cancer agents because of their ability to inhibit cell proliferation, angiogenesis, oxidative stress and promote apoptosis<sup>36,37</sup> in a variety of cancer cells *in vitro* including brain, breast, colon, pancreas, prostate, and ovary without causing toxicity and changes and body weight in rats, mice, and rabbits.<sup>38-40</sup>

### Steroidal Alkaloids

Steroidal alkaloids (SAs) are a diverse class of plant steroids with a steroid nucleus containing nitrogen atoms attached to a ring or side chains.<sup>41</sup> Some examples of steroidal alkaloids are  $\alpha$  solanine, solamargine, tomatidine, solasonine,  $\alpha$ -solanine, briofilin, and  $\alpha$ -chaconine with anti-cancer activity<sup>42</sup> *via* induction of either intrinsic or extrinsic pathways of apoptosis.<sup>43,44</sup> The cell cycle arrest and anti-metastatic effect of some SAs have been also reported. Solanidine and spirosolane types are also known to possess pregnane skeleton and exhibit anti-fungal and anti-viral roles.<sup>45</sup> Antifungal, antiviral, antitumor and embryotoxic activities of steroidal alkaloid glycosides (spirosolane and solanidine) have been proven via various spectroscopic analyses.<sup>46,47</sup> Recently, both *in vitro* and *in vivo* investigation on *Sarcococca saligna*, the hepatoprotective and immunosuppressive potential of isolated SAs was defined. According to the results in a dose-dependent treatment, human T-cells proliferation, IL-2 production and phytohemagglutinin stimulated T-cell proliferation have been suppressed on a significant scale.<sup>48</sup>

### Withanolides

Withanolides are steroidal lactones carrying oxidized C22 and C26 ergostane skeleton and have been found to show immunomodulatory, anti-inflammatory, and anti-microbial activities by altering NF- $\kappa$ B and JAK/STAT signaling. Therefore, their application in inflammation-mediated chronic diseases has been studied in several studies. Besides, like other plant steroids, withanolides showed antitumor activity in several cancer cell lines for example, the most potent withanolide, withaferin A caused cell cycle arrest in MCF-7, SUM159, and SK-BR-3 breast cancer cell lines.<sup>49</sup> Withaferin A exhibited an antiproliferative effect in melanoma, head and neck squamous cell carcinoma, and human glioblastoma by altering Akt/mTOR and MAPK signaling pathways. Another important effect is that withanolides can target breast cancer stem cells by decreasing mammospheres and aldehyde dehydrogenase activity.<sup>50-52</sup>

### Phytosterols

Phytosterols (plant sterols) are a ubiquitous group of plant steroids. Phytosterols (PS), a member of the triterpene family, are steroidal alcohols. They are known as natural plant metabolites that exhibit functional similarity with sterol-structured cholesterol in mammalian cells. Unlike cholesterol, they are

not synthesized endogenously in the human body. More than 250 phytosterols of dietary origin such as legumes, fruits, vegetables, tubers, beans, nuts, wheat germ, whole grains, sunflower seeds and vegetable oil have been defined. Among them, campesterol,  $\beta$ -Sitosterol, and stigmasterol are the most sterols present in edible fats of PSs. Sterols and stanols both in PSs represent a class of sterol composites that modulate essential physiological functions such as membrane fluidity, permeability and signal transduction in plant cells. While sterols are in "free" unbound form, they can be covalently bonded through their ester or glycosidic bonds additionally.<sup>53-55</sup> Various studies emphasize that phytosterol glucosides are critical in the functional organization of plasma membrane lipid rafts, plasma membrane enzymes and receptor proteins. PSs also act as precursors in the synthesis of main bioactive compounds such as steroidal glycoalkaloids, steroidal saponins, phytoecdysteroids, and brassinosteroids.<sup>2,56,57</sup> As a new functional food group, extensive research has been conducted on the anticancer, anti-diabetes, anti-obesity, cytotoxic, insecticidal/larvicidal, anti-atherosclerosis, anti- Alzheimer and hepatoprotective effects of PSs related to the management of human health and metabolic disorders.<sup>57</sup> Plant sterols have been proven to increase mitochondrial ATP content, reduce dyslipidemia, insulin resistance and dysfunction of cells, improve gut microbiota dysbiosis and barrier dysfunction, increase adipose inflammatory signal, reduce oxidative stress, and modulate inflammatory signals. The fact that PSs interact directly and / or indirectly with free radicals and specific proteins in redox signaling pathways involved in various physiological processes is actually thought to be due to their antioxidant properties.<sup>58</sup> Ergosterol, campesterol,  $\beta$ -sitosterol, and stigmasterol, inhibit the production of inflammatory enzymes and pro-inflammatory cytokines in different cell lines. In LPS-stimulated HaCaT human keratinocytes and J774A.1 mouse macrophages, TNF- $\alpha$ , interleukin (IL)-8, IL-1 $\beta$  and IL-6 secretion have been reduced after the application of  $\beta$ -sitosterol isolated from moringa oleifera.<sup>59</sup> Scientific evidence reveals that PSs modulate the gut microbiota composition and play a protective role against pathologies. In addition, functionality has a beneficial effect on gut inflammation and barrier integrity. *In vitro* faeces analysis of morbidly obese individuals during the fermentation process determined that sterol supplementation decreased the population of *Erysipelotrichaceae*, a family of bacteria associated with lipidemic imbalances.<sup>60</sup> The same microbial changes have been confirmed in mouse and hamster models of hypercholesterolaemia.<sup>61</sup>

## ANTI-VIRAL ACTIVITIES OF PLANT STEROIDS

Due to the inevitable reality of viral infection risks, modern medical science aims to prevent the transmission and spread of viral infection and also to minimize the treatment and financial burden. In this regard, scientific research and pharmaceutical companies have been examining their potential com-

pounds for the identification and production of new antivirals. Most plants have hormonal functionality and are considered to be steroid synthesis factories. Recent research proves that although there is a structural distinction of plant steroids, they have a viral transcription/replication alteration effect, along with their inhibitory, antioxidant, and immunomodulatory activities, support host defense mechanisms and cell survival in the event of viral infection.<sup>62,63</sup> With the known details of the preventive role of functional foods and medicine herbs with natural nutraceutical ingredients such as polyphenols, terpenoids, flavonoids, alkaloids, sterols in noncommunicable diseases (NCDs), their preventive and / or therapeutic roles associated with the immune system in viral infectious diseases (CDs) in particular remain a mystery in many respects.<sup>63,64</sup>

In a recent study, 4 biomarker extracts of *Guiera senegalensis*, a phytoestrogen family were examined against hepatitis B virus in HuH7 liver cell lines, and their antioxidative, antiviral and hepatoprotective potential have been confirmed.<sup>65</sup> Molecular investigations of  $\beta$ -sitosterol as a common phytosterol in Chinese traditional medicine have been designed in influenza (IAV) infected mouse models in a dose dependent manner  $\beta$ -sitosterol (150–450  $\mu$ g/mL) that is able to suppress inflammation *via* p38 mitogen-activated protein kinase (MAPK) and NF- $\kappa$ B signaling. Additionally, RIG-I signaling, harmful IFN production and acute lung injury inhibition have been reported.<sup>66</sup>

Activation of the resistance mechanisms of BRs against DNA and RNA viruses is the main characteristic of their defense strategies. As a result of the host cell's special sensors (PRRs) encountering with expressed structural motifs (PAMPs) unique to the pathogen virus, immune response mechanisms that inactivate bacteria, viruses, fungi and oomycetes are triggered.<sup>20,67,68</sup> Recent studies indicated that brassinosteroids and their derivatives inhibited the *in vitro* replication of herpes simplex type 1 (HSV-1) thymidine kinase (TK)+ and TK- strains, and the arenaviruses Junin (agent of Argentine hemorrhagic fever), Pichinde, and Tacaribe viruses.<sup>69</sup> The structural alterations determine their efficacy on antiviral responses through increasing host recognition mechanisms. BR treatment in tobacco plants substantially reduced *Tobacco mosaic virus* (TMV) viral infection and increased crop yields by 56% with induced resistance to TMV.<sup>70</sup> The exogenous application of brassinolides to *Nicotiana benthamiana*, was shown as an antiviral mechanism during TMV infection. Brassinosteroids could activate different cellular targets such as MEK2 (MAPKK)-SIPK (salicylic acid-induced protein kinase) and RBOHB (respiratory burst oxidase homolog protein B)-dependent ROS burst. Additional targets such as BES1/BZR1 could inhibit RBOHB dependent ROS generation and maintain growth function as a hallmark of plant immunity.<sup>20</sup>

In a case study, it was shown that the *Arabidopsis thaliana* plant belonging to the cruciferous family, BAK1 and/or BKK1 proteins in the steroid signaling are mandatory to maintain plant

immunity against RNA viruses' infection such as Turnip crinkle virus (TCV).<sup>71</sup> Enhancement of antioxidative enzymatic performance and gene expression regulation have been observed in *A. thaliana* infected with cucumber mosaic virus (CMV) after BR treatment.<sup>72</sup> Shamsabadipour et al. determined the structural properties of triterpene and steroid compounds obtained from *E. denticulate* plant endemic to Iran by NMR and mass spectroscopic approaches. Toxicity and antiviral analysis results proved that both types of compounds have protective effects against Herpes Simplex Type 1 (HSV-1) virus infection.<sup>73</sup>

The anti-viral activity of bufadienolides and cardenolides has been reviewed by Kamano et al. Buadienolide derivatives showed selective inhibition of Rhinovirus at very low concentrations. In addition, bufadienolides isolated from *Kalanchoe pinnata* were shown to inhibit the activation of Epstein Barr virus.<sup>74</sup> Besides, a potential anti-bovine viral diarrhoea virus (BVDV) activity of nine members of cucurbitacins was found. In addition, some of the members, namely cucurbitacin B, D and E, have been shown to inhibit Hepatitis C replicon replication in HuH-7 cells.<sup>75,76</sup>

Tomatidine in green tomatoes is a steroidal alkaloid with enzymatic activity. An in vitro research focused on antiviral reaction of tomatidine versus Chikungunya virus (CHIKV), highlighting the strong controlling role of this compound on CHIKV replication processes and a significant decrease in the count of infected cells both early or post infection.<sup>77</sup> The quest for effective anti-PEDV drugs to control the swine epidemic diarrhoea virus (PEDV), defined by the fatal diarrhoea symptom in piglets, continues. Wang and colleagues, by designing *in silico* and in vitro assays, draws attention to the inhibitory role of tomatidine during PEDV replication cycle by targeting the 3CL protease in IPEC-J2 and Vero cell lines. Findings suggest that tomatidine has an antiviral activity against porcine reproductive and respiratory syndrome virus (PRRSV), infectious gastroenteritis virus (TGEV), seneca virus A (SVA), and encephalomyocarditis virus (EMCV) strongly.<sup>78</sup>

## SARS-CoV-2 AND COVID-19

Coronavirus family members (CoVs), which cause respiratory infections of human beings and other mammals, represent an enveloped and large group of single-stranded RNA viruses. Since the genome of these viruses can be directly translated into viral proteins by the host cell's ribosomes, they are defined as positive-sense viruses (viral mRNA). It is known that CoVs belong to the Nidovirales family including Roniviridae, Arteriviridae, Coronaviridae and Mesoniviridae main four members.<sup>79–81</sup> Phylogenetic analysis disclosed that the viral genome ranging from 27–32 kb has 29,903 nucleotides and shows 89.1% nucleotide similarity with SARS-like coronaviruses.<sup>82,83</sup> The viral ORF1ab gene encodes the envelope glycoprotein or spike protein (S), membrane (M) pro-

tein, nucleocapsid (N) protein, and envelope (E) proteins, which are defined as structural proteins.<sup>84</sup> Follow-up of clinical reports reveals that coronavirus members, SARS-CoV, SARS-CoV-2 and MERSCoV, show the potential to infect mammals, causing very serious symptoms. The SARS-CoV-2 virus is the seventh in this regard.<sup>85</sup> SARS-CoV-2 was raised in December 2019 in China from an unidentified zoonotic source, which might be generated from pangolin or bat coronaviruses. The disease is characterized by hypoxemic respiratory failure, which requires air-ventilation support at the severe stages of the disease. COVID-19 patients can also show asymptomatic or mild symptoms of the disease such as fever, dry cough, fatigue, lung failure mainly acute respiratory distress syndrome (ARDS), and cytokine storm at the very late stage of the disease. Until now, different candidates have been suggested for therapy including novel or repurposed antibodies, anti-inflammatory drugs, and corticosteroids. The World Health Organization (WHO) guidelines that were published in September 2020 recommend the systemic corticosteroids rather than no corticosteroids for the treatment of patients with severe and critical COVID-19 who required mechanical ventilation.<sup>86</sup> On the other hand, the same guideline also indicated not to use corticosteroids in the treatment of patients with non-severe which was based on certainty evidence. Conversely, guidelines from the Infectious Diseases Society of America that were published in April 2020 issued a weak recommendation against corticosteroids, except for patients with COVID-19 and ARDS treated in the context of a clinical trial.<sup>86</sup>

While early observational data from China suggested a potential mortality benefit of corticosteroids in COVID-19, previous studies of corticosteroids in other viral pneumonia, especially severe acute respiratory syndrome (SARS) and the Middle East respiratory syndrome (MERS), found an association with delayed viral clearance and reinforced concerns that corticosteroids may impair host response to SARS-CoV-2. Furthermore, a meta-analysis of observational studies suggested increased mortality with corticosteroid treatment in influenza pneumonia. As the COVID-19 pandemic spread across the world, clinicians struggled to weigh the potential benefits of corticosteroids against the many potential harms associated with these drugs. Despite being overwhelmed with critically ill patients, multiple clinical trial groups around the world launched high-quality RCTs of corticosteroids for severe COVID-19. Additionally, recognizing the urgency of aggregating data from these trials to guide management, WHO coordinated a prospective meta-analysis of these ongoing RCTs (PROSPERO CRD42020197242). The clinical trial groups agreed to share data, even before acceptance of their trial data for primary publication. With a press released on June 16, 2020, reporting the results of the UK-based RECOVERY trial, the existing approach for treating and studying patients with COVID-19 underwent a major change. In this large open-label randomized trial enrolling 6425 patients (2104 randomized to

receive dexamethasone and 4321 randomized to receive usual care), treatment with dexamethasone (6 mg/d for 10 days) reduced mortality by one-third in patients receiving mechanical ventilation (29.3% vs 41.4%, respectively; rate ratio, 0.64 [95% CI, 0.51-0.81]) and by one-fifth in patients receiving supplemental oxygen (23.3% vs 26.2%, respectively; 0.82 [95% CI, 0.72-0.94]) compared with usual care alone.<sup>13</sup> However, there was no benefit among patients not receiving respiratory support (1.19 [95% CI, 0.91-1.55]), and the possibility of harm could not be excluded.<sup>86</sup>

### Potential Effects of Plant Steroids as Natural Therapeutics Against Coronaviruses

With the lack of a specific/successful drug in the treatment of SARS-CoV-2 infection, most researchers focus on the antiviral effects of phytomedicines against SARS coronaviruses simultaneously. In the process defined as the term 'molecular farming', plants' secondary metabolites are preferred in the production of alternative drugs and recombinant vaccines, since they exhibit fewer side effects compared to allopathic drugs.<sup>87,88</sup>

Drug design studies are mainly focused on S protein RBD (receptor binding region) region of SARS-CoV-2, which targets angiotensin converting enzyme 2 (ACE2) receptors for the initial attachment process.<sup>89,90</sup> Understanding the lipid rafts and lipid-activated molecular troughs in the plasma membrane areas that support the entry of the SARS-CoV-2 virus into the host cell (endocytosis) and infection suggests valuable clues to the emergence of powerful antiviral strategies.<sup>91</sup>

Recent studies on lipophilic naturally derived phytosterols emphasize that these substances interact with lipid rafts, destabilize the structure of membrane cholesterol and impress biochemical activities associated with lipid rafts.<sup>92</sup> Experimental research on *Lycoris radiata* has shown that four herbal steroidal alkaloids derived from this plant may be candidates for the development of anti-SARS-CoV therapeutics.<sup>93</sup> In an *in vitro* study targeting the anti-coronaviral activity and mechanisms of action of saicosaponins (A, B2, C and D), it has been proven that saicosaponin B2 significantly inhibits human coronavirus 229E infection by interfering with viral absorption and replication processes.<sup>94</sup> Research results examining the antiviral properties and therapeutic potential of cardenolides and bufadienolides against SARS-CoV-2, HCoV-229E and HCoV-OC43 belonging to the coronavirus family report that these steroid compounds are the remarkable inhibitors of selected coronaviruses.<sup>95</sup>

Very recent comprehensive *in silico* analysis on the interaction between various plant secondary metabolites (4,704 ligands) and the four structural target proteins of SARS-CoV-2 reveals in detail the possible physicochemical, bioavailability, and binding energy scores during interaction. The virtual screening and molecular docking results demonstrate that the steroidal

lactones, triterpene sterols, coagulins, steroidal saponins, triterpene glycosides, triterpene saponins and steroidal glycoalkaloids were similar, showing lower and favorable binding energy scores against the target amino acid residues of the S protein.<sup>96</sup> Molecular Simulation approach using the University of Bristol Insertion Engine recommends steroids, vitamins, retinoids as ligands that bind the free fatty acid pocket of SARS-CoV-2 S Protein.<sup>97</sup>

The pathophysiology of COVID-19 is complex as various signaling pathways and molecules are involved in the inflammatory state. SARS-CoV-2 initiates pro-IL-1 secretion, inflammation and IL-1 beta hyper activation and up-regulation by binding to toll-like receptors. This hyperactive proinflammatory response is described as Cytokine Storm (CS). The severity of the infection that has occurred is marked by the levels of circulating cytokines and chemokines (monocyte chemoattractant protein 1, IL-2, IL-6, IFN $\gamma$ , TNF). Cytokine Storm (CS) is known to cause severe fibrosis induction in the lung tissues of infected patients, which can result in death unfortunately.<sup>98,99</sup> Obtained results of *in vitro* and *in vivo* studies focusing on the anti-inflammatory properties of Cucurbitacin against viral infections prove that Cucurbitacin II B decreased the expression of IFN $\gamma$ , TNF $\alpha$  and IL-6. In addition, Cucurbitacin E and R, respectively, downregulate IL-1 and TNF $\alpha$  expression by suppressing NF- $\kappa$ B translocation and the STAT3 signaling pathways.<sup>100,101</sup>

### CONCLUSION

Viral diseases are very common in spreading, like in the case of COVID-19, and become pandemic. To treat or prevent viral infections is a challenge since it is usually impossible to control the replicative cycle of the virus without interfering the host one, or to estimate the mutations that it will carry after each replicative cycle. Plant steroids are divided into several subclasses, and some of them have been shown as good candidates to treat viral infections since they have few side effects to the host. The exemplary studies described above indicate that plant steroid family members have a high potential for clinical efficacy, especially against SARS-CoV-2 infection. It is thought that the pharmacological manipulation of these compounds may show promising results in the course of the pandemic including COVID-19.

**Peer Review:** Externally peer-reviewed.

**Author Contributions:** Conception/Design of Study-P.O.Y.; Data Analysis/Interpretation-P.O.Y.; Drafting Manuscript-P.O.Y., E.D.A., L.M., P.U.O., A.C.G.; Critical Revision of Manuscript-P.O.Y., E.D.A., L.M., P.U.O., A.C.G.; Final Approval and Accountability-P.O.Y., E.D.A., L.M., P.U.O., A.C.G.

**Conflict of Interest:** Authors declared no conflict of interest.

**Financial Disclosure:** Authors declared no financial support.

## ORCID IDs of the authors

Pinar Obakan Yerlikaya	0000-0001-7058-955X
Elif Damla Arisan	0000-0002-4844-6381
Leila Mehdizadehtapeh	0000-0001-8759-5016
Pinar Uysal-Onganer	0000-0003-3190-8831
Ajda Coker-Gurkan	0000-0003-2298-5755

## REFERENCES

1. Trautwein EA, McKay S. The role of specific components of a plant-based diet in management of dyslipidemia and the impact on cardiovascular risk. *Nutrients*. 2020; 12(9), 71-91.
2. Kreis W, Müller-Uri F. Biochemistry of sterols, cardiac glycosides, brassinosteroids, phytoecdysteroids and steroid saponins. *Annu Rev Plant Biol*. 2010;304–363.
3. Beg S, Hasan H, Hussain MS, et al. Systematic review of herbals as potential anti-inflammatory agents: Recent advances, current clinical status and future perspectives. *Pharmacogn Rev*. 2011;5(10):120-137.
4. Gunaherath GMK, Gunatilaka AAL. Plant steroids: occurrence, biological significance and their analysis. *Encyc of Anal Chem*. 2014;1–26.
5. Li Y, Li J, Zhou K, et al. A review on phytochemistry and pharmacology of cortex periplocae. *Molecules*. 2016;21(12):2702-2718.
6. Bhandari J, Muhammad B, Thapa P, et al. Study of phytochemical, anti-microbial, anti-oxidant, and anti-cancer properties of *Allium wallichii*. *BMC Complement Altern Med*. 2017;17(1):102.
7. Moosavi B, Liu S, Wang N, et al. The anti-fungal  $\beta$ -sitosterol targets the yeast oxysterol-binding protein Osh4. *Pest Management Science*, 2019; 76(2):4–11.
8. Yang L, He J. Traditional uses, phytochemistry, pharmacology and toxicological aspects of the genus *Hosta* (Liliaceae): A comprehensive review. *J Ethnopharmacol*. 2021; (265):113-123.
9. Grove MD, Spencer GF, Rohwedder WK, et al. Brassinolide, a plant growth-promoting steroid isolated from *Brassica napus pollen*. *Nature*. 1979;281(5728):216–217.
10. Yokota T, Takahashi N. Chemistry, physiology and agricultural application of brassinolide and related steroids. *Proceed in Life Sci*. 1986;129–138.
11. Kour J, Kohli SK, Khanna K, et al. Brassinosteroid signaling, crosstalk and, physiological functions in plants under heavy metal stress. *Front Plant Sci*. 2021;24(12):608061. doi:10.3389/fpls.2021.608061.
12. Khamsuk O, Sonjaroon W, Suwanwong S, et al. Effects of 24-epibrassinolide and the synthetic brassinosteroid mimic on chili pepper under drought. *Acta Physiol. Plant*. 2018;(40):106-118.
13. Sondhi N, Bhardwaj R, Kaur S, et al. Isolation of 24-epibrassinolide from leaves of *Aegle marmelos* and evaluation of its antigenotoxicity employing *Allium cepa* chromosomal aberration assay. *Plant Growth Reg*. 2007;54(3):217–224.
14. Carange J, Longpre F, Daoust B, et al. 24-epibrassinolide, a phytosterol from the brassinosteroid family, protects dopaminergic cells against MPP-induced oxidative stress and apoptosis. *J Toxicol*. 2011;392859.
15. Clouse SD, Sasse JM. Brassinosteroids: Essential regulators of plant growth and development. *Ann Rev Plant Physiol Plant Mol Biol*. 1998;(49): 427-451.
16. Singh I, Shono M. Physiological and molecular effects of 24-epibrassinolide, a brassinosteroid on thermotolerance of tomato. *Plant Growth Reg*. 2005; 47(2–3): 111-119.
17. Coskun D, Obakan P, Arisan ED, et al. Epibrassinolide alters PI3K/MAPK signaling axis via activating Foxo3a-induced mitochondria-mediated apoptosis in colon cancer cells. *Exp Cell Res*. 2015; 15;338(1):10-21.
18. Ramirez JA, Michelini FM, Galagovsky LR, Berra A, Alche LE. Antiangiogenic brassinosteroid compounds. U.S. Patent 2013088400, 17 November 2015
19. Zhabinskii VN, Khripach NB, Khripach VA. Steroid plant hormones: effects outside plant kingdom. *Steroids*. 2015;(97):87-97.
20. Kaur Kohli S, Bhardwaj A, Bhardwaj V, Sharma A, Kalia N, Landi M, et al. Therapeutic potential of brassinosteroids in biomedical and clinical research. *Biomolecules*. 2020;10(4):572.
21. Puschett JB, Agunanne E, Uddin MN. Emerging role of the bufadienolides in cardiovascular and kidney diseases. *Am J Kidney Dis*. 2010;56(2):359-370.
22. Tang HJ, Ruan LJ, Tian HY, et al. Novel stereoselective bufadienolides reveal new insights into the requirements for Na(+), K(+)-ATPase inhibition by cardiotonic steroids. *Sci Rep*. 2016;6:29155.
23. Gao H, Popescu R, Kopp B, Wang Z. Bufadienolides and their antitumor activity. *Nat Prod Rep*. 2011;28(5):953-969.
24. Li H, Cao X, Chen X, et al. Bufadienolides induce apoptosis and autophagy by inhibiting the AKT signaling pathway in melanoma A-375 cells. *Mol Med Rep*. 2019;20(3):2347-2354.
25. Kaushik U, Aeri V, Mir SR. Cucurbitacins-An insight into medicinal leads from nature. *Pharmacogn Rev*. 2015;9(17):12-18.
26. Oi T, Asanuma K, Matsumine A, et al. STAT3 inhibitor, cucurbitacin I, is a novel therapeutic agent for osteosarcoma. *Int J Oncol*. 2016; 49(6):2275-2284.
27. Chen X, Bao J, Guo J, et al. Biological activities and potential molecular targets of cucurbitacins: a focus on cancer. *Anticancer Drugs*. 2012; 23(8):777-787.
28. Dinan L. Phytoecdysteroids: biological aspects. *Phytochemistry*. 2001;57(3):325-339.
29. Chadin I, Volodin V, Whiting P, Shirshova T, Kolegova N, Dinan L. Ecdysteroid content and distribution in plants of genus *Potamogeton*. *Biochem Syst and Ecol*. 2003; 31(4): 407-415.
30. Lafont R, Dinan L. Practical uses for ecdysteroids in mammals including humans: an update . *J Insect Sci*. 2003;3:7.
31. Festucci-Buselli RA, Contim LA, Barbosa LCA, Stuart J, Otoni WC. Biosynthesis and potential functions of the ecdysteroid 20-hydroxyecdysone-a review. *Botany*. 2008;86(9): 978-987.
32. Shakhmurova GA, Mamadalieva NZ, Zhanibekov AA, Khushbaktova ZA, Syrov VN. Effect of total ecdysteroid preparation from *Silene viridiflora* on the immune state of experimental animals under normal and secondary immunodeficiency conditions. *Pharm Chem J*. 2012;46 (4), 222–224.
33. Ishola, IO, Ochieng, CO, Olayemi SO, Jimoh MO, Lawal SM. Potential of novel phytoecdysteroids isolated from *Vitex doniana* in the treatment depression: Involvement of monoaminergic systems. *Pharmacol Biochem Behav*. 2014;127, 90–100.
34. Kregiel D, Berlowska J, Witonska I, et al. Saponin-based, biological-active surfactants from plants. In application and characterization of surfactants. Edited by Reza Najjar InTech. doi: 10.5772/65591, 2017



35. Marrelli M, Conforti F, Araniti F, et al. Effects of saponins on lipid metabolism: a review of potential health benefits in the treatment of obesity. *Molecules*. 2016;21(10):1404.
36. Du JR, Long FY, Chen C. Research progress on natural triterpenoid saponins in the chemoprevention and chemotherapy of cancer. *Enzymes*. 2014;(36):95-130.
37. Sarkar FH, Li Y, Wang Z, et al. Cellular signaling perturbation by natural products. *Cell Signal*. 2009;21(11):1541-1547.
38. Haridas V, Higuchi M, Jayatilake GS, et al. Avicins: triterpenoid saponins from *Acacia victoriae* (Benth) induce apoptosis by mitochondrial perturbation. *Proc Natl Acad Sci USA*. 2001;98(10):5821-5826.
39. Patlolla JM, Raju J, Swamy MV, et al. Beta-escin inhibits colonic aberrant crypt foci formation in rats and regulates the cell cycle growth by inducing p21(waf1/cip1) in colon cancer cells. *Mol Cancer Ther*. 2006;5(6):1459-1466.
40. Fukumura M, Ando H, Hirai Y, et al. Achyranthoside H methyl ester, a novel oleanolic acid saponin derivative from *Achyranthes fauriei* roots, induces apoptosis in human breast cancer MCF-7 and MDA-MB-453 cells via a caspase activation pathway. *J Nat Med*. 2009;63(2):181-188.
41. Ooh KF, Ong HC, Wong FC, et al. High performance liquid chromatography profiling of health-promoting phytochemicals and evaluation of antioxidant, anti-lipoxygenase, iron chelating and anti-glucosidase activities of wetland macrophytes. *Pharmacogn Mag*. 2014;10(3):443-455.
42. Dey P, Kundu A, Chakraborty HJ, et al. Therapeutic value of steroidal alkaloids in cancer: Current trends and future perspectives. *Int J Cancer*. 2019;145(7):1731-1744.
43. Dirsch VM, Müller IM, Eichhorst ST, et al. Cephalostatin 1 selectively triggers the release of Smac/DIABLO and subsequent apoptosis that is characterized by an increased density of the mitochondrial matrix. *Cancer Res*. 2003;63(24):8869-8876.
44. Moser BR. Review of cytotoxic cephalostatins and ritterazines: isolation and synthesis. *J Nat Prod*. 2008;71(3):487-491.
45. Lacour TG, Guo C, Bhandaru S, et al. Interphylal Product Splicing: The First Total Syntheses of Cephalostatin 1, the North Hemisphere of Ritterazine G, and the Highly Active Hybrid Analogue, Ritterostatin GN1N1. *J Am Chem Soc*. 1998; 120(4): 692-707.
46. Torres MC, das Chagas L, Pinto F, et al. Antiophidic solanidane steroidal alkaloids from *Solanum campaniforme*. *J Nat Prod*. 2011;74(10):2168-2173.
47. Wang K, Sasaki T, Li W, et al. Two novel steroidal alkaloid glycosides from the seeds of *Lycium barbarum*. *Chem Biodivers*. 2011;8(12):2277-2284.
48. Jan NU, Ahmad B, Ali S, et al. Steroidal alkaloids as an emerging therapeutic alternative for investigation of their immunosuppressive and hepatoprotective potential. *Front Pharmacol*. 2017; (8):114.
49. Antony ML, Lee J, Hahn ER, et al. Growth arrest by the antitumor steroidal lactone withaferin A in human breast cancer cells is associated with down-regulation and covalent binding at cysteine 303 of  $\beta$ -tubulin. *J Biol Chem*. 2014;289(3):1852-1865.
50. Zhang H, Samadi AK, Gallagher RJ, et al. Cytotoxic withanolide constituents of *Physalis longifolia*. *J Nat Prod*. 2011;74(12):2532-2544.
51. Zhang H, Bazzill J, Gallagher RJ, et al. Antiproliferative withanolides from *Datura wrightii*. *J Nat Prod*. 2013;76(3):445-449.
52. Grogan PT, Sleder KD, Samadi AK, et al. Cytotoxicity of withaferin A in glioblastomas involves induction of an oxidative stress-mediated heat shock response while altering Akt/mTOR and MAPK signaling pathways. *Invest New Drugs*. 2013;31(3):545-557.
53. Srigley CT, Haile EA. Quantification of plant sterols/stanols in foods and dietary supplements containing added phytosterols. *J Food Comp Anal*. 2015;(40):163-176.
54. Miras-Moreno B, Sabater-Jara AB, Pedreno MA, et al. Bioactivity of phytosterols and their production in plant in vitro cultures. *J Agric Food Chem*. 2016; 64(38):7049-7058.
55. Salehi-Sahlabadi A, Varkaneh HK, Shahdadian F, et al. Effects of Phytosterols supplementation on blood glucose, glycosylated hemoglobin (HbA1c) and insulin levels in humans: a systematic review and meta-analysis of randomized controlled trials. *J Diabetes Metab. Disord*. 2020;19(1):625-632.
56. Moreau RA, Nystrom L, Whitaker BD, et al. Phytosterols and their derivatives: Structural diversity, distribution, metabolism, analysis, and health-promoting uses. *Prog Lipid Res*. 2018;(70):35-61
57. Hannan MA, Sohag AAM, Dash R, et al. Phytosterols of marine algae: Insights into the potential health benefits and molecular pharmacology. *Phytomedicine*. 2020;(69):153201.
58. Vezza T, Canet F, de Maranon AM, et al. Phytosterols: Nutritional health players in the management of obesity and its related disorders. *Antioxidants (Basel)*. 2020;9(12):1266.
59. Liao PC, Lai MH, Hsu KP, et al. Identification of  $\beta$ -Sitosterol as in vitro anti-inflammatory constituent in *Moringa oleifera*. *J Agric Food Chem*. 2018;66(41):10748-10759.
60. Turnbaugh PJ, Backhed F, Fulton L, et al. Diet-induced obesity is linked to marked but reversible alterations in the mouse distal gut microbiome. *Cell Host Microbe*. 2008;3(4):213-223.
61. Martínez I, Perdicaro DJ, Brown AW, et al. Diet-induced alterations of host cholesterol metabolism are likely to affect the gut microbiota composition in hamsters. *Appl Environ Microbiol*. 2013;79(2):516-524.
62. Castilla V, Ramirez J, Coto CE. Plant and animal steroids a new hope to search for antiviral agents. *Curr Med Chem*. 2010;17(18):1858-1873.
63. Denaro M, Smeriglio A, Barreca D, et al. Antiviral activity of plants and their isolated bioactive compounds: An update. *Phytother Res*. 2020;34(4):742-768.
64. Alkhatib A, Tsang C, Tiss A, et al. Functional foods and lifestyle approaches for diabetes prevention and management. *Nutrients*. 2017;9(12):1310.
65. Parvez MK, Alam P, Arbab AH, et al. Analysis of antioxidative and antiviral biomarkers  $\beta$ -amyrin,  $\beta$ -sitosterol, lupeol, ursolic acid in *Guiera senegalensis* leaves extract by validated HPTLC methods. *Saudi Pharm J*. 2018;26(5):685-693.
66. Zhou BX, Li J, Liang XL, et al.  $\beta$ -sitosterol ameliorates influenza A virus-induced proinflammatory response and acute lung injury in mice by disrupting the cross-talk between RIG-I and IFN/STAT signaling. *Acta Pharmacol Sin*. 2020;41(9):1178-1196.
67. Yuan M, Jiang Z, Bi G, et al. Pattern-recognition receptors are required for NLR-mediated plant immunity. *Nature*. 2021;592(7852):105-109.
68. Calil IP, Fontes EPB. Plant immunity against viruses: antiviral immune receptors in focus. *Ann Bot*. 2017;119(5):711-723.
69. Wachsmann MB, Lopez EM, Ramirez JA, et al. Antiviral effect of brassinosteroids against herpes virus and arenaviruses. *Antivir Chem Chemother*. 2000;11(1):71-77.

70. Nakashita H, Yasuda M, Nitta T, et al. Brassinosteroid functions in a broad range of disease resistance in tobacco and rice. *Plant J*. 2003; 33(5):887-898.
71. Yang H, Gou X, He K, et al. BAK1 and BKK1 in *Arabidopsis thaliana* confer reduced susceptibility to turnip crinkle virus. *Eur J Plant Pathol*. 2010; 127(1):149–156.
72. Zhang DW, Deng XG, Fu FQ, et al. Induction of plant virus defense response by brassinosteroids and brassinosteroid signaling in *Arabidopsis thaliana*. *Planta*. 2015; 241(4):875-885.
73. Shamsabadipour S, Ghanadian M, Saeedi H, et al. Triterpenes and steroids from *Euphorbia denticulata* Lam. with anti-herpes simplex virus activity. *Iran J Pharm Res*. 2013;12(4):759-767.
74. Supratman U, Fujita T, Akiyama K, et al. Insecticidal compounds from *Kalanchoe daigremontiana* x *tubiflora*. *Phytochemistry*. 2001;58(2):311-314.
75. Munakarmi S, Chand L, Shin HB, et al. Anticancer effects of *Poncirus fructus* on hepatocellular carcinoma through regulation of apoptosis, migration, and invasion. *Oncol Rep*. 2020;44(6):2537-2546
76. Liu Y, Yang H, Guo Q, et al. Cucurbitacin E Inhibits Huh7 Hepatoma Carcinoma Cell Proliferation and Metastasis via Suppressing MAPKs and JAK/STAT3 Pathways. *Molecules*. 2020;25(3):560.
77. Troost B, Mulder LM, Diosa-Toro M, et al. Tomatidine, a natural steroidal alkaloid shows antiviral activity towards chikungunya virus in vitro. *Sci Rep*. 2020;10(1):6364.
78. Wang P, Bai J, Liu X, et al. Tomatidine inhibits porcine epidemic diarrhea virus replication by targeting 3CL protease. *Vet Res*. 2020;51(1):136.
79. Brian DA, Baric RS. Coronavirus genome structure and replication. *Curr Top Microbiol Immunol*. 2005;(287):1-30.
80. Fehr AR, Perlman S. Coronaviruses: an overview of their replication and pathogenesis. *Methods Mol Biol*. 2015;(1282):1-23.
81. Mahmood N, Nasir SB, Hefferon K. Plant-Based Drugs and Vaccines for COVID-19. *Vaccines (Basel)*. 2020;9(1):15.
82. Dent SD, Xia D, Wastling JM, et al. The proteome of the infectious bronchitis virus Beau-R virion. *J Gen Virol*. 2015;96(12):3499-3506.
83. Wu F, Zhao S, Yu B, et al. A new coronavirus associated with human respiratory disease in China. *Nature*. 2020;579(7798):265-269.
84. Tang X, Wu C, Li X, et al. On the origin and continuing evolution of SARS-CoV-2. *Natl Sci Rev*. 2020;7(6):1012-1023.
85. Corman VM, Muth D, Niemeyer D, et al. Hosts and Sources of Endemic Human Coronaviruses. *Adv Virus Res*. 2018;(100):163-188.
86. van Paassen J, Vos JS, Hoekstra EM, et al. Corticosteroid use in COVID-19 patients: a systematic review and meta-analysis on clinical outcomes. *Crit Care*. 2020;24(1):696.
87. Fischer R, Buyel JF. Molecular farming-The slope of enlightenment. *Biotechnol. Adv*. 2020; (40):107519.
88. Capell T, Twyman RM, Armario-Najera V, et al. Potential applications of plant biotechnology against SARS-CoV-2. *Trends Plant Sci*. 2020 25(7):635-643.
89. Shang J, Ye G, Shi K, et al. Structural basis of receptor recognition by SARS-CoV-2. *Nature*. 2020; 581(7807):221-224.
90. Bhuiyan FR, Howlader S, Raihan T, et al. Plants metabolites: Possibility of natural therapeutics against the COVID-19 pandemic. *Front Med (Lausanne)*. 2020;(7):444.
91. Fernandez-Oliva A, Ortega-Gonzalez P, Risco C. Targeting host lipid flows: Exploring new antiviral and antibiotic strategies. *Cell Microbiol*. 2019;21(3):e12996.
92. Baglivo M, Baronio M, Natalini G, et al. Natural small molecules as inhibitors of coronavirus lipid-dependent attachment to host cells: a possible strategy for reducing SARS-COV-2 infectivity? *Acta Biomed*. 2020;91(1):161-164.
93. Li SY, Chen C, Zhang HQ, et al. Identification of natural compounds with antiviral activities against SARS-associated coronavirus. *Antiviral Res*. 2005;67(1):18-23.
94. Cheng PW, Ng LT, Chiang LC, et al. Antiviral effects of saikosaponins on human coronavirus 229E in vitro. *Clin Exp Pharmacol Physiol*. 2006;33(7):612-616.
95. Yang CW, Lee YZ, Hsu HY, et al. Inhibition of SARS-CoV-2 by highly potent broad-spectrum anti-coronaviral tylophorine-based derivatives. *Front Pharmacol*. 2020;(11):606097.
96. Puttaswamy H, Gowtham HG, Ojha MD, et al. In silico studies evidenced the role of structurally diverse plant secondary metabolites in reducing SARS-CoV-2 pathogenesis. *Sci Rep*. 2020;10(1):20584.
97. Shoemark DK, Colenso CK, Toelzer C, et al. Molecular simulations suggest vitamins, retinoids and steroids as ligands of the free fatty acid pocket of the SARS-CoV-2 spike protein. *Angew Chem Int Ed Engl*. 2021; 60(13):7098-8010.
98. Alka H, Akhilesh A, Archana S, et al. Cucurbitacin: As a candidate against cytokine storm in severe COVID-19 infection. *Int J Res Pharm Sci*. 2020;11(1): 928–930.
99. Conti P, Ronconi G, Caraffa A, et al. Induction of pro-inflammatory cytokines (IL-1 and IL-6) and lung inflammation by Coronavirus-19 (COVI-19 or SARS-CoV-2): anti-inflammatory strategies. *J Biol Regul Homeost Agents*. 2020;34(2):327-331.
100. Qiao J, Xu LH, He J, et al. Cucurbitacin E exhibits anti-inflammatory effect in RAW 264.7 cells via suppression of NF- $\kappa$ B nuclear translocation. *Inflamm Res*. 2013;62(5):461-469.
101. Escandell JM, Recio MC, Manez S, et al. Cucurbitacin R reduces the inflammation and bone damage associated with adjuvant arthritis in lewis rats by suppression of tumor necrosis factor-alpha in T lymphocytes and macrophages. *J Pharmacol Exp Ther*. 2007;320(2):581-590.

#### How cite this article

Obakan Yerlikaya P, Arisan ED, Mehdizadehtapeh L, Uysal-Onganer P, Coker-Gurkan A. The Use of Plant Steroids in Viral Disease Treatments: Current Status and Future Perspectives. *Eur J Biol* 2023;82(1): 86-94. DOI: 10.26650/EurJBiol.2023.1130357

# The Role of Akt Signalling Pathway in Neurological and Cardiovascular Pathologies

Akshat D. Modi<sup>1,2</sup>,  Aahmad Ali Mahoon<sup>3</sup>,  Dharmeshkumar M. Modi<sup>4</sup> 

<sup>1</sup>Department of Biological Sciences, University of Toronto, Scarborough, Ontario, Canada

<sup>2</sup>Department of Genetics and Development, Krembil Research Institute, Toronto, Ontario, Canada

<sup>3</sup>Department of Molecular Genetics, University of Toronto, Toronto, Ontario, Canada

<sup>4</sup>Department of Pharmacy, Silver Oak University, Ahmedabad, Gujarat, India

## ABSTRACT

The PI3K/Akt/mTOR signalling pathway plays a crucial role in several biological processes, including cell proliferation, survival, and apoptosis, as well as regulates numerous signalling pathways, including JNK, NF- $\kappa$ B, and ERK pathways. The recent proliferation of signal transduction studies in neurological and cardiovascular diseases/injuries sheds light on Akt-dependent pathogenesis. The downregulation of the Akt signalling pathway 24 hours post-injury prevents neurogenesis and promotes the progression of severe secondary injuries, including neuroinflammation, scar formation, and neuronal and glial necrosis, following traumatic brain and spinal cord injury, suggesting designing therapeutic approaches within a 24-hour window post-injury. Similarly, the downregulation of the Akt signalling pathway in myocardial infarction lowers cardiovascular protection, limits neurovascularization, and inhibits cell survival. Following myocarditis, the Akt signalling network is upregulated, leading to aggravated inflammation, and increased myocardial damage. Also, the upregulation of the PI3K/Akt/mTOR pathway in chordoma promotes tumor progression and invasion, leading to neuronal damage and impaired physiological functions. Future therapeutics that target the aberrant expression of key players in the PI3K/Akt/mTOR signalling pathway present a promising approach to treating several neurological and cardiovascular pathologies. This narrative review discusses the role of PI3K/Akt/mTOR signalling pathway in traumatic central nervous system injuries (brain and spinal cord), cardiac injury (myocardial infarction), inflammatory disease (myocarditis), and rare neurological cancer (chordoma) along with therapeutic targets that are known to prevent worsened outcomes and promote recovery following those conditions.

**Keywords:** PI3K/Akt/mTOR Signalling Pathway, Traumatic Spinal Cord Injury, Traumatic Brain Injury, Myocardial Infarction, Myocarditis, Chordoma.

## INTRODUCTION

The Akt signalling is essential for cell survival, the cell cycle, and proliferation and is regulated by the phosphorylation of several growth factors and receptors that transduces the signal to transcription factors (i.e., activated Akt acts as a secondary messenger).<sup>1,2</sup> Akt is made from  $\nu$ -Akt and Akt-8 and has 68% homology with PKA and 73% homology with PKC; this high homology rate leads Akt to be termed as PKA/PKC-associated kinase.<sup>3</sup> Akt is divided into three homologous subtypes encoded by distinct genes: Akt1/PKB, Akt2/PKB, and Akt3/PKB, where each isoform has a pleckstrin homology (PH) domain at the N-terminus, and a central fragment, with a regulatory domain at the C-terminus, as well as a kinase catalytic domain.<sup>2</sup> The kinase catalytic domain has homologous regions to PKA and PKC where the Thr308 site and Ser473 (located on the C-

terminal) site are needed for complete activation of Akt.<sup>4</sup> Despite their similarities, the three Akt subtypes conduct diverse physiological functions; Akt1, for example, is ubiquitously expressed and involved in cell formation, apoptosis, size, proliferation, angiogenesis, and tumour cell invasiveness.<sup>1,2,5,6</sup> Akt2 is present in insulin-sensitive tissues, as well as mammalian skeletal muscle and adipose tissue, and has been proven to regulate glucose homeostasis and cell growth and proliferation, while Akt<sup>3</sup> is related to the brain (i.e., required for brain size and malignant glioma cell survival), lung, heart, kidney, testis, and skeletal muscle.<sup>1,5,6</sup> Akt is the primary mediator of the Akt signalling pathway, resulting in phosphorylation of downstream targets, and is active in various biological pathways like cAMP, p27 inhibition, pathways that comprise upstream PI3K and PTEN, and downstream TSC2, FOXO, eIF4E, activating

**Corresponding Author:** Akshat D. Modi **E-mail:** akshat.modi@mail.utoronto.ca

**Submitted:** 21.01.2023 • **Revision Requested:** 14.03.2023 • **Last Revision Received:** 07.05.2023 • **Accepted:** 10.05.2023



This article is licensed under a Creative Commons Attribution-NonCommercial 4.0 International License (CC BY-NC 4.0)

PI3P and mTOR (Figure 1).<sup>5,7</sup> Furthermore, several negative regulators, such as PTEN, prevent the activation of the Akt signalling pathway by hydrolysing PIP-3 to PIP-2, decreasing downstream p-Akt activity (Figure 1).<sup>5,8</sup>

The PI3K and Akt signalling pathway is enhanced by EGF, sonic hedgehog, IGF-1, insulin, and calmodulin; conversely, Akt can be antagonized by PTEN, glycogen synthase kinase 3 $\beta$ , and the HB9 transcription factor.<sup>9,10</sup> PI-(3,4,5)-P3 is necessary for the Akt activation and attracts Akt from the cytoplasm, causing ring-phosphorylation and conformational changes to the Akt via a combination of PDK1 and PI-(3,4,5)-P3.<sup>11</sup> PDK2 phosphorylates the Akt hydrophobic terminal, and double-phosphorylated Akt separates from the membrane, resulting in a cellular reaction with the substrate that includes PDK2, ILK, mTORC, and DNA-PK. The PI3K/Akt pathway is activated by PI-(3,4,5)-P3, Akt conformational alterations, and double-phosphorylation of Akt. PTEN transforms PI-(3,4,5)-P3 into a different compound inhibiting the Akt pathway (Figure 1). However, when PTEN is inhibited, the Akt pathway activates again; furthermore, carboxyl-terminal modulator protein C may decrease Akt phosphorylation and impede the PI3K/Akt signalling pathway.<sup>2,12</sup> Overall, the activation of Akt pathways promotes genetic stability, cell survival, NO production, glucose uptake, neuroregeneration, and NF- $\kappa$ B pathway, and inhibition of cellular apoptosis, neuroprotection, JNK, and ERK pathways (Figure 1).

In this narrative review, we elaborate on the role of PI3K/Akt/mTOR signalling pathways in life-changing and life-threatening neurological and cardiovascular pathologies, including traumatic brain injury, traumatic spinal cord injury, myocardial infarction, myocarditis, and chordoma. These findings have reshaped our insights into Akt signalling network-mediated pathogenesis and highlight its differential regulation in cell survival/death (i.e., traumatic injuries), cell inflammation (i.e., viral infection), and uncontrollable cell proliferation (i.e., cancer). We expect the studies of Akt signalling and neurological and cardiovascular pathologies to provide deeper insight into the pathogenesis and progression of diseases while providing opportunities for exploring novel therapies.

## AKT SIGNALLING PATHWAY IN NEUROLOGICAL PATHOLOGIES

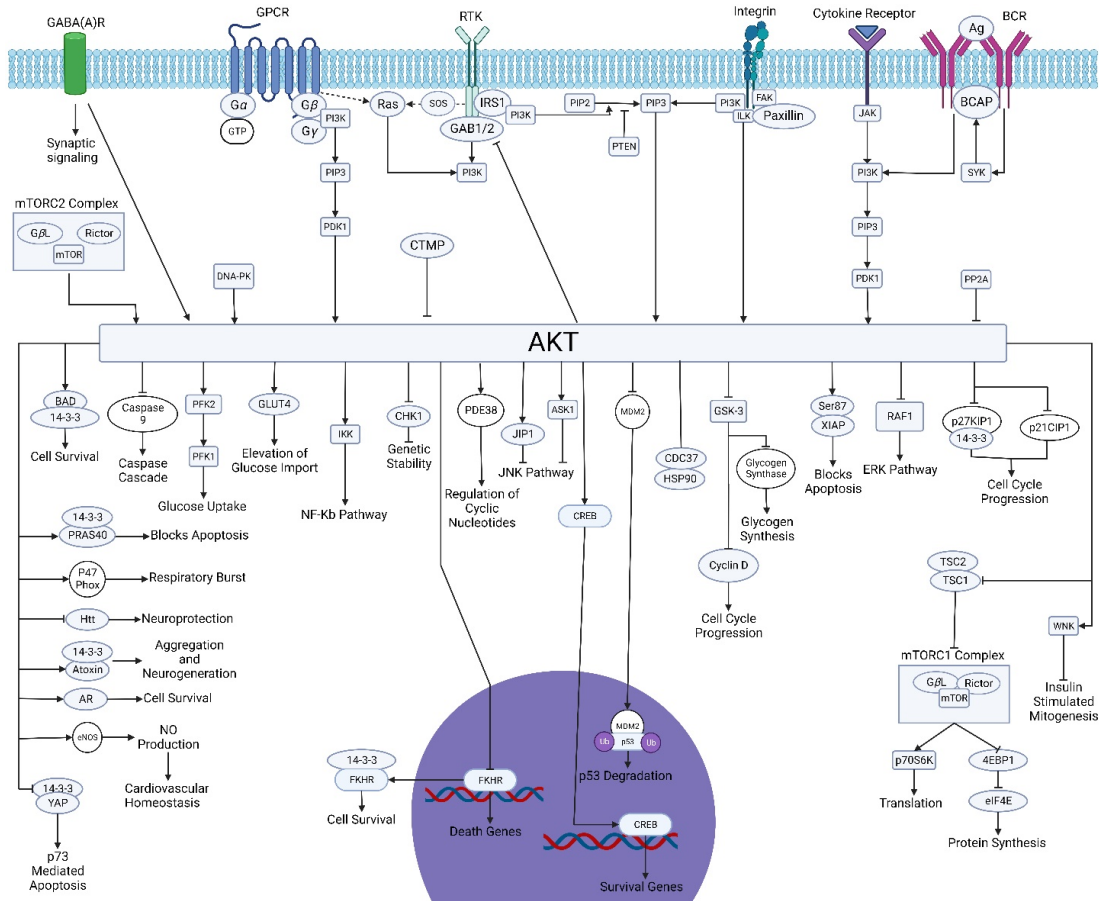
### Downregulated Akt Signalling Pathway in Traumatic Brain Injury

Traumatic brain injury (TBI) is a life-threatening event that results in motor and cognitive dysfunction, long-term disability, and/or death due to the inability of cerebral tissue to repair and regenerate following blunt (i.e., blows or jolts) or invasive sharp objects (i.e., bullets) trauma.<sup>13</sup> Along with its striking annual prevalence of 200 per 100,000 people and mortality rate of 18 per 100,000 people worldwide, it has affected more than 2.5

million people in the United States alone.<sup>13–15</sup> Hence, ensuring its place in one of the most heavily researched diseases globally, with the common aim of saving mankind.<sup>13</sup> The sudden mechanical damage initiates the primary mechanism of TBI, which involves deformities in the brain tissue, hemorrhage, concussion, diffuse axonal injury, necrosis, the release of cytokines and chemokines, and the leakage of crucial ions, proteins, fluid, and immune cells' transmigration due to the dysfunctioning of the vascular and blood-brain barrier.<sup>13</sup> This distortion in brain anatomy and increased intracranial pressure induces the activation of secondary injuries such as oxidative stress, excitotoxicity, and demyelination leading to inflammation, apoptosis, autoimmune reaction, and neurodegeneration.<sup>13</sup> The onset of secondary injuries has been debated in the literature with a range of hours to days post-primary injury, which causes gradual alteration in neurotransmitters (i.e., dopamine and serotonin), metabolic disorders, and morphological changes of mitochondria.<sup>13,16</sup> The delayed occurrence of secondary injuries provides an opportunity for therapeutic intervention to prevent neurological deficits, including cognitive decline, impairment in neurological functions, psychological alterations, and long-term disability.<sup>13</sup> Alteration of several signalling pathways, including PI3K/Akt/mTOR, is associated with the onset of secondary injuries and promotes neuronal death following TBI; hence, it presents a promising therapeutic target for pre-clinical and clinical trials.<sup>13,17</sup>

The Akt signalling pathway plays a key role as a survival signalling pathway by blocking apoptosis through the activation of Ser87, XIAP, and PRAS40 while inhibiting YAP.<sup>18</sup> The alteration in Akt kinase expression initiated at 15 mins, rapidly increased till 4 hours, peaked between 4 to 24 hours, and started to significantly subside after 72 hours post-TBI.<sup>18,19</sup> Interestingly, the induction of the Akt pathway was observed in the lesion side/ipsilateral hemisphere (i.e., injured hippocampus and cerebral cortex) while no significant alteration in the contralateral hemisphere of the brain.<sup>18,20</sup> In the hippocampus (dentate gyrus, CA1, and CA3 regions), the hallmarks of Akt hyperactivation (specific to the hippocampus), including mTORC1 complex (i.e., comprising G $\beta$ L, Rictor, and mTOR) dependent phosphorylation of ribosomal protein S6 and mTORC2 complex (i.e., comprising G $\beta$ L, Raptor, and mTOR) associated Ser473 phosphorylation was observed at 15 to 24 hours and 4 hours post-TBI, respectively (Figure 2).<sup>18,21</sup> Moreover, a decreased expression of phospho-Akt (p-Akt) along with phosphorylated phosphatase and tensin homolog deleted on chromosome 10 (p-PTEN) was observed in cortical and CA3 hippocampal neurons following TBI, which may have caused excessive inflammation in and around the lesion site of the brain and eventually worsening the condition of the patient.<sup>22</sup>

Following traumatic brain injury, the inhibition of the Akt signalling pathway occurs, resulting in inflammation and cerebral necrosis, while its therapeutic upregulation leads to neurogenesis. Several studies have shown a strong relationship

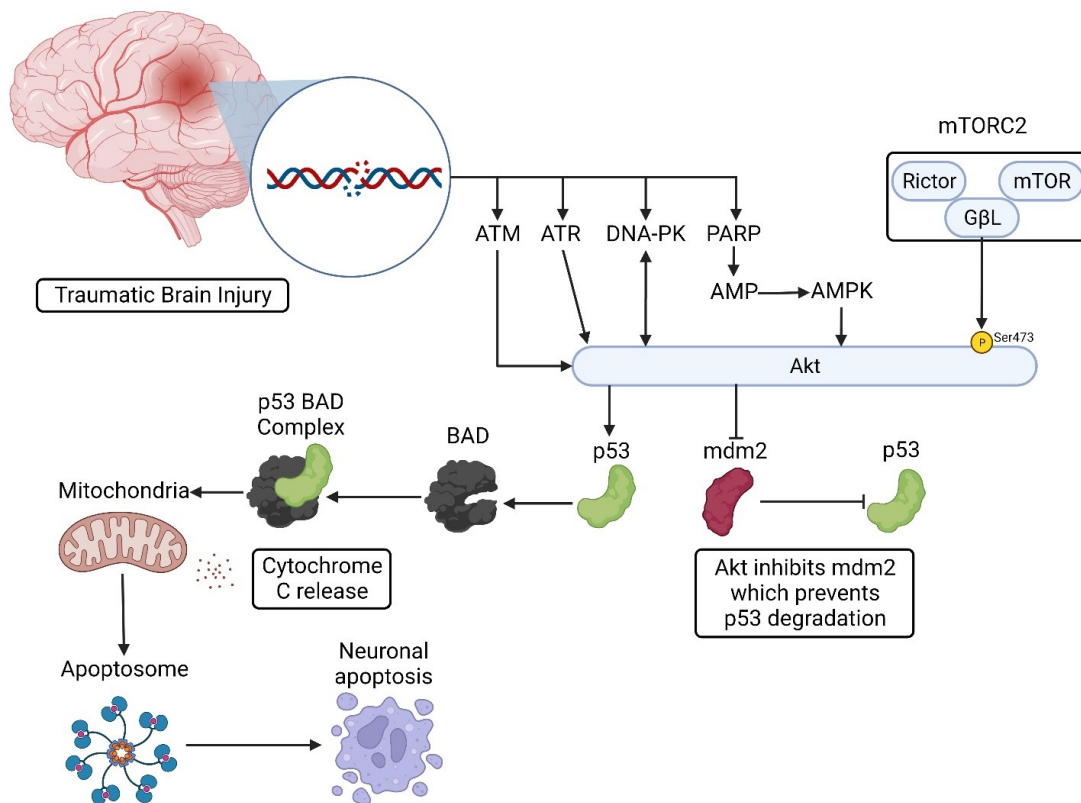


**Figure 1.** An Overview of the Akt Signalling Pathways Network. Akt signalling cascades are activated by the stimulation of gamma-aminobutyric acid (GABA) receptors, G-protein-coupled receptors (GPCR), receptor tyrosine kinases (RTKs), B-cell receptor, integrin, and cytokine receptors through neurotransmitter GABA, inflammatory cytokines, and growth factors. The set of adaptors (*Gα/β/γ*, IRS1, GAB1/2, FAK, ILK, JAK, and BCAP) links the activated receptor to other factors (SOS, PI3K, and PIP3) leading to signal transduction through small GTP-binding proteins such as Ras. The Akt is the central mediator of every pathway that transduces the signal downstream to dictate cell functioning and alteration in gene expression through the mediating of transcription factors such as FKHR and CREB. The figure was created in BioRender (BioRender.com).

between the inhibition of the Akt signalling pathway with the progression of inflammation and cerebral necrosis as well as lowering the effects of neuroprotective medications such as valproic acid that acts by inhibiting histone-deacetylases to delay apoptosis in degenerating neurons.<sup>23,24</sup> Research conducted at The State University of New Jersey and Harvard Medical School showed the role of activating Akt and mTORC1 pathways in improving memory and learning, reducing neuron apoptosis, and showed no effect on inflammation, while the inhibition of those pathways yielded no beneficial effects following TBI.<sup>18,20</sup> A 14-day-long TBI treatment using Simvastatin, a cholesterol-lowering medication, promoted the upregulation of Akt signalling, causing increased expression of growth factors and neurogenesis, leading to improved cognition.<sup>18,25</sup> In the research conducted at the Washington University School of Medicine, the use of Rapamycin, an immunosuppressant medication, inhibits the mTORC1 signalling to reduce neuron apoptosis and posttraumatic epilepsy in mice following four weeks of treatment post-TBI (i.e., the specific model of

TBI was controlled cortical impact as the mTORC1 pathway was hyperactivated following injury.<sup>18,26</sup> Furthermore, Stachydrine activated the Akt pathway and stimulated the expression of Akt/PI3k/m-TOR proteins that had anti-apoptotic and anti-inflammatory effects following TBI.<sup>23,27</sup> Another TBI treatment using a volatile anesthetic, Sevoflurane, activated the Akt signalling pathway that reduced inflammation, blocked programmed cell death, and controlled autophagy responses.<sup>28-31</sup>

Despite the crucial role of the Akt signalling pathway in preventing cell death and inflammation, it is also involved in maintaining the blood-brain barrier (BBB) to treat TBI.<sup>32</sup> The activation of the Akt signalling pathway leads to the inhibition of BBB-weakening RhoA proteins, thereby increasing the integrity of the BBB.<sup>32</sup> To conclude, the recent proliferation of TBI studies suggests that the appropriate timing of therapeutic interventions and targeting the activation of Akt/mTOR/PI3K pathways could lead to recovery from TBI and provide insights into novel drug discovery for TBI.<sup>18,19,33</sup> Furthermore, the activation of Akt interacts with several other signalling



**Figure 2.** The Akt Signalling Pathway in Traumatic Brain Injury. The Akt signalling pathway is activated by ATM, ATR, DNA-PK, PARP, and mTORC2 when DNA damage occurs due to traumatic brain injury. mTORC2 is composed of Rictor, mTOR, and GβL and it phosphorylates the Ser473 residue of Akt. These proteins activate the Akt signalling pathway till 24 hours post-injury, which inhibits mdm2. This promotes the p53 survival and binds to BAD to form a p53-BAD complex, which triggered cytochrome C release and the formation of an apoptosome leading to neuronal apoptosis. The figure was created in BioRender (BioRender.com).

pathways following TBI that further inhibited neuronal cell death, cytotoxicity, and inflammation: downregulation of ERK pathway via inhibition of Raf1 and JNK pathway via inhibition of ASK1 and binding with JIP1, while upregulation of NF-κB pathway via activation of IKKs and overexpression to promote Akt expression.<sup>34</sup> Conversely, the NF-κB pathway is known to be activated in innate neurodegenerative diseases, including Alzheimer's disease, to promote neuroinflammation and neuronal apoptosis. It should be noted that the crosstalk of NF-κB and Akt signalling pathways is highly complex and context-dependent; hence, further investigation is required.

### Downregulated Akt Signalling Pathway in Traumatic Spinal Cord Injury

Traumatic spinal cord injury (SCI) induces physical damage to the superstructure of neural circuits and vascular networks, impairing sensorimotor and autonomous functions.<sup>35</sup> Despite the advancement in neuroscience research, the inability of the spinal cord to undergo innate regeneration and no currently available treatments lead to a compromise in the patient's independence and personal, social, and economic aspects of life.<sup>35</sup> Globally, the annual incidence rate of 60 cases per 1 million and

mortality rate of 19% of SCI patients emerges the need to understand the pathogenesis and the development of novel therapeutic strategies to treat SCI.<sup>35</sup> The pathological and physiological alterations following SCI comprise the primary and secondary injury cascades that determine the severity of neuronal loss, scar formation, and subsequent behavioral dysfunction below the injury site.<sup>35</sup> The primary injury comprises mechanical injury (i.e., compressive, and shearing forces) and vasculature disruptions that cause neuronal and glial cell death, neurogenic shock, structural damage (i.e., myelin sheath, axon and axonal connections, and nerve membrane), ionic imbalance, the release of inflammatory mediators (i.e., cytokines), and synaptic alteration (i.e., neurotransmitter levels).<sup>35</sup> The primary injury is inevitable and irreversible; hence, the treatment following SCI must focus on inhibiting harmful secondary injury cascade to promote neuroplasticity.<sup>35-38</sup> The secondary injury cascade is characterized by ischemia/hemorrhage (i.e., excessive ROS and  $Ca^{+2}$  production), inflammation (i.e., astrogliosis, infiltration of lymphocytes in the lesion, activation of monocytes), and excitotoxicity (i.e., excess level of glutamate, oxidative stress due to  $Ca^{+2}$  overproduction, and apoptosis) that gradually leads to cystic cavitation, glial scar formation, and complex apoptosis-associated signal transduction systems.<sup>35</sup>

The activation of PI3K and Akt signalling pathways plays a significant role in neuron and glial cell survival and cell cycle progression by limiting the apoptotic cell signalling triggered by injury-induced growth-inhibiting extracellular matrix.<sup>35</sup> The activated PI3K kinase dimer can be transferred to the cytomembrane's interior surface for promoting PIP3 or the conversion of PIP2 to PIP3, which phosphorylates and activates the Akt kinase.<sup>35</sup> Several cascades are involved in activated Akt-mediated blocking of apoptosis: activation of the Ser87 and XIAP along with PRAS40 and inhibition of YAP.<sup>35</sup> Interestingly, the activated Akt is also known to inhibit cell survival, and cell cycle progression cascades through the inhibition of BAD, p21CIP1, p27KIP1, FKHR, and GSK-3 (Figure 3).<sup>35</sup> The inhibition of cell survival-promoting FKHR transcription factor could be explained due to its additional role in death genes that outweighs its beneficial role; however, the mystery behind inhibiting other cell proliferating cascades remains unexplored.<sup>35</sup>

The recent proliferation of cell signalling studies suggests the activation of PI3K and Akt signalling pathways is critical for protecting neural tissue from ischemia and anoxia neuron damage, boosting cell proliferation, preventing neuronal apoptosis in the spinal cord by regulating the permeability of the blood-spinal cord barrier (BSCB) and regulating autophagy through medications such as Baicalin.<sup>39–42</sup> Despite the importance of Akt in SCI, it has a remarkable contribution to autophagy regulation that was previously thought to stabilize neuronal microtubules through promoting degradation of the microtubule-destabilizing protein (i.e., superior-cervical ganglia protein 10).<sup>42</sup> The Akt-mediated autophagy modulation is known to improve gait post-SCI through axon regeneration and attenuated axon retraction.<sup>42</sup> Moreover, autophagy promotes BSCB restoration and integrity by preventing the loss of tight and adherents junction proteins following SCI; hence, future research should emphasize the relationship between autophagy and apoptosis (i.e., crosstalk of signal transduction).<sup>42</sup> The impact of altered autophagy following neurotrauma shows discrepancies throughout the literature; however, its involvement in the removal of accumulating pro-inflammatory factors helps reduce the prolonged inflammation following SCI and has consistently improved axonal regeneration and locomotor functionality.<sup>42</sup>

Exploring the transcriptomic studies, the cytoplasmic Akt, PI3K, and pAkt had an upregulated expressional pattern for the first 24 hours post-SCI, and then it gradually decreased over time, which strengthens the concept of secondary injuries in promoting spinal cord healing at the initial stage and has a detrimental effect at the prolonged stage (i.e., after 24 hours post-SCI).<sup>35</sup> In accordance with Dobkin's 'window stage' hypothesis, these findings suggest the presence of a vital phase (i.e., within 7 to 14 days) following spinal cord damage that is a critical period for the effective restoration of the defense system through ectogenic intervention treatments (i.e., drug therapy and stem cell transplantation).<sup>35</sup> During this vital phase,

those treatments will not just avoid the adverse environment of the acute secondary injury phase but also generate a favorable microenvironment for tissue repair, stem cell regeneration, and therapeutic action, therefore preventing the formation of glial scars and promoting functional recovery.<sup>35</sup>

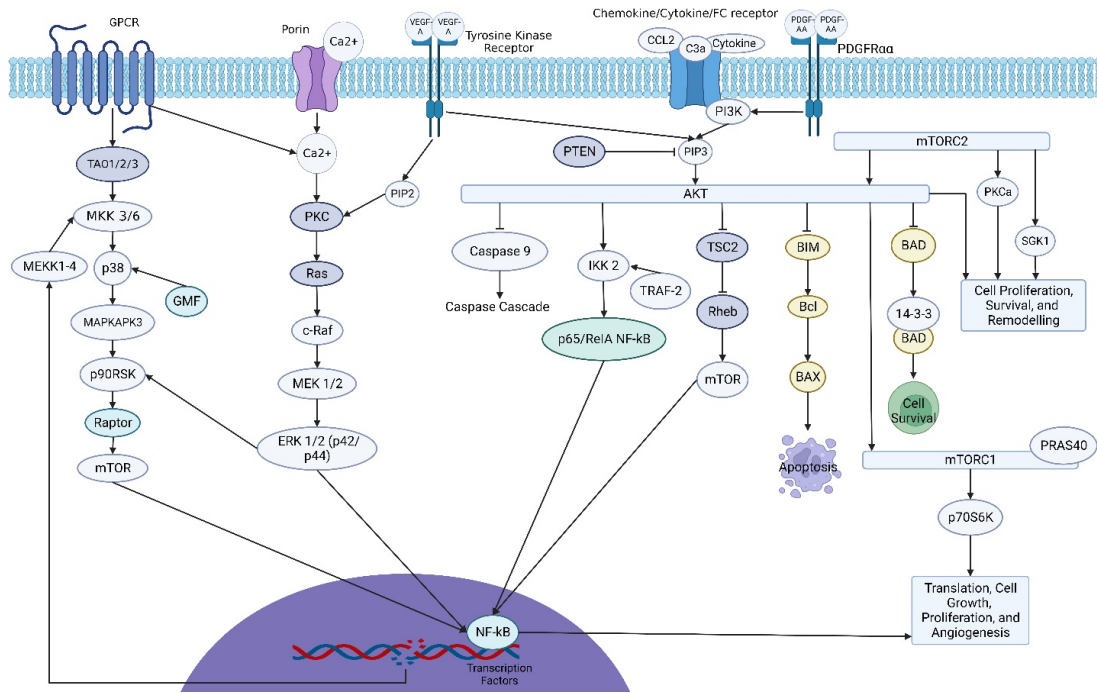
Furthermore, olfactory ensheathing cells (OECs) promote neuroplasticity/neuroregeneration following SCI, acting as a possible candidate for SCI cell transplant treatment.<sup>43</sup> Previous research has shown that activating the PI3K/Akt pathway can boost vascular endothelial cell proliferation and migration through the VEGF-A or PDGF-AA cascade.<sup>43–46</sup> The research emphasizing the association between activated OECs and the PI3K/Akt signalling pathway revealed the participation of the PI3K/Akt signalling pathway in pro-angiogenic events generated by the incorporation of conditioned medium (i.e., extracted from activated OEC) into the vascular endothelial cell, which suggest the involvement of PI3K/Akt pathway in promoting the effectiveness of various neurotherapeutics.<sup>43</sup>

## AKT SIGNALLING PATHWAY IN CARDIOVASCULAR PATHOLOGIES

### Downregulated Akt Signalling Pathway in Myocardial Infarction

Myocardial infarction (MI), one of the leading causes of death, has an annual prevalence of 3 million people worldwide and an annual mortality of more than 1 million in the United States alone.<sup>47</sup> Myocardial infarction, categorized into non-ST-segment elevation and ST-segment elevation, results in irreversible damage to the cardiac tissue due to oxygen deprivation and may lead to arrhythmias due to impaired heart function.<sup>47,48</sup> The narrowing of coronary arteries, coronary microembolization, and transient occlusion results in non-ST-segment elevation MI, while the ST-segment elevation MI is caused by complete and prolonged epicardial coronary occlusion leads to insufficient collateral circulation.<sup>48</sup> An effective strategy for dealing with these issues is restoring blood flow to hypoxic-ischemic tissue, rescuing the tissue in that area, and preventing it from further stress damage and cell-programmed death.<sup>49</sup> The most common methods for treating MI are thrombolysis, heparin with tPA, balloon angioplasty (PCI), and coronary artery bypass grafting.<sup>49</sup> While these treatments help reduce the death rate of MI, there is a high risk of subsequent hemorrhages and coronary restenosis that can further complicate the patient's condition.<sup>49</sup> Despite those clinically available treatments, the innate recovery of cardiac tissue following MI remains questionable; hence, exploring therapeutic options to promote innate cardiac repair and regeneration would be beneficial to save many people's lives.

Regarding the pathogenesis and therapeutic opportunities for myocardial infarction, the upregulation of the Akt signalling pathway is known to be advantageous for the repair and re-



**Figure 3.** The Akt Signalling Pathway in Traumatic Spinal Cord Injury. The Akt signalling pathway is activated by PIP3, which is activated by PI3K. Akt then begins to initiate survival pathways by inhibiting caspase cascades, apoptosis, and activation of transcription factors that promote survival and growth pathways. It is also involved in activating Raptor and mTOR, which also triggers transcription factors for growth and survival. Furthermore, you have Tyrosine kinase receptors which bind VEGF-A resulting in activation of PIP2 which then activates PKC leading to the PKC pathway depicted. This PKC pathway is also activated by the Chemokine/Cytokine/FC receptor. This leads to PIP3 and then Akt activation. The figure was created in BioRender (BioRender.com).

generation of cardiomyocytes.<sup>50</sup> Research conducted by Feng et al. demonstrated that the aerobic and resistance exercise-induced upregulation of IGF-1/IGF-1R-phosphatidylinositol 3-kinase (PI3K) and Akt signalling pathway resulted in protein synthesis, increased expression of myogenic regulatory factors, reduced protein degradation, and inhibited the apoptosis of myocytes following MI.<sup>51</sup> In cardiac tissue, the overexpression of PI3K kinase dimer resulted in the conversion of PIP2 to PIP3 lipid that binds to the PH domain of Akt kinase, causing a conformational change, which exposes the Ser473 and Thr308 sites of the Akt kinase.<sup>52</sup> The PDK1 and PDK2 phosphorylate the Ser473 and Thr308 sites, which allows for the Akt-based regulation of cardiac recovery following myocardial infarction.<sup>53</sup> The activation of Akt/PI3K pathways promotes the proliferation of endothelial cells in MI patients leading to angiogenesis due to the accumulation of myeloid cells, transducing pro-inflammatory signals, collagen production, and activation of the JAK/STAT pathway.<sup>54,55</sup> Moreover, activating the PI3K, Akt, and MAPK pathways promotes the production of functional vasculatures, which aid in the organization and development of complex blood vessel networks for efficient oxygen and nutrition delivery.<sup>56,57</sup>

Following MI, the therapeutic activation of the Akt signalling pathway resulted in the activation of the Notch signalling pathway that, in response, promoted the overexpression of PI3K

and Akt signalling pathway; hence, several therapeutics are designed to take advantage of the Notch signalling pathway activation through Oestrogen receptor  $\beta$ .<sup>50,58</sup> This inter-activation and crosstalk between the two pathways establish a positive feedback loop, which is essential for cardiovascular protection, regulating cardiac regeneration, promoting neurovascularization, and improving angiogenesis.<sup>59,60</sup> Moreover, when targeted by platelet-derived growth-factor-BB, the Akt phosphorylation accomplished through Notch leads to the upregulation of ERK1/2 (i.e., MAPK signalling pathway) that promotes vascular endothelial cell migration and recruitment.<sup>50,61</sup>

Several studies have studied the involvement of various kinds of RNAs in cell proliferation and recovery through their interaction with Akt and PTEN signalling pathways following MI.<sup>50</sup> Recent proliferation in studies emphasizing the importance of long non-coding RNAs revealed that the binding of small nucleolar RNA host gene 1 binds to PTEN and forms a positive feedback loop with Akt, PTEN, and c-Myc to induce cardiomyocyte proliferation.<sup>50,62</sup> Here, the Akt pathway not only aids in regeneration but also promotes cell survival in the myocardium through increasing anti-apoptotic signals and reducing inflammation.<sup>63</sup> This effect is consistent with medication such as Rosuvastatin that activates the PI3K and Akt pathways, where the medication successfully reduces the caspase-3 levels due to active Akt pathways and inhibits NF- $\kappa$ B p65.<sup>63</sup>



Around the globe, stem cells (i.e., especially Human-Induced Pluripotent Stem Cells (hiPSC)) have received great attention as one of the best regenerative therapeutics following MI or other cardiac disorders. Human-induced pluripotent stem cell-derived cardiomyocytes (hiPSC-CMs) are known to improve myocardial recovery by replacing the injured cardiomyocytes; however, they are significantly more prone to hypoxia due to the downregulation of the Akt signalling pathway following MI.<sup>64</sup> The treatment with thymosin  $\beta$ 4 (Tb4) activated the integrin-linked kinase that promoted the Akt signalling pathway, which resulted in the activation of transcription factors responsible for the overexpression of caspase inhibitors in hiPSC-CMs that protected them from hypoxia-induced cellular damage.<sup>64</sup>

Following myocardial infarction, nerve growth factor (NGF) poly (lactic-co-glycolic acid) (PLGA) nanoparticles exerted a protective effect on human umbilical cord mesenchymal stem cell (hUCMSC) and enhanced the paracrine effects of hUCMSCs on protecting cardiomyocyte and promoting angiogenesis through the regulation of the TrkA (tyrosine kinase A) and PI3K/Akt signalling pathways.<sup>65</sup> To further investigate the role of those pathways in the NGF-induced protection of hUCMSCs, the inhibition of TrkA or Akt signalling pathways using K252a or MK-2206, respectively, led to the complete failure of the anti-apoptotic effect of NGF and the subsequent angiogenesis (i.e., reversed the effects of NGF).<sup>65</sup> Research conducted at Duke University demonstrated a similar role of the Akt signalling pathway in inhibiting hypoxia-induced apoptosis and ventricular remodeling, limiting infarct size, and promoting cardiac/ventricular function (i.e., effectively contracting cardiomyocytes) following Akt-overexpressing mesenchymal stem cells (Akt-MSCs) therapy for myocardial infarction.<sup>66</sup> Lastly, the inhibition of Akt activity through nitrosylation increased the infarct size and reduced the capillary density, hence, delaying the revascularization and subsequent cardiac recovery.<sup>67</sup>

### Upregulated Akt Signalling Pathway in Myocarditis

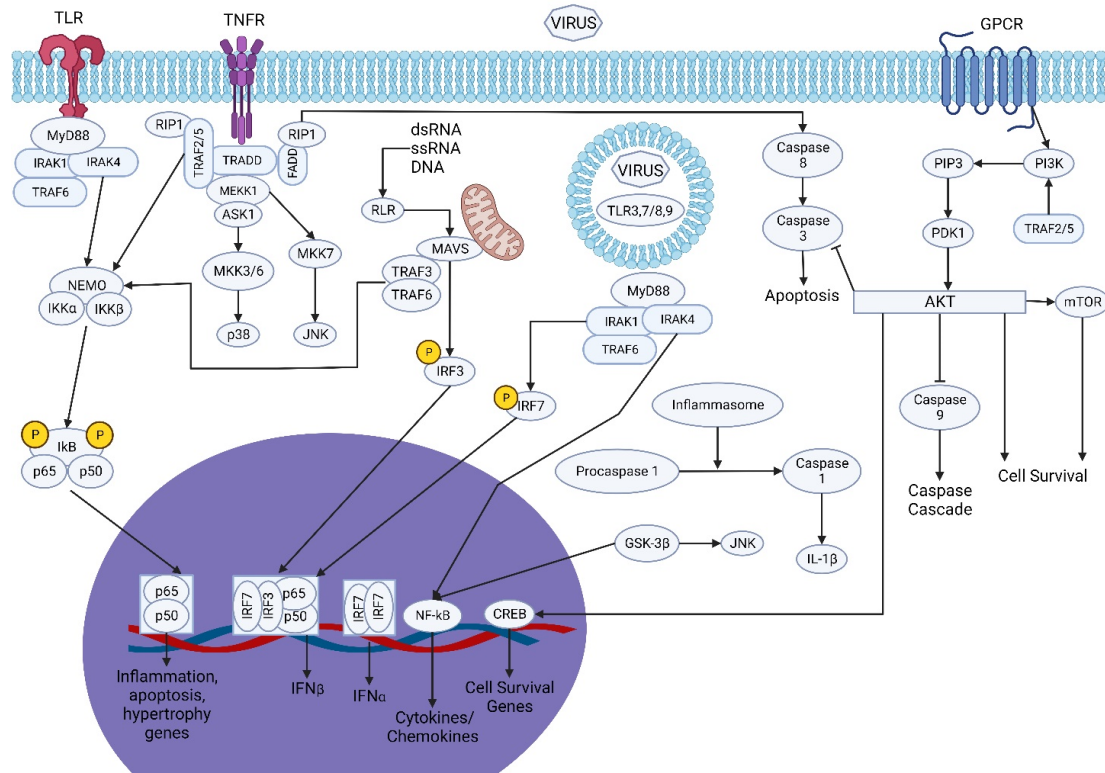
In the nineteenth century, the term "myocarditis" was first used in medical literature to characterize disorders of the heart muscle that were not connected with valve abnormalities.<sup>67</sup> The currently accepted definition of myocarditis refers to the heart muscle inflammation characterized by necrosis, inflammatory cell infiltration (i.e., monocyte and lymphocyte infiltration, pro-inflammatory chemokines, cytokines, and autoantibodies) in the myocardial interstitium, fibrosis, and edema.<sup>68</sup> Certain medical conditions are known to elevate the risk of developing myocarditis, including diabetes, AIDS, HIV, autoimmune disorders, and viral, bacterial, parasitic, and fungal infections.<sup>68</sup> Myocarditis, a silent illness with few physiological symptoms, is one of the top causes of unexplained sudden death (i.e., accounting for around 20% of cases) in the age group under 40 years, young athletes, US Air Force recruits, and elite Swedish orienteers.<sup>68</sup>

The recent proliferation of cardiology studies demonstrated that inhibiting the PI3K/Akt pathway significantly reduced the development of myocarditis (i.e., myocarditis patients had significantly increased p-Akt levels) (Figure 4), hence, protein kinase B (Akt) is an essential therapeutic target for the development, progression, and inhibition of myocarditis.<sup>68–71</sup> When testing the effect of inhibiting and activating the PI3K and Akt signalling pathway, it was found that lowering Akt phosphorylation using LY294002 (a PI3K inhibitor) promoted apoptosis in Coxsackievirus (CVB) 3 infected cells, decreased myocardial damage, and improve cardiac function in experimental autoimmune myocarditis animals.<sup>72,73</sup> Moreover, the CVB3 infection-induced autophagic response aggravated in Akt1-overexpressing cells through direct inhibition of Akt, hence, suppressing the disease progression, while Akt-/- mice increased the occurrence of experimental autoimmune encephalomyelitis.<sup>68,74,75</sup> Several transcriptomic studies (i.e., RNA-Seq and microarray) showed the activation of the Akt signalling pathway in myocarditis, causing alterations to genes related to the Akt network.<sup>76,77</sup>

Some naturally occurring compounds such as salidroside, curcumin, and *Scutellaria baicalensis* Georgi are known to inhibit PI3K/Akt/GSK-3 $\beta$ , PI3K/Akt/NF- $\kappa$ B, and Akt/p38 signalling pathways, respectively, from sepsis and CVB3-myocarditis.<sup>72,73,78–81</sup> Hence, those compounds act as natural antiviral agents that can help downregulate the mRNA levels of myocarditis-promoting signalling pathways, and their administration within 48 hours post the onset of symptomatic infection yields the best results.<sup>81</sup> Andrographolide, a labdane diterpenoid, downregulates the levels of p-PI3K and p-Akt while causing no alteration to the PI3K and Akt levels, indicating that this compound inhibits myosin-induced proliferation.<sup>82,83</sup> Also, andrographolide appears to suppress the formation of experimental autoimmune myocarditis, which may be related to its ability to inhibit the Akt signalling pathway and its anti-inflammatory effects.<sup>83</sup> SC79, an Akt phosphorylation activator, and Akt-PH domain translocation inhibitor, is known to counter the effects of this compound.<sup>83</sup> Contradictorily, the constitutive Akt activation in a healthy heart increased cardiomyocyte growth/size and resulted in concentric left ventricular hypertrophy, whereas Akt knockout mice had smaller heart sizes.<sup>84</sup> Furthermore, Akt activation elevated the expression of angioprotein-2 and VEGF in cardiomyocytes leading to increased cardiac capillary density and physiological hypertrophic remodeling.<sup>85</sup> Therefore, future research should emphasize the impact of Akt downregulation during myocarditis on cardiomyocyte regenerability, function, and cellular structure.

### UPREGULATED AKT SIGNALLING PATHWAY IN CHORDOMA

Chordoma, a slow-growing and invasive malignant tumor, arises from the remnants of the non-disintegrating notochord cells post-birth in proximity to the tailbone (i.e., sacral tumor)



**Figure 4.** The Akt Signalling Pathway in Myocarditis. An Akt signalling pathway is also involved in myocarditis by promoting cell survival pathways. It does this by inhibiting caspase cascades via the inhibition of caspase 9 which also helps with the inhibition of caspase 3. This helps the cell survive and is also assisted by the Akt activation of mTOR. Furthermore, Akt activates transcription factors that are involved in cell survival which help prevent cell death, protein degradation, increased protein synthesis, and increased myogenic regulatory factors to deal with myocarditis. Furthermore, IRAK4 (which is activated with MyD88, IRAK1, and TRAF6) leads to the activation of the NF-κB transcription factor which leads to the release of cytokines and chemokines. This NF-κB activity is also promoted by GSK-3β which also signals to JNK for its pathway. The figure was created in BioRender (BioRender.com).

and articulation of the spine and skull (i.e., clival tumor).<sup>86</sup> Patients are usually diagnosed with chordoma in their 50s and 60s (i.e., accounting for 95% of cases); hence, its detection and diagnosis mostly occur at the severe stage due to no clinically relevant presentation at previous stages.<sup>86</sup> In some cases, such as children’s chordomas, the tumor grows at a prominent rate accounting for 5% of cases with high prevalence in female children than male children.<sup>86</sup>

The focus on the association of PI3K/Akt/mTOR pathway and chordoma initially developed with the numerous chordoma patients demonstrating tuberous sclerosis syndrome, which involved the alteration of TSC1/2 genes (i.e., critical downstream effectors of PI3K/Akt/mTOR pathway).<sup>86</sup> Further genomic investigation of chordoma tissue revealed the activation of the PI3k/Akt/mTOR pathway; hence, the regulation of PI3k, Akt, and mTOR is crucial to lessen the severity and pathogenesis of chordoma.<sup>87</sup> To evaluate those therapeutic targets, several molecular, pre-clinical, and clinical studies have shown excellent outcomes in restricting chordoma growth via inhibiting cellular proliferation and promoting apoptosis.<sup>86</sup>

Throughout the literature, the molecular evidence pertaining to the expression of certain proteins, signalling pathway activ-

ity, chromosomal alteration, and mutations plays a key role in the development of chordoma. Chromosomal aberrations are unique for chordoma, including the loss of PI3KCA, mTOR, and PTEN at 3q26, 1p36.2, and 10q23 harboring gene regions, respectively.<sup>88-91</sup> The mTOR, RPS6, and S6 have shown gene copy number variation, while it is not observed TSC1/2 suggesting the involvement of other mechanisms for inactivating the TSC1/2 complex (i.e., promotes mTOR pathway).<sup>89</sup> Moreover, 20% of patients showed biallelic inactivation of the TSC1/2 complex (i.e., germline TSC1/2 mutation), abolishing its mTOR-inhibiting effect.<sup>86</sup> Nonsense germline TSC1 mutation was also detected in chordoma patients with a family history of tuberous sclerosis (TSC), which led to the termination of translation.<sup>91</sup> In addition, somatic mutations in Rheb, PI3KCA, PTEN, and mTOR are mainly absent (i.e., a mutation in 1-5% of cases); hence, it is not the primary reason for aberrant signalling regulation.<sup>89,92-94</sup> The lack of TSC1/2 mutations and high expression of Akt, p-Akt, and TSC1/2 proteins suggest the Akt-induced phosphorylation of TSC2 that causes the inactivation of TSC1/2 complex instead of genetic mutation.<sup>85,95,96</sup> Compared to fetal nucleus pulposus tissue, significant expression of p-Akt was observed, which is associated with activation of the Akt signalling pathway and decreased survival

rate.<sup>90</sup> Also, PI3K, mTOR, p-mTOR (> 50% of samples), p-p70S6K (> 50% of samples), p-RPS6K, p-PKD-1, PTEN (correlated with the degree of bone invasion), 4E-BP1, p-4E-BP1, and eIF-4E was differentially expressed in chordoma.<sup>89,95–99</sup> The p-mTOR and p-p70S6K (i.e., better than p-mTOR) have been adequate biomarkers for PI3K/Akt/mTOR pathway activation that demonstrated the upregulation of those pathways in 46–65% of chordoma.<sup>95</sup> Hypermethylation of several cancer-related gene loci in chordoma samples suggested regulating several cellular proliferative pathways, including PI3K/Akt/mTOR pathway.<sup>93,100</sup> Moreover, transcriptomic studies showed: 1) the association between expression of brachyury in tumors and activity of the PI3K/Akt signalling pathway, 2) clival and sacral chordomas had considerably differing expression levels of the PI3K/ACT signalling pathway, and 3) highly expressed YBX1 triggered the EGFR/Akt pathway in chordoma.<sup>101–103</sup>

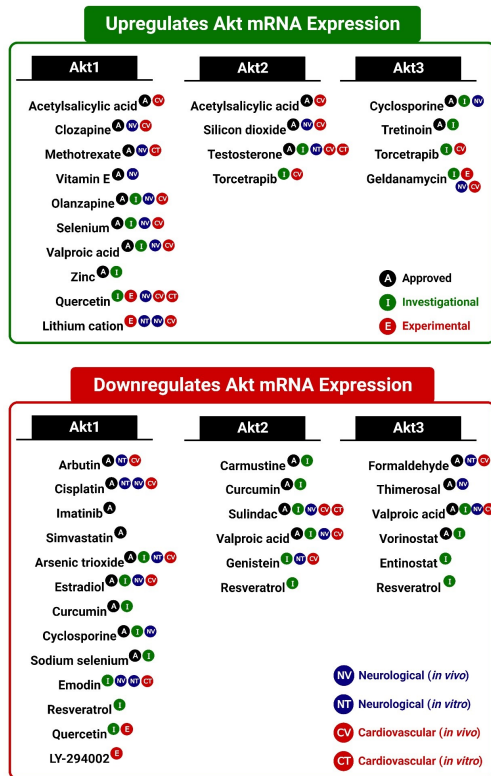
Numerous prospective therapies are supported by the abundance of pre-clinical research that shows both their *in-vitro* and *in-vivo* efficacy. Treatment with rapamycin, an mTOR complex 1 (mTORC1), has shown: 1) tumor suppressive effects (i.e., decreased tumor volume-cell number, growth, and proliferation), 2) lowered the p-Akt and p-P70S6K levels, 3) delayed the initiation of tumor formation in zebrafish, and 4) increased the survival rate of tumor-bearing fish.<sup>104</sup> Wortmannin, a PI3K inhibitor, lowered the p-Akt levels and brachyury mRNA expression in chordoma cell lines, U-CH1 and U-CH2, respectively.<sup>105</sup> PI-103, a dual PI3K/mTOR inhibitor, decreased cell proliferation and promoted apoptosis while showing tumor-suppressive effects when combined with chemotherapy drugs.<sup>94</sup> In U-CH2, Ly2094002 suppressed the brachyury mRNA expression, while it was also observed in BEZ235 treatment along with its impact on inhibiting cell growth and brachyury protein expression.<sup>105</sup>  $\beta$ - $\beta$ -dimethylacrylshikonin possesses antitumor activity by lowering the Akt, p-Akt, and p-Erk levels in chordoma cell lines.<sup>106</sup> Antagomirs, inhibiting miR-140-3p and miR-155-5p, promoted the PTEN protein expression that significantly downregulated the PI3K-Akt-mTOR signalling and tumor-cell proliferation.<sup>107</sup> MLN0128, an ATP-competitive dual mTORC1/2 inhibitor, suppressed the activity of the PI3K/Akt/mTOR signalling pathway, while LY294002, a PI3K inhibitor, showed no effect on tumor growth (i.e., mTOR, not activated by PI3K but through Ras oncogene).<sup>108,109</sup>

In terms of clinical evidence, several case reports on the use of rapamycin (slowed chordoma recurrence by six times post-surgery and treatment for ten months), imatinib, and sirolimus (89% improvement in patients and reached stable disease state), everolimus (promoted stable disease state following slight progression during four months of PDGFR inhibitor treatment), and temsirolimus showed positive results for treating chordoma patients.<sup>104,110</sup> A phase 2 clinical study evaluated the impact of imatinib and everolimus treatment for progressively advanced chordoma in 43 adult patients.<sup>111</sup> Although the data demonstrated minimal anticancer activity, certain patients with

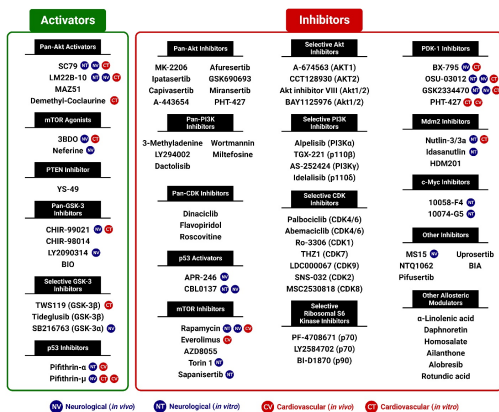
highly phosphorylated mTOR effectors had better treatment outcomes, indicating a link between mTOR pathway activation and responsiveness to imatinib plus everolimus therapy.<sup>111</sup>

## CONCLUSION

Traumatic brain injury, especially the secondary injury following primary physical trauma, results in a wide range of physiological/functional impairments due to neuronal and glial apoptosis, neuroinflammation, excitotoxicity, mitochondrial dysfunction, and axonal damage. Within 24 hours of the onset of TBI, the Akt kinase is significantly upregulated, promoting cell survival and an innate preventive mechanism against the physical trauma; however, the Akt signalling pathway is significantly downregulated after 24 hours leading to severe secondary injury pathologies. This suggests that the therapeutic upregulation of the Akt signalling pathway can be extremely beneficial if performed within 24 hours post-TBI to promote neurogenesis, prevent cell programmed death, control autophagy, and reduce neuroinflammation. Moreover, the crosstalk of the Akt signalling network suggests the role of the downregulation of ERK and JNK pathways and the upregulation of the NF- $\kappa$ B pathway in promoting recovery following TBI. A similar observation of downregulated Akt signalling pathway following 24 hours post-injury inhibits recovery in traumatic spinal cord injury. In cardiovascular injuries such as myocardial infarction, the PI3K/Akt signalling pathway is downregulated; however, the therapeutics upregulation is known to limit infarct size, promote cardiovascular protection and neurovascularization, improve angiogenesis, and increase the efficiency of stem cell therapy. Following myocarditis, the therapeutic inhibition of several Akt signalling networks promoted cardiac regeneration and reduced myocardial damage: PI3K/Akt/GSK-3 $\beta$ , PI3K/Akt/NF- $\kappa$ B, and Akt/p38. Interestingly, the activation of the Akt signalling pathway in myocarditis led to an increase in cardiomyocyte size, resulting in ventricular hypertrophy and lowered cardiac output. Moreover, the pre-clinical and clinical research suggested that the upregulation of the PI3K/Akt/mTOR pathway in chordoma aggravated the invasion and progression of cancerous tissue. In conclusion, the PI3K/Akt/mTOR pathway is downregulated in traumatic injuries (i.e., cell apoptosis) and upregulated in cancer (i.e., uncontrollable cell proliferation) and inflammatory traumas (i.e., cell size growth). Several therapeutic drugs can modulate the aberrant activity of the PI3K/Akt/mTOR pathway through upregulating or downregulating Akt mRNA expression (Figures 5 and 6) and through activating or inhibiting the PI3K/Akt/mTOR pathway, which can be used to treat several neurological and cardiovascular diseases.



**Figure 5.** Comprehensive Overview of Akt mRNA Expression-Modulating Drugs. List of approved, investigational, and experimental drugs that are categorized based on their regulatory effect (i.e., upregulate or downregulate) on Akt mRNA expression. Data for the figure was obtained from DrugBank.<sup>112</sup> The figure was created in BioRender (BioRender.com).



**Figure 6.** Comprehensive Overview of Akt Signalling Pathway Activators and Inhibitors in Cardiovascular and Neurological Research. List of drugs that act as pan-Akt activators, mTOR agonists, PTEN inhibitors, pan/selective GSK-3 inhibitors, and p53 inhibitors to activate the Akt signalling pathway. List of drugs that act as pan/selective Akt, pan/selective PI3K, pan/selective CDK, mTOR, selective ribosomal S6 kinase, PDK-1, Mdm2, c-Myc, and other inhibitors along with p53 activators and allosteric modulators that deactivate/inhibit the Akt signalling pathway. The activators/inhibitors are divided into 3 categories based on their application in literature: cardiovascular (*in vivo/in vitro*), neurological (*in vivo/in vitro*), and potential candidates. Data for the figure was obtained from IUPHAR/BPS Guide to Pharmacology<sup>113</sup> and PubMed literature search. The figure was created in BioRender (BioRender.com).

**Peer Review:** Externally peer-reviewed.

**Author Contributions:** Conception/Design of Study- A.D.M., D.M.M.; Data Acquisition- A.D.M., A.A.M.; Data Analysis/Interpretation- A.D.M., A.A.M.; Drafting Manuscript- A.D.M., A.A.M.; Critical Revision of Manuscript- A.D.M., D.M.M.; Final Approval and Accountability- A.D.M., A.A.M., D.M.M.

**Conflict of Interest:** Authors declared no conflict of interest.

**Financial Disclosure:** Authors declared no financial support.

**ORCID IDs of the authors**

Akshat D. Modi 0000-0003-1086-3670  
 Aahmad Ali Mahoon 0000-0002-6850-3910  
 Dharmeshkumar M. Modi 0000-0002-4011-0533

**REFERENCES**

- Wang Z, Cui X, Hao G, He J. Aberrant expression of PI3K/AKT signaling is involved in apoptosis resistance of hepatocellular carcinoma. *Open Life Sci.* 2021;16(1):1037-1044.
- Xie Y, Shi X, Sheng K, et al. PI3K/Akt signaling transduction pathway, erythropoiesis and glycolysis in hypoxia (Review). *Mol Med Rep.* 2019;19(2):783-791.
- Staal SP, Hartley JW. Thymic lymphoma induction by the AKT8 murine retrovirus. *J Exp Med.* 1988;167(3):1259-1264.
- Woodgett JR. Recent advances in the protein kinase B signaling pathway. *Curr Opin Cell Biol.* 2005;17(2):150-157.
- Zhang Z, Yao L, Yang J, Wang Z, Du G. PI3K/Akt and HIF 1 signaling pathway in hypoxia ischemia (Review). *Mol Med Rep.* 2018;18(4):3547-3554.
- Linnerth-Petrik NM, Santry LA, Moorehead R, Jücker M, Wootton SK, Petrik J. Akt isoform specific effects in ovarian cancer progression. *Oncotarget.* 2016;7(46):74820-74833.
- Zhang F, Ding T, Yu L, Zhong Y, Dai H, Yan M. Dexmedetomidine protects against oxygen-glucose deprivation-induced injury through the I2 imidazoline receptor-PI3K/AKT pathway in rat C6 glioma cells. *J Pharm Pharmacol.* 2012;64(1):120-127.
- Ciuffreda L, Falcone I, Incani UC, et al. PTEN expression and function in adult cancer stem cells and prospects for therapeutic targeting. *Adv Biol Regul.* 2014;56:66-80.
- Ojeda L, Gao J, Hooten KG, et al. Critical role of PI3K/Akt/GSK3β in motoneuron specification from human neural stem cells in response to FGF2 and EGF. *PLoS One.* 2011;6(8):e23414. doi: 10.1371/journal.pone.0023414.
- Wyatt LA, Filbin MT, Keirstead HS. PTEN inhibition enhances neurite outgrowth in human embryonic stem cell-derived neuronal progenitor cells. *J Comp Neurol.* 2014;522(12):2741-2755.
- Fruman DA, Meyers RE, Cantley LC. Phosphoinositide kinases. *Annu Rev Biochem.* 1998;67:481-507.
- Zhao S, Fu J, Liu F, Rastogi R, Zhang J, Zhao Y. Small interfering RNA directed against CTMP reduces acute traumatic brain injury in a mouse model by activating Akt. *Neurol Res.* 2014;36(5):483-490.
- Rana A, Singh S, Sharma R, Kumar A. Traumatic brain injury altered normal brain signaling pathways: Implications

- for novel therapeutics approaches. *Curr Neuropharmacol*. 2019;17(7):614-629.
14. Marklund N. Rodent Models of Traumatic Brain Injury: Methods and Challenges. In: Kobeissy FH, Dixon CE, Hayes RL, Mondello S, eds. *Injury Models of the Central Nervous System*. Vol 1462. Methods in Molecular Biology. Springer New York; 2016:29-46.
  15. Bryan-Hancock C, Harrison J. The global burden of traumatic brain injury: preliminary results from the Global Burden of Disease Project. *Injury Prevention*. 2010;16:A17. <http://dx.doi.org/10.1136/ip.2010.029215.61>
  16. Chen CC, Hung TH, Lee CY, et al. Berberine protects against neuronal damage via suppression of glia-mediated inflammation in traumatic brain injury. *PLoS One*. 2014;9(12):e115694. doi:10.1371/journal.pone.0115694.
  17. Lagraoui M, Sukumar G, Latoche JR, Maynard SK, Dalgard CL, Schaefer BC. Salsalate treatment following traumatic brain injury reduces inflammation and promotes a neuroprotective and neurogenic transcriptional response with concomitant functional recovery. *Brain Behav Immun*. 2017;61:96-109.
  18. Nikolaeva I. Targeting the PI3K/Akt/mTOR pathway in traumatic brain injury and developmental disease (Thesis). 2016.
  19. Noshita N, Lewén A, Sugawara T, Chan PH. Evidence of phosphorylation of Akt and neuronal survival after transient focal cerebral ischemia in mice. *J Cereb Blood Flow Metab*. 2001;21(12):1442-1450.
  20. Park J, Zhang J, Qiu J, et al. Combination therapy targeting Akt and mammalian target of rapamycin improves functional outcome after controlled cortical impact in mice. *J Cereb Blood Flow Metab*. 2012;32(2):330-340.
  21. Zhao S, Fu J, Liu X, Wang T, Zhang J, Zhao Y. Activation of Akt/GSK-3 $\beta$ /beta-catenin signaling pathway is involved in survival of neurons after traumatic brain injury in rats. *Neurological Research*. 2012;34(4):400-407.
  22. Wang G, Jiang X, Pu H, et al. Scriptaid, a novel histone deacetylase inhibitor, protects against traumatic brain injury via modulation of PTEN and AKT pathway : scriptaid protects against TBI via AKT. *Neurotherapeutics*. 2013;10(1):124-142.
  23. Yu N, Hu S, Hao Z. Beneficial effect of stachydrine on the traumatic brain injury induced neurodegeneration by attenuating the expressions of Akt/mTOR/PI3K and TLR4/NF $\kappa$ -B pathway. *Transl Neurosci*. 2018;9:175-182.
  24. Zhang C, Zhu J, Zhang J, et al. Neuroprotective and anti-apoptotic effects of valproic acid on adult rat cerebral cortex through ERK and Akt signaling pathway at acute phase of traumatic brain injury. *Brain Research*. 2014;1555:1-9.
  25. Rozas NS, Redell JB, Hill JL, et al. Genetic activation of mTORC1 signaling worsens neurocognitive outcome after traumatic brain injury. *J Neurotrauma*. 2015;32(2):149-158.
  26. Guo D, Zeng L, Brody DL, Wong M. Rapamycin attenuates the development of posttraumatic epilepsy in a mouse model of traumatic brain injury. *PLoS ONE*. 2013;8(5):e64078. doi:10.1371/journal.pone.0064078.
  27. Zhao L, Wu D, Sang M, Xu Y, Liu Z, Wu Q. Stachydrine ameliorates isoproterenol-induced cardiac hypertrophy and fibrosis by suppressing inflammation and oxidative stress through inhibiting NF- $\kappa$ B and JAK/STAT signaling pathways in rats. *Int Immunopharmacol*. 2017;48:102-109.
  28. He H, Liu W, Zhou Y, et al. Sevoflurane post-conditioning attenuates traumatic brain injury-induced neuronal apoptosis by promoting autophagy via the PI3K/AKT signaling pathway. *DDDT*. 2018;12:629-638.
  29. Gao Y, Li J, Wu L, et al. Tetrahydrocurcumin provides neuro-protection in rats after traumatic brain injury: autophagy and the PI3K/AKT pathways as a potential mechanism. *J Surg Res*. 2016;206(1):67-76.
  30. Miao J, Wang L, Zhang X, et al. Protective effect of aliskiren in experimental ischemic stroke: Up-regulated p-PI3K, p-AKT, Bcl-2 expression, attenuated Bax expression. *Neurochem Res*. 2016;41(9):2300-2310.
  31. Zhang L, Ding K, Wang H, Wu Y, Xu J. Traumatic brain injury-induced neuronal apoptosis is reduced through modulation of PI3K and autophagy pathways in mouse by FTY720. *Cell Mol Neurobiol*. 2016;36(1):131-142.
  32. Wang ZG, Cheng Y, Yu XC, et al. bFGF protects against blood-brain barrier damage through junction protein regulation via PI3K-Akt-Rac1 pathway following traumatic brain injury. *Mol Neurobiol*. 2016;53(10):7298-7311.
  33. Wang C, Hu Z, Zou Y, et al. The post-therapeutic effect of rapamycin in mild traumatic brain-injured rats ensuing in the upregulation of autophagy and mitophagy. *Cell Biol Int*. 2017;41(9):1039-1047.
  34. Sun J, Nan G. The extracellular signal-regulated kinase 1/2 pathway in neurological diseases: A potential therapeutic target (Review). *Int J Mol Med*. 2017;39(6):1338-1346.
  35. Zhang P, Zhang L, Zhu L, et al. The change tendency of PI3K/Akt pathway after spinal cord injury. *Am J Transl Res*. 2015;7(11):2223-2232.
  36. Yu WR, Fehlings MG. Fas/FasL-mediated apoptosis and inflammation are key features of acute human spinal cord injury: implications for translational, clinical application. *Acta Neuropathol*. 2011;122(6):747-761.
  37. Saxena T, Loomis KH, Pai SB, et al. Nanocarrier-mediated inhibition of macrophage migration inhibitory factor attenuates secondary injury after spinal cord injury. *ACS Nano*. 2015;9(2):1492-1505.
  38. Calvo M, Zhu N, Grist J, Ma Z, Loeb JA, Bennett DLH. Following nerve injury neuregulin-1 drives microglial proliferation and neuropathic pain via the MEK/ERK pathway. *Glia*. 2011;59(4):554-568.
  39. Renfu Q, Rongliang C, Mengxuan D, et al. Anti-apoptotic signal transduction mechanism of electroacupuncture in acute spinal cord injury. *Acupunct Med*. 2014;32(6):463-471.
  40. Zhang L, Gu S, Zhao C, Wen T. Combined treatment of neurotrophin-3 gene and neural stem cells is propitious to functional recovery after spinal cord injury. *Cell Transplant*. 2007;16(5):475-481.
  41. Peviani M, Tortarolo M, Battaglia E, Piva R, Bendotti C. Specific induction of Akt3 in spinal cord motor neurons is neuroprotective in a mouse model of familial amyotrophic lateral sclerosis. *Mol Neurobiol*. 2014;49(1):136-148.
  42. Zhao R, Wu X, Bi XY, Yang H, Zhang Q. Baicalin attenuates blood-spinal cord barrier disruption and apoptosis through PI3K/Akt signaling pathway after spinal cord injury. *Neural Regen Res*. 2022;17(5):1080-1087.
  43. Wang X, Jiang C, Zhang Y, et al. The promoting effects of activated olfactory ensheathing cells on angiogenesis after spinal cord injury through the PI3K/Akt pathway. *Cell Biosci*. 2022;12(1):23. doi:10.1186/s13578-022-00765-y.
  44. Zheng Z, Zeng Y, Zhu X, et al. ApoM-S1P modulates Ox-LDL-induced inflammation through the PI3K/Akt signaling pathway in HUVECs. *Inflammation*. 2019;42(2):606-617.
  45. Zhu GS, Tang LY, Lv DL, Jiang M. Total flavones of abel-

- moschus manihot exhibits pro-angiogenic activity by activating the VEGF-A/VEGFR2-PI3K/Akt signaling Axis. *Am J Chin Med*. 2018;46(3):567-583.
46. Zhang X, Zhao F, Zhao JF, Fu HY, Huang XJ, Lv BD. PDGF-mediated PI3K/AKT/ $\beta$ -catenin signaling regulates gap junctions in corpus cavernosum smooth muscle cells. *Exp Cell Res*. 2018;362(2):252-259.
  47. Choi AR, Jeong MH, Hong YJ, et al. Clinical characteristics and outcomes in acute myocardial infarction patients with versus without any cardiovascular risk factors. *Korean J Intern Med*. 2019;34(5):1040-1049.
  48. Goloroush P, Yellon DM, Davidson SM. Mouse models of atherosclerosis and their suitability for the study of myocardial infarction. *Basic Res Cardiol*. 2020;115(6):73. doi:10.1007/s00395-020-00829-5.
  49. Sabatine MS, Braunwald E. Thrombolysis in myocardial infarction (TIMI) study group: JACC focus seminar 2/8. *J Am Coll Cardiol*. 2021;77(22):2822-2845.
  50. Zhang Q, Wang L, Wang S, et al. Signaling pathways and targeted therapy for myocardial infarction. *Signal Transduct Target Ther*. 2022;7(1):78. doi:10.1038/s41392-022-00925-z.
  51. Feng L, Li B, Xi Y, Cai M, Tian Z. Aerobic exercise and resistance exercise alleviate skeletal muscle atrophy through IGF-1/IGF-1R-PI3K/Akt pathway in mice with myocardial infarction. *Am J Physiol Cell Physiol*. 2022;322(2):C164-C176.
  52. Hua H, Zhang H, Chen J, Wang J, Liu J, Jiang Y. Targeting Akt in cancer for precision therapy. *J Hematol Oncol*. 2021;14(1):128. doi:10.1186/s13045-021-01137-8.
  53. Eisenreich A, Rauch U. PI3K inhibitors in cardiovascular disease. *Cardiovasc Ther*. 2011;29(1):29-36.
  54. Mo XG, Chen QW, Li XS, et al. Suppression of NHE1 by small interfering RNA inhibits HIF-1 $\alpha$ -induced angiogenesis in vitro via modulation of calpain activity. *Microvasc Res*. 2011;81(2):160-168.
  55. Gao W, Chang G, Wang J, et al. Inhibition of K562 leukemia angiogenesis and growth by selective Na<sup>+</sup>/H<sup>+</sup> exchanger inhibitor cariporide through down-regulation of pro-angiogenesis factor VEGF. *Leuk Res*. 2011;35(11):1506-1511.
  56. Liang X, Ding Y, Lin F, et al. Overexpression of ERBB4 rejuvenates aged mesenchymal stem cells and enhances angiogenesis via PI3K/AKT and MAPK/ERK pathways. *FASEB J*. 2019;33(3):4559-4570.
  57. Fan J, Xu W, Nan S, Chang M, Zhang Y. MicroRNA-384-5p promotes endothelial progenitor cell proliferation and angiogenesis in cerebral ischemic stroke through the delta-like ligand 4-mediated Notch signaling pathway. *Cerebrovasc Dis*. 2020;49(1):39-54.
  58. Du M, Shan J, Feng A, Schmill S, Gu J, Xue S. Oestrogen receptor  $\beta$  activation protects against myocardial infarction via Notch1 signalling. *Cardiovasc Drugs Ther*. 2020;34(2):165-178.
  59. Huang H, Huang F, Huang JP. Transplantation of bone marrow derived endothelial progenitor cells overexpressing Delta like 4 enhances functional neovascularization in ischemic myocardium. *Mol Med Rep*. 2013;8(5):1556-1562.
  60. Zhou XL, Fang YH, Wan L, et al. Notch signaling inhibits cardiac fibroblast to myofibroblast transformation by antagonizing TGF- $\beta$ 1/Smad3 signaling. *J Cell Physiol*. 2019;234(6):8834-8845.
  61. Yao Q, Renault MA, Chapouly C, et al. Sonic hedgehog mediates a novel pathway of PDGF-BB-dependent vessel maturation. *Blood*. 2014;123(15):2429-2437.
  62. Li M, Zheng H, Han Y, et al. LncRNA Snhg1-driven self-reinforcing regulatory network promoted cardiac regeneration and repair after myocardial infarction. *Theranostics*. 2021;11(19):9397-9414.
  63. Baraka SA, Tolba MF, Elsherbini DA, El-Naga RN, Awad AS, El-Demerdash E. Rosuvastatin and low-dose carvedilol combination protects against isoprenaline-induced myocardial infarction in rats: Role of PI3K/Akt/Nrf2/HO-1 signalling. *Clin Exp Pharmacol Physiol*. 2021;48(10):1358-1370.
  64. Tan SH, Loo SJ, Gao Y, et al. Thymosin  $\beta$ 4 increases cardiac cell proliferation, cell engraftment, and the reparative potency of human induced-pluripotent stem cell-derived cardiomyocytes in a porcine model of acute myocardial infarction. *Theranostics*. 2021;11(16):7879-7895.
  65. Luo W, Gong Y, Qiu F, et al. NGF nanoparticles enhance the potency of transplanted human umbilical cord mesenchymal stem cells for myocardial repair. *Am J Physiol Heart Circ Physiol*. 2021;320(5):H1959-H1974.
  66. Gneccchi M, He H, Noiseux N, et al. Evidence supporting paracrine hypothesis for Akt-modified mesenchymal stem cell-mediated cardiac protection and functional improvement. *FASEB J*. 2006;20(6):661-669.
  67. Li X, Zhang H, An G, et al. S-Nitrosylation of Akt by organic nitrate delays revascularization and the recovery of cardiac function in mice following myocardial infarction. *J Cell Mol Med*. 2021;25(1):27-36.
  68. Li S, Wang Y, Zhao C, et al. Akt inhibitor deguelin aggravates inflammation and fibrosis in myocarditis. *Iran J Basic Med Sci*. 2019;22(11):1275-1282.
  69. Zhang Q, Hu L qun, Li H qi, Wu J, Bian N na, Yan G. Beneficial effects of andrographolide in a rat model of autoimmune myocarditis and its effects on PI3K/Akt pathway. *Korean J Physiol Pharmacol*. 2019;23(2):103.
  70. Liu HS, Zhang J, Guo JL, Lin CY, Wang ZW. Phosphoinositide 3-kinase inhibitor LY294002 ameliorates the severity of myosin-induced myocarditis in mice. *Curr Res Transl Med*. 2016;64(1):21-27.
  71. Song Y, Ge W, Cai H, Zhang H. Curcumin protects mice from coxsackievirus B3-induced myocarditis by inhibiting the phosphatidylinositol 3 kinase/Akt/nuclear factor- $\kappa$ B pathway. *J Cardiovasc Pharmacol Ther*. 2013;18(6):560-569.
  72. Chen Z, Yang L, Liu Y, et al. LY294002 and Rapamycin promote coxsackievirus-induced cytopathic effect and apoptosis via inhibition of PI3K/AKT/mTOR signaling pathway. *Mol Cell Biochem*. 2014;385(1-2):169-177.
  73. Liu HS, Zhang J, Guo JL, Lin CY, Wang ZW. Phosphoinositide 3-kinase inhibitor LY294002 ameliorates the severity of myosin-induced myocarditis in mice. *Curr Res Transl Med*. 2016;64(1):21-27.
  74. Ouyang S, Zeng Q, Tang N, et al. Akt-1 and Akt-2 differentially regulate the development of experimental autoimmune encephalomyelitis by controlling proliferation of thymus-derived regulatory T cells. *J Immunol*. 2019;202(5):1441-1452.
  75. Chang H, Li X, Cai Q, et al. The PI3K/Akt/mTOR pathway is involved in CVB3-induced autophagy of HeLa cells. *Int J Mol Med*. 2017;40(1):182-192.
  76. Henao-Martínez AF, Agler AH, Watson AM, et al. AKT network of genes and impaired myocardial contractility during murine acute Chagasic myocarditis. *Am J Trop Med Hyg*. 2015;92(3):523-529.
  77. Henao-Martínez AF, Parra-Henao G. Murine heart gene expression during acute Chagasic myocarditis. *Genom Data*. 2015;4:76-77.

78. He H, Chang X, Gao J, Zhu L, Miao M, Yan T. Salidroside mitigates sepsis-induced myocarditis in rats by regulating IGF-1/PI3K/Akt/GSK-3 $\beta$  signaling. *Inflammation*. 2015;38(6):2178-2184.
79. Li Q, Li Y, Li J, et al. FBW7 suppresses metastasis of colorectal cancer by inhibiting HIF1 $\alpha$ /CEACAM5 functional axis. *Int J Biol Sci*. 2018;14(7):726-735.
80. Hussain I, Waheed S, Ahmad KA, Pirog JE, Syed V. *Scutellaria baicalensis* targets the hypoxia-inducible factor-1 $\alpha$  and enhances cisplatin efficacy in ovarian cancer. *J Cell Biochem*. 2018;119(9):7515-7524.
81. Fu Q, Gao L, Fu X, Meng Q, Lu Z. *Scutellaria baicalensis* inhibits Cocksackievirus B3-induced myocarditis via AKT and p38 pathways. *J Microbiol Biotechnol*. 2019;29(8):1230-1239. doi:10.4014/jmb.1904.04050.
82. Chen HW, Lin AH, Chu HC, et al. Inhibition of TNF- $\alpha$ -induced inflammation by andrographolide via down-regulation of the PI3K/Akt signaling pathway. *J Nat Prod*. 2011;74(11):2408-2413.
83. Lu CY, Yang YC, Li CC, Liu KL, Lii CK, Chen HW. Andrographolide inhibits TNF $\alpha$ -induced ICAM-1 expression via suppression of NADPH oxidase activation and induction of HO-1 and GCLM expression through the PI3K/Akt/Nrf2 and PI3K/Akt/AP-1 pathways in human endothelial cells. *Biochem Pharmacol*. 2014;91(1):40-50.
84. Shioi T. The conserved phosphoinositide 3-kinase pathway determines heart size in mice. *EMBO J*. 2000;19(11):2537-2548.
85. Shiojima I. Disruption of coordinated cardiac hypertrophy and angiogenesis contributes to the transition to heart failure. *J Clin Invest*. 2005;115(8):2108-2118.
86. Ulici V, Hart J. Chordoma. *Arch Pathol Lab Med*. 2022;146(3):386-395.
87. Williams BJ, Raper DMS, Godbout E, et al. Diagnosis and treatment of chordoma. *J Natl Compr Canc Netw*. 2013;11(6):726-731.
88. Rinner B, Weinhaeusel A, Lohberger B, et al. Chordoma characterization of significant changes of the DNA methylation pattern. *PLoS One*. 2013;8(3):e56609. doi:10.1371/journal.pone.0056609.
89. Tamborini E, Virdis E, Negri T, et al. Analysis of receptor tyrosine kinases (RTKs) and downstream pathways in chordomas. *Neuro Oncol*. 2010;12(8):776-789.
90. Dewaele B, Maggiani F, Floris G, et al. Frequent activation of EGFR in advanced chordomas. *Clin Sarcoma Res*. 2011;1(1):4.
91. Shalaby A, Presneau N, Ye H, et al. The role of epidermal growth factor receptor in chordoma pathogenesis: a potential therapeutic target. *J Pathol*. 2011;223(3):336-346.
92. Choy E, MacConaill LE, Cote GM, et al. Genotyping cancer-associated genes in chordoma identifies mutations in oncogenes and areas of chromosomal loss involving CDKN2A, PTEN, and SMARCB1. *PLoS One*. 2014;9(7):e101283. doi:10.1371/journal.pone.0101283.
93. Tauziède-Espariat A, Bresson D, Polivka M, et al. Prognostic and therapeutic markers in Chordomas: A study of 287 tumors. *J Neuropathol Exp Neurol*. 2016;75(2):111-120.
94. Tarpey PS, Behjati S, Young MD, et al. The driver landscape of sporadic chordoma. *Nat Commun*. 2017;8(1):890. doi:10.1038/s41467-017-01026-0.
95. Meng T, Jin J, Jiang C, et al. Molecular targeted therapy in the treatment of Chordoma: A systematic review. *Front Oncol*. 2019;9:30. doi:10.3389/fonc.2019.00030.
96. de Castro CV, Guimaraes G, Aguiar S, et al. Tyrosine kinase receptor expression in chordomas: phosphorylated AKT correlates inversely with outcome. *Hum Pathol*. 2013;44(9):1747-1755.
97. Wu Z, Wang L, Guo Z, et al. Experimental study on differences in clivus chordoma bone invasion: an iTRAQ-based quantitative proteomic analysis. *PLoS One*. 2015;10(3):e0119523. doi:10.1371/journal.pone.0119523.
98. Chen K, Mo J, Zhou M, et al. Expression of PTEN and mTOR in sacral chordoma and association with poor prognosis. *Med Oncol*. 2014;31(4):886. doi:10.1007/s12032-014-0886-7.
99. Scheipl S, Barnard M, Cottone L, et al. EGFR inhibitors identified as a potential treatment for chordoma in a focused compound screen. *J Pathol*. 2016;239(3):320-334.
100. Alholle A, Brini AT, Bauer J, et al. Genome-wide DNA methylation profiling of recurrent and non-recurrent chordomas. *Epigenetics*. 2015;10(3):213-220.
101. Otani R, Mukasa A, Shin M, et al. Brachyury gene copy number gain and activation of the PI3K/Akt pathway: association with upregulation of oncogenic Brachyury expression in skull base chordoma. *J Neurosurg*. 2018;128(5):1428-1437.
102. Li G, Cai L, Zhou L. Microarray gene expression profiling and bioinformatics analysis reveal key differentially expressed genes in clival and sacral chordoma cell lines. *Neurol Res*. 2019;41(6):554-561.
103. Liang C, Ma Y, Yong L, et al. Y-box binding protein-1 promotes tumorigenesis and progression via the epidermal growth factor receptor/AKT pathway in spinal chordoma. *Cancer Sci*. 2019;110(1):166-179.
104. Ricci-Vitiani L, Runci D, D'Alessandris QG, et al. Chemotherapy of skull base chordoma tailored on responsiveness of patient-derived tumor cells to rapamycin. *Neoplasia*. 2013;15(7):773-782.
105. Wang K, Tian K, Wang L, et al. Brachyury: A sensitive marker, but not a prognostic factor, for skull base chordomas. *Mol Med Rep*. 2015;12(3):4298-4304.
106. Jahanafrooz Z, Stallinger A, Anders I, et al. Influence of silibinin and  $\beta$ - $\beta$ -dimethylacrylshikonin on chordoma cells. *Phytomedicine*. 2018;49:32-40.
107. Lee DH, Zhang Y, Kassam AB, et al. Combined PDGFR and HDAC inhibition overcomes PTEN disruption in Chordoma. *PLoS One*. 2015;10(8):e0134426. doi:10.1371/journal.pone.0134426.
108. Davies JM, Robinson AE, Cowdrey C, et al. Generation of a patient-derived chordoma xenograft and characterization of the phosphoproteome in a recurrent chordoma. *J Neurosurg*. 2014;120(2):331-336.
109. Burger A, Vasilyev A, Tomar R, et al. A zebrafish model of chordoma initiated by notochord-driven expression of HRASV12. *Dis Model Mech*. 2014;7(7):907-913.
110. Lebellec L, Chauffert B, Blay JY, et al. Advanced chordoma treated by first-line molecular targeted therapies: Outcomes and prognostic factors. A retrospective study of the French Sarcoma Group (GSF/GETO) and the Association des Neuro-Oncologues d'Expression Française (ANOCEF). *Eur J Cancer*. 2017;79:119-128.
111. Stacchiotti S, Morosi C, Lo Vullo S, et al. Imatinib and everolimus in patients with progressing advanced chordoma: A phase 2 clinical study. *Cancer*. 2018;124(20):4056-4063.
112. Wishart DS, Feunang YD, Guo AC, et al. DrugBank 5.0: a major update to the DrugBank database for 2018. *Nucleic Acids Res*. 2018;46(D1):D1074-D1082.

113. Harding SD, Armstrong JF, Faccenda E, et al. The IUPHAR/BPS guide to PHARMACOLOGY in 2022: curating pharmacology for COVID-19, malaria and antibacterials. *Nucleic Acids Res.* 2022;50(D1):D1282-D1294.

### **How cite this article**

Modi AD, Mahoon AA, Modi DM. The Role of Akt Signalling Pathway in Neurological and Cardiovascular Pathologies. *Eur J Biol* 2023;82(1): 95-108. DOI: 10.26650/Eur-JBiol.2023.1240220



# Impact of Toxic Heavy Metals and Their Concentration in *Zygophyllum* Species, *Mentha longifolia*, and *Thymus vulgaris* Traditional Medicinal Plants Consumed in Setif-Algeria

Meriem Djarmouni<sup>1</sup>,  Ilham Sekia<sup>1</sup>,  Djamila Ameni<sup>1</sup>,  Tassadit Ikessoulen<sup>1</sup>,   
Abderrahmane Baghiani<sup>1</sup> 

<sup>1</sup>Ferhat Abbas Setif1University, Faculty of Nature and Life Sciences, Laboratory of Applied Biochemistry, Setif, Algeria

## ABSTRACT

Heavy metals (HM) are essential for living cells to maintain their equilibrium. This survey focuses on the problem of medicinal plant contamination due to environmental pollution produced by many different industrial activities and the atmospheric deposition of some toxic compounds. This analysis is important since plants can easily absorb organic and inorganic compounds from all environmental compartments (water, soil, air), which can enter and be transferred in the trophic chain, up to humans. Medicinal plants are relevant for a study about their interactions with different contaminants, in particular those inorganic persistent as HM, because they are used in the entire world for their beneficial properties and represent a significant part of traditional medicine. This review was undertaken to give readers a comprehensive understanding of chemical contaminants, such as HM, which are significant and frequent pollutants of herbal medicines and pose considerable health concerns to the human body. The information was obtained from several sources to figure out the levels of HM in three traditional medicinal plants used in Algeria's Setif region. The gathered data demonstrated that *Zygophyllum* species, *Mentha longifolia*, and *Thymus vulgaris* accumulate higher quantities of HM when cultivated in polluted soil as opposed to unpolluted soil. The data's conclusions imply that these plants contained different hazardous concentrations of HM over the World Health Organization's allowable limits. Rational herb consumption is necessary for a healthy diet. However, the exact mechanisms through which this HM affect human health are not well understood.

**Keywords:** Heavy metal, health risk, polluted soil, *Zygophyllum* species, *Mentha longifolia*, *Thymus vulgaris*.

## INTRODUCTION

Heavy metal contamination is a general phenomenon known to pose major dangers to human health and ecosystem stability. The three main challenges are increasing urbanization, real estate transformation, and industrial development, particularly in highly populous and developing nations.<sup>1</sup> Environmental concern over the poisoning of the water and air with toxic metals has affected hundreds of millions of people worldwide. Another concern for human and animal health is the poisoning of food with heavy metals (HM). In this regard, the amount of HM in the resources (water, air, and food) is assessed.<sup>2</sup> Some of these metals can be found in a wide range of amounts. The essential elements (micro- and macro-elements) are crucial for the normal development and growth of living organisms. Additionally, medicinal plants may contain high amounts of HM, which can be poisonous and cause serious metabolic disturbances. Essential metals in the form of micro- and macro-elements (Zn, Cu,

Fe, Mn, Na, K, Ca, Cr, and Mg) are required in trace amounts for the healthy functions of enzymatic systems, vitamin synthesis, the production of hemoglobin, and the growth, development, and photosynthesis of plants.<sup>3</sup>

In actuality, air pollution or contact with contaminated soil are the two main causes of natural food contamination. The accumulation of HM in a human body and adipose tissue results in the loss of essential nutrients and deficits in the central nervous system, in addition to heart, digestive, hematological, neurological, hepatocellular, renal, reproductive, immune, and intrauterine growth retardation problems.<sup>1</sup> For many years, using plants as medicine has been a significant component of the global primary health care system. However, several areas still lack information regarding therapeutic plants and their preservation.<sup>4</sup> The safety and toxicity of natural herbs and product formulations on the market have come under scrutiny in tandem with the growing interest in the medicinal advantages of herbal remedies. Although it is generally believed that nat-

Corresponding Author: Djarmouni M E-mail: djarmouni.meriem@hotmail.com

Submitted: 18.08.2022 • Revision Requested: 02.12.2022 • Last Revision Received: 21.01.2023 • Accepted: 23.05.2023



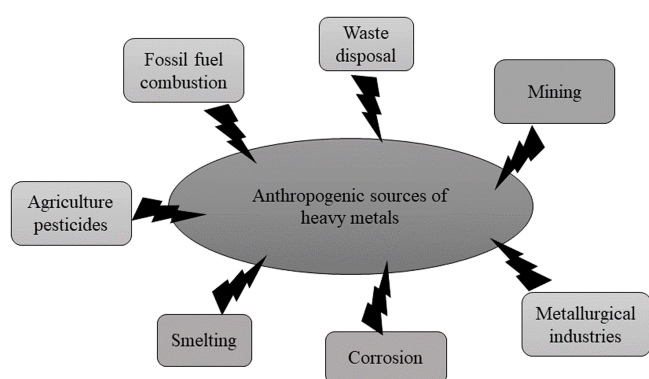
This article is licensed under a Creative Commons Attribution-NonCommercial 4.0 International License (CC BY-NC 4.0)

ural herbs and plants are intrinsically harmless, several reports have been reported on toxicity and unfavorable effects associated with the use of plants and their preparations in various parts of the world.<sup>5</sup>

Our goal was to review the literature on the origin, accessibility, toxicity associated with HM, and health effects of HM in some medicinal plants grown in Setif, Algeria, including *Zygophyllum* species, *Mentha longifolia*, and *Thymus vulgaris*. This review will increase our knowledge of their harmful effects on the body's organs and result in better management of metallic intoxications.

## HEAVY METAL CONTAMINATION

HM, such as Cr, Hg, Pb, Cu, and Cd are significant environmental pollutants. Heavy metal contamination of the air, water, and soil may have serious negative effects on all living organisms. HM added to soil have adverse effects on food production, population growth rates, and environmental health. Human health can be seriously endangered by the bioaccumulation of HM in food. These substances enter the body through food and breathing. The mobility and bioavailability of the soil influence this pollution.<sup>6</sup> Certain metals (Mn, Cr, Cu and Zn) are present in green plants as necessary metals often in low amounts, and the organisms that consume these plants are unaffected. However, the high levels of HM in plants can rise as a result of environmental contamination.<sup>7</sup> Human and anthropogenic factors are the primary causes of the rising environmental toxicity of HM. The naturally occurring sources of HM include forest fires, volcanic eruptions, wind-blown soil debris, biogeochemical processes, and marine salt. The use of herbicides, pesticides, agricultural practices, sewage evaporation, and industrial processes are among the human-caused factors contributing to the contamination of the HM<sup>8</sup> (Figure 1).



**Figure 1.** Anthropogenic activity leads to soil contamination by heavy metals.

Numerous factors, including the pH of the soil, the amounts of metals there, the oxidoreduction capacity of the soil, as well as other chemical and physical parameters, all have an impact on

the bioavailability of metals. Additionally, contamination could happen at the time of sale or during storage. Herbs can generally become contaminated during cultivation, harvest, and processing. The sources of contamination by HM in herbs may include irrigation water, industrial, emissions, contaminated soil, pesticide and fertilizers, transportation traffic, and harvesting and storage procedures. The average daily dietary consumption affects the health risk posed by metal exposure.<sup>5</sup> HM could be found on the water's surface as a result of either natural or anthropogenic causes. HM ions are found in the form of silicates, phosphates, sulfates, oxides, sulfurs and hydroxydes.<sup>9,10</sup> Other natural source mechanisms that generate heavy metal pollution of water include water interaction with rocks, water interaction with soil, and the deposition of dry and moist air sand. Examples of these compounds are cuprite, calcite, kaolinite, chromite, siderite, and arsenic trioxide. Industry and urbanization are two anthropogenic sources of water contamination, and their fast rise is another.<sup>11-14</sup> These HM in the river can have a severe impact on the aquatic system's biological balance, and as the contamination increases, the variety of aquatic organisms becomes limited.<sup>15</sup> The presence of certain HM causes diseases such as Minamata, an organic Hg poisoning. When HM bioaccumulate, they pose a threat to the human and animal population who drink this water.<sup>16</sup> This necessitates the determination of pollution levels, which allows for the development of strategies to solve the problem<sup>17,18</sup> (Table 1).

**Table 1.** Permissible limits of heavy metals in water.<sup>19</sup>

Heavy Metals	World Health Organization's (WHO) Permissible Limit (ppm)
Mn	5.00
Zn	5.00
Cr	0.1
Cd	0.001-0.005
Fe	5.00
As	10.00
Pb	0.1
Cu	3.00

Pb, Ni and Cd have a variety of toxic effects on plants at the physiological, morphological, and biochemical levels when they enter cells in high concentrations. The effects of Pb, Ni, and Cd on plants may be caused by direct (metal toxicity from tissue accumulation) and/or indirect factors including the alteration of the photosynthetic process, the disruption of nitrogen/mineral nutrition, and the development of oxidative stress via excessive reactive oxygen species (ROS) generation.<sup>20</sup> ROS, such as superoxide anion ( $O_2^\bullet$ ), hydroxyl radical ( $^\bullet OH$ ), hydrogen peroxide ( $H_2O_2$ ), and singlet oxygen ( $O_2$ ) are produced in excess by

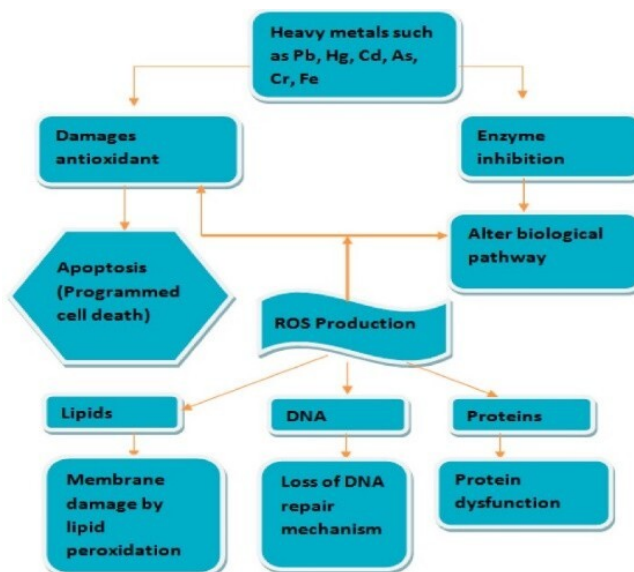
several HM, including Pb. According to recent research, Pb may interact with oxy-Hb to produce ROS, which can induce peroxidation of erythrocyte membranes. The pro-oxidant/antioxidant equilibrium is upset by the toxic metals, which induce oxidative damage. ROS are produced as a result of lead exposure, which causes oxidative stress, reduces the cellular defense mechanism by depleting glutathione (GSH), inhibits sulfhydryl-dependent enzymes, or increases cellular sensitivity to oxidative damage by altering membrane integrity.<sup>4</sup>

## HEAVY METAL-MEDIATED CHANGES IN PLANTS

Plants defend themselves against free radical damage by avoiding the oxidation of some lipid, protein, and nucleic acid components. The strategies used by plants to defend themselves from the effects of HM include the buildup of secondary metabolic products such as phenolic compounds, flavonoids, glutathione, proline, and antioxidant enzymes. These strategies depend on the plant's species used as well as the potential concentration of metal contamination<sup>21</sup> (Figure 2). It's also important to note that plants have a common ROS-scavenging mechanism, called superoxide dismutase (SOD), which converts oxygen to hydrogen peroxide. The H<sub>2</sub>O<sub>2</sub> is then detoxified to water molecules H<sub>2</sub>O by the enzymes catalase (CAT), peroxidase (POX), or glutathione peroxidase (GPX), which prevent the production of OH• radicals.<sup>22</sup> The main intracellular antioxidant molecule inside the cell is glutathione. It has been found practically in every cell compartment, including the cytosol, chloroplasts, endoplasmic reticulum, vacuole, and mitochondria. GSH is one of the main non-protein thiol sources in most plant cells, where it plays a crucial role in numerous cellular detoxification processes and protects cells from oxidative stress induced by HM.<sup>22</sup>

## POTENTIAL IMPLICATIONS OF HEAVY METALS ON HUMAN HEALTH

In recent years, the impact of heavy metal toxicity on human health has received a lot of attention. The primary pathway for HM from contaminated soil to humans is through plants. HM possess low rates of rein excretion, which means that even at very low amounts, they may have harmful effects on human health. Metals like Mn, Cu, Zn, Cr, and Fe are necessary nutrients because they are crucial for physiological processes. However, if it's consumed more than permissible limits it may become toxic.<sup>24,25</sup> The increased dietary HM intake was generally linked to several health problems, including decreased immune system defenses, fetal deformity, gastrointestinal cancer, heart disease, altered neurological and psychosocial behavior, and many others.<sup>26,27</sup>



**Figure 2.** Attack of heavy metals on a cell resulting in the production of reactive oxygen species (ROS) (from Anyanwu et al.<sup>23</sup> according to the provisions MDPI).

## Various Heavy Metals and Their Toxicity

The literature was examined for information on the toxic effects of HM. Table 2 outlines the toxic effects of five HM (As, Cr, Hg, Cd, and Pb) on body organs as well as the underlying mechanisms that cause these effects.<sup>28–46</sup>

Excessive exposure to Pb can cause hypertension, appetite loss, stomach pain, headaches, renal dysfunction, arthritic symptoms, lethargy, vertigo, insomnia and hallucinations. Also, Pb can cause urological, respiratory, gastrointestinal, neurological symptoms, muscular, cerebral, as well as reproductive impairments and cardiovascular problems due to immunological modulation, oxidative and inflammation processes.<sup>2,5,8</sup> Pb is classified as a possible carcinogen. It is a protoplasmic toxin with a preference for grey matter in the brain. It infiltrates neurons, destroys cells, nerve synapses, dendrites, and decreases the quantity of oxygen-carrying red blood cells. It binds to phosphorous and enters the bloodstream, where it is transported to the liver, spleen, and kidneys.<sup>47</sup>

Zn is an essential oligo-element required for blood clotting, growth, thyroid function, and DNA and protein synthesis. There is little evidence on the toxicity of Zn; nevertheless, an excess of Zn level has deleterious effects on the immune system, Cu levels, and blood lipoprotein levels. The legal limit for iron in medicinal herbs has not yet been determined. Iron is important in the human body for various reasons, including energy production, oxygen supply, and the immune system.<sup>5</sup> The high level of iron is stored in the pancreas, heart, liver, hypophysis, skeletal muscles, and suprarenal glands. When the organ body receives too much Fe, it escapes from its storage sites and enters the bloodstream, where it is carried to the brain. High levels

**Table 2.** Comparison of the organ effects, permissible limits, and mechanisms of some heavy metal toxicity.

Toxic Metals	Organ Toxicity	Permissible limits (mg/l)	Disrupted Macromolecule/Mechanism of Action	Reference
<b>As</b>	-Cardiovascular dysfunction	0.02	-Alterations in neurotransmitter homeostasis	28-31
	- Central nervous system (CNS) injury		-Uncoupled of oxidative phosphorylation	
	-Skin and hair changes		(Inhibition of ATP formation)	
	-Liver damage		-Damaged capillary endothelium	
<b>Cr</b>	-Gastrointestinal (GI) discomfort	0.05	-Thiol binding (GSH conjugation)	32,33
	-Kidney dysfunction		-DNA damage	
	-GI disorders		-Genomic instability	
	-Dermal diseases		-Oxidative stress and ROS generation	
	-Increased occurrence of cancers, including bladder, kidneys, lungs, larynx, testicular, bone, and thyroid			
<b>Hg</b>	-CNS injuries	0.01	-Aquaporin mRNA reduction	31,34-37
	-Renal dysfunction		-Glutathione peroxidase inhibition	
	-Hepatotoxicity		-Increased c-fos expression	
			-ROS production	
			-Enzyme inhibition	
<b>Cd</b>		0.06	-Thiol binding (GSH conjugation)	31,38-42
	-Degenerative bone disease		-miRNA expression dysregulation	
	-Kidney dysfunction		-Apoptosis	
	-Liver damage		-Endoplasmic reticulum stress	
	-Lung injuries		-Cd-MT absorption by the kidneys	
	-GI disorders		-Dysregulation of Ca, Zn, and Fe homeostasis	
	-Metabolic syndromes associated with Zn and Cu		-Low serum PTH levels	
-Cancer	-ROS generation			
<b>Pb</b>		0.1	-Altered phosphorylation cascades	31,43-46
	-CNS injury		-Enhanced levels of inflammatory cytokines: IL-1 $\beta$ , TNF- $\alpha$ , and IL-6 in the CNS	
	-Hematological changes (anemia)		-Increased serum ET-1, NO, and EPO levels	
	-Pulmonary dysfunction		-Inactivation of $\delta$ -ALAD and ferrochelatase (inhibition of heme biosynthesis)	
	-GI colic		-Reduced GSH, SOD, CAT, and GPx levels	
	-Liver damage			
	-Reduced pulmonary function			
-Cardiovascular dysfunction				

of iron in the brain destroys neurons, resulting in neurodegenerative diseases and neurological dysfunction with symptoms similar to Alzheimer's disease.<sup>47</sup>

Cd at high doses has a negative toxicological effect on the human body. The kidney is the most vulnerable organ in the exposed population. Cd excretion is slow and it accumulates in the kidney for a long time, resulting in irreversible renal damage. Cd has substantial effects on the liver, vascular and immunological systems, respiratory system, as well as renal and cardiovascular issues.<sup>5,48</sup>

As is a toxic heavy metal that is one of the most serious threats

to human health. It is well-known as the king of poisons and the poison of kings.<sup>49</sup> As poisoning, both acute and chronic, is linked to the malfunctioning of various essential enzymes.<sup>2</sup>

The Hg toxicity causes acrodynia or pink disease. Cumulative Hg exposure may alter the structure of the brain, resulting in shyness, cognitive loss, tremors, irritability, and vision or hearing impairment.<sup>2</sup> Exposure to higher concentrations of metallic Hg vapours over a shorter period may cause pulmonary edema, diarrhea, nausea, vomiting, skin eruptions, and an increase in arterial pressure. The symptoms of organic Hg toxicity include fatigue, memory problems, depression, hair loss, headaches,

and tremors. Because these signs are frequently combined with other disorders, the circumstances can be difficult to identify.<sup>8</sup>

### Heavy Metal-Mediated ROS Generation

The production of free radicals, primarily ROS and reactive nitrogen species (RNS), by toxic metals has the potential to cause oxidative stress. For example, Cd may indirectly produce radicals such as hydroxyls (OH $\cdot$ ), O $_2^{\cdot-}$ , and NO $\cdot$ , which could weaken the antioxidant defense of cells.<sup>50</sup> Pb significantly decreased antioxidative parameters such as SOD, CAT, GST, GPx and GSH while increasing oxidative parameters such as H $_2$ O $_2$  and MDA.<sup>51</sup> It has been shown that As produces oxygen (O $_2$ ), H $_2$ O $_2$ , O $_2^{\cdot-}$ , nitric oxide (NO $\cdot$ ) and peroxy radicals (ROO $\cdot$ ). The production of ROS and RNS induced by Cr decreases the antioxidant cellular capacity causing oxidative stress which increases the toxicity of proteins, lipids and DNA.<sup>52,53</sup> High Hg affinity for -SH groups can inhibit several intracellular receptor signaling as well as reduce glutathione peroxidase capacity. Moreover, Me-Hg increases the activation of phospholipase D (PLD), which is involved in many human diseases such as cancer.<sup>54,55</sup> The toxicity of Hg and Pb induced directly the ROS production or indirectly via reducing the antioxidant cellular system. However, it is believed that the Cd indirectly generates ROS. This may be caused by the substitution of Cd by Fe and Cu in cellular proteins. The result of this excessive accumulation of Fe and Cu is oxidative stress<sup>56,57</sup> (Figure 3).

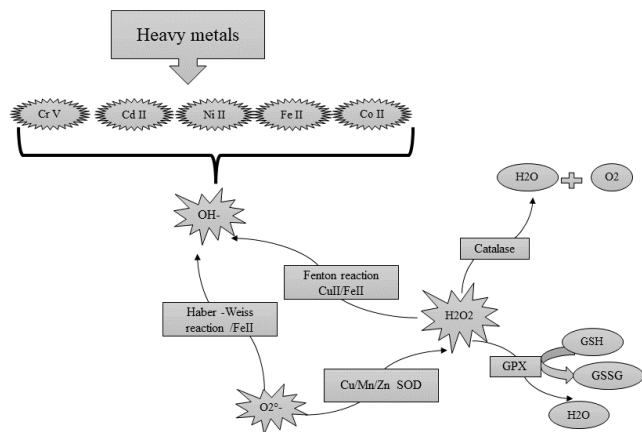


Figure 3. Generation of ROS by heavy metals.

### IMPORTANCE OF MEDICINAL PLANTS AND THEIR HEAVY METAL CONTENT

Plant and herbal treatments have begun to receive more attention even in developed nations. For thousands of years, phytotherapy has been used and trusted over the world due to its ease of availability and limited side effects. The therapeutic properties of these plants are usually related to the presence

of phytochemical content, with the most important of these phytochemicals being alkaloids, tannins, flavonoids, and phenolic compounds. However, the transportation and storage of medicinal plants may cause the loss of active components, and the production of inactive metabolites and toxic metabolites plays a key role in plant contamination.<sup>31</sup> In the present study, we focused on three different species of plants found in Setif, Algeria, which are *Zygophyllum* species, *Thymus vulgaris*, and *Mentha longifolia* about their chemical composition, medicinal properties as well as HM content.

### Zygophyllaceae Family

The Zygophyllaceae is a family of about 25 genera and 240 species adapted to Mediterranean and semi-desert climates.<sup>58</sup> The *Zygophyllum* species are a class of succulent plants that can be resistant to salt and/or dryness tolerant and live in dry and severe climates. Moreover, several authors have listed it as one of the crucial species of desert vegetation.<sup>59</sup> It is believed that *Zygophyllum* species' growth and distribution are influenced by the chemical composition of the soil in their habitats.<sup>59</sup> There are 100 species in the genus *Zygophyllum*, which are found in steppe and desert habitats from the Mediterranean, South Africa, Central Asia, and Australia.<sup>60</sup> It is a perennial herb with fleshy flowers and leaves. The majority of *Zygophyllum* species include *Z. album*, *Z. simplex*, *Z. fabago*, *Z. coccenium*, and *Z. dumosum*.<sup>61–98</sup> (Table 3). The species of *Zygophyllum* has indicated several biological properties including antidiabetic, antioxidant, antimicrobial, antitumor and anti-inflammatory activities.<sup>62–67</sup> These activities are attributed to their phytochemical compounds including phenolic, flavonoids, essential oils, triterpenes, sterols esters and saponins.<sup>68–73</sup>

The therapeutic uses of *Zygophyllum* species are reported together with that of *Mentha longifolia* and *Thymus vulgaris* in Table 3.<sup>62,64,66,67,74–100</sup>

### *Thymus vulgaris* L. (Thym)

*T. vulgaris* L. (Thym), belonging to the Lamiaceae family, is a living herbaceous plant. The plant is indigenous to southern Italy and the western Mediterranean region. There are 350 different species of thyme grown around the world.<sup>101</sup> Thym has different volatile oils as the primary chemical components. The most significant components of volatile oils in Thym species are thymol and carvacrol, however, this genus also contains several chemotypes. Some other chemical components of the Thymus species are caffeic acid, flavonoids (e.g. thymonin, cirsilineol, and 8-methoxycirsilineol), "Labiatae tannin" (rosmarinic acid), triterpenoids, aliphatic aldehydes, and long-chain saturated hydrocarbons.<sup>102</sup> The chemical nature of medicinal plants has a significant impact on their biological activity. Thymol has numerous biological proper-

**Table 3.** Reported the therapeutic uses of *Zygophyllum* species, *Menta longifolia* and *Thymus vulgaris*.

Medicinal Plants	Therapeutic Uses
<b><i>Zygophyllum</i> species</b>	
<i>Z. dumosum</i>	Antimicrobial and antifungal <sup>74</sup>
<i>Z. cornutum</i>	Antioxidant <sup>75</sup> ; Antidiabetic <sup>76</sup>
<i>Z. fabago</i>	Antioxidant and cytotoxic activity <sup>77</sup> ; Antimicrobial and antifungal <sup>78</sup> ; Urease inhibitor <sup>79</sup>
<i>Z. album</i>	Anticancer <sup>80</sup> Anti-acetylcholinesterase <sup>81</sup> Antihyperlipidemic <sup>82</sup> Weight lowering <sup>83</sup> Antihyperglycemic, and the protective hematological proprieties <sup>84</sup> Antidiabetic <sup>64,82, 85</sup> Antioxidant <sup>80,81,85</sup> Anti-inflammatory <sup>80,84</sup>
<i>Z. coccienium</i>	Antioxidant <sup>86</sup> Anti-hypertensive <sup>87</sup> Antimicrobial and antifungal <sup>88</sup> Cytotoxic activity <sup>89</sup>
<i>Z. gaetulum</i>	Antidiabetic <sup>90,91</sup> Antiinflammatory <sup>92</sup> Hepatoprotective and antioxidant <sup>90</sup>
<i>Z. geslini</i>	Antidiabetic <sup>62,93</sup>
<i>Z. hamiense</i>	Hepatoprotective and antioxidant <sup>94</sup>
<i>Z. macropodum</i>	Analgesic and anti-inflammatory <sup>95</sup>
<i>Z. qatarense</i>	Antimicrobial and antifungal <sup>96</sup>
<i>Z. simplex</i>	Antioxidant <sup>66,97</sup> Anti-inflammatory <sup>97,98</sup> Analgesic <sup>98</sup> Antimicrobial <sup>67</sup>
<b>Thyme (<i>Thymus vulgaris</i>)</b>	Antispasmodic and antioxidant, Anthelmintic, as a substitute for cancer prevention <sup>99</sup>
<b>Mint (<i>Mentha longifolia</i>)</b>	Antimicrobial, Antispasmodic, Anticancer properties, used as antioxidants in food preservatives <sup>100</sup>

ties, including antioxidant<sup>103</sup>, antifungal<sup>104</sup>, antibacterial<sup>105</sup>, immunomodulating<sup>106</sup>, and anti-inflammatory.<sup>107</sup> Carvacrol

also has antioxidant antifungal, antimicrobial<sup>108–110</sup>, anticarcinogenic and antimutagenic activities.<sup>111</sup>

### *Mentha longifolia* L. (Mint)

Wild Mint (*M. longifolia* L.), also known as *M. sylvestris* L., is a herbaceous plant that belongs to the Lamiaceae family. There are about 20 species of the genus *Mentha*, with numerous variants and subspecies, including a wide range of culinary and medicinal herbs. The species *M. longifolia* is widespread in southern Africa, Eurasia, Egypt, the Atlas Mountains and the Arabian Peninsula.<sup>112</sup> The essential oil and extract of wild mint have a variety of pharmacological properties, including antispasmodic, antimicrobial, and anticancer activities. It can be used as an antioxidant in food preservation products.<sup>100</sup> Moreover, the volatile oil components of mentha have been linked to its biological activity, while phenolic compounds can also have a significant effect. The flavonoid containing is eriocitrin, hesperidin, luteolin-7-O-rutinoside and narirutin. The phenolic acid contained is caffeic acid, rosmarinic acid, and protocatechuic acid.<sup>113</sup>

### Content of Heavy Metals in *Zygophyllum* Species

The number of metals found in plant species varies from type to type and from one region to another. Moreover, it is increasingly concentrated in contaminated areas than in non-contaminated ones. Where their concentration varies in seeds, leaves, roots, and flower parts. The concentrations of heavy metal Fe, Zn, Cu, and Al in the *Z. album* from the polluted area were  $3.82 \mu\text{g g}^{-1}$ ,  $0.615 \mu\text{g g}^{-1}$ ,  $0.035 \mu\text{g.g}^{-1}$  and  $99.3 \mu\text{g g}^{-1}$  compared to  $2.35 \mu\text{g g}^{-1}$ ,  $0.405 \mu\text{g g}^{-1}$ , 0 and  $56 \mu\text{g g}^{-1}$  from the unpolluted area of Southern Sinai, Egypt. While the results of *Z. coccineum* were close to the concentrations of *Z. album*.<sup>114</sup> The highest concentration of Pb,  $10.98 \mu\text{g/g}$ , was found in the root of *Z. album* in the Adrar region, while Cd has the highest concentration,  $2.145 \mu\text{g/g}$ , in the root of *Zygophyllum* sp. in Oued Souf.<sup>115</sup> The higher level of Cd in the root of *Zygophyllum* sp. might be explained by pollution of the soil in the area where the harvest was performed.

*Z. album* can accumulate and extract 13 HM, including Al, Cu, Fe, Mn, Mo, Zn, Cr, Pb, Co, Ni, Ag, Cd, and Ba from soil that has been contaminated by wastewater used in Jeddah City, Saudi Arabia.<sup>116</sup> Al was the most abundant metal found in the *Z. album* at a location near the sewage water discharge zone, where it had a concentration of 3166 mg/L, compared to 85.2 mg/L in an unpolluted area. Therefore, the species *Z. album* is a hyper-accumulator of the HM.<sup>116</sup> *Z. album* accumulated HM in its leaves at concentrations higher than those found in the stem and root, including Cu, Zn, Al, Ba, Cd, B, Ag, Ni, Mn, Fe, and Cr.

According to Khairia<sup>117</sup>, seven plant species *Cassia italika*, *Cyprus laevigatus*, *Calotropus procera*, *Citrullus colocynthis*, *Argemone maxicana*, *Phragmite australis*, and *Rhazya stricta* accumulate HM such as Cr, Cd, Ni, Cu, Pb, Co, Fe, Zn in the

Reiyad area in Saudi Arabia and the strongest accumulation was found in the roots, followed by the stem, then the leaves, with the exception of Cd, which is about equally accumulated in the stem, root, and leaves.

Al-Sodany et al.<sup>118</sup> found that the *Phragmite australis* species in Egypt had the strongest accumulations of HM in the root when compared to the shoot. Mazhoudi et al.<sup>119</sup> determined that aerial parts of plant accumulated metals at a lower rate than roots and proposed that the root might play a significant role in the retention of metals by preventing a toxic build-up in the shoot.

Metal accumulators should adopt three criteria related to their ability to store metals. These criteria are improved metal absorption by the root, effectiveness in moving metal from the root to the shoot, and plant tolerance to a high level of this toxic HM.<sup>97</sup> Sathiyamoorthy et al.<sup>120</sup> measured HM from 42 medicinal plants found in the Néguev Desert. The Fe concentration is the highest, with  $3020 \mu\text{g/g}$  in *Gundelia tournefortii* and  $2485 \mu\text{g/g}$  in *Anchusa strigosa*. The levels of iron obtained in *Z. geslini* are comparatively very low, with a maximum of  $2.4 \text{ g/g}$  at the leaf and  $2.16 \text{ g/g}$  at the fruit.<sup>115</sup> Zinc concentrations are significantly higher in *Z. geslini* leaves, reaching  $119.10 \mu\text{g/g}$ .<sup>115</sup> This value is rather close to that reported by Lefevre et al.<sup>121</sup> for a nearby species, *Z. fabago*, which has a range of  $150 \mu\text{g/g}$ . The maximum concentration of Mn,  $24.89 \mu\text{g/g}$ , and Nickel, was  $19.78 \mu\text{g/g}$ . is found in *Z. geslini* leaves and *Z. album* root part respectively<sup>115</sup>, however Mg is concentrated in the stems in *Z. album*.<sup>118</sup> The Cr concentration obtained is  $4.06 \mu\text{g/g}$  in the stem and  $3.94 \mu\text{g/g}$  in the root of *Z. geslini*. However, the concentration of As, determined in *Z. geslini*, is higher in the root and leaf,  $0.07 \mu\text{g/g}$ , than in the root and fruit.<sup>115</sup> *Z. album* accumulates Al, Cu, Mn and Zn. Zn is higher in the roots while Al, Cu and Mn are more concentrated in the stems.<sup>122</sup> Table 4 shows the content of heavy metals in *Zygophyllum* species.<sup>115,116,123,124</sup>

### Content of Heavy Metals in *T. vulgaris*

The heavy metal concentrations Cr and Cd in *T. vulgaris* and *T. serpyllum* in the Ash-shoubak region are not detected.<sup>125</sup> The undetected levels of Cr and Cd in thymus herbs might result from low Cd soil content in Jordan's suburban regions or the cultivation of these plants away from industrial operations like the glass and steel industries, which have been demonstrated to be a source of chromium pollution.<sup>126,127</sup> However, a high concentration of Cd has been found along roads in urban areas of Jordan and its level has increased as traffic density has increased.<sup>126,128</sup>

Pb levels in *T. serpyllum* and *T. vulgaris* were 1.26 and 32.03, respectively.<sup>125</sup> The amount of Pb in *T. vulgaris* was higher than that found in the wild *T. serpyllum* growing in the Ash-shoubak region. However, it was less than that found in the northern

**Table 4.** Content of heavy metals (mg/g) in *Zygophyllum* species.

Locality	Plant	Area	Part uses	The concentration of metals (mg/g) D.W								Reference
				Cd	Cu	Ni	Pb	Zn	Co	Mn	Fe	
South Sinai, Egypt	<i>Z. album</i>	unpolluted	Shoot	Nd	Nd	Nd	Nd	0.410 ± 0.021	Nd	Nd	2.35 ± 0.21	114
South Sinai, Egypt	<i>Z. album</i>	polluted	Shoot	Nd	0.035 ± 0.007	Nd	Nd	0.623 ± 0.012	Nd	Nd	3.82 ± 0.25	114
South Sinai, Egypt	<i>Z. coccineum</i>	unpolluted	Shoot	Nd	0.015 ± 0.007	Nd	Nd	0.303 ± 0.011	Nd	Nd	1.37 ± 0.19	114
South Sinai, Egypt	<i>Z. coccineum</i>	polluted	Shoot	Nd	0.232 ± 0.023	Nd	Nd	0.761 ± 0.042	Nd	Nd	2.40 ± 0.007	114
Oued Souf, Algeria	<i>Zygophyllum.spS</i>	unpolluted	Leaves	0.058	10.60	12844	3.35	Nd	Nd	Nd	Nd	115
Oued Souf, Algeria	<i>Zygophyllum.sp</i>	unpolluted	Fruit	0.143	9.19	5.52	3.81	Nd	Nd	Nd	Nd	115
Oued Souf, Algeria	<i>Zygophyllum.sp</i>	unpolluted	Stem	0.093	9.71	8.13	2.99	Nd	Nd	Nd	Nd	115
Oued Souf, Algeria	<i>Zygophyllum.sp</i>	unpolluted	Root	2.145	9.1	6.89	3.48	Nd	Nd	Nd	Nd	115
Adrar, Algeria	<i>Z. album</i>	unpolluted	Leaves	0.209	7.92	8.00	8.35	Nd	Nd	Nd	Nd	115
Adrar, Algeria	<i>Z. album</i>	unpolluted	Fruit	0.058	11.42	13.89	10.54	Nd	Nd	Nd	Nd	115
Adrar, Algeria	<i>Z. album</i>	unpolluted	Stem	0.131	9.78	7.82	9.39	Nd	Nd	Nd	Nd	115
Adrar, Algeria	<i>Z. album</i>	unpolluted	Root	0.107	11.5	19.78	10.98	Nd	Nd	Nd	Nd	115
Ouargla, Algeria	<i>Z. gelsini</i>	unpolluted	Leaves	0.34	6.53	5.31	1.12	102.6	Nd	19.86	Nd	115
Ouargla, Algeria	<i>Z. gelsini</i>	unpolluted	Fruit	0.23	5.76	6.10	1.30	74.39	Nd	15.58	Nd	115
Ouargla, Algeria	<i>Z. gelsini</i>	unpolluted	Stem	0.18	7.10	1.43	1.10	57.33	Nd	13.64	Nd	115
Ouargla, Algeria	<i>Z. gelsini</i>	unpolluted	Root	0.09	6.89	2.08	1.17	22.28	Nd	4.27	Nd	115
Yanbu city, Saudi Arabia	<i>Z. coccinum</i>	Yanbu Petroleum refinery	Whole plant	19 ± 0.3	Nd	Nd	18 ± 1.0	Nd	16 ± 0.9	33 ± 1.8	Nd	123
Yanbu city, Saudi Arabia	<i>Z. coccinum</i>	Sanitary landfill	Whole plant	14 ± 0.2	Nd	Nd	19 ± 0.5	Nd	13 ± 0.8	30 ± 1.5	Nd	123
Yanbu city, Saudi Arabia	<i>Z. coccinum</i>	Light industrial park	Whole plant	13 ± 0.5	Nd	Nd	18 ± 0.3	Nd	13 ± 0.3	19 ± 0.4	Nd	123
Yanbu city, Saudi Arabia	<i>Z. coccinum</i>	Alsawary area	Whole plant	3.5 ± 0.1	Nd	Nd	10 ± 0.6	Nd	3.4 ± 0.4	9 ± 0.1	Nd	123
Jeddah city, Saudi Arabia	<i>Z. album</i>	unpolluted	Leaves	Nd	2.2 ± 0.0003	1.28 ± 0.004	Nd	24.3 ± 0.04	0.08	38.7 ± 0.002	328 ± 32	116
Jeddah city, Saudi Arabia	<i>Z. album</i>	polluted	Leaves	0.23 ± 0.001	22.3 ± 0.09	9.4 ± 0.001	8.9 ± 0.002	231 ± 0.04	0.97	88.4 ± 0.008	1493 ± 13	116
Jeddah city, Saudi Arabia	<i>Z. album</i>	npolluted	Stems	Nd	1.3 ± 0.0003	1.15 ± 0.003	Nd	9.6 ± 0.01	0.02	13.1 ± 0.001	115 ± 10	116
Jeddah city, Saudi Arabia	<i>Z. album</i>	polluted	Stems	0.08 ± 0.001	14.3 ± 0.002	4.2 ± 0.004	19.4 ± 0.001	104 ± 0.01	0.12	43.7 ± 0.003	736 ± 8	116
Jeddah city, Saudi Arabia	<i>Z. album</i>	unpolluted	Roots	Nd	4.2 ± 0.0003	1.82 ± 0.001	Nd	5.6 ± 0.05	0.03	12.2 ± 0.022	112 ± 23	116
Jeddah city, Saudi Arabia	<i>Z. album</i>	polluted	Roots	0.02 ± 0.001	17.6 ± 0.002	3.53 ± 0.01	14.9 ± 0.02	83.2 ± 0.01	0.45	24.1 ± 0.002	602 ± 12	116
South of Riyadh Capital in Saudi Arabia	<i>Z. simplex</i>	Industrial area	Whole plant	0.3	4.76	7.46	2.71	12.1	Nd	Nd	412.46	124

regions.<sup>129</sup> The concentration of Zn in *Thymus spp.* ranged from 16.01 mg kg<sup>-1</sup> (*T. fallax*) to 33.71 mg kg<sup>-1</sup> (*Thymus praecox*), which was higher than the concentration of Zn in *T. vulgaris* in Turkey (14.30 mg kg<sup>-1</sup>).<sup>130</sup> In previous studies on this species, the Zn concentration in *T. fallax* decreased in the range (13.7 to 34.7 mg kg<sup>-1</sup>)<sup>131</sup>. The location of the *T. vulgaris* cultivation region, may help to clarify the contamination of

these species by Pb, in particular, as it is well known that motor vehicles are the main source of Pb contamination. However, Pb was below the toxic level in wild *T. serpyllum* growing in its natural environment.<sup>132</sup> Additionally, the availability of the plant to accumulate the metal and store it, as well as the kind of soil and plant species, may all contribute to variations in the amount of Pb in the plants study.<sup>133,134</sup> The Cu concentrations



**Table 5.** Content of metals (mg/g) in *T. vulgaris*.

Locality	Plant	Area	Part uses	The concentration of metals (mg/g) D.W									Reference
				Co	Cu	Cr	Mn	Ni	Fe	Pb	Zn	Cd	
Jordan	<i>T. vulgaris</i>	Ash-shouback	Aerial parts	Nd	13.23 ± 0.13	Nd	15.52 ± 0.16	23.85 ± 0.03	141.3 ± 0.67	32.03 ± 0.04	16.18 ± 0.24	Nd	139
Egypt	<i>T. vulgaris</i>	Cairo and Giza governorates	Whole plant	0.151	Nd	0.606	ND	2.55	Nd	11.16	Nd	0.454	140
Morocco	<i>T. vulgaris</i>	Ounarha town	Leaves, woods, and flowers	Nd	4.88	8.76	22.4	Nd	405	Nd	14.3	Nd	141
Iraq	<i>T. vulgaris</i>	Erbil	Stem, seeds, root, inner bark, flowers and leaves	Nd	0.61 ± 0.05	Nd	6.33 ± 0.55	0.34 ± 0.28	57.57 ± 3.83	0.41 ± 0.03	5.44 ± 0.52	Nd	142
Libya	<i>T. vulgaris</i>	Misurata city	Whole plant	Nd	0.99 ± 0.18	0.66 ± 0.18	Nd	Nd	5.26 ± 2.97	0.43 ± 0.07	6.53 ± 1.08	0.34 ± 0.52	143
United Arab Emirates	<i>T. vulgaris</i>	Market in Dubai	Whole plant	Nd	3.52 -13.16	Nd	Nd	Nd	120.75 -764.51	9.07-23.52	Nd	-0.63	5
Iran	<i>T. vulgaris</i>	Tehran drugstores	Herbal drops	Nd	0.782 ± 0.057	Nd	Nd	Nd	Nd	0.264 ± 0.071	Nd	0.012 ± 3.388	144

**Table 6.** Content of heavy metals (mg/g) in *M. longifolia*.

Locality	Plant	Area	Part uses	The concentration of metals (mg/g) D.W							Reference
				Cu	Cr	Mn	Ni	Fe	Pb	Zn	
Bosnia and Herzegovina	<i>M. longifolia</i> L.	Bugojno	Leaves	7.00 ± 0.01	Nd	40.30 ± 0.01	7.00 ± 0.01	645 ± 0.01	0.10 ± 0.01	13.90 ± 0.01	3
Bosnia and Herzegovina	<i>M. longifolia</i> L.	Rudo	Leaves	7.30 ± 0.01	Nd	21.30 ± 0.01	3.70 ± 0.01	755 ± 0.01	0.60 ± 0.01	14.50 ± 0.01	3
Bosnia and Herzegovina	<i>M. longifolia</i> L.	Sarajevo	Leaves	10.00 ± 0.01	Nd	37.80 ± 0.01	6.60 ± 0.01	659 ± 0.01	0.90 ± 0.01	29.90 ± 0.01	3
Pakistan	<i>M. longifolia</i> L.	Chumra derai	Root, shoot, and leaves	Nd	2.00 ± 0.04	Nd	0.38 ± 0.20	Nd	0.40 ± 0.14	20.54 ± 1.14	153
Egypt	<i>M. longifolia</i> L.	Polluted canals in summer	Shoot	354.6 ± 168.1	8.2 ± 1.6	98.5 ± 31.2	168.1 ± 9.9	919.3 ± 108.16	2.6 ± 1.0	282.6 ± 70.5	100
Egypt	<i>M. longifolia</i> L.	Polluted canals in summer	Root	646.7 ± 193.7	16.0 ± 4.6	156.4 ± 47.2	420.1 ± 47.6	2054.3 ± 436.9	0.6 ± 0.1	544.9 ± 191.7	100
Egypt	<i>M. longifolia</i> L.	Unpolluted canals	Shoot	194.7 ± 86.0	3.2 ± 1.1	39.9 ± 27.9	156.4 ± 58.1	573.4 ± 351.9	6.7 ± 6.2	233.7 ± 67.2	100
Egypt	<i>M. longifolia</i> L.	Unpolluted canals	Root	372.7 ± 97.3	8.8 ± 2.0	79.4 ± 50.6	288.4 ± 101.4	1270.1 ± 714.2	1.7 ± 2.5	455.9 ± 123.6	100
Montenegro	<i>M. longifolia</i> L.	Slopes of Mount Bjelasica	Root	32.8 ± 2.61	Nd	78.8 ± 4.21	2.91 ± 0.35	1457 ± 92	Nd	58.2 ± 4.47	154
Montenegro	<i>M. longifolia</i> L.	Slopes of Mount Bjelasica	Stem	28.2 ± 2.33	Nd	49.1 ± 2.21	0.37 ± 0.03	94.1 ± 12	Nd	10.6 ± 1.32	154
Montenegro	<i>M. longifolia</i> L.	Slopes of Mount Bjelasica	Leaf	20.7 ± 2.39	Nd	52.3 ± 4.67	3.06 ± 0.32	183 ± 13	Nd	25.5 ± 4.12	154

in the *Tymus* species were within legal limits (2-20 ppm). The Cu concentration ranged from 13.23 ppm in *T. vulgaris* to 10.4 ppm in *T. serpyllum*<sup>125</sup> This difference in the Cu concentration may be caused by genetic variation across plant species<sup>135</sup> or by varying plant heavy metal selectivity<sup>126</sup>, or it influenced by the effect of anthropogenic activities and high heavy traffic levels, which could cause accumulation of Cu metal in the

soil.<sup>126,136</sup> The concentration of Zn in *T. vulgaris* was higher than that found in *T. serpyllum*, while the concentrations of Mn were found to be close in *T. vulgaris* and *T. serpyllum*.<sup>125</sup> (Table 5). The high amount of Mn may be attributed to the development of industrial and residential locations rich in Mn and Ni and their use as fuel additives similar to Pb.<sup>137</sup> The optimal range for Co concentration in *T. serpyllum* was between

0.02 and 1.0 mg/kg.<sup>9</sup> The presence of cobalt in *T. serpyllum* and its absence in the other species may be explained by the fact that the occurrence of Co is essentially dependent upon the species. The absorption is controlled by various mechanisms in various species. Physical factors including pH, temperature, the salinity of the environment, and the presence of some metals influence the effect of Co absorption and accumulation in different plant species.<sup>138</sup> Table 5 shows the content of metals in *T. vulgaris*.<sup>139,140–144</sup>

### Content of Heavy Metals in *M. longifolia*

The mentha herb may contain harmful elements, such as HM derived from the environment during cultivation, storage or harvesting. Furthermore, contamination of the herb by various HM may also occur during plant cultivation as a result of soil content, the presence of nutritive elements, fertilizers and during the treatment and packaging of herbaceous materials.<sup>5,143,145</sup> Metal concentration ranged from 0.10 mg/g for Pb to 755.00 mg/g for Fe in *M. longifolia* L. (wild species), while metal ranged from 0.40 mg/g for Pb to 1108.40 mg/g for Fe in *M. piperita* L. (cultivated species). Cr and Cd content in wild species were lower than WHO standards.<sup>143,146</sup> Furthermore, the highest concentration was found in Fe, and the lowest concentration was found in Pb. A relatively low Cu concentration in wild species compared to Zn concentration occurs because higher Cu content in soil can reduce Zn availability in plants, due to competition for the same absorption sites in the root of plant.<sup>145,147,148</sup> The highest quantities of trace oligo-elements found in *Mentha* species are Fe (619.30–1108.40 mg/g), Mn (21.30–94.00 mg/g), Zn (13.90–39.30 mg/g), Cu (4.46–12.50 mg/g) and Cr (0.70–0.90 mg/g). The high amount of Fe is a result of the fact that Fe is mostly found in soil and rock. Cr concentrations in wild *Mentha* were below detection limits.<sup>3</sup> These findings indicate that both *Mentha* species (*M. longifolia* L. and *M. piperita* L.) are good sources of low HM concentrations and are safe for usage as a beverage and in various herbal preparations.<sup>3</sup> HM levels in target species growth in contaminated areas may be doubled or tripled when compared to the noncontaminated area. For example, the Fe content in the root of *M. longifolia* was 14.56 (mg/kg) DW in contaminated soil, and this value was decreased to around half (6.35 mg/kg DW) in non-contaminated soil (Table 6). Sometimes the metal amount of growing plants in a contaminated area yields values that are 10 times higher than those in a non-contaminated area. Furthermore, the metal uptake and accumulation capacities vary significantly among wetland species<sup>123</sup>. This finding may support the concept of employing *M. longifolia* as a phytoremediator, which is consistent with research investigating the phytoremediation potentiality of several species in wetlands.<sup>149–152</sup> Table 6 shows the content of heavy metals in *M. longifolia*.<sup>3,100,153,154</sup>

Our research found that the same medicinal plant species

(*Zygophyllum*, *M. longifolia*, and *T. vulgaris*) that grow in different geographical areas accumulate different levels of HM. The concentration of HM varies for different plant species derived from the same geographical location. The amounts of HM detected in the plants collected in some areas were within the legal limits, but levels in other geographical areas exceeded the recommended ranges. As a result, medicinal plants for herbal remedies must be collected from non-polluting natural areas. Our findings also suggest that medicinal plants, whether used for local or medicinal applications, should be obtained from areas free of HM contamination.

### CONCLUSION

HM accumulation in plant species is a stress factor that causes a variety of growth problems for plants. As a result, it is critical to avoid harvesting medicinal plants that show signs of stress, because they may be the result of heavy metal accumulation. Toxic metal bioaccumulation has a variety of toxic effects on many organisms, tissues, and organs. Metal poisoning can show as either acute or chronic symptoms. HM interfere with biological functions such as proliferation, growth, differentiation, repair of cellular damage, as well as apoptosis. The main goal of utilizing medicinal plants in disease treatment is to acquire a cure with few or no side effects, yet the presence of HM in plants may pose substantial health risks to consumers if absorbed. Even when they are low toxic levels, those with a long biological half-life tend to accumulate in the body over time, and as a result, long-term absorption of extremely high amounts can result in death.

**Peer Review:** Externally peer-reviewed.

**Author Contributions:** Conception/Design of Study- M.D.; Data Acquisition- M.D.; Data Analysis/Interpretation- M.D.; Drafting Manuscript- I.S., T.I.; Critical Revision of Manuscript- I.S.; Final Approval and Accountability- A.B., D.A., M.D., I.S.

**Conflict of Interest:** Authors declared no conflict of interest.

**Financial Disclosure:** Authors declared no financial support.

### List of Author orcid

Meriem Djarmouni	0000-0003-0303-6263
Ilham Sekia	0009-0006-4506-961X
Djamila Ameni	0000-0002-1884-6050
Tassadit Ikessoulen	0009-0004-4396-7294
Abderrahmane Baghiani	0000-0002-6881-011X

### REFERENCES

1. Munir N, Jahangeer M, Bouyahya A, et al. Heavy metal contamination of natural foods is a serious health issue: a review. *Sustainability*. 2022;14(1):161. doi:10.3390/su14010161.
2. Balali-Mood M, Naseri K, Tahergorabi Z, Khazdair MR,

- Sadeghi M. Toxic mechanisms of five heavy metals: Mercury, lead, chromium, cadmium, and arsenic. *Front Pharmacol.* 2021;227. doi:10.3389/fphar.2021.764227.
3. Mandal Š. Essential and heavy metal content in wild and cultivated *Mentha* species from Bosnia and Herzegovina. *Kemija u industriji.* 2021;70(7-8):393. doi:10.15255/KUI.2021.093.
  4. Aouacheri O, Saka S. Cytoprotective effects of *Zingiber officinale* against the oxidative stress induced by lead acetate toxicity in rats. *Phytothérapie.* 2021;19(5-6):297-305.
  5. Dghaim R, Al Khatib S, Rasool H, Ali Khan M. Determination of heavy metal concentration in traditional herbs commonly consumed in the United Arab Emirates. *J Environ Public Health.* 2015;2015. doi:10.1155/2015/974256.
  6. Islam EU, Yang XE, He ZL, Mahmood Q. Assessing potential dietary toxicity of heavy metals in selected vegetables and food crops. *J Zhejiang Univ Sci B.* 2007;8(1):1-13.
  7. Asiminicesei DM, Vasilachi IC, Gavrilesco MARIA. Heavy metal contamination of medicinal plants and potential implications on human health. *Revista de Chimie.* 2020;71(7):16-36.
  8. Zaynab M, Al-Yahyai R, Ameen A, et al. Health and environmental effects of heavy metals. *J King Saud Univ Sci.* 2022;34(1):101653. doi: 10.1016/j.jksus.2021.101653.
  9. Kabata-Pandias A, Kabata-Pandias A, Pendias H. Trace elements in soils and plants. CRC Press, Incorporated; 1984.
  10. Salgarello M, Visconti G, Barone-Adesi L. Interlocking circumareolar suture with undyed polyamide thread: a personal experience. *Aesthetic Plast Surg.* 2013;37:1061-1062.
  11. Wedepohl KH. The composition of the continental crust. *Geochim Cosmochim Acta.* 1995;59(7):1217-1232.
  12. Ball JW, Izbicki JA. Occurrence of hexavalent chromium in ground water in the western Mojave Desert, California. *Appl Geochem.* 2004;19(7):1123-1135.
  13. Viers J, Oliva P, Nonell A, Gélabert A, Sonke JE, Freyrier R, Dupré B. Evidence of Zn isotopic fractionation in a soil-plant system of a pristine tropical watershed (Nsimi, Cameroon). *Chem Geol.* 2007;239(1-2):124-137.
  14. Hüffmeyer N, Klasmeier J, Matthies M. Geo-referenced modeling of zinc concentrations in the Ruhr river basin (Germany) using the model GREAT-ER. *Sci Total Environ.* 2009;407(7):2296-2305.
  15. Ayandiran TA, Fawole OO, Adewoye SO, Ogundiran MA. Bioconcentration of metals in the body muscle and gut of *Clarias gariepinus* exposed to sublethal concentrations of soap and detergent effluent. *J Cell Anim Biol.* 2009;3(8):113-118.
  16. Sonone SS, Jadhav S, Sankhla MS, Kumar R. Water contamination by heavy metals and their toxic effect on aquaculture and human health through food Chain. *Lett Appl NanoBioScience.* 2020;10(2):2148-2166.
  17. Means B. Risk-assessment guidance for superfund. Volume 1. Human health evaluation manual. Part A. Interim report (Final) (No. PB-90-155581/XAB; EPA-540/1-89/002). Environmental Protection Agency, Washington, DC (USA). Office of Solid Waste and Emergency Response; 1989.
  18. Wu B, Zhao DY, Jia HY, Zhang Y, Zhang XX, Cheng SP. Preliminary risk assessment of trace metal pollution in surface water from Yangtze River in Nanjing Section, China. *Bull Environ Contam Toxicol.* 2009;82:405-409.
  19. Olayinka-Olagunju JO, Dosumu AA, Olatunji-Ojo AM. Bioaccumulation of heavy metals in pelagic and benthic fishes of Ogbese River, Ondo State, South-Western Nigeria. *Water Air Soil Pollut.* 2021;232:1-19.
  20. Rouidi S, Hadeif A, Dziri H. The state of metallic contamination of Saf-Saf river sediments (Skikda-Algeria). *Pollution.* 2022;8(3):717-728.
  21. Asiminicesei DM, Vasilachi IC, Gavrilesco MARIA. Heavy metal contamination of medicinal plants and potential implications on human health. *Revista de Chimie.* 2020;71(7):16-36.
  22. Amari T, Ghnaya T, Abdelly C. Nickel, cadmium and lead phytotoxicity and potential of halophytic plants in heavy metal extraction. *S Afr J Bot.* 2017;111:99-110.
  23. Anyanwu BO, Ezejiofor AN, Igweze ZN, Orisakwe OE. Heavy metal mixture exposure and effects in developing nations: an update. *Toxics.* 2018;6(4):65. doi: 10.3390/toxics6040065.
  24. Korfali SI, Hawi T, Mroueh M. Evaluation of heavy metal content in dietary supplements in Lebanon. *Chem Cent J.* 2013;7:1-13.
  25. Korfali SI, Mroueh M, Al-Zein M, Salem R. Metal concentration in commonly used medicinal herbs and infusion by Lebanese population: health impact. *J Food Res.* 2013;2(2):70. doi: 10.5539/jfr.v2n2p70.
  26. Mahan L, Escott-Stump S, Raymond L. Krause's Food and Nutrition Care Process, edited by: Y. Alexopoulos, Saunders, St. Louis, Mo, USA, 2016.
  27. Singh R, Gautam N, Mishra A, Gupta R. Heavy metals and living systems: An overview. *Indian J Pharmacol.* 2011;43(3):246. doi:10.4103/0253-7613.81505.
  28. Jolliffe DM, Budd AJ, Gwilt DJ. Massive acute arsenic poisoning. *Anaesthesia.* 1991;46(4):288-290.
  29. Luo JH, Qiu ZQ, Zhang L, Shu WQ. Arsenite exposure altered the expression of NMDA receptor and postsynaptic signaling proteins in rat hippocampus. *Toxicol Lett.* 2012;211(1):39-44.
  30. Shen S, Li XF, Cullen WR, Weinfeld M, Le XC. Arsenic binding to proteins. *Chem Rev.* 2013;113(10):7769-7792.
  31. Shaban NS, Abdou KA, Hassan NEHY. Impact of toxic heavy metals and pesticide residues in herbal products. *Beni-suef Univ J Basic Appl Sci.* 2016;5(1):102-106.
  32. Deng Y, Wang M, Tian T, et al. The effect of hexavalent chromium on the incidence and mortality of human cancers: a meta-analysis based on published epidemiological cohort studies. *Front Oncol.* 2019;9:24. doi: 10.3389/fonc.2019.00024.
  33. Pavesi T, Moreira JC. Mechanisms and individuality in chromium toxicity in humans. *J Appl Toxicol.* 2020;40(9):118-1197.
  34. Cheng JP, Wang WH, Jia JP, Zheng M, Shi W, Lin XY. Expression of c-fos in rat brain as a prelude marker of central nervous system injury in response to methylmercury-stimulation. *Biomed Environ Sci.* 2006;19(1):67-72.
  35. Bottino C, Vázquez M, Devesa V, Laforenza U. Impaired aquaporins expression in the gastrointestinal tract of rat after mercury exposure. *J Appl Toxicol.* 2016;36(1):113-120.
  36. Chen R, Xu Y, Xu C et al. Associations between mercury exposure and the risk of nonal fatty liver disease (NAFLD) in US adolescents. *Environ Sci Pollut Res.* 2019;26:31384-31391.
  37. Zhang C, Gan C, Ding L, Xiong M, Zhang A, Li P. Maternal inorganic mercury exposure and renal effects in the Wanshan mercury mining area, southwest China. *Ecotoxicol Environ Saf.* 2020;189:109987.
  38. Schutte R, Nawrot TS, Richart T, et al. Bone resorption and environmental exposure to cadmium in women: a population study. *Environ Health Perspect.* 2008;116(6):777-783.
  39. Pan C, Liu HD, Gong Z, Yu X, Hou XB, Xie DD, et al. Cadmium

- is a potent inhibitor of PPM phosphatases and targets the M1 binding site. *Sci Rep*. 2013;3:2333. doi: 10.1038/s02333.
40. Pi H, Xu S, Reiter RJ, et al. SIRT3-SOD2-mROS-dependent autophagy in cadmium-induced hepatotoxicity and salvage by melatonin. *Autophagy*. 2015;11(7):1037-1051.
  41. Fay MJ, Alt LA, Ryba D, et al. Cadmium nephrotoxicity is associated with altered microRNA expression in the rat renal cortex. *Toxics*. 2018;6(1):16. doi: 10.3390/toxics6010016.
  42. Wang Y, Mandal AK, Son YO, et al. Roles of ROS, Nrf2, and autophagy in cadmium-carcinogenesis and its prevention by sulforaphane. *Toxicol Appl Pharmacol*. 2018;353:23-30.
  43. Strużyńska L, Dąbrowska-Bouta B, Koza K, Sulkowski G. Inflammation-like glial response in lead-exposed immature rat brain. *Toxicol Sci*. 2007;95(1):156-162.
  44. Dongre NN, Suryakar AN, Patil AJ, Ambekar JG, Rathi DB. Biochemical effects of lead exposure on systolic & diastolic blood pressure, heme biosynthesis and hematological parameters in automobile workers of north Karnataka (India). *Indian J Clin Biochem*. 2011;26:400-406.
  45. Wang J, Zhu H, Yang Z, Liu Z. Antioxidative effects of hesperetin against lead acetate-induced oxidative stress in rats. *Indian J Pharmacol*. 2013;45(4):395. doi: 10.4103/0253-7613.115015.
  46. Boskabady MH, Tabatabai SA, Farkhondeh T. Inhaled lead affects lung pathology and inflammation in sensitized and control guinea pigs. *Environ Toxicol*. 2016;31(4):452-460.
  47. Dzomba P, Chayamiti T, Togarepi E. Heavy metal content of selected raw medicinal plant materials: implication for patient health. *Bull. Environ. Pharmacol Life Sci*. 2012;10(1):28-33.
  48. Begum HA, Hamayun M, Zaman K, Shinwari ZK, Hussain A. Heavy metal analysis in frequently consumable medicinal Plants of khyber paktunkhwa, Pakistan. *Pak J Bot*. 2017;49(3):1155-1160.
  49. Gupta DK, Tiwari S, Razafindrabe BHN, Chatterjee S. Arsenic contamination from historical aspects to the present. In: *Arsenic Contamination in the Environment: The Issues and Solutions*. Elsevier; 2017:1-12.
  50. Rani A, Kumar A, Lal A, Pant M. Cellular mechanisms of cadmium-induced toxicity: a review. *Int J Environ Health Res*. 2014;24(4):378-399.
  51. Wang J, Zhu H, Yang Z, Liu Z. Antioxidative effects of hesperetin against lead acetate-induced oxidative stress in rats. *Indian J Pharmacol*. 2013;45(4):395. doi: 10.4103/0253-7613.115003.
  52. Yao H, Guo L, Jiang BH, Luo J, Shi X. Oxidative stress and chromium (VI) carcinogenesis. *J En Pathol Toxicol Oncol*. 2008;27(2). doi: 10.1615/JEnvironPatholToxicolOncol.v27.i2.10.
  53. Aggarwal V, Tuli HS, Varol A, Thakral F, Yerer MB, Sak K, et al. Role of reactive oxygen species in cancer progression: molecular mechanisms and recent advancements. *Biomolecules*. 2019;9(11):735. doi: 10.3390/biom9110735.
  54. Fernandes Azevedo B, Barros Furieri L, Peçanha FM, Wiggers GA, Frizzera Vassallo P. Toxic effects of on the cardiovascular and central nervous systems. *Biomed Res Int*. 2012;949048. doi: 10.1155/2012949048.
  55. Brown HA, Thomas PG, Lindsley CW. Targeting phospholipase D in cancer, infection and neurodegenerative disorders. *Nat Rev Drug Discov*. 2017;16(5):351-367.
  56. Liu J, Qu W, Kadiiska MB. Role of oxidative stress in cadmium toxicity and carcinogenesis. *Toxicol Appl Pharmacol*. 2009;238(3):209-214.
  57. Wu X, Cobbina SJ, Mao G, Xu H, Zhang Z, Yang L. A review of toxicity and mechanisms of individual and mixtures of HM in the environment. *Environ Sci Pollut Res*. 2016;23:8244-8259.
  58. Hammada HM, Ghazy NM, Harraz FM, Radwan MM, ElSohly MA, Abdallah II. Chemical constituents from *Tribulus terrestris* and screening of their antioxidant activity. *Phytochemistry*. 2013;92:153-159.
  59. Shawky E, Gabr N, El-gindi M, Mekky R. A comprehensive review on genus *Zygophyllum*. *J Adv Pharm Res*. 2019;3(1):1-16.
  60. Amini-Chermahini F, Ebrahimi M, Farajpour M, Taj Bordbar Z. Karyotype analysis and new chromosome number reports in *Zygophyllum* species. *Caryologia*. 2014;67(4):321-324.
  61. Bourgou S, Megdiche W, Ksouri R. The halophytic genus *Zygophyllum* and *Nitraria* from North Africa: A phytochemical and pharmacological overview. In: *Medicinal and Aromatic Plants of the World-Africa Volume 3*. Springer. 2017;345-356.
  62. Medjdoub H, Tabti B. Antidiabetic effect of the aerial part ethanolic extracts of *Zygophyllum geslini* Coss. in streptozotocin induced-diabetic rats. *Met Funct Res Diab*. 2012;5:17-20.
  63. Barzegar R, Safaei HR, Nemati Z, Ketabchi S, Talebi E. Green synthesis of silver nanoparticles using *Zygophyllum qatarense* Hadidi leaf extract and evaluation of their antifungal activities. *J Appl Pharm Sci*. 2018;8(3):168-171.
  64. Mnafgui K, Kchaou M, Hamden K, Derbali F, Slama S, Nasri M, et al. Inhibition of carbohydrate and lipid digestive enzymes activities by *Zygophyllum album* extracts: effect on blood and pancreas inflammatory biomarkers in alloxan-induced diabetic rats. *J Physiol Biochem*. 2014;70:93-106.
  65. Elbadry MA, Elaasser MM, Elshiekh HH, Sherif MM. Evaluation of antimicrobial, cytotoxic and larvicidal activity of *Zygillum coccineum* North Sinai, Egypt. *Med Aromat Plants*. 2015;4(5):214. doi: 10.4172/2167-0412.1000214.
  66. Sharma V, Ramawat KG. Salt stress enhanced antioxidant response in callus of three halophytes (*Salsola baryosma*, *Trianthema triquetra*, *Zygophyllum simplex*) of Thar Desert. *Biologia*. 2014;69:178-185.
  67. Emad MA, Gamal EG. Screening for antimicrobial activity of some plants from Saudi folk medicine. *GJRMJ*. 2013;2(4):210-218.
  68. Zaki AA, Ali Z, El-Amier YA, Khan IA. A new lign from *Zygophyllum aegyptium*. *Magn Reson Chem*. 2016;54(9):771-773.
  69. He J, Lv X, Niu Y, et al. Four new compounds from *Zygophyllum fabago* L. *Phytochem Lett*. 2016;15:116-120.
  70. Ganbaatar C, Gruner M, Tunsag J, et al. Chemical constituents isolated from *Zygophyllum melongena* Bunge growing in Mongolia. *Nat Prod Res*. 2016;30(14):1661-1664.
  71. Abdel-Hamid RA, Ross SA, Abilov ZA, Sultanova NA. Flavonoids and sterols from *Zygophyllum fabago*. *Chem Nat Compd*. 2016;52:318-319.
  72. Hassanean HA, Desoky EK. An acylated isorhamnetin glucoside from *Zygophyllum simplex*. *Phytochemistry*. 1992;31(9):3293-3294.
  73. Elgamal MHA, Shaker KH, Pöllmann K, Seifert K. Triterpenoid saponins from *Zygophyllum* species. *Phytochemistry*. 1995;40(4):1233-1236.
  74. Kaplan D, Maymon M, Agapakis CM, et al. A survey of the microbial community in the rhizosphere of two dominant shrubs of the Negev Desert highlands, *Zygophyllum dumosum* (Zygophyllaceae) and *Atriplex halimus* (Amaranthaceae), using

- cultivation-dependent and cultivation-independent methods. *Am J Bot.* 2013;100(9):1713-1725.
75. Belguidoum M, Dendougui H, Kendour Z, Belfar A, Bensaci C, Hadjadj M. Antioxidant activities, phenolic, flavonoid and tannin contents of endemic *Zygophyllum cornutum* Coss. from Algerian Sahara. *Der Pharma Chemica.* 2015;7(11):312-317.
  76. Boumaza A, Ferdi S, Sbayou H, Touhami FK, Belmahi MH, Benlatreche C. Therapeutic effect of *Zygophyllum cornutum* on metabolic disturbances, oxidative stress in heart tissue and histological changes in myocardium of streptozotocin-induced diabetic rats. *J Life Sci.* 2016;10:192-197.
  77. Yaripour S, Delnavazi MR, Asgharian P, Valiyari S, Tavakoli S, Nazemiyeh H. A survey on phytochemical composition and biological activity of *Zygophyllum fabago* from Iran. *Adv Pharm Bull.* 2017;7(1):109. doi: 10.15171/apb.2017.014.
  78. AL-Qaissi E. Antimicrobial activity of petroleum ether extracts from leaves, seeds and roots of *Zygophyllum fab L.* towards some microorganisms. *Ibn AL-Haitham J Pure Appl Sci.* 2017;21(2):1-14.
  79. Khan SS, Khan A, Khan A, et al. Urease inhibitory activity of urbane type sulfated saponins from the aerial parts of *Zygophyllum fabago* Linn. *Phytomedicine.* 2014;21(3):379-382.
  80. Ksouri WM, Medini F, Mkadmini K, Legault J, Magné C, Abdely C, et al. LC-ESI-TOF-MS identification of bioactive secondary metabolites involved in the antioxidant, anti-inflammatory and anticancer activities of the edible halophyte *Zygophyllum album* Desf. *Food Chem.* 2013;139(1-4):1073-1080.
  81. Kchaou M, Salah HB, Mhiri R, Allouche N. Anti-oxidant and anti-acetylcholinesterase activities of *Zygophyllum album.* *Bangladesh J Pharmacol.* 2016;11(1):5462. doi: 10.3329/bjp.v11i1.5462.
  82. Ghoull JE, Boughattas NA, Ben-Attia M. Antihyperglycemic and antihyperlipidemic activities of ethanolic extract of *Zygophyllum album* in streptozotocin-induced diabetic mice. *Toxicol Ind Health.* 2013;29(1):43-51.
  83. Mnafigui K, Hamden K, Ben Salah H, et al. Inhibitory activities of *Zygophyllum album*: A natural weight-lowering plant on key enzymes in high-fat diet-fed rats. *Evid Based Complement Alternat Med.* 2012;620384. doi: 10.1155/2012/620384.
  84. Mnafigui K, Kchaou M, Ben Salah H, Hajji R, Khabbabi G, Elfeki A, et al. Essential oil of *Zygophyllum album* inhibits key digestive enzymes related to diabetes and hypertension and attenuates symptoms of diarrhea in alloxan-induced diabetic rats. *Pharm Biol.* 2016;54(8):1326-1333.
  85. Kchaou M, Ben Salah H, Mnafigui K, Abdennabi R, Gharsallah N, Elfeki A, Allouche N. Chemical composition and activities of *Zygophyllum album* (L.) essential oil from Tunisia. *J Essent Oil Res.* 2018;30(6):401-408.
  86. El-Shora HM, El-Amier YA, Awad MH. Antioxidant activity of leaf extracts from *Zygophyllum coccineum* L. collected from desert and coastal habitats of Egypt. *Int J Curr Microbiol App Sci.* 2016;5(4):635-641.
  87. Gibbons S, Oriowo MA. Antihypertensive effect of an aqueous extract *Zygophyllum coccineum* L. in rats. *Phytother Res.* 2001;15(5):452-455.
  88. Elbadry MA, Elaasser MM, Elshiekh HH, Sheriff MM. Evaluation of antimicrobial, cytotoxic and larvicidal activity of *Zygophyllum coccineum* North Sinai, Egypt. *Med Aromat Plants.* 2015;4(5):214. doi: 10.4172/2167-0412.1000214
  89. Khafagi IK, Dewedar A. The efficiency of random versus ethno-directed research in the evaluation of Sinai medicinal plants for bioactive compounds. *J Ethnopharmacol.* 2000;71(3):365-376.
  90. Guenzet A, Krouf D, Zennaki S, Berzou S. *Zygophyllum gaetulum* aqueous extract protects against diabetic dyslipidemia and attenuates liver and kidney oxidative damage in streptozotocin-induced-diabetic rats. *Int J Pharm Sci Res.* 2014;5(11):4709-4717.
  91. Jaouhari JT, Lazrek HB, Jana M. The hypoglycemic activity of *Zygophyllum gaetulum* extracts in alloxan-induced hyperglycemic rats. *J Ethnopharmacol.* 2000;69(1):17-20.
  92. Ait El Cadi M, Makram S, Ansar M, Khabbal Y, Alaoui K, Faouzi MA, Taoufik J. Anti-inflammatory activity of aqueous and ethanolic extracts of *Zygophyllum gaetulum*. *Ann Pharm Fr.* 2011;70(2):113-116.
  93. Boudjelthia K, Hammadi K, Kouidri M, Djebli N. Evaluation of antidiabetic activity of two plants *Berberis vulgaris* and *Zygophyllum geslini*. *J Phys Chem Biophys.* 2017;7(1):1-7.
  94. Shehab NG, Abu-Gharbieh E, Bayoumi FA. Impact of phenolic composition on hepatoprotective and antioxidant effects of four desert medicinal plants. *BMC Complement Altern Med.* 2015;15:1-12.
  95. Yang XR, Zhang XF, Zhang XM, Gao HY. Analgesic and anti-inflammatory activities and mechanisms of 70% ethanol extract of *Zygophyllum macropodium* in animals. *Chin Herb Med.* 2018;10(1):59-65.
  96. Barzegar R, Safaei HR, Nemati Z, Ketabchi S, Talebi E. Green synthesis of silver nanoparticles using *Zygophyllum qatarense* Hadidi leaf extract and evaluation of their antifungal activities. *J Appl Pharm Sci.* 2018;8(3):168-171.
  97. Abdallah HM, Esmat A. Antioxidant and anti-inflammatory activities of the major phenolics from *Zygophyllum simplex* L. *J Ethnopharmacol.* 2017;205:51-56.
  98. Kakrani HKN, Kakrani PH, Saluja AK. Evaluation of analgesic and anti-inflammatory activity of Ethyl acetate extract of *Zygophyllum simplex* Linn. herb. *Int J Res Phytochem Pharmacol.* 2011;1(3):180-183.
  99. Abd El Kader MA, Mohamed NZ. Evaluation of protective and antioxidant activity of thyme (*Thymus vulgaris*) extract on paracetamol-induced toxicity in rats. *Aust J Basic Appl Sci.* 2012;6(7):467-474.
  100. Gharib FA, Mansour KH, Ahmed EZ, Galal TM. HM concentration, and antioxidant activity of the essential oil of the wild mint (*Mentha longifolia* L.) in the Egyptian watercourses. *Int J Phytoremediation.* 2021;23(6):641-651.
  101. Stahl-Biskup E, Sáez F, eds. Thyme: The Genus *Thymus*. CRC Press; 2002.
  102. Varga E, Bardocz A, Belak A, et al. Antimicrobial activity and chemical composition of thyme essential oils and the polyphenolic content of different *Thymus* extracts. *Farmacina.* 2015;63(3).
  103. Aeschbach R, Löliger J, Scott BC, et al. Antioxidant actions of thymol, carvacrol, 6-gingerol, zingerone and hydroxytyrosol. *Food Chem Toxicol.* 1994;32(1):31-36.
  104. Šegvić Klarić M, Kosalec I, Mastelić J, Piecková E, Pepeljak S. Antifungal activity of thyme (*Thymus vulgaris* L.) essential oil and thymol against moulds from damp dwellings. *Lett Appl Microbiol.* 2007;44(1):36-42.
  105. Didry N, Dubreuil L, Pinkas M. Activity of thymol, carrol, cinnamaldehyde and eugenol on oral bacteria. *Pharm Acta Helv.* 1994;69(1):25-28.
  106. Suzuki Y, Furuta H. Stimulation of guinea pig neutrophil superoxide anion-producing system with thymol. *Inflammation.* 1988;12:575-584.
  107. Braga PC, Dal Sasso M, Culici M, Bianchi T, Bordoni L, Mara-

- bini L. Anti-inflammatory activity of thymol: Inhibitory effect on the release of human neutrophil elastase. *Pharmacology*. 2006;77(3):130-136.
108. Bozin B, Mimica-Dukic N, Samojlik I, Jovin E. Antimicrobial and antioxidant properties of rosemary and sage (*Rosmarinus officinalis* L. and *Salvia officinalis* L., *Lamiaceae*) essential oils. *J Agric Food Chem*. 2007;55(19):7879-7885.
109. Horošová K, Bujňáková D, Kf V. Effect of oregano essential oil on chicken lactobacilli and *E. coli*. *Folia Microbiol(Praha)*. 2006;51(4):278-280.
110. Alma MH, Mavi A, Yildirim A, Digrak M, Hirata T. Screening chemical composition and in vitro antioxidant and antimicrobial activities of the essential oils from *Origanum syriacum* L. growing in Turkey. *Biol Pharm Bull*. 2003;26(12):1725-1729.
111. Arcila-Lozano CC, Loarca-Piña G, Lecona-Urbe S, González de Mejía E. Oregano: Properties, composition and biological activity. *Arch Latinoam Nutr*. 2004;54(1):100-111.
112. Patonay K, Korozs M, Muranyi Z, Konya EP. Polyphenols in northern Hungarian *Mentha longifolia* (L.) L. treated with ultrasonic extraction for potential oenological uses. *Turk J Agric For*. 2017;41(3):208-217
113. Elansary HO, Szopa A, Kubica P, et al. Polyphenol profile and antimicrobial and cytotoxic activities of natural *Mentha piperita* and *Mentha longifolia* populations in Northern Saudi Arabia. *Processes*. 2020;8(4):479. doi: 10.3390/pr8040479.
114. Morsy AA, Ali Salama KH, Kamel HA, Fahim Mansour MM. Effect of HM on plasma membrane lipids and antioxidant enzymes of *Zygophyllum* species. *Eurasian J Biosci*. 2012;6:1-8. doi: 10.5053/ejobios.2012.6.0.1.
115. Smati D, Hammiche V, Azzouz M, Alamir B. Dosage des métaux lourds dans les *Zygophyllum* réputés antidiabétiques. *Ann Toxicol Anal*. 2011;23(3):125-132.
116. Saeed AZ, Zaki AH. Effect of discharged sewage water on accumulation of HM in three plant species *Zygophyllum album*, *Suaeda aegyptiaca* and *Cyprus rotundus*. *J Biosci Appl Res*. 2017;3(4):181-190.
117. Al-Qahtani KM. Assessment of HM accumulation in native plant species from soils contaminated in Riyadh City, Saudi Arabia. *Life Sci J*. 2012;9(2):384-392.
118. Al-Sodany Y, El-Sheikh M, Baraka D, Shaltout K. Elements Accumulation and Nutritive Value of Phragmites Australis (Cav.) Trin. ex Steudel in Lake Burullus: A Ramsar site, Egypt. *Catrina: The Int J Environ Sci*. 2013;8(1):51-63.
119. Mazhoudi S, Chaoui A, Ghorbal MH, El Ferjani E. Response of antioxidant enzymes to excess copper in tomato (*Lycopersicon esculentum*, Mill.). *Plant Sci*. 1997;127(2):129-137.
120. Sathiyamoorthy P, Van Damme P, Oven M, Golan-Goldhirsh A. HM in medicinal and plants of the Negev desert. *J Environ Sci Health Part A*. 1997;32(8):2111-2123.
121. Lefèvre I, Corréal E, Lutts S. Cadmium tolerance and accumulation in the noxious weed *Zygophyllum fabago*. *Botany*. 2005;83(12):1655-1662.
122. Hashem AR, Alfarhan AH. Minerals content of wild plants from Ashafa, Toroba, Wahat and Wehait (Saudi Arabia). *JKS Unio Sci*. 1993;5(2):101-106.
123. Hashem. Mineral content of soil and wild plants from Saudi Arabia. 1996.
124. Aloud SS, Alotaibi KD, Almutairi KF, Albarakah FN. Assessment of HM accumulation in soil and native plants in an industrial environment, Saudi Arabia. *Sustainability*. 2022;14(10):5993. doi: 10.3390/su14105993.
125. Abu-Darwish MS. Essential oils yield and HM content of some aromatic medicinal plants grown in Ash-Shoubak region, south of Jordan. *Adv Environ Biol*. 2009;3(3):296-301.
126. Jaradat QM, Momani KA. Contamination of roadside soil, plants, and air with HM in Jordan, a comparative study. *Turk J Chem*. 1999;23(2):209-220.
127. Al-Shayeb SM, Al-Rajhi MA, Seaward MRD. The date palm (*Phoenix dactylifera* L.) as a biomonitor of lead and other elements in arid environments. *Sci Total Environ*. 1995;168(1):1-10.
128. Ubavi M, Dozet D, Bogdanovi D. Te ki metali u zemlji tu. In: Kastori R, ed. Te ki metali i pesticidi u zemlji tu te ki metali ipesticidi uzemlji tima Vojvodine, Poljoprivredni fakultet Institut za ratarstvo i povrtar-stvo. *Novi Sad*. 1993:31-46.
129. Meister A, Bernhardt G, Christoffel V, Buschauer A. Antispasmodic activity of *Thymus vulgaris* extract on the isolated guinea-pig trachea: discrimination between drug and ethanol effects. *Planta Med*. 1999;65(06):512-516.
130. Özcan M. Mineral contents of some plants used as condiments in Turkey. *Food Chem*. 2004;84(3):437-440
131. Özcan MM, Ünver A, Uç T, Arslan D. Mineral content of some herbs and herbal teas by infusion and decoction. *Food Chem*. 2008;106(3):1120-1127.
132. Başgel S, Erdemoğlu SB. Determination of mineral and trace elements in some medicinal herbs and their infusions consumed in Turkey. *Sci Total Environ*. 2006;359(1-3):82-89.
133. Nookabkaew S, Rangkadilok N, Satayavivad J. Determination of trace elements in herbal tea products and their infusions consumed in Thailand. *J Agric Food Chem*. 2006;54(18):6939-6944.
134. alenčić ĐP, Kevrešan ŽS, Popović MT. Mineral composition of selected Sal species growing wild in the Vojvodina province. *Zbornik Matice srpske za prirodne nauke*. 2003;(105):25-33.
135. Johnsson L. Selenium in Swedish soils. Factors influencing soil content and plant uptake. *Ambio*. 1992;21(4):292-296.
136. Al-Khlaifat AL, Al-Khashman OA. Atmospheric heavy metal pollution in Aqaba city, Jordan, using Phoenix dactylifera L. leaves. *Atmos Environ*. 2007;41(39):8891-8897.
137. Loranger S, Zayed J. Manganese and lead concentrations in ambient air and emission rates from unleaded and leaded gasoline between 1981 and 1992 in Canada: a comparative study. *Atmos Environ*. 1994;28(9):1645-1651.
138. Palit S, Sharma A, Talukder G. Effects of cobalt on plants. *Bot Rev*. 1994;60(2):149-181.
139. Hlihor RM, Roşca M, Hagiuzaleschi L, Simion IM, Daraban GM, Stoleru V. Medicinal plant growth in HM contaminated soils: Responses to metal stress and induced risks to human health. *Toxics*. 2022;10(9):499. doi: 10.3390/toxics10090499.
140. Thabit TM, Elgeddawy DI, Shokr SA. Determination of some common HM and radionuclides in some medicinal herbs using ICP-MS/MS. *JAOAC Int*. 2020;103(5):1282-1287
141. Bennouna MA, Arjouni Y, Belaqqiz R, Romane A. Assessment of some oligo-elements and HM in different parts of the *Thymus broussonettii* growing in Morocco. *J Mater Environ Sci*. 2014;5(1):293-297.
142. Ciftci H, Caliskan CE, Cakar AE, Ramadan MS, Olcucu A. Determination of mineral and trace element in some medicinal plants by spectroscopic method. *Sigma J Eng Nat Sci*. 2020;38(4):2133-2144.
143. Alkherraz AM, Amer AM, Mlitan AM. Determination of some HM in four medicinal plants. *World Acad Sci Eng Technol*.

- 2013;78:1568-1570.
144. Ravanbakhsh M, Mahernia S, Bagherzadeh K, Dadrass OG, Amanlou M. Determination of HM (Cd, Pb, Cu) in some herbal drops by Polarography. *Iran J Pharmacol Ther.* 2017;1:4-7.
  145. Jezler CN, Mangabeira PAO, Almeida AAFD, Jesus RMD, Oliveira RAD, Silva DDC, Costa LCDB. Pb and Cd on growth, leaf ultrastructure and essential oil yield mint (*Mentha arvensis L.*). *Ciência Rural.* 2015;45:392-398.
  146. Rubio C, Lucas JRD, Gutiérrez AJ, Glez-Weller D, Marrero BP, Caballero JM, Hardisson A. Evaluation of metal concentrations in mentha herbal teas (*Mentha piperita*, *Mentha pulegium* and *Mentha species*) by inductively coupled plasma spectrometry. *J Pharm Biomed Anal.* 2012;71:11-17.
  147. Yener İ. Trace element analysis in some plants species by inductively coupled plasma optical emission spectrometry (ICP-OES). *J Inst Sci Technol.* 2019;9(3):1492-1502.
  148. Kočevar Glavač N, Djogo S, Ražić S, Kreft S, Veber M. Accumulation of HM from soil in medicinal plants. *Arch Hig Rada Toksikol.* 2017;68(3):236-244.
  149. Farrag HF, Al-Sodany YM, Otiby FG. Phoremediation and accumulation characteristics of HM by some plants in Wadi Alargy-Wetland, Taif-KSA. *World Appl Sci J.* 2013;28(5):644-653.
  150. Cardwell AJ, Hawker DW, Greenway M. Metal accumulation in aquatic macrophytes from southeast Queensland, Australia. *Chemosphere.* 2002;48(7):653-663.
  151. Deng H, Ye ZH, Wong MH. Accumulation of lead, zinc, copper and cadmium by 12 wetland plant species thriving in metal-contaminated sites in China. *Environ Pollut.* 2004;132(1):29-40.
  152. Soda S, Hamada T, Yamaoka Y, Ike M, Nakazato H, Saeki Y, Sakurai Y. Constructed wetlands for advanced treatment of wastewater with a complex matrix from a metal-processing plant: bioconcentration and translocation factors of various metals in *Acorus gramineus* and *Cyperus alternifolius*. *Ecol Eng.* 2012;39:63-70.
  153. Shahnaz M, Khan B, Sardar Khan JI, Mian IA, Muhammad MW. Contamination and bioaccumulation of HM in medicinal plants of District Dir Upper, Khyber Pakhtunkhwa, Pakistan. *Pak J Bot.* 2021;53(6):2179-2186.
  154. Kastratć V, Blagojević N, Vukašinović-Pešić V. Bioaccumulation and translocation of some transition metals in *Mentha spicata* and *Mentha longifolia*. *Pol J Environ Stud.* 2022;31(5):4065-4073.

### How cite this article

Djarmouni M, Sekia I, Ameni D, Ikessoulen T, Baghiani A. Impact of Toxic Heavy Metals and Their Concentration in *Zygophyllum* Species, *Mentha longifolia*, and *Thymus vulgaris* Traditional Medicinal Plants Consumed in Setif-Algeria. *Eur J Biol* 2023;81(2): 109-123. DOI: 10.26650/Eur-JBiol.2023.1163155